



Faculteit Farmaceutische, Biomedische en Diergeneeskundige Wetenschappen

Departement Farmaceutische Wetenschappen

Development of scientifically based and quality controlled herbal products

Ontwikkeling van wetenschappelijk onderbouwde en kwaliteitsgecontroleerde kruidenpreparaten

Proefschrift voorgelegd tot het behalen van de graad van Doctor in de Farmaceutische

Wetenschappen aan de Universiteit Antwerpen te verdedigen door

Ines VAN DOOREN

Promotoren: Prof. dr. S. Apers

Prof. dr. L. Pieters

Antwerpen, 2016

Table of contents

Chapter 1 INTRODUCTION

1.1	Herbal products.....	2
1.1.1	Introduction.....	2
1.1.2	Herbal medicinal products	2
1.1.2.1	Definitions	2
1.1.2.2	Legislation.....	3
1.1.2.3	Quality	4
1.1.3	Food supplements.....	5
1.1.3.1	Definitions	5
1.1.3.2	Legislation.....	6
1.1.3.3	Health claims	7
1.1.3.4	Quality	7

Chapter 2 AIM AND OUTLINE OF THIS WORK

Chapter 3 MATERIALS AND METHODS

3.1	Solvents and reagents	16
3.2	General apparatus.....	18
3.3	Methods	19
3.3.1	Chromatographic and spectroscopic methods	19
3.3.1.1	Introduction.....	19
3.3.1.2	Thin layer chromatography	19
3.3.1.3	Gas chromatography	19
3.3.1.4	Liquid chromatography	20
3.3.1.5	Nuclear magnetic resonance spectroscopy.....	26
3.3.1.6	Optical rotation	28
3.3.1.7	Fluorescence.....	29
3.3.1.8	UV/visible light spectroscopy and fluorescence spectrophotometry	29
3.3.2	Biological methods	29
3.3.2.1	Gastro-intestinal dialysis model	29

Chapter 4 DEVELOPMENT AND VALIDATION OF ANALYTICAL METHODS

4.1	Method development	34
4.2	Method validation	35
4.2.1	Introduction.....	35
4.2.2	Validation characteristics	36
4.2.2.1	Range	36
4.2.2.2	Linearity – calibration model.....	36
4.2.2.3	Precision	37

4.2.2.4	Accuracy	39
4.2.2.5	Specificity.....	40
4.2.2.6	Robustness	40
Chapter 5 <i>DESMODIUM ADSCENDENS</i>		
5.1	General introduction	44
5.1.1	Botanical description and use	44
5.1.2	Pharmacological activity.....	44
5.1.2.1	Antiasthmatic and anti-inflammatory activity	44
5.1.2.2	Hepatoprotective effects.....	46
5.1.2.3	Other properties.....	46
5.1.3	Toxicity studies	47
5.1.4	Phytochemical investigations.....	47
5.2	Development and validation of a gas chromatographic method for the quantification of D-pinitol in decoctions of <i>Desmodium adscendens</i>	50
5.2.1	Introduction.....	50
5.2.1.1	D-Pinitol	50
5.2.1.2	Herbal medicinal products and food supplements containing <i>Desmodium adscendens</i>	50
5.2.1.3	Analytical methods for the quantification of D-pinitol	51
5.2.2	Materials and methods	51
5.2.2.1	Plant material, decoction, and food supplements	51
5.2.2.2	General experimental procedures.....	52
5.2.2.3	Method development.....	52
5.2.2.4	Final method.....	54
5.2.2.5	Method validation	54
5.2.3	Results and discussion.....	55
5.2.3.1	Analytical technique	55
5.2.3.2	Method development.....	55
5.2.3.3	Method validation	58
5.2.3.4	Food supplements and decoctions.....	63
5.2.4	Conclusion	65
5.3	Antihepatotoxic activity of a quantified <i>Desmodium adscendens</i> decoction and D-pinitol against chemically-induced liver damage in rats	66
5.3.1	Introduction.....	66
5.3.2	Materials and methods	66
5.3.2.1	Plant material and preparation of the decoction.....	66
5.3.2.2	General experimental procedures.....	67
5.3.3	Results and discussion.....	67
5.3.3.1	Protective effect against acute D-galactosamine-induced liver damage.....	67

5.3.3.2	Curative effect against chronic D-galactosamine-induced liver damage	67
5.3.3.3	Curative effect against acute acetaminophen-induced hepatotoxicity	67
5.3.3.4	Protective effect against chronic ethanol-induced liver damage	68
5.3.4	Conclusions.....	68
5.4	Phytochemical analysis.....	69
5.4.1	Introduction.....	69
5.4.2	Materials and methods	69
5.4.2.1	Quick screening by HPLC-UV and TLC.....	69
5.4.2.2	Optimization of chromatographic parameters for flavonoid isolation and analysis ..	70
5.4.2.3	Compound isolation and structure elucidation.....	70
5.4.2.4	Total flavonoid content of five food supplements containing <i>D. adscendens</i> and different plant parts	73
5.4.3	Results and discussion	73
5.4.3.1	Quick screening by HPLC-UV and TLC.....	73
5.4.3.2	Optimization of chromatographic parameters for flavonoid isolation and analysis ..	74
5.4.3.3	Isolation and structure elucidation	77
5.4.3.4	Total flavonoid content of five food supplements containing <i>D. adscendens</i> and of different plant parts	115
5.4.4	Conclusions.....	116
5.5	Biological activity and metabolization.....	117
5.5.1	Introduction.....	117
5.5.1.1	General introduction	117
5.5.1.2	Metabolization	117
5.5.1.3	Advanced glycation end products	119
5.5.2	Materials and methods	120
5.5.2.1	Gastro-intestinal dialysis model	120
5.5.2.2	Analysis.....	121
5.5.2.3	Advanced glycation end products	122
5.5.3	Results	124
5.5.3.1	Gastro-intestinal dialysis model	124
5.5.3.2	Advanced glycation end products	127
5.5.4	Conclusions.....	129
Chapter 6 <i>HERNIARIA HIRSUTA</i>		
6.1	General introduction	140
6.1.1	<i>Herniaria hirsuta</i>	140
6.1.2	Kidney stones and gallstones	143
6.2	Saponins and flavonoids from an infusion of <i>Herniaria hirsuta</i>	147
6.2.1	Introduction.....	147

6.2.2	Materials and methods	147
6.2.2.1	Plant material	147
6.2.2.2	General experimental procedures.....	147
6.2.3	Results and discussion.....	150
6.2.3.1	Isolation	150
6.2.3.2	Structure elucidation.....	151
6.2.3.3	Discussion	182
6.3	Development and validation of an HPLC-UV method for the quantification of flavonoids and saponins in infusions of <i>Herniaria hirsuta</i> L.	184
6.3.1	Introduction.....	184
6.3.2	Materials and methods	184
6.3.2.1	Plant material and infusion	184
6.3.2.2	Method development.....	184
6.3.2.3	Final method.....	185
6.3.2.4	Method validation	185
6.3.3	Results and discussion.....	186
6.3.3.1	Method development.....	186
6.4	Coumarin, flavonoid and saponin profiles of different <i>Herniaria hirsuta</i> extracts and comparison with <i>Herniaria glabra</i> and <i>Herniariae herba</i>	192
6.4.1	Introduction.....	192
6.4.2	Material and methods.....	192
6.4.2.1	Plant material	192
6.4.2.2	General experimental methods.....	193
6.4.3	Results and discussion.....	193
6.4.3.1	Coumarins.....	193
6.4.3.2	Saponins	194
6.4.3.3	Flavonoids.....	196
6.5	Cholesterol lowering effect in the gallbladder of dogs by a standardized infusion of <i>Herniaria hirsuta</i> L.	199
6.5.1	Introduction.....	199
6.5.2	Materials and methods	199
6.5.2.1	Experimental protocol for the in vivo evaluation.....	199
6.5.2.2	Genotoxicity: Ames test	200
6.5.3	Results and discussion.....	201
6.5.3.1	In vivo evaluation	201
6.5.3.2	Genotoxicity: Ames test	203
6.5.4	Conclusions.....	204
Chapter 7 <i>VACCINIUM MACROCARPON</i>		
7.1	General introduction	210

7.1.1	Urinary tract infections.....	210
7.1.2	<i>Vaccinium macrocarpon</i>	210
7.1.3	Proanthocyanidins.....	214
7.1.4	Herbal medicinal products and food supplements containing <i>V. macrocarpon</i>	216
7.1.5	Methods of analysis.....	217
7.2	Development and validation of a UPLC-MS/MS method for the quantification of A-type dimeric and trimeric procyanidins in a cranberry extract.....	221
7.2.1	Materials and methods	221
7.2.1.1	Plant material	221
7.2.1.2	General experimental procedures.....	221
7.2.1.3	Method development.....	222
7.2.1.4	Method validation	225
7.2.2	Results and discussion	226
7.2.2.1	Method development.....	226
7.2.2.2	Final method.....	236
7.2.2.3	Method validation	236
7.2.3	Conclusions.....	246
7.3	Comparison of twelve cranberry-containing extracts using different commonly used analytical techniques.....	247
7.3.1	Materials and methods	247
7.3.1.1	Plant material	247
7.3.1.2	General experimental procedures.....	247
7.3.1.3	Analysis.....	247
7.3.2	Results and discussion.....	249
7.3.2.1	Analysis.....	249
7.3.3	Conclusion	263
Chapter 8 GENERAL CONCLUSIONS AND FUTURE PERSPECTIVES		
Chapter 9 SUMMARY		
ACKNOWLEDGMENTS - DANKWOORD		
SCIENTIFIC CURRICULUM VITAE		

List of abbreviations

ACN	acetonitrile
AFSSA	Agence Française de Sécurité Sanitaire des Aliments - French Health Products Safety Agency
Ag	aglycone
AGEs	advanced glycation end products
ALP	alkaline phosphatase
ALT	alanine aminotransferase
ANOVA	analysis of variance
AST	aspartate aminotransferase
BSA	bovine serum albumin
BSTFA	<i>N,O</i> -bis(trimethylsilyl)trifluoroacetamide
CE	crude extract
CFU	colony forming units
CG	control group
<i>D. adscendens</i>	<i>Desmodium adscendens</i>
DAD	diode array detection/detector
DC	direct current
DMAC	4-(dimethylamino)cinnamaldehyde
DMSO	dimethyl sulfoxide
DP	degree of polymerization
DPPH	2,2-diphenyl-1-picrylhydrazyl
DQF-COSY	double quantum-filtered correlation spectroscopy
EFSA	European Food Safety Authority
EI	electron ionization
ELSD	evaporative light scattering detection/detector
EMA	European Medicines Agency
ESI	electrospray ionization
EU	European Union
FA	formic acid
FAGG	Federaal Agentschap voor Geneesmiddelen en Gezondheidsproducten
FAMPH	Federal Agency for Medicines and Health Products
FID	flame ionization detection/detector
FS	food supplements
GC	gas chromatography
GIDM	gastro-intestinal dialysis model
GP	general phase
<i>H. hirsuta</i>	<i>Herniaria hirsuta</i>
HG	<i>H. hirsuta</i> group
HMBC	heteronuclear multiple bond correlation
HMPs	Herbal medicinal products
HMPC	Committee on Herbal Medicinal Products
HP	herbal preparations
HPLC	high-performance liquid chromatography
HRMS	high-resolution mass spectrometry
HS	herbal substances

HSQC	heteronuclear single quantum coherence
ICH	International Conference on Harmonization of Technical Requirements for Registration of Pharmaceuticals for Human Use
IM	intramuscular
IV	intravenous
LC	liquid chromatography
LOF	lack of fit
<i>m/z</i>	mass to charge ratio
MALDI	matrix-assisted laser desorption ionization
MRM	multiple reaction monitoring
MS	mass spectrometry
NBT	nitrobluetetrazolium
NMR	nuclear magnetic resonance
NP	normal phase
NSAIDs	non-steroidal anti-inflammatory drugs
OECD	Organization for Economic Co-operation and Development
PACs	proanthocyanidins
PDA	photo diode array
PEG	polyethylene glycol
P-gp	P-glycoprotein
RAGEs	AGEs receptors
RF	radio-frequency
R _f	retardation factor
RP	reversed phase
RSD	relative standard deviation
SIM	single ion monitoring
SPE	solid phase extraction
TFA	trifluoroacetic acid
TIC	total ion chromatogram
TLC	thin layer chromatography
TMCS	trimethylchlorosilane
TOCSY	total correlated spectroscopy
TOF	time of flight
TQD	triple quadrupole detection/detector
UDCA	ursodeoxycholic acid
UG	UDCA group
UPLC	ultra-performance liquid chromatography
UTIs	urinary tract infections
UV	ultraviolet
<i>V. macrocarpon</i>	<i>Vaccinium macrocarpon</i>
VIS	visible
VOG	vitexin-2''-O-glucoside
VOR	vitexin-2''-O-rhamnoside
WCB	Wilkins-Chalgren broth
WCOT	wall coated open tubular column

Chapter 1

INTRODUCTION

1.1 Herbal products

1.1.1 Introduction

Medicinal plants are used for centuries in different parts of the world. Nowadays, herbal medicines are still the only form of health care for large parts of the populations in developing countries, but also in industrialized developed countries the public interest and use of herbal products has tremendously increased during the past decades.¹⁻⁷ In Europe, these products are available as registered medicines (herbal medicinal products) or food supplements and are subjected to a different legislation. In the following part, this will be further elaborated in order to obtain an overview of their differences and similarities.

1.1.2 Herbal medicinal products

1.1.2.1 Definitions

The definitions are according to the directive 2004/24/EC.⁸

Herbal medicinal products

Herbal medicinal products (HMPs) are defined as medicinal products, which exclusively contain as active ingredients one or more herbal substances, or one or more herbal preparations, or a combination of one or more herbal substances and one or more of such herbal preparations.

Herbal substances

Herbal substances (HS) are all mainly whole, fragmented or cut plants, plant parts, algae, fungi, lichen in an unprocessed, usually dried form, but sometimes fresh. Certain exudates that have not been subjected to a specific treatment are also considered to be HS. They are precisely defined by the plant part used and the botanical name according to the binomial system (genus, species, variety, and author).

Herbal preparations

Herbal preparations (HP) are defined as preparations obtained by subjecting HS to treatments such as extraction, distillation, expression, fractionation, purification, concentration, or fermentation. These include comminuted or powdered HS, tinctures, extracts, essential oils, expressed juices, and processed exudates.

Traditional herbal medicinal products

Traditional HMPs need to fulfill the following conditions:

- they have indications exclusively appropriate to traditional HMPs which, by virtue of their composition and purpose, are intended and designed for use without the supervision of a medical practitioner for diagnostic purposes or for prescription or monitoring of treatment
- they are exclusively for administration in accordance with a specified strength and posology
- they are oral, external, and/or inhalation preparations
- they are used at least for 30 years, including 15 years in the European Community
- the data on the traditional use of the medicinal product are sufficient; in particular the product proves not to be harmful in the specified conditions of use and the pharmacological effects or efficacy of the medicinal product are plausible on the basis of long-standing use and experience

1.1.2.2 Legislation

In Europe, HMPs enter the market following different regulatory paths, i.e. following a registration procedure in order to obtain a marketing authorization as for medicinal products or following a simplified registration procedure to obtain a traditional use registration. The difference between these application procedures is situated in the safety and efficacy part (modules 4 and 5 of an application). In the first case, the authorization application is based on scientific literature establishing that the active substances of the medicinal products have been in well-established use within the European Union (EU) for at least ten years, with recognized efficacy and an acceptable level of safety. In addition, the application can also consist of only safety and efficacy data from the company's own development, called a 'stand-alone application', or a combination of their own studies combined with bibliographic data which is called a mixed application. The simplified

registration procedure is only possible when an HMP is classified as a traditional use medicine, i.e. an HMP with a long tradition for which scientific literature and data, in order to demonstrate a well-established use, are not available.

All these applications can be filed with a national competent authority of a member state, for national, mutual recognition, where the application is first filed in one member state and after approval in other member states of the EU, and decentralized procedures, while applications of well-established use medicines and stand-alone and mixed applications can also be filed with the European Medicines Agency (EMA) for a centralized procedure, where one central application is filed and the decision and approval are done by and for the whole EU, if it applies.^{1,8-10}

In order to increase the harmonization in the EU, the Committee on Herbal Medicinal Products (HMPC) was founded, one of the seven committees of the EMA. In addition, the committee drafts herbal monographs, which contain scientific opinions on safety and efficacy of a herbal substance or preparation with medicinal use based on all available information, including nonclinical and clinical data and data concerning long term use in the EU. Another core task of the HMPC is the establishment of the community list of HS, preparations, and combinations thereof for use in traditional HMPs. These two document types can be used by the applicants and facilitate the registration.¹⁰⁻¹¹ For example, if an applicant of a traditional HMP can demonstrate that his medicinal product complies with the community list, no further safety and traditional use evidence is required from the applicant.¹²

At a national level in Belgium, the Federal Agency for Medicines and Health Products (FAMHP-FAGG) ensures the safety, quality and efficacy of HMPs and processes applications. Within the FAMHP-FAGG a scientific committee for herbal medicines can be considered as the national equivalent of the HMPC.¹³

For all of these classes of HMPs, the quality must be documented in the application.

1.1.2.3 Quality

The quality requirements for HMPs and synthetic drugs are the same.^{2,9} However, their nature, i.e. a complex mixture of constituents, causes the need for a different approach. The quality of an HMP starts with a good quality of the starting material. The herbal substance material needs to be well characterized botanically, by microscopic and macroscopic determination, and phytochemically since

the content of active constituents can be influenced by growing conditions, such as climate and soil quality and by harvesting and storage conditions. Guidelines concerning cultivation, harvesting and collection are described in 'good agricultural and collection practice for starting materials of herbal origin' of the EMA.¹⁴ Phytochemical characterization of the herbal substance can be done by chromatographic fingerprinting, purity tests, and assays of certain constituents. Starting from the HS, HP, such as extracts, expressed juices and comminuted and powdered plants, are prepared using validated manufacturing processes. These preparations also require quantitative analysis. HS and HP are classified in three groups being either standardized, quantified, or other HS or HP. Standardized HS or HP are adjusted to a defined content of one or more constituents with known therapeutic activity by blending batches of the HS or HP or by mixing the HS or HP with inert excipients; quantified HS or HP are adjusted to a defined range of one or more active markers, i.e. constituents or groups of constituents which are generally accepted to contribute to the therapeutic activity. They are adjusted by blending batches of HS or HP. Other HS and HP are not adjusted to a particular content of constituents. They do not contain constituents with known therapeutic activity nor active markers. One or more constituents can be used as analytical markers, for which a minimum content is given in individual monographs, with respect to quality control of these extracts.¹⁵⁻¹⁶

The European Pharmacopoeia contains general guidelines for herbal drugs, herbal drug preparations, and herbal drug extracts and monographs comprising methods for the characterization and assays of a certain number of herbal substances and preparations.^{10,17-20} Up till now 278 of such monographs are available in the European Pharmacopoeia. If no monograph is available, new analytical methods for the quantification of active constituents or markers need to be developed and validated.

1.1.3 Food supplements

1.1.3.1 Definitions

Food supplements are defined by Regulation No 1924/2006 as pre-dosed foodstuffs, in addition to normal diet, which contain one or more nutrients, plants, plant preparations, or other compounds which possess a nutritional or physiological effect.²¹ Pre-dosed forms include capsules, tablets, gelules, granulate and similar forms and powder sachets, ampulla, dropper bottles, and similar forms of fluids and powders intended for unidose administration.

1.1.3.2 Legislation

The European directive 2002/46/EC is a first step in the harmonization of food supplements legislations in the different member states and consists of requirements concerning labeling and advertising. In addition, a list of vitamins and minerals allowed in food supplements are part of this directive.²²

In Belgium, three royal decrees and two ministerial decrees are applicable to food supplements, of which the Royal Decree of 29 August 1997 deals with manufacturing and marketing of foodstuffs, which contain or consist of plants and plant preparations. Before a food supplement is introduced on the market, it has to be notified to the Ministry of Health. This notification procedure is described in the royal decree and should include the nature of the product, a qualitative and quantitative list of ingredients including the plant name and its name in Latin, the plant part and the preparation used, a nutritional analysis of the product, qualitative and quantitative information on known significantly active constituents or 'markers' for one dosage unit and for a daily dosage, and information on toxicity and stability. In contrast to HMPs, no clinical trials or bibliographic evidence are required.²³ Recently the European Food Safety Authority (EFSA) published a guidance for the assessment of botanicals and botanical preparations to be used in food supplements, which could be of assistance to the notification procedure.²⁴ The notification procedure implies the commitment of the manufacturer to analyze his food supplement at different time points and to be able to provide these data to the Authorities.

In addition, the Royal Decree of 29 August 1997 includes three plant lists. List 1 contains toxic plants which are forbidden in food supplements, list 2 contains a list of edible mushrooms which are allowed in food supplements, and list 3 contains plants which are allowed to be processed in food supplements. For plants on list 3, the minimal and maximal amounts of active constituents and markers can be fixed. At the moment, Belgium, France, and Italy have submitted the Belfrit list to the European Commission. This is a positive list containing plants that are allowed in foodstuffs, mutually recognized by the three aforementioned countries.²³

Plants which do not belong to list 2 or 3 and that were not consumed at a significant degree in the European Union before 15 May 1997 can be considered as novel foods and are covered by regulation (EC) No 258/97. The registration procedure is centralized in Europe and the EFSA conducts a safety risk assessment on the novel food applications.^{25,26}

1.1.3.3 Health claims

Since food supplements can contain ingredients which can have nutritional or physiological effects, manufacturers can claim a certain relationship between the food supplement and health. These health claims are regulated by regulation (EC) No 1924/2006, the Royal Decree of 17 April 1980 and the Royal Decree of 29 March 2012, and are divided in functional health claims, risk reduction claims, and claims referring to children's development.^{21,27,28} Functional health claims are related to the growth, development and function of the body, to psychological or behavioral functions, or to slimming and weight control. Risk reduction claims are related to the reduction of a risk factor in the development of a disease. All claims should be based on scientific evidence and are subjected to different restrictions defined in the regulation and the abovementioned royal decrees. For example, health claims suggesting that not consuming the food supplement will affect health are not allowed as well as mentioning names of diseases or pictures of organs. A Community list of permitted claims published by the Commission is available. For claims mentioned on this list, no authorization procedure is necessary. All other claims need to undergo an authorization procedure whereby the authority verifies the scientific evidence of the claim and considers whether the claim complies with the criteria of the abovementioned regulation.

1.1.3.4 Quality

Although less extensively described in guidelines, the quality requirements of food supplements containing plants show many agreements with HMPs. In this way, the plant material should be botanically and phytochemically characterized and the content of plant constituents described in lists 2 and 3 or content of active constituents or markers need to be quantified. For this latter purpose, developed and validated analytical methods are necessary.

References

1. Furst, R.; Zundorf, I. Evidence-based phytotherapy in Europe: where do we stand? *Planta Med.* **2015**, *81* (12-13), 962-967.
2. Wegener, T.; Deitelhoff, B.; Silber-Mankowsky, A. Drug safety aspects of herbal medicinal products. *Wien. Med. Wochenschr.* **2015**, *165* (11-12), 243-250.
3. Popović, Z.; Matić, R.; Bojović, S.; Stefanović, M.; Vidaković, V. Ethnobotany and herbal medicine in modern complementary and alternative medicine: An overview of publications in the field of I&C medicine 2001–2013. *J. Ethnopharmacol.* **2016**, *181*, 182-192.
4. Tilburt, J.; Kaptchuk, T. Herbal medicine research and global health: an ethical analysis. *Bul. W. H. O.* **2008**, *86* (8), 90.
5. Bardia, A.; Nisly, N. L.; Zimmerman, M. B.; Gryzlak, B. M.; Wallace, R. B. Use of herbs among adults based on evidence-based indications: findings from the National Health Interview Survey. *Mayo Clin. Proc.* **2007**, *82* (5), 561-566.
6. Ekor, M. The growing use of herbal medicines: issues relating to adverse reactions and challenges in monitoring safety. *Front. Pharmacol.* **2014**, *4*, 177.
7. Wachtel-Galor, S.; Benzie, I. F. F. Herbal medicine: An introduction to its history, usage, regulation, current trends, and research needs. In *Herbal Medicine: Biomolecular and Clinical Aspects*, Benzie, I. F. F.; Wachtel-Galor, S., Eds. CRC Press/Taylor & Francis Llc.: Boca Raton (FL), 2011.
8. European Parliament and Council. *Directive 2004/24/EC of the European parliament and of the council of 31 March 2004, amending as regards traditional herbal medicinal products, directive 2001/83/EC on the Community code relating to medicinal products for human use.* Strasbourg, 2004.
9. European Medicines Agency. Herbal medicinal products.
http://www.ema.europa.eu/ema/index.jsp?curl=pages/regulation/general/general_content_000208.jsp (accessed November, 2016).
10. Vlietinck, A.; Pieters, L.; Apers, S. Legal requirements for the quality of herbal substances and herbal preparations for the manufacturing of herbal medicinal products in the European union. *Planta Med.* **2009**, *75* (7), 683-688.
11. European Medicines Agency. HMPC: overview.
http://www.ema.europa.eu/ema/index.jsp?curl=pages/about_us/general/general_content_000122.jsp&mid=WC0b01ac0580028e7d (accessed June 15, 2016).
12. European Medicines Agency. European Community list entries.
http://www.ema.europa.eu/ema/index.jsp?curl=pages/regulation/document_listing/document_listing_000213.jsp. (accessed June 15, 2016).
13. Federal Agency for Medicines and Health Products. Wat doet het FAGG? http://www.fagg-afmps.be/nl/public_information/que_fait_afmps. (accessed June 15, 2016).
14. European Medicines Agency. Guideline on good agricultural and collection practice for starting materials of herbal origin. *EMEA/HMPC/246816/2005*. London, 2006.

15. European Medicines Agency. Guideline on the quality of herbal medicinal products/traditional herbal medicinal products. *EMA/CPMP/QWP/2819/00 Rev. 2; EMA/CVMP/814/00 Rev. 2; EMA/HMPC/201116/2005 Rev. 2*. London, 2011.
16. European Medicines Agency. Reflection paper on markers used for quantitative and qualitative analysis of herbal medicinal products and traditional herbal medicinal products. *EMA/HMPC/253629/2007*. London, 2008.
17. Council of Europe. Monographs on herbal drug extracts (information chapter). In: European Pharmacopoeia 8.7 [Online]; Council of Europe: Strasbourg, 2016. <http://online6.edqm.eu/ep807/> (accessed June 15, 2016).
18. Council of Europe. Herbal drug extracts. In: European Pharmacopoeia 8.7 [Online]; Council of Europe: Strasbourg, 2016. <http://online6.edqm.eu/ep807/> (accessed June 15, 2016).
19. Council of Europe. Herbal drug preparations. In: European Pharmacopoeia 8.7 [Online]; Council of Europe: Strasbourg, 2016. <http://online6.edqm.eu/ep807/> (accessed June 15, 2016).
20. Council of Europe. Herbal drugs. In: European Pharmacopoeia 8.7 [Online]; Council of Europe: Strasbourg, 2016. <http://online6.edqm.eu/ep807/> (accessed June 15, 2016).
21. European Parliament and Council. *Regulation No 1924/2006 of the European Parliament and of the council of 20 December 2006 on nutrition and health claims made on foods*. Brussels, 2007.
22. European Parliament and Council. *Directive 2002/46/EC of the European parliament and of the council of 10 June 2002 on the approximation of the laws of the member states relating to food supplements*. Luxembourg, 2002.
23. *Royal Decree of 29 August 1997 on the manufacture and trade of foods composed of or containing plants and plant preparations*. Brussels, 1997.
24. European Food Safety Authority. Guidance on the safety assessment of botanicals and botanical preparations intended for use as ingredients in food supplements. http://www.efsa.europa.eu/sites/default/files/scientific_output/files/main_documents/1249.pdf. (accessed June 15, 2016).
25. European Commission. Novel Foods. http://ec.europa.eu/food/safety/novel_food/index_en.htm. (accessed June 15, 2016).
26. European Parliament and Council. *Regulation No 258/97 of the European parliament and of the council of 27 January 1997 concerning novel foods and novel food ingredients*. Brussels, 1997.
27. *Royal Decree of 17 April 1980 concerning advertising of foodstuffs*. Brussels, 1980.
28. *Royal Decree of 29 March 2012 changes of Royal Decree of 17 April 1980*. Brussels, 2012.

Chapter 2

AIM AND OUTLINE OF THIS WORK

Because of the enormous importance of herbal products in developing countries and the growing interest in plant-based medicines in the developed countries, as discussed in **Chapter 1**, this work aimed to contribute to the development of scientifically based and quality controlled herbal products (**Chapter 2**).

In this work, three plant species were selected: *Desmodium adscendens* (Sw.) DC., *Herniaria hirsuta* L., and *Vaccinium macrocarpon* Aiton.

All techniques and materials used in this work are described in **Chapter 3**.

In **Chapter 4**, an overview is given of the development and validation of analytical methods, in particular for herbal products.

In **Chapter 5**, *Desmodium adscendens* is discussed. *D. adscendens* is used in traditional medicine for many years for the treatment of pain, fever, asthma, seizures, hepatitis, muscle spasms, ovary inflammation, and snake bites. A patent has been taken on the use of *Desmodium*, especially *D. adscendens*, in the treatment of viral or chemically-induced hepatitis. However, at the start of this work, no studies had been performed with a quantified extract of *D. adscendens*. Previous experiments of our research group characterized D-pinitol, a compound with hepatoprotective activity, as the major constituent of a decoction of *D. adscendens*.

This work aimed to develop a quantified extract with known levels of D-pinitol, to be used in *in vivo* studies. An analytical method for the quantification of D-pinitol was developed and validated. Afterwards, the protective and curative effect of this decoction, in which D-pinitol was quantified, and of pure D-pinitol, against liver damage induced by various chemicals in rats, was investigated. According to the results of the *in vivo* study, further phytochemical research needed to be done to characterize accompanying constituents. Finally, the metabolization of the decoction and its constituents was investigated together with the evaluation of the biological activity of the extract against advanced glycation end products.

The second plant species selected was *Herniaria hirsuta* (**Chapter 6**). An infusion of *H. hirsuta* is traditionally used in Morocco for the treatment of biliary dyskinesia, (uro)lithiasis, or as a diuretic.

The efficacy of this plant species against cholelithiasis had already been reported. However, the efficacy and use of a standardized extract against cholelithiasis have never been investigated. Therefore, a scientifically based and quality controlled extract was developed. The workflow consisted of the phytochemical characterization of the main constituents by means of isolation and structure elucidation, the development and validation of an analytical method for the quantification of the characterized constituents, and an *in vivo* study in dogs with the standardized extract. In addition, its genotoxicity was evaluated.

In **Chapter 7**, *Vaccinium macrocarpon* Aiton, widely used for the prevention of urinary tract infections, is discussed. This plant is a rich source of proanthocyanidins, including the rather rare A-type procyanidins, considered to be the pharmacologically active constituents of cranberry. In literature, only a few potentially qualitative methods for quantification of dimeric and trimeric A-type proanthocyanidins are described and none of them was thoroughly developed and validated. Therefore, this study aimed to develop and validate a fast and reliable LC-MS² method for the simultaneous quantification of both A-type dimers and trimers in cranberry extracts. In the last part, the quality of different cranberry extracts was evaluated by means of some generally accepted methods for proanthocyanidin analysis and the correlation with the newly developed LC-MS² method was investigated.

The general conclusions including future perspectives are described in **Chapter 8**.

Chapter 3

MATERIALS AND METHODS

3.1 Solvents and reagents

Solvents and gasses	acetonitrile (ACN) Far UV (HPLC grade), methanol (HPLC grade)	Fisher Scientific Hampton, NH, USA
	absolute ethanol (HPLC grade), acetone (HPLC grade), butanol (99%), dichloromethane (HPLC grade), dimethyl sulfoxide (DMSO) (p.a.), ethyl acetate (HPLC grade), pyridine (99+%)	Acros organics Geel, Belgium
	acetone-d ₆ (CD ₃ CN 99.8%), DMSO-d ₆ , methanol-d ₃ (CD ₃ OD 99.5%)	Sigma Aldrich St. Louis, MI, USA
	helium, hydrogen, nitrogen, compressed air	Air Liquide Liège, Belgium
Reagents	acetic acid (99.8%), formic acid (FA) (99+%), phosphoric acid (p.a. 85%), sulphuric acid (85%) and trifluoroacetic acid (TFA) (p.a. >99%)	Acros organics
	<i>p</i> -anisaldehyde, bile salt (B-8631, porcine), bovine serum albumin (98%), L-cysteine, 4-(dimethylamino) cinnamaldehyde (≥98%), diphenylboric acid 2-aminoethyl ester (98%), disodium phosphate dihydrate, glycerol suitable for culture, hydrochloric acid (p.a. 25%), nitrotetrazolium blue chloride (TLC grade), pancreatin (76 190, from dog pancreas, 149 USP U/mg amylase), pepsin (P-7000, from porcine stomach mucosa, 800-2500 U/mg protein), resazurin sodium salt, sodium azide (>99,5%) sodium dihydrogen phosphate anhydrous, sodium thioglycolate broth, vanillin (>99%)	Sigma Aldrich
	<i>N,O</i> -bis(trimethylsilyl)trifluoroacetamide (BSTFA) containing 1% trimethylchlorosilane (TMCS), Wilkins-Chalgren broth (WCB)	Thermo Fisher Scientific Waltham, MA, USA
	potassium hydroxide (p.a.)	VWR International Radnor, PA, USA
polyethylene glycol (PEG) 4000, sodium hydroxide, sodium bicarbonate	Merck Darmstadt, Germany	

Chemicals for <i>in vivo</i> experiment (Chapter 6, <i>H. hirsuta</i>)	acepromazine (Calmivet®), ketamine (Clorketam 1000®), marbofloxacin 2% (Marbocyl®), tolfenamic acid 4% (Tolfidin®)	Vétoquinol, Lure, Cedex, France
	oxibendazole and niclozamide (Vitaminthe®)	BCI®
	atropine	Promopharm Casablanca, Morocco
	sodium thiopental (Nesdonal®)	Sanofi-Aventis Paris, France
	isoflurane	Cooper Maroc, Casablanca, Morocco
	a kit for cholesterol determination	DiaSYS Diagnostic Systems GmbH Holzeim, Germany
	ursodeoxycholic acid (UDCA) as Ursofalk® 250 mg	Dr. Falk Pharma Benelux B.V.
	praziquantel (Droncit®), xylazine (Rompun®)	Bayer Leverkusen, Germany

3.2 General apparatus

The device used for ultrasonication was an ultrasonic cleaner Branson MHT 3510 (VWR). A small microprocessor-controlled centrifuge, a SIGMA 1-15PK from Fisher scientific and a Heraeus labofuge 400 centrifuge from Thermo scientific were used. PH measurements were performed on a PHM 92 LAB pH-meter from Radiometer (Copenhagen, Denmark). Concentration under reduced pressure was done using a rotavapor from IKA (VWR) and a Büchi RE111 Rotavapor (Büchi, Flawil, Switzerland). Round bottom flasks were heated using an Isopad Labmasters heating mantle (VWR).

3.3 Methods

3.3.1 Chromatographic and spectroscopic methods

3.3.1.1 Introduction

Separations by chromatographic techniques are based on the distribution of the analytes between a mobile and a stationary phase. In this work, thin layer chromatography, gas chromatography and liquid chromatography are used and will be briefly discussed including the detection systems used.

3.3.1.2 Thin layer chromatography

For thin layer chromatography (TLC), the distribution takes place between a liquid mobile phase and a solid stationary phase on a glass or plastic support. Frequently used stationary phases are silica, aluminum oxide, or cellulose. Samples are applied on the TLC plates and placed in a developing chamber, containing mobile phase, and are developed. Visualization of analytes can be performed by ultraviolet (UV)-light when using plates with a fluorescence indicator or by spraying with a derivatization reagent to obtain colored spots for the analytes of interest.¹

Normal phase HPTLC plates (20 x 20 cm, silica gel 60 F₂₅₄, Merck) and normal phase TLC plates (20 x 20 cm, silica gel 60 F₂₅₄, Merck) were used. Samples were spotted either manually or by using an automatic TLC sampler 4 (Camag, Muttenz, Switzerland) and the plates were developed using a glass developing tank or an automatic developing chamber (Camag) and heated on a TLC Plate Heater III (Camag). The following spraying reagents were used: a KOH solution (5% in ethanol), the NEU-reagent (1% diphenylboric acid 2-aminoethyl ester in methanol), a PEG solution (5% in ethanol), and the anisaldehyde reagent (anisaldehyde/sulphuric acid/acetic acid/methanol 0.5:5:10:85). The plates were scanned or visualized using a TLC scanner 3 or a reprostar 3 (Camag). Software was from Wincats.

3.3.1.3 Gas chromatography

Gas chromatography (GC) uses a gaseous mobile phase, such as nitrogen or helium, and a liquid stationary phase placed on a support, such as polysiloxane. The analyte is injected on the column and is eluted by heating the column using a temperature gradient so that the analyte reaches the gas phase. Different detectors are used in combination with gas chromatography such as a thermal

conductivity detector, a flame ionization detector, and an electron capture detector. In this work, a flame ionization detector (FID), and electron ionization mass detector were used. This first detector type is a universal detector. The eluate is mixed with H₂ and air and burned in the flame giving rise to ionization of organic compounds. These ions increase the electric current of the collecting electrode which is recorded by the computer system. Using the electron ionization (EI) mass detector, ions are formed by a beam of high-energy electrons and ions are separated based on their m/z ratio by a quadrupole (see liquid chromatography).¹

The system used for the experiments was a Trace GC Ultra with flame ionization detection (Interscience, Louvain-la-Neuve, Belgium) equipped with an autosampler AS 3000 and a Trace Ultra GC. In addition, a Trace 2000 GC with a Combi Pal injector (CTC Analytics, Zwingen, Switzerland) and a Voyager quadrupole mass spectrometer equipped with an electron ionization source (Interscience) was used. The GC-FID and GC-MS instruments were equipped with EZchrome and Xcalibur software, respectively.

Different columns were used: column 1: HP-5 (30 m x 0.32 mm, 0.25 μ m) (5% phenyl, 95% methyl polysiloxane) (WCOT) (Agilent, Santa Clara, CA, USA); ATTM-5MS/Rtx[®]-5MS (30 m x 0.25 mm, 0.25 μ m) (5% phenyl, 95% polysilphenylene siloxane), (Alltech, Columbia, MD, USA); and column 2: ATTM-264, (30 m x 0.32 mm, 1.8 μ m) (6% cyanopropylphenyl, 94% methyl siloxane) (WCOT) (Alltech).

3.3.1.4 *Liquid chromatography*

Liquid chromatography (LC) uses a liquid mobile phase and a solid stationary phase, as for TLC, but the stationary phase is located in a column. Frequently used stationary phases are silica and different types of modified silica to which a wide variety of functional groups is linked. The column and particle size can vary depending on the purpose of the experiment. Bigger columns with larger particle size are used for preparative separations, while smaller particles and column sizes are more suitable for analytical purposes. A large range of mobile phases is used, ranging from water to hexane. Depending on the polarity of the mobile and stationary phase, different types of LC are distinguished: the term normal phase (NP) is used for a system consisting of a polar stationary phase and an apolar mobile phase, whereas reversed phase (RP) is used to denote that an apolar stationary phase is used in combination with a polar mobile phase.

Different detection systems are used in combination with LC including diode array detectors (DAD), mass spectrometry (MS) detectors, evaporative light scattering detectors (ELSD), and refractive index detectors. In this work, the first three detector types were used. The ELSD works by evaporating the eluate into a fine spray by mixing it with a nebulizing gas. By heating, the solvent of the droplets evaporates leading to small particles containing the compounds. These particles flow through a light source and, depending on the size and amount of the particles, the light is scattered. This degree of scattering is measured.

A DAD measures the UV absorbance of the eluate running through the flow cell of the detector over a wavelength range. When the energy level of the light, in the ultraviolet range, emitted by the light source of the spectrophotometer is the same as the difference in energy levels in the molecule, the light will be absorbed and the electron moves to a higher energy state. The amount of absorption is directly proportional to the concentration of the analyte and is described by Lambert-Beer's Law:

$$A = \epsilon \cdot c \cdot d$$

where A is the absorbance, ϵ the molar extinction coefficient expressed in $\text{L}\cdot\text{mol}^{-1}\cdot\text{cm}^{-1}$, c the concentration expressed in mol/L, and d the path length, expressed in cm.

Since these electronic transitions often involve π electrons and lone pair ions (n), molecules with double bonds and conjugated systems are able to absorb light in the ultraviolet range (100-400 nm).¹

Flash chromatography

Flash chromatography was done on a Reveleris® iES Flash Chromatography System (Grace) equipped with a sample injection system which allows dry or liquid sample loading, a binary pump and four solvent reservoirs, a UV detector (simultaneous detection of 2 wavelengths between 200-400 nm) and ELSD, and a fraction collector with 2 collection trays. Collection criteria were either slope detection or threshold detection. A Reveleris silica column (80 g, 40 μm) and a Reveleris C18 column (40 g, 40 μm) were used.

Manual flash chromatography was done by means of a Gilson® 306-pump (Gilson, Middleton, USA) coupled to a GraceResolv® column (150 g, 40-63 μm) (Grace).

Semi-preparative liquid chromatography

An Agilent 1200 Series HPLC with degasser, quaternary pump, automated liquid sampler, thermostatic column compartment and DAD (Agilent) was used. The system was equipped with Chemstation software. In addition, a Gilson 322 HPLC with a binary pump, automated liquid sampler, and UV detector was used. This system was equipped with Unipoint software.

An autoPurification™ system from Waters with a binary gradient module, sample manager, make-up pump, system fluidics organizer, DAD, and Micromass Quattro micro TQD-MS analyzer (Milford, Massachusetts, USA) was used. The system was equipped with Masslynx software.

Two different semi-preparative columns were used: An Apollo C18 column (250 x 10 mm, 5 µm) (Phenomenex, Torrance, CA, USA) and a Luna C18 (2) column (250 x 10 mm, 5 µm) (Phenomenex).

High-performance liquid chromatography

An Agilent 1200 and 1260 Series HPLC with degasser, quaternary pump, automated liquid sampler, thermostatic column compartment and DAD, and ChemStation software (Agilent Technologies, Eindhoven, The Netherlands) and a Beckmann HPLC system consisting of a model 125 pump, a model 507e autosampler, a model 168 DAD and 32 Karat™ software (Beckmann Coulter, Fullerton, CA, USA) were used.

Different columns were used: A Grace Smart RP-18 column (250 x 4.6 mm, 5 µm) (Grace), a Lichrospher 100 RP-18 (250 x 4, 5 µm) (Merck), an Apollo C18 column (250 x 4.6 mm, 5 µm) (Phenomenex), an Econosphere C18 (250 x 4.6 mm, 5 µm) (Grace), a Luna C18 (2) column (250 x 4.6 mm, 5 µm) (Phenomenex) and a Kinetex EVO C18 (250 x 4.6 mm, 5 µm) (Phenomenex). For NP chromatography a Purospher STAR Si column (250 x 4 mm, 5 µm) (Merck) was used.

HPLC – solid phase extraction

An Agilent 1200 HPLC as described above, was coupled to an online solid phase extraction (SPE) system Prospekt 2 consisting of a high-pressure dispenser, an automated cartridge exchange unit (Spark Holland, Emmen, The Netherlands), a Knauer pump and a Liquid handler (Bruker BioSpin, Rheinstetten, Germany). HySpere Resin general phase (GP) cartridges, of which the sorbent is polydivinyl-benzene, were used, after conditioning with methanol and equilibrating with water.

Detection was done at 330 nm. When a peak appears in the chromatogram, the trapping is started and the analyte is transferred to the selected cartridge. At the end of the peak, the trapping is stopped. To increase the concentration of the compound, the HPLC run is repeated and the same compound is trapped several times on the same cartridge. After trapping, the cartridges are dried with N₂ and compounds are eluted with CD₃CN into an NMR tube (3 mm). The column used for the experiments was a Luna C18 (2) column (250 x 4.6 mm, 5 μm).

HPLC – mass spectrometry

A Surveyor LC system equipped with a degasser, a quaternary pump, an autosampler and a DAD (Thermo Fisher) was used. The LC system was coupled to an LXQ linear ion trap (Thermo Fisher). The LXQ linear ion trap detector is shown in Figure 3.1 and consists of an atmospheric pressure ionization source, ion optics, a mass analyzer, and an ion detection system. In the ion source, ion formation takes place. In our experiments, electrospray ionization (ESI) was used. The sample solution travels through the ESI needle on which a high voltage is applied resulting in a spray of sample solution consisting of electrically charged (at surface) droplets. As the solvent evaporates, the charge density increases and the droplets divide into smaller droplets. From very small droplets, ions are desorbed or ejected through electrostatic repulsion. The ions are transferred through the ion sweep cone, acting as a physical barrier, and an ion transfer capillary of the ion source interface to the ion optics. From this interface part on, the detector is held under vacuum. The ion optics consist of different lenses, a skimmer, and a quadrupole and an octapole. The lenses act as ion focusing devices and lens L0 and L1 also act as a vacuum baffle between the different ion guide compartments. The application of a radio frequent (RF) voltage on the lenses creates an electrical field, focusing the ions along their axis. The quadrupole and octapole act as ion transmission devices. By applying an RF voltage to the rods, an electrical field is obtained, which guides the ions along the axis of the quadrupole and octapole to the mass analyzer, the heart of the detector.

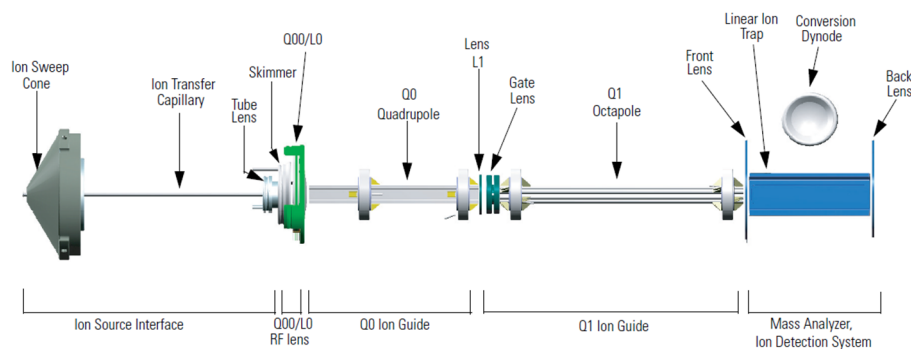


Figure 3.1 Overview of the LXQ linear ion trap detector.²

The mass analyzer, shown in Figure 3.2, consists of a front lens, the linear ion trap, which consists of four hyperbolic rods and a back lens.

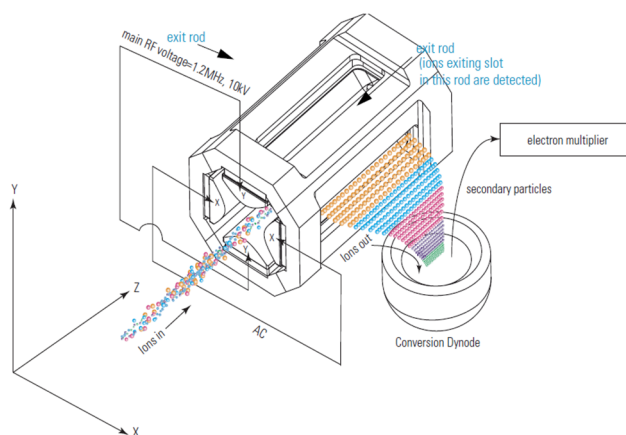


Figure 3.2 Overview of the ion trap mass analyzer of the LXQ detector.²

On these three components, voltages are applied in order to trap ions or to scan them out. Scanned out ions reach the ion detection systems and are converted into signals, which are processed by the software system.

In this way, different experiments can be performed. A full scan experiment provides a full mass spectrum of all precursor ions (one-stage full scan) or product ions after collision (two-stage full scan or product ion scan), between a predetermined mass range. During selected ion monitoring, precursor ions of one or more mass to charge ratios are trapped and measured, whereas during a selected reaction monitoring experiment, one selected precursor ion (single reaction monitoring) or more selected precursor ions (multiple reaction monitoring) collide with a background gas giving rise to product ions. Product ions of one or more m/z values are selected and all other ions are scanned

out. Then the selected product ions are scanned out and measured. This process can be repeated multiple times. In this way, an enormous quantity of structural information is obtained making this detector ideal for structure elucidation.²

A non-linear ion trap works in a similar way. The ion trap mass analyzer comprises a ring electrode and 2 end-cap electrodes, one entrance and one exit cap electrode. By using an RF voltage, ions can be trapped and scanned out as described for the linear ion trap mass analyzer.³

The experimental data were recorded in positive and negative mode using ESI. The system was equipped with Xcalibur software. Different columns were used: A Grace Smart RP-18 column (250 x 4.6 mm, 5 μ m) (Grace), an Apollo C18 column (250 x 4.6 mm, 5 μ m) (Phenomenex), a Luna C18 (2) column (250 x 4.6 mm, 5 μ m), a Purospher STAR C18 (Merck Millipore), and an Hypersil Gold column (150 x 2.1 mm, 3 μ m) (Thermo Fisher).

An Agilent 1100 Series HPLC equipped with a binary pump, automated liquid sampler and an Agilent 1100 Series MSD ion trap ChemStation software (Agilent Technologies) was used. The experimental data were recorded in positive and negative mode using ESI. Different columns were used: A Grace Smart RP-18 column (250 x 4.6 mm, 5 μ m) (Grace), an Apollo C18 column (250 x 4.6 mm, 5 μ m)(Phenomenex), and a Luna C18 (2) column (250 x 4.6 mm, 5 μ m).

Ultra-performance liquid chromatography – mass spectrometry

An Acquity ultra-performance liquid chromatography (UPLC) system (Waters) with a sample manager, binary solvent manager, photo diode array (PDA) detector and triple quadrupole detector (TQD) was used. The TQD consists of an ion source, ion optics, and a mass analyzer. Ions are formed in the ion source using ESI as described for the LQX system. These ions are transferred through the sample cone into a vacuum system. The ion optics, a hexapole, guides the ions to the mass analyzer which consists of two quadrupoles and a collision cell. By applying a direct current (DC) and RF potentials on the rods of the quadrupoles, ions with a predetermined mass to charge ratio are selected and enter the collision cell. Here, ions collide with neutral gas molecules leading to product ions, which are transferred to the second quadrupole. This quadrupole can be set to scan all product ions or filter ions of only one or more m/z ratios. In this way, high sensitivity is achieved. The same experiments can be performed as described above: full scan, single/selected ion monitoring/recording, single and multiple reaction monitoring, but also a precursor ion scan and

neutral loss experiment can be performed. For a precursor ion scan, the first quadrupole scans all the ions coming through. They collide in the collision cell and the second quadrupole filters the product ion of interest. In this way, all precursors leading to the product ion of interest are found. In a neutral loss experiment, the first and second quadrupole are synchronized and the second quadrupole searches for product ions with the predetermined mass losses.⁴

The system was equipped with Masslynx software. A BEH C18 (2.1 x 100 mm; 1.8 μm) (Waters) column and an HSS T3 column (2.1 x 100 mm; 1.8 μm) (Waters) were used.

High-resolution mass spectrometry

Accurate mass measurements were carried out using an Orbitrap mass spectrometer (Q Exactive™, Thermo Fisher Scientific) equipped with an Ion Max™ ESI source (Thermo Fisher Scientific). High-resolution mass spectrometric experiments were performed using a hybrid mass spectrometer that combines a quadrupole for ion selection with an accurate mass high-resolution orbitrap detector system (Q Exactive™). After ions are selected by the quadrupole mass filter, the ions are stored in the C-trap before they are injected to the orbitrap. The instrument also comprises a high-energy collision detector with a collision cell where fragmentation takes place before entering the orbitrap. The orbitrap consists of an outer barrel like electrode and an inner spindle like electrode. Ions are trapped by the balance between the electrostatic attraction to the inner electrode and their centrifugal forces. They cycle round the inner axis in elliptical trajectories and move back and forward. This axial motion is only dependent of the m/z ratio and gives rise to an image current that can be detected and results in a mass spectrum after Fourier Transformation.^{5,6}

3.3.1.5 Nuclear magnetic resonance spectroscopy

Nuclear magnetic resonance (NMR) spectroscopy is based on the following principle. Some nuclei, more specifically those of elements with an odd atom number or odd mass, have a nuclear spin (I) and therefore they behave like magnets when they are placed in a strong magnetic field (B_0). According to their spin quantum number, they can orient in $2I + 1$ ways. The most used elements are ^1H and ^{13}C which both have a spin quantum number of $1/2$ and therefore have two orientations, i.e. one with and one opposed to the applied field, a parallel and an anti-parallel orientation,

respectively. The ratio of low-energy state or parallel (N_α) and high-energy state or anti-parallel (N_β) oriented nuclei is described by the Boltzmann distribution:

$$\frac{N_\beta}{N_\alpha} = e^{-\frac{\Delta E}{kT}}$$

with

$$\Delta E = \frac{h\gamma B_0}{2\pi}$$

where k is the Boltzmann constant, T the temperature, E the energy, h Planck's constant, and γ the gyromagnetic ratio. However, when an RF signal is applied the distribution changes and more nuclei will change from the low-energy state to the high-energy state. The resonance frequency at which the nuclei come into resonance is given by:

$$\nu = \frac{\gamma B_0}{2\pi}$$

After the nuclei are excited, they gradually relax to return to their ground state. These decaying signals are called free induction decays and undergo a Fourier Transformation to give a spectrum containing frequency signals. Modern systems generate a powerful pulse covering the whole range of frequencies to be detected.⁶

To obtain ^1H , ^{13}C -NMR and 2D-NMR (^1H - ^1H correlation spectroscopy (COSY), ^1H - ^1H total correlated spectroscopy (TOCSY), ^1H - ^{13}C heteronuclear single quantum coherence (HSQC) and ^1H - ^{13}C heteronuclear multiple bond correlation (HMBC)) spectra, a Bruker DRX 400 instrument (Figure 3.3) equipped with a z-gradient 5 mm dual probe and a 3 mm broadband inverse probe using standard Bruker pulse sequences (Rheinstetten, Germany) was used operating at 400 MHz for ^1H and 100 Hz for ^{13}C . Chemical shifts are given in ppm and coupling constants (J) in Hz.



Figure 3.3 NMR 400 MHz from Bruker.

3.3.1.6 Optical rotation

Substances containing one or more chiral centra are able to rotate the plane of polarized light. This phenomenon is called optical rotation. When the plane is rotated in a clockwise direction, these substances are dextrorotatory, whereas laevorotatory substances rotate the plane in an anti-clockwise direction. The angle of rotation can be measured in a polarimeter. The specific optical rotation (α_D^{20}) is characteristic for each substance and is the angle of rotation (α) measured at 20 °C, at the D-line of sodium ($\lambda = 589.3$) for a concentration (c) of 1 g/L of the substance and a path length (l) of 1 dm, and can be calculated as ⁷:

$$\alpha_D^{20} = \frac{\alpha \cdot 1000}{l \cdot c}$$

To measure the optical rotation a Jasco P-2000 digital polarimeter (Jasco, VA Ijsselstein, The Netherlands) equipped with a Tungsten-Halogen lamp was used. Measurements were performed at 589 nm and 20 °C using a sample holder of 100 mm (\varnothing 2.5 mm). The specific optical rotation was calculated using the abovementioned formula.

3.3.1.7 Fluorescence

After a molecule has absorbed light and has become excited it will go back to its ground state. When this is done by emitting light, it is called fluorescence. This can be measured by a fluorescence spectrometer.¹

3.3.1.8 UV/visible light spectroscopy and fluorescence spectrophotometry

A Lambda 35 double beam UV/ visible light (VIS) spectrophotometer (Perkin-Elmer, Waltham, MA, USA) equipped with a deuterium and Tungsten lamp was used. Measurements were performed with a bandwidth of 1 nm.

An Infinite 200 well plate reader (Tecan, Männedorf, Switzerland) was used for VIS and fluorescence spectrophotometrical measurements.

3.3.2 Biological methods

3.3.2.1 Gastro-intestinal dialysis model

This model consists of four Amicon stirred dialysis cells (Figure 3.4) equipped with a dialysis membrane with a molecular weight cutoff of 1000 and a diameter of 63.5 mm (Millipore). Tubular dialysis membranes for the preparation of dialysis bags (molecular mass cut off of 12 to 14 kDa (Visking size 6 Inf Dia 27/32 – 21.5 mm: 30 M) were obtained from Medicell Ltd. (London, UK). A thin flexible plastic tube was attached to each cell for transportation of dialyzed fluid, called dialysate, out of the cells into a collection recipient. All four dialysis cells were attached in parallel to a system that feeds the cells with either water or gas (N₂) to mimic the transport mechanism of water from plasma into the chyme in humans. The cells are placed on a shaking hot water bath during the gastric phase and in a Jacomex Globe-box T₃ (TCPS, Rotselaar, Belgium) during the duodenum and colonic phase.⁸

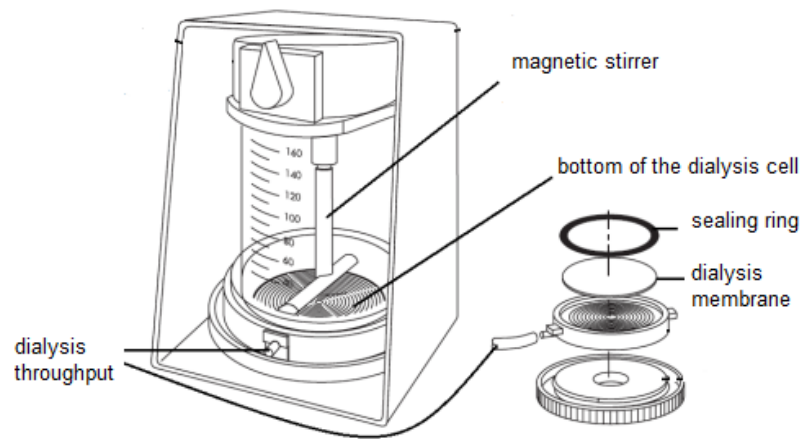


Figure 3.4 Dialysis cell of the gastro-intestinal dialysis model.⁸

References

1. Hage, D; Carr, J. *Analytical chemistry and quantitative analysis*; Pearson Education: New Jersey, 2001.
2. Thermo Fisher Scientific. Finnigan LXQ hardware manual. 2006.
<http://tools.thermofisher.com/content/sfs/manuals/Man-97055-97043-LXQ-HardwareMan9705597043-B-EN.pdf> (accessed, June 2016)
3. Agilent Technologies. Agilent 6300 Ion Trap LC/MS Systems. 2006.
https://www.agilent.com/cs/library/usermanuals/Public/G2440-90096_Concepts_6.1.pdf. (accessed, July 2016.)
4. Waters TQ Detector quick guide to start. 2007.
http://jg.xauat.edu.cn/labs/hjgch/files/pdf/2014/20141216105217_9573.pdf June (accessed, 2016).
5. Thermo Fisher Scientific. Orbitrap LC-MS. How does the orbitrap function in MS?
<https://www.thermofisher.com/be/en/home/industrial/mass-spectrometry/liquid-chromatography-mass-spectrometry-lc-ms/lc-ms-systems/orbitrap-lc-ms.html>. (accessed, June 2016).
6. Williams, D; Flemming, I. *Spectroscopic Methods in Organic Chemistry*; 6th edition; MacGraw-Hill Higher Education: Berkshire, 2008.
7. Council of Europe. 2.2.7 Optical rotation. In: European Pharmacopoeia 8.8 [Online]; Council of Europe: Strasbourg, 2016. <http://online6.edqm.eu/ep807/> (accessed June 15, 2016).
8. Breynaert, A; Bosscher, D; Kahnt, A; Claeys, M; Cos, P; Pieters, L; Hermans, N. *Planta Med.* **2015**, 81, 1075-183.

Chapter 4

DEVELOPMENT AND VALIDATION OF ANALYTICAL METHODS

4.1 Method development

Method development for phytochemical analysis has to deal with some specific challenges in comparison with the quantification of synthetic drugs.

Since herbal products are complex mixtures of constituents, embedded in different matrices, of which the content is influenced by growing conditions, such as climate and soil quality, and by harvesting and storage conditions.¹⁻³ Care has to be taken to completely extract the constituents of interest. Therefore, the extraction method needs to be thoroughly evaluated during method development using a range of solvents and extraction techniques, different solvent volumes, and extraction times.²

In addition, their complex composition makes the separation of active constituents harder than it is for synthetic drugs and phytochemical analysis is often hampered by co-elution and matrix effects. Sample clean-up can be carried out to remove concomitant compounds which cause these problems, but also the use of an optimal chromatographic system can prevent co-elution and matrix effects. Therefore, a broad range of columns, mobile phases, and gradients are tested during method development, especially when there is prior knowledge about a specific herbal product, in order to obtain an optimal separation of the analytes of interest.² Another way to deal with matrix effects is standard addition. When no suitable sample clean-up is available and the chromatographic system cannot be further improved, standard addition is often a solution.

Another challenge is the lack of commercially available reference materials since many herbal constituents are hard to synthesize and isolation of large amounts is time and material consuming.³ Therefore, the choice of the standard used for quantification needs to be well selected during method development. When sufficient amounts of commercially unavailable constituents are isolated in the lab, correction factors can be calculated, otherwise, the content can be expressed as the chosen standard as it described in the European Pharmacopoeia, for example for procyanidins in *Crataegi fructus* samples.

4.2 Method validation

4.2.1 Introduction

After developing a method it is necessary to demonstrate that the method is fit for its intended purpose(s). Therefore, a validation of the method is performed. The guideline of the International Conference on Harmonization of technical requirements for registration of pharmaceuticals for human use (ICH) describes and discusses the validation of analytical procedures.⁴

Depending on the type of analytical procedure, different validation characteristics are required. An overview of the different characteristics is given in Table 4.1.

Table 4.1 Overview of analytical procedures and their validation characteristics.⁴

Type of analytical procedure	Identification	Testing for impurities		Assay
Characteristics		Quantitative / limit		- dissolution - content/potency
Accuracy	-	+	-	+
Precision	-			
Repeatability	-	+	-	+
Intermediate precision	-	+(1)	-	+(1)
Specificity (2)	+	+	+	+
Detection limit	-	-(3)	+	-
Quantification limit	-	+	-	-
Linearity	-	+	-	+
Range	-	+	-	+

- signifies that this characteristic is normally not evaluated

+ signifies that this characteristic is normally evaluated

(1) intermediate precision is not needed in cases where reproducibility has been performed

(2) lack of specificity of one analytical procedure could be compensated by other supporting analytical procedure(s)

(3) may be needed in some cases

Since this work comprises the development of different assays the validation characteristics, which are normally evaluated, will be discussed in depth based on the ICH guidelines and Ermer and Miller.⁵

4.2.2 Validation characteristics

4.2.2.1 Range

The range of an analytical method is defined as the interval between upper and lower concentrations of analyte in the sample for which it has been demonstrated that the analytical procedure has a suitable level of precision, accuracy, and linearity. For the assay of a drug substance or a finished drug product the range normally covers 80% to 120% of the test concentration. Since the content of herbal products is highly variable, a larger range of validation will be needed as described further.

4.2.2.2 Linearity – calibration model

The linearity of an analytical procedure is defined as the ability to obtain results which are directly proportional to the concentration of the analyte.

For the evaluation, at least 5 concentration points, between 40% and 200% of the theoretical concentration should be injected twice. Results are plotted as a function of the concentration and are visually inspected. If there is a visible linear relationship, other tests are performed in order to verify the assumed linear calibration model. A regression line is fitted using the least squares method and the correlation coefficient is calculated. A correlation coefficient higher than 0.99 is desirable. In addition, the residuals, which are the deviations of the actual data points to the regression line are plotted in a residual plot. Residuals should be randomly scattered and the condition of homoscedasticity should be fulfilled (Figure 4.1 A). Otherwise, a trend is present or the data show heteroscedasticity (Figure 4.1 B and C), and a transformation of the data should be performed or another model should be considered. The maximum residual value in relation to the value of the 100% concentration should not be higher than the precision of the analytical technique. For example, 5% is acceptable for HPLC-UV with an automatic injector.

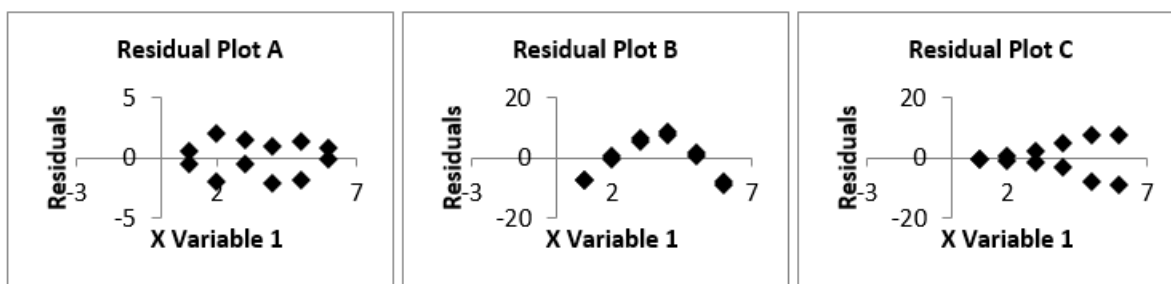


Figure 4.1 Different residual plots: A) residuals are randomly scattered; B) a trend is present; C) residual values increase with increasing concentrations, homoscedasticity condition is not fulfilled.

When these aforementioned requirements are met, the following tests are performed. The 95% confidence interval of the intercept is calculated to evaluate if it includes the point (0,0) meaning that the regression line statistically includes the origin. When this is the case a single calibration point can be used for calculations of each analysis, while if this is not the case, a regression line consisting of three calibration points should be used for calculations. In addition, the significance of the slope of the regression line is evaluated by means of a t-test where the definition of the null hypothesis says that the slope is equal to zero and the alternative hypothesis says that the slope is significantly different from zero. In order to have a linear relationship between concentration and response, the slope should be significantly different from zero and therefore the null hypothesis should be rejected.

4.2.2.3 Precision

The precision of an analytical method expresses the closeness of agreement between a series of measurements obtained from multiple sampling from the same homogeneous sample under the prescribed conditions and can be performed at different levels of precision: repeatability, intermediate precision, and reproducibility, and is expressed as standard deviation, variance, and/or relative standard deviation (RSD). Repeatability is the precision under the same operating condition over a short period of time, for example within one day, whereas intermediate precision expresses the within-laboratories variation meaning that one factor is changed, for example, analysis is performed on different days or by different analysts. In contrast to the intermediate precision, reproducibility expresses the precision between laboratories.

For the evaluation of the repeatability, minimum 9 determinations covering the range of the method or 6 determinations at 100% of the test conditions should be performed.

For the evaluation of the intermediate precision, one factor is varied. For example, the analysis is performed 6 times each day during 3 different days. The factor should be chosen depending on the intended use of the analytical method. For example, when different analysts will have to perform the analysis, the factor “analyst” should be included and tested in the intermediate precision.

For the assays developed in this work no evaluation of the reproducibility was performed.

For all determinations, the mean, standard deviation, variance and relative standard deviation have to be calculated to express the precision. The homogeneity of the variances of the intermediate precision results is evaluated by means of a Cochran or Levene’s test. If these tests confirm that equal variances can be assumed an Analysis of Variance (ANOVA) test is performed which divides the total variation in “within variation” and “between variation” expressed in the ANOVA table as mean squares within (MS_{within}) and means squares between ($MS_{between}$). This test estimates the effect of the factor on the obtained results by comparing the generated critical F-value with the calculated F-value. When the calculated F-value is higher than the critical F-value this means that the factor has a significant effect on the results. Even though an effect is present, the precision of the method can still be acceptable. Therefore, the within relative standard deviation ($RSD_{within}\%$) and the between relative standard deviation ($RSD_{between}\%$) are calculated as follows:

$$RSD_{within}\% = \frac{\sqrt{MS_{within}}}{\langle x \rangle} * 100$$

$$RSD_{between}\% = \frac{\sqrt{\frac{MS_{between} - MS_{within}}{n_j} + MS_{within}}}{\langle x \rangle} * 100$$

The $RSD_{between}$ is compared with the maximal RSD. This maximal RSD can be calculated as 2/3 of the $RSD_{Horwitz}$ or can be fixed at a realistic value based on experience with the analytical technique and sample preparation in the lab. The $RSD_{Horwitz}$ is calculated as follows:

$$RSD_{Horwitz}\% = 2^{(1-0.5\log C)} \text{ with concentration in m/m}$$

and is used to estimate the maximal variation for reproducibility experiments, whereas for intermediate precision experiments the following formula is used:

$$RSD_{max}\% = \frac{2}{3} RSD_{Horwitz}\%$$

If the $RSD_{between}\%$ is smaller than the $RSD_{max}\%$ the method can still be considered precise. Furthermore, results should be plotted and visually inspected. Ideally, the results of the different conditions should show some overlap.

4.2.2.4 Accuracy

The accuracy is defined as the closeness of agreement between the accepted true value and the found value and is also called trueness.

This can be determined by three different methods. One method is the analysis of synthetic mixtures of the drug product components to which a known amount of the analyte is added. This method is only applicable when all components of the drug product and their amounts are known, which is often the case for synthetic drug products. For herbal medicinal products, this method is hardly applicable since the composition of the herbal substances or preparations varies and it is impossible to fully characterize the herbal matrix. In addition, it is not always possible to have access to the herbal substance without the analytes. Therefore, another method is more applicable for herbal products, namely the standard addition method. Known amounts of the analyte are added to the drug product, called spiking, at three different concentration levels within the linear region of the method. The recovery of the analyte is calculated as follows:

$$Recovery\% = \frac{X_{after} - X_{before}}{X_{added}} * 100$$

X_{after} = amount of analyte found in mixture

X_{before} = amount of analyte found in drug product

X_{added} = amount of analyte added to drug product

This method will demonstrate losses during analysis but will not prove that the extraction has been complete. Another method to determine the accuracy of the method is comparison with the results obtained with another well-characterized accepted method with known accuracy.

4.2.2.5 Specificity

The specificity of a method is defined as the ability to unequivocally determine the analyte in the presence of other components present in the sample such as impurities and matrix components. A method needs to be specific in order to accurately determine the content of the analyte in a sample. For the determination of the specificity, analysis of the matrix without the analyte is performed in order to demonstrate that this matrix is not giving a response. Because it is not always possible to obtain blank matrices, specificity can also be evaluated by peak purity testing by comparison of the UV-spectra or the fragmentation pattern at the beginning and the end of the peak for respectively DAD and mass spectrometric detection.

4.2.2.6 Robustness

The robustness of a method is defined as the capacity to remain unaffected by small but deliberate variations in method parameters and provides an indication of its reliability during normal usage. The robustness needs to be considered during method development, during which variations such as extraction time, pH of mobile phases, mobile phases, columns, temperatures and flow rate and the stability of analytical solutions should be tested.

References

1. Vlietinck, A; Pieters, L; Apers, S. Legal requirements for the quality of herbal substances and herbal preparations for the manufacturing of herbal medicinal products in the European union. *Planta Med.* **2009**, 75 (7), 683-688.
2. Ong, ES. Extraction methods and chemical standardization of botanicals and herbal preparations. *J. Chromatogr. B, Anal. Technol Biomedical Life Sci.* **2004**, 812 (1-2), 23-33.
3. Betz, JM; Brown, PN; Roman, MC. Accuracy, precision, and reliability of chemical measurements in natural products research. *Fitoterapia* **2011**; 82 (1), 44-52.
4. International Conference on Harmonization. Validation of analytical procedures: text and methodology Q2 (R1). 2005.
5. Ermer, J; Miller, J. *Method validation in pharmaceutical analysis. A guide to best practice.* Weinheim: Wiley-VCH Verlag; 2005.

Chapter 5

DESMODIUM ADSCENDENS

5.1 General introduction

5.1.1 Botanical description and use

Desmodium adscendens (Sw.) DC. is a small herb belonging to the Fabaceae family. The stems are erect, slender angular and have spreading hairs. The elliptic, obovate leaves are 3-foliolate with two lateral leaves and one bigger terminal leaf. The upper surface is green and smooth and the lower surface is gray and hairy (Figure 5.1). The inflorescences are racemes and pods are broad and glabrescent.¹⁻²



Figure 5.1 Leaves and flowers of *Desmodium adscendens*.³

Desmodium adscendens occurs in Africa and South America and is used in traditional medicine for many years for the treatment of pain, fever, asthma, seizures, hepatitis, muscle spasms, ovary inflammation, and snake bites. For this purpose, a decoction or infusion is prepared from the leaves and/or stems of the plant.^{1,4,5}

5.1.2 Pharmacological activity

5.1.2.1 Antiasthmatic and anti-inflammatory activity

In 1977 the "Magazine of the WHO" reported a double-blind clinical trial, in which 12 randomly selected patients were treated against bronchial asthma with placebo herbs for three months, and then for a second period of three months with combinations of *D. adscendens*, *Deinbollia pinnata*, and *Thonningia sanguinea*. All patients continued to have asthmatic attacks during placebo treatment, but eight of them had no attacks during the herbal therapy. Some of the remaining four had decreased attacks, but the response of the combined herbs was judged less than satisfactory.⁶

Only very few pharmacological studies about *D. adscendens* were performed. Addy et al.⁷ carried out the first studies in Ghana. They investigated the effect of *D. adscendens* on anaphylaxis in the guinea-pig and demonstrated that aqueous and ethanolic extracts from *D. adscendens* reduced smooth muscle contraction, both anaphylactic as well as histamine-induced contractions, and decreased the release of substances which activate smooth muscle cells in the lungs.⁷ Further research was performed on this topic in several follow-up studies. A hot water extract of *D. adscendens* inhibited histamine-induced ileal contractions in a competitive way and reduced the anaphylactically released spasmogens and the anaphylactic-induced contractions of ileal muscles.⁸ Three different fractions of the aqueous extract were evaluated for their effect on ovalbumin and arachidonic acid-induced contraction in the guinea-pig airways. The results suggested that *D. adscendens* contained several constituents with the ability to inhibit the allergic smooth muscle contraction in the lungs.⁹ A subsequent bio-guided fractionation was performed based on the inhibition of electrically induced contraction of ileal pieces. Preliminary characterization of the active components of one of the fractions suggested the presence of triterpenoid saponins.¹⁰ This fraction was evaluated for its pharmacological activity, using contractions of tracheal spirals and lung parenchymal strips caused by ovalbumin, arachidonic acid, histamine, and carbachol. The results suggested that this fraction might inhibit the release of arachidonic acid.¹¹ In a subsequent study, the effect of a *D. adscendens* extract, an *n*-butanol fraction of the extract and hordenine, tyramine and saponins, known to be present in the plant, on the cytochrome P450-dependent arachidonic acid metabolism was evaluated using cortical microsomes of human kidneys. Saponins, a sapogenin, and the abovementioned phenolic compounds, hordenine and tyramine, did not inhibit the oxygenation of arachidonic acid.¹² Further research was done on this topic. Therefore, the effect of three groups of compounds known to be present in *D. adscendens* was investigated on plasma membrane ion channels, cytochrome P450 NADPH-dependent oxygenation of arachidonic acid, and the production of prostaglandins by cyclooxygenase. The very high-conductance calcium-activated potassium ion channel, which is responsible for the tone in smooth muscles, was activated by saponins. The cytochrome P450 NADPH-dependent monooxygenase reaction which is responsible for the formation of epoxy- and hydroxy eicosanoids was inhibited by a tetrahydroquinoline analog present in the plant. This analog together with the β -phenylethylamines present in the plant increased the cyclooxygenase activity resulting in an increased formation of prostaglandins.¹³ The effect of these compounds present in *D.*

adscendens could contribute to its reported anti-asthmatic property. McManus et al.¹⁴ isolated soyasaponins I, II, and III and dehydrosoyasaponin from *D. adscendens*. The latter compound was found to act as a high-affinity activator of calcium-dependent potassium channels.¹⁴ Irié-N'guessan et al.¹⁵ confirmed that *D. adscendens* induced a relaxant effect on mice-isolated trachea. In addition, the traditional use of *D. adscendens* in the treatment of ovary inflammation was evaluated. The results suggested that a blockade of voltage-sensitive calcium channels contributes to this property.¹⁶

5.1.2.2 Hepatoprotective effects

In 1989, patent EP0309342 "Use of *Desmodium* in the treatment of hepatitis, and medicaments thereof" was published.¹⁷ It concerned *Desmodium*, especially *D. adscendens*, which permitted a rapid cure of viral hepatitis (A or B) or of viral hepatitis (non-A, non-B). The effect of *D. adscendens* was monitored both clinically, by the disappearance of icterus, of the digestive and general symptomatology, over at most 2 weeks, if the treatment had been timely, and biologically by the normalization of the transaminases. In addition, *D. adscendens* was also used for the treatment of hepatitis induced by chemical products, whether involving drug addiction or secondary effects of chemotherapy. The daily posology ranged from 5 to 10 g of dried whole plant, employed either as a decoction or gelatin capsules of dried plant powder. Results were obtained for 34 cases of viral hepatitis (A, B, or non-A, non-B). In 11 cases where treatment had started before the third day of icterus, the color of the teguments and of urine was normalized after 5 days of treatment, and the level of serum transaminases had significantly decreased. In these 11 cases, a complete normalization was achieved within 20 days. In 14 cases where treatment had started between the third and the twentieth day after icterus had appeared, the level of the transaminases was lowered to 1/3 of the initial value before the tenth day of treatment. For the 9 remaining cases, clinical and biological parameters were still perturbed after the twentieth day of icterus. In various cases of toxic hepatitis due to chemical agents, such as anticancer drugs, transaminases were normalized within 10 days of treatment.

5.1.2.3 Other properties

Another study added an aqueous extract of *D. adscendens* to the medium of an *in vitro* evaluation of insulin release by pancreatic beta-islet cells by another plant (*Ocimum canum*). This addition did not

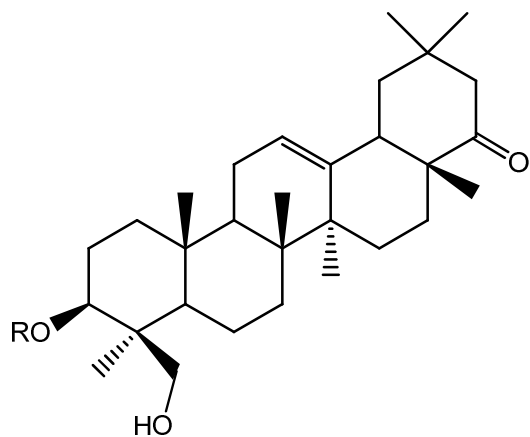
increase but rather inhibited the insulin secretion.¹⁷ An effect on the central nervous system was found for an ethanolic extract of the leaves of *D. adscendens*. Moreover, the extract induced hypothermia and showed an analgesic and anti-epileptic effect in mice.⁵ Both Muanda et al.¹⁹ and Zielinska-Pisklak et al.²⁰ demonstrated the antioxidative activity of *D. adscendens* and the protective effect against oxidative stress in kidney cells was proven by François et al.²¹ These results were in contrast with the findings of Gyamfi et al.²² who did not find a DPPH radical scavenging effect for *D. adscendens*.

5.1.3 Toxicity studies

N'guemou et al.⁵ investigated the acute toxicity of *D. adscendens* after intraperitoneal administration in mice. At doses up to 100 mg/kg, no neurological deficit was observed. At a dose of 300 mg/kg, 25% of the mice showed abdominal contractions 20-25 min after injection, but these effects were reversed within 60 min and might be due to the administration route.

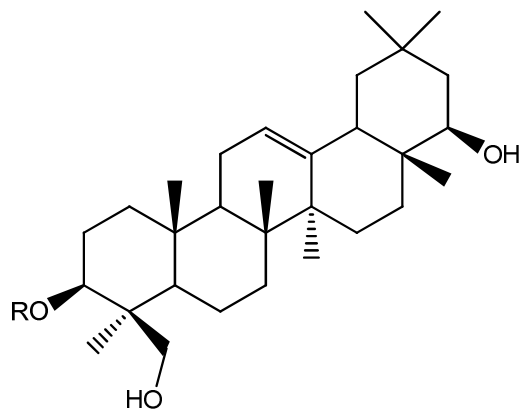
5.1.4 Phytochemical investigations

Phytochemical investigations resulted in the isolation and identification of triterpenoid saponins as soyasaponin I, soyasaponin III, dehydrosoyasaponin I, sapogenol B and sapogenol E, a tetrahydroquinolone named salsoline, phenylethylamines such as hordenine, tyramine and dimethoxyphenylethylamine, indole-3-alkyl amines such as dimethyltryptamine, and flavonoids such as vitexin, isovitexin, and rutin.^{1,4,13,20,23} Muanda et al.¹⁹ reported the presence of gallic acid, protocatechuic acid, rutin, quercetrin-3-*O*-glucoside, quercetrin dihydrate and cinnamic acid after comparison with standard compounds by HPLC. Since the HPLC separation was rather poor, these latter findings are doubtful. Biaocchi et al.²³ reported the presence of 22 flavonoid C-glycosides and 13 flavonoid O-glycosides by high-resolution mass spectrometry. All these glycosides were apigenin, diosmetin or kaempferol derivatives. In previous investigations carried out by our research group, D-pinitol was isolated as the major component of the decoction of *Desmodium adscendens*.²⁴ An overview of the most important constituents of *D. adscendens* is given in Figure 5.2.



soyasapogenol E R = H

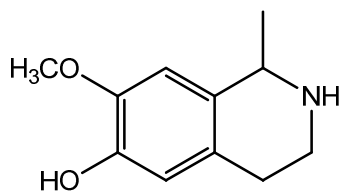
dehydrosoyasaponin I R = Glc-Rha-GlcA



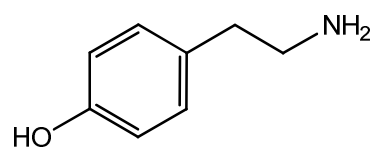
soyasapogenol B R = H

soyasaponin I R = Glc-Rha-GlcA

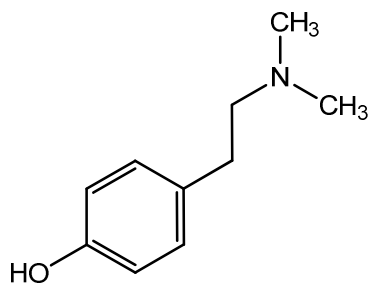
soyasaponin III R = Rha-GlcA



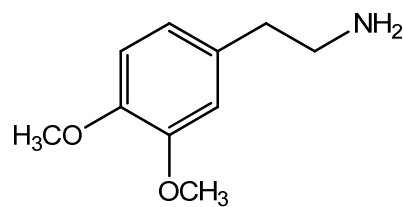
salsoline



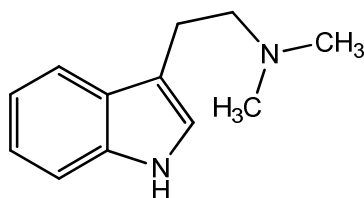
tyramine



hordenine

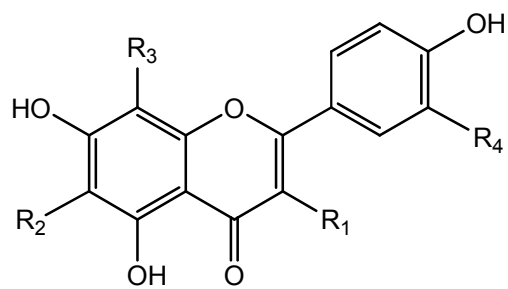


dimethoxyphenylethylamine

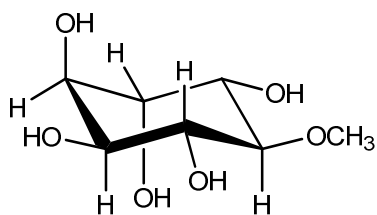


dimethyltryptamine

Figure 5.2 Overview of constituents isolated from *D. adscendens*.



	R1	R2	R3	R4
Apigenin	H	H	H	H
Diosmetin	H	H	H	OCH ₃
Kaempferol	OH	H	H	H
Rutin	Glc-Rha	H	H	OH
Vitexin	H	H	Glc	H
Isovitexin	H	Glc	H	H



D-pinitol

Figure 5.2 continued Overview of constituents isolated from *D. adscendens*.

5.2 Development and validation of a gas chromatographic method for the quantification of D-pinitol in decoctions of *Desmodium adscendens**

5.2.1 Introduction

5.2.1.1 D-Pinitol

D-Pinitol is a sugar alcohol with a low molecular weight, i.e. the 3-*O*-methyl derivative of D-chiro-inositol.^{25,26} It has hypoglycemic and antiatherogenic activity *in vitro* and an influence on the immune system was also observed.²⁷⁻³² *In vivo* antihyperglycemic, hepatoprotective and anti-inflammatory effects have been reported.^{25,26,33-39} A patent has been awarded for the "use of pinitol or *chiro*-inositol for protecting the liver".⁴⁰ In asthmatic conditions hyperreactivity and inflammation were reduced through an influence on the immune system.³⁰ Since D-pinitol had been characterized in our research group as the major component of a *D. adscendens* decoction, it was decided to develop and validate an analytical method (chapter 4) for this constituent, with the aim of preparing a quantified extract of *D. adscendens* with a known level of D-pinitol. This extract could then be used for *in vivo* experiments to assess its hepatoprotective properties. In addition, there is a growing need for quality control of food supplements, including those containing D-pinitol, and a validated method is required for their evaluation.

5.2.1.2 Herbal medicinal products and food supplements containing *Desmodium adscendens*

An evaluation of HMPs or food supplements, containing *Desmodium adscendens*, on the market in Belgium, was performed. Therefore, the information of the Belgian Center for Pharmacotherapeutic Information, which gives an overview of all registered drugs and Pharmacopendium Plus, which contains all food supplements currently on the market, was consulted.^{41,42} This search indicated that there are 3 food supplements but no herbal medicinal products containing *D. adscendens*. Two supplements were mono-preparations and one was a combination preparation, which also contained *Cynara scolymus* L. and *Curcuma longa* L. and was part of a detox box. The food supplements used in this research and described under 5.2.2.1 were obtained from France via an industrial partner.

*Published: van Dooren, I.; Hermans, N.; Dhooghe, L.; Naessens, T.; Vermeylen, R.; Claeys, M.; Vlietinck, A.; Pieters, L.; Apers, S. Development and validation of a gaschromatographic method for the quantification of D-pinitol in decoctions of *Desmodium adscendens*. *Phytochem. Lett.* **2014**, *7*, 19-25.

5.2.1.3 Analytical methods for the quantification of D-pinitol

Although many GC methods for pinitol quantification are developed and applied in different domains⁴³⁻⁴⁷, only one was validated.⁴⁸ This method published by Lein et al.⁴⁸ was used to quantify carbohydrates, including the sugar alcohol D-pinitol and simmondsins in jojoba seed meal. However, it was necessary to develop and validate a new method for quantification of D-pinitol in *D. adscendens* for several reasons: First of all, the difference in type and composition of the matrix, i.e. aerial parts for *Desmodium* instead of seed meal for jojoba, which has a major impact on the extraction and chromatographic conditions. Secondly, the incompleteness of this research work with respect to possible extraction techniques. Next to ultrasonication and maceration (rotary mixing) for a fixed time, we included reflux extraction and ultrasonication with additional heating. In addition, other parameters influencing the extraction such as time and solvent volume were not evaluated. Furthermore, the authors did not specify which Tri-Sil reagent was used for silylation. Finally, our validation procedure is more thorough, especially with respect to the precision on different concentration levels. In this way, the completeness of extraction was proven which is important in assessing accurately the content of active metabolites in plant materials.

5.2.2 Materials and methods

5.2.2.1 Plant material, decoction, and food supplements

Leaves and twigs from *Desmodium adscendens* (Sw.) DC. were collected in February 2009 (Batch A from which two decoctions (A1 and A2) were made at different time points) and June 2010 (Batch B) in the central region of Ghana. The plant was identified by D.K. Donkor. Voucher specimens are kept at Biosources International, Inc. (Ghana) (no. BRI 03910), and at the University of Ghana (no. GC 03910). The aqueous decoction of *Desmodium adscendens* was prepared from 1 kg powdered leaves and twigs, in portions of 200 g, each portion was boiled for 1 h in 3 L of distilled water. The decoction was cooled down, portions were combined, filtered, and lyophilized. Typically, 1 kg of plant material yielded about 65 g lyophilizate.

Five food supplements were analyzed for their D-pinitol content. One food supplement was a drinkable solution from *D. adscendens*. 20 mL of this solution should correspond with 10 g of dry plant material or 40 g of fresh plant material. The other food supplements were capsules. According

to their label, two of these supplements contained 200 mg of *D. adscendens*, while the others listed *D. adscendens* in an amount of 450 mg and 2.5 g, respectively.

In addition, the amount of D-pinitol was quantified in twigs (batch B), leaves (batch B and an additional batch delivered from Ghana) and roots (origin Ghana) separately and in decoctions (Batch B) prepared with 2 L and 1 L of water instead of 3 L.

5.2.2.2 General experimental procedures

The systems used for the experiments were a Trace GC Ultra with flame ionization detection and a Trace 2000 GC with a Voyager quadrupole mass spectrometer equipped with an electron ionization source.

Different columns were used: column 1: HP-5 (30 m x 0.32 mm, 0.25 µm) (5% phenyl, 95% methylpolysiloxane) (wall coated open tubular column (WCOT)); ATTM-5MS/Rtx[®]-5MS (30 m x 0.25 mm, 0.25 µm) (5% phenyl, 95% polysilphenylene-siloxane); and column 2: ATTM-264, (30 m x 0.32 mm, 1.8 µm) (6% cyanopropylphenyl, 94% methyl siloxane) (WCOT). Reaction vials (Reacti-VialTM) and a heating block were obtained from Pierce. The device used for ultrasonication was an ultrasonic cleaner Branson MHT 3510. The reflux extraction was done in a round bottom flask, which was heated by a heating mantle and attached to a condenser and cooling system.

5.2.2.3 Method development

Internal standard

Different commercially available sugar alcohols were evaluated in the search for a suitable internal standard, including sorbitol, mannitol, dulcitol, xylitol, and inositol.

Derivatization: acetylation

For the acetylation derivatization, a mixture of acetic acid anhydride and pyridine (2:1, v/v) was used. 600 µL of this reagent was added to D-pinitol (0.85 mg) and sorbitol (1 mg) and the mixture was put in an oven at 60 °C for half an hour or was kept overnight at room temperature. After derivatization, the samples were dried under a nitrogen flow and redissolved in 500 µL ethyl acetate.⁴⁶ These samples were analyzed on the ATTM-264 column (column 2).⁵⁰

Chromatographic system: the starting temperature was 200 °C and then the temperature was increased with 5 °C/min to 220 °C, which was held for 20 min.⁴⁹

Trimethylsilylation

For the trimethylsilylation reaction, a mixture of BSTFA + TMCS 1% and pyridine (2.5:1, v/v) was used. First, 100 µL of D-pinitol (0.2 – 1 mg/mL, in methanol) and sorbitol (0.5 – 1 mg/mL, in methanol) was evaporated under a nitrogen flow. 140 µL of the derivatization reagent was added and the mixture was placed in an oven for three hours at 70 °C. After evaporating the derivatization reagent, the standards were redissolved in 300 µL hexane and analyzed (injected in triplicate). To choose a good internal standard, also xylitol, mannitol, inositol and dulcitol (0.2 – 0.4 mg/mL) were tested in this way.

After the internal standard was chosen (see 5.2.3.2), the experiment was repeated. 500 µL of methanolic solutions of 31.3 µg/mL – 87.5 µg/mL D-pinitol and 40 µg/mL xylitol were evaporated under a nitrogen flow. To each vial, 100 µL derivatization reagent was added and the vials were put in an oven (70 °C) for 3 h, 6 h, or one night. After derivatization, the samples were dried under a nitrogen flow, redissolved in 300 µL hexane, and analyzed (injected in duplicate).

The experiment was also performed using reaction vials and a heating block. 50 µL of a solution of 31.3 µg/mL – 87.5 µg/mL D-pinitol and 40 µg/mL xylitol was pipetted into reaction vials and dried under a nitrogen flow. 50 µL derivatization reagent was added and the vials were heated for 1 h in a heating block (70 °C). The experiment was repeated using a higher concentration of xylitol and without adding hexane at the end of the derivatization. The samples were analyzed in duplicate on an HP-5 column (column 1). The chromatographic system used by Medeiros and Simoneit⁵¹ was used: the starting temperature was 65 °C and was held for two min. Then, the temperature was increased with 6 °C/min to 300 °C. This temperature was held for 15 min.

Extraction

Sonication, in presence and absence of heat, and reflux extraction were evaluated on 100 mg of the lyophilized decoction. For the sonication experiment, different volumes were used (10, 20, 50, and 100 mL of methanol) and the process (30 min) was repeated (1 time – 4 times). Also, the influence of the time of sonication was tested and the sonication was carried out for 30 min (as for all the

previous experiments) and for 1 h with 50 mL and 100 mL. Sonication in presence of heat and reflux extraction were performed with a volume of 50 mL. The procedure was also repeated (1-4 times). One of the samples was refluxed for 1 h instead of 0.5 h, to check the influence of time.

5.2.2.4 Final method

A D-pinitol standard solution and an internal standard solution were prepared as follows: about 10.5 mg xylitol was accurately weighed in a 100.0 mL flask and dissolved in methanol. 25.0 mL of this solution was pipetted in a flask and diluted to 250.0 mL.

The sample was prepared by weighing about 100.0 mg of the decoction accurately in a round bottom flask. 50.0 mL of the internal standard stock solution was added and the mixture was heated under reflux for 0.5 h. After cooling down, the mixture was centrifuged for 5 min at 1760 *g* (3000 rpm). From the supernatant, 150 μ L was transferred to a reaction vial and was dried under a nitrogen current. 50 μ L of derivatization reagent was added and the mixture was vortexed and derivatized in a heating block at 70 °C for 1 h. After cooling the vials, the mixture was transferred to a GC vial with an insert and was analyzed by GC-FID using the HP-5 column (column 1). The temperature gradient was as follows: 2 min at 65 °C, from 65 °C to 300 °C at 6 °C/min, and at 300 °C for 15 min. Injector and detector temperatures were 280 °C and 285 °C. The split ratio was 30 and the split flow 39 mL/min. The flow of the carrier gas (helium) was 1.3 mL/min. The injection volume was 1 μ L.

5.2.2.5 Method validation

The method was validated according to the ICH guidelines (Chapter 4). The calibration model, range, linearity, precision, accuracy and specificity were investigated.

For the investigation of the calibration model, five standard solutions, starting from one stock solution of D-pinitol and one stock solution of xylitol, were prepared. The concentration was between 40 and 200% of the true amount of D-pinitol in the samples, i.e. 5.4 μ g/mL and 27 μ g/mL. All solutions were injected twice.

For the repeatability of the injection, one sample was analyzed 6 times. For the precision six independent samples (about 100 mg freeze-dried decoct) were analyzed. For the intermediate precision, six samples were analyzed on three different days. The intermediate precision was also

tested on different concentration levels. Six samples with half the amount (50 mg) and double the amount (200 mg) were analyzed.

The accuracy was investigated by means of the standard addition method. To 50% of the freeze-dried decoct, a standard solution of D-pinitol was added until the amount of D-pinitol was 100%, 150%, and 175%. Every concentration level was prepared in triplicate. About 50 mg freeze-dried powder was weighed in a round-bottom flask, and 5, 10 and 12.5 mL of a stock solution of D-pinitol (67.5 µg/mL) was added.

The specificity of the method was investigated with GC with mass spectrometric detection. Also, samples with and without internal standard were compared.

5.2.3 Results and discussion

5.2.3.1 Analytical technique

Different techniques are used to analyze sugars and sugar alcohols. HPLC with refractive index detection has been widely used for many years in sugar analysis, although this technique has several drawbacks, for example, baseline instability with changing temperature or mobile phase composition.⁵² An ELSD detector has been used to determine *D-chiro*-inositol in buckwheat.⁵³ HPLC-ELSD was also evaluated for the determination of D-pinitol in *D. adscendens*, but it gave no satisfactory results. Peaks were broad and the baseline was not stable. Other methods to determine sugars and sugar alcohols are HPLC with UV, fluorescence, or electrochemical detection. The first two detection systems require derivatization of the sugar and sugar alcohol molecules.⁵² This is also the case for analysis using GC since sugars and sugar alcohols are not volatile. The derivatization of sugars and sugar alcohols for GC analysis is well described by Bauer et al.⁵⁴ and by Medeiros and Simoneit.⁵¹ Furthermore, since GC with FID detection is more common than HPLC with electrochemical detection, we chose to develop a GC-FID method for the determination and quantification of D-pinitol.

5.2.3.2 Method development

Internal standard

Five sugar alcohols were considered as internal standards, i.e., inositol, dulcitol, mannitol, sorbitol, and xylitol. Of these, dulcitol and xylitol have been used in previous work as internal recovery

standards for the determination of the fungal spore markers, mannitol and arabitol, respectively, in atmospheric aerosols.⁵⁴ In the present study, the internal standard was added after the preparation of the extract; hence, its use only compensates for losses of the analyte in the following sample work-up steps such as derivatization. Two of the five selected sugar alcohols, i.e. inositol and dulcitol, are soluble in water, but almost insoluble in methanol. Because water and also traces of water can cause degradation of trimethylsilyl derivatives, these sugar alcohols were not chosen as internal standard. Mannitol, sorbitol and xylitol are soluble in methanol; of these, xylitol was chosen as internal standard because the structure is more similar to that of D-pinitol (same number of hydroxyl groups) and because mannitol and sorbitol co-eluted with other components present in the decoct.

Derivatization: acetylation

When acetylation was used for derivatization, a large variation in retention time and peak area between injections and between samples was observed. Possible reasons are that these derivatives are not sufficiently volatile, and/or that the acetylation was not complete.

Trimethylsilylation

When trimethylsilylation was used to derivatize the samples, no shifts in retention time were observed and the preliminary experiments showed that a linear model could be applied. There was a big intervariability, though, between the peak area of two standard solutions of the same concentration, after three or six hours, or after derivatization overnight. The optimal derivatization time could not be determined. The vials were also not suitable for trimethylsilylation because they appeared not to be air tight and some of the reagent was lost.

Because of these problems we changed to reaction vials that could be heated in a heating block. This protocol resulted in repeatable and linear data.

Extraction

In the evaluation of sonication as extraction technique, we found that the extraction was not completed, even after 4 times using 10.0 mL of solvent. When sonicated twice in twice as much solvent (20.0 mL), there was also more D-pinitol extracted. Hence, as expected, the volume is an

influencing factor. Consequently, also 50.0 mL and 100.0 mL were used to dissolve the samples. There was no difference between the results of both volumes but the amount D-pinitol extracted increased with doubling the sonication time (1 h). However, the amount of D-pinitol was still lower than after four times sonicating in 10.0 mL. Because the time seemed to be an important factor, this was further investigated. During sonicating for a longer time, the mixture warms up, hence, an ultrasonic bath with heating was used. After sonicating twice in the heated ultrasonic bath, the amount of D-pinitol did not increase any more. Besides the heated ultrasonic bath, reflux with heating was also evaluated. After a one time reflux with heating, the maximum amount of D-pinitol was extracted. The amount of D-pinitol extracted with reflux was a little bit higher than for all the other sonication procedures.

From this, it is clear that optimization of the extraction procedure, taking into account variables as time, temperature and solvent composition, was necessary for developing a reliable quantitative method. Lein et al.⁴⁸ only compared solvent composition and no other influencing parameters. Because they also quantify D-pinitol, in addition to sugars and simmondsins, there is an existing chance that D-pinitol is not fully extracted from the jojoba seed meal and that as a consequence, the amount of D-pinitol is underestimated.

A chromatogram of the standards and a sample prepared according to the final optimized method are shown in Figures 5.3 and 5.4.

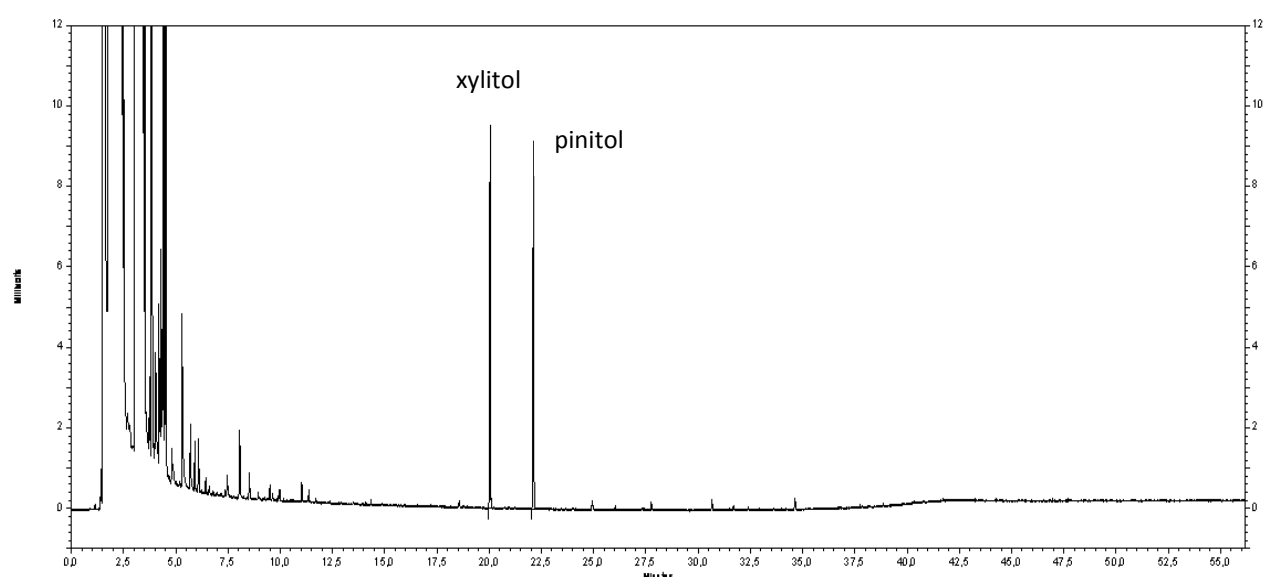


Figure 5.3 Chromatogram of a standard solution containing both D-pinitol and the internal standard xylitol.

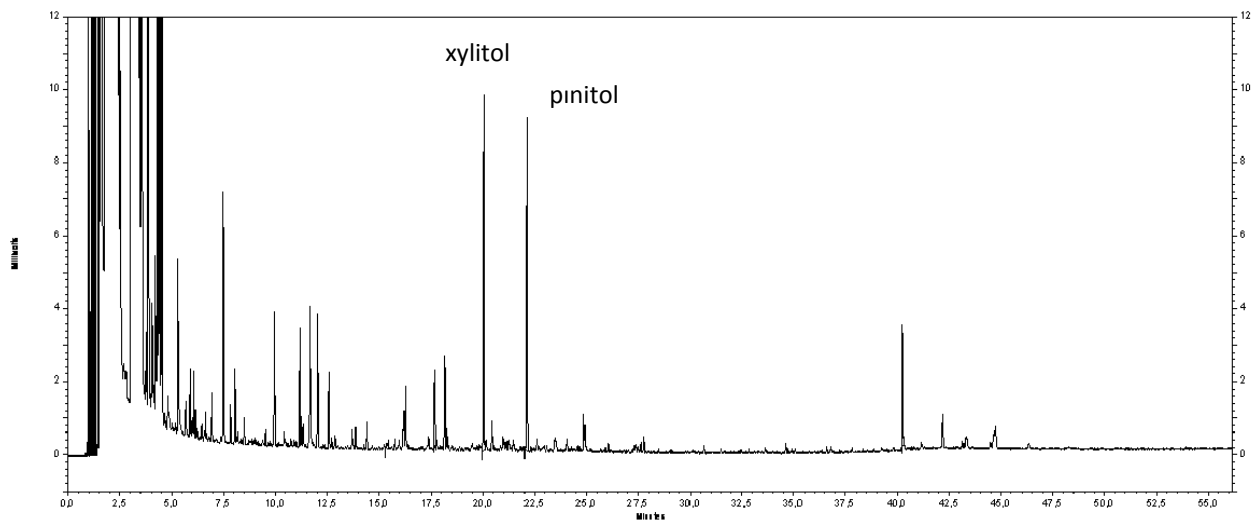


Figure 5.4 Chromatogram of a decoction of *D. adscendens*.

5.2.3.3 Method validation

Calibration model

The linear response of D-pinitol was investigated. The regression line was constructed and the equation was generated. The correlation coefficient was also calculated. The slope and intercept were investigated with a Student t-test. The residuals were graphically evaluated. In addition, an ANOVA lack of fit (LOF) test was performed.

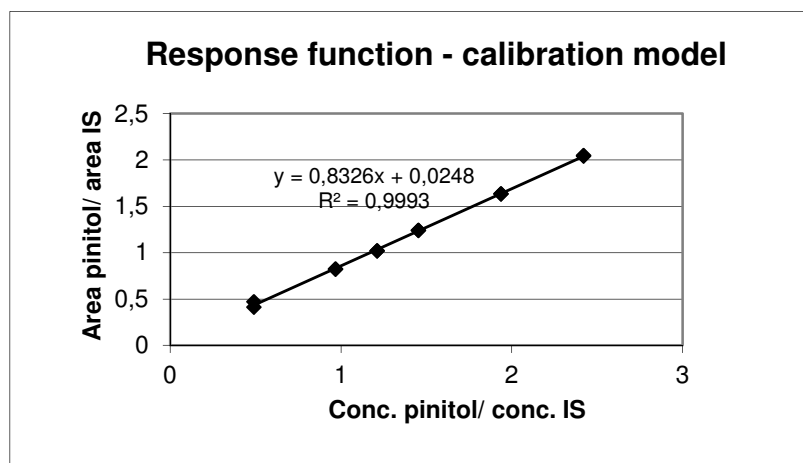


Figure 5.5 Response curve of D-pinitol.

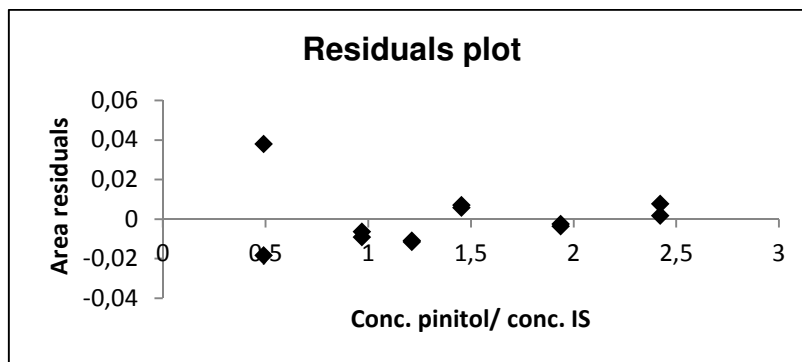


Figure 5.6 Residuals plot.

A visual inspection of the regression line (Figure 5.5) and residuals plot (Figure 5.6) showed that the method was linear and homoscedastic. The correlation coefficient was higher than 0.99. The slope of the regression line was significant and the intercept of the line did not include the point (0,0) (Table 5.1). The F-value was smaller than the critical value for the ANOVA/LOF test. Based on those results it could be concluded that a linear calibration model could be applied for the quantification of D-pinitol. Since point (0,0) was not included, a calibration curve of at least 3 concentration levels needed to be used.

Table 5.1 Linearity data of D-pinitol.

Correlation coefficient	0.9997
Slope	0.8326
Intercept	0.0248
95% CI intercept	[0.7709.10 ³ ;48.86.10 ³]
F_{critical} ANOVA Lack of fit	4.284
F_{calculated} ANOVA Lack of fit	0.7

Precision

The mean, the standard deviation and the RSD% were calculated for each day and each concentration level, while Lein et al.⁴⁸ only evaluated precision on different days. The overall mean, standard deviation and RSD% were calculated for the three days and also for the three different concentration levels. The repeatability and intermediate precision were evaluated by an ANOVA single factor. For the repeatability, the within mean squares were used to calculate the standard deviation and RSD%. For the intermediate precision, the standard deviation was calculated using the following formula:

$$s = \sqrt{\frac{MS_{between} - MS_{within}}{n_j} + MS_{within}}$$

Before performing the ANOVA single factor, a Cochran test was done. The results are shown in Table 5.2.

In case of the different days, the calculated Cochran value was smaller than the critical C-value, implying that the variances are not significantly different and an ANOVA single factor could be carried out.

The calculated F-value is higher than the theoretical F-value, meaning that the results between the days are significantly different. Although the ANOVA single factor shows a significant difference, the $RSD_{between}$ is still smaller than the calculated maximum RSD%, based on $RSD_{Horwitz}$, indicating that the method is still precise.

Table 5.2 Precision on different days.

	Day 1	Day 2	Day 3
Mean	0.6275%	0.6271%	0.6378%
Standard deviation	0.0052%	0.0026%	0.0051%
RSD%	0.83%	0.41%	0.80%
Critical Cochran value		0.7070	
Calculated Cochran value		0.4530	
S_{within}		0.0044%	
RSD_{within}		0.71%	
S_{between}		0.0073%	
RSD_{between}		1.16%	
RSD_{Horwitz}		4.29%	
RSD_{max} (= 2/3 Horwitz)		2.86%	

In case of the different concentration levels, the calculated C-value was smaller than the critical C-value and an ANOVA single factor could also be applied to the results.

Also for the different concentration levels, the calculated F-value was higher than the critical F-value. Since the $RSD_{between}$ is smaller than the calculated maximum RSD% and RSD between concentrations is in the same order as RSD between days, it could be concluded that the method is precise (Table 5.3).

Table 5.3 Precision on different concentration levels (n=6).

	50 mg	100 mg (day 1)	100 mg (day 2)	100 mg (day 3)	200 mg
Mean	0.6397%	0.6275%	0.6271%	0.6376%	0.6374%
Standard deviation	0.0063%	0.0052%	0.0026%	0.0051%	0.005%
RSD%	0.98%	0.83%	0.41%	0.80%	0.79%
Critical Cochran value	0.5060				
Calculated Cochran value	0.3162				
S _{within}	0.0050%				
RSD _{within}	0.78%				
S _{between}	0.0080%				
RSD _{between}	1.27%				
RSD _{Horwitz}	4.28%				
RSD _{max (= 2/3 Horwitz)}	2.86%				

The graphical representation of the results (Figure 5.7) reveals that no trend could be observed between the results obtained at different concentration levels, proving the completeness of extraction. The overall mean D-pinitol content was 0.634%.

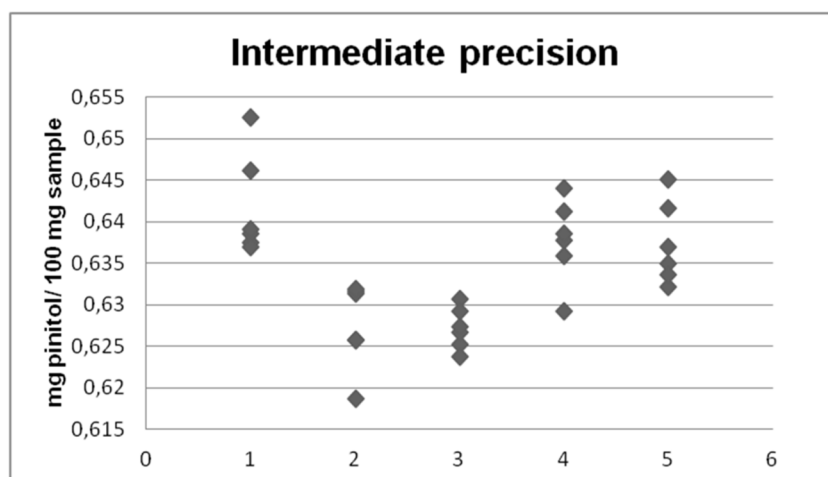


Figure 5.7 Results from intermediate precision: 1 = concentration level 50%; 2 = concentration level 100%, day 1; 3 = concentration level 100%, day 2; 4 = concentration level 100%, day 3; 5 = concentration level 200%.

Accuracy

The recovery was calculated for each sample. Also, the mean, the RSD%, and the confidence interval were calculated. The results are shown in Table 5.4.

The mean recovery was 104.61% and the standard deviation 1.594%. Based on the confidence interval which ranges from 103.38% to 105.84%, it is clear that the recovery is significantly different from 100% and exceeds the acceptance limits [97 – 103 %] (Table 5.4). In this case, the recovery should be explicitly mentioned with every result obtained with the method, so that the true amount of D-pinitol can be calculated. The recovery experiment was carried out with a repeatability in compliance with the precision of the method and no level of dependency could be observed. It could be concluded that all D-pinitol was recovered.

Table 5.4 Recovery results

	Added amount pinitol (%)	Recovery (%)
1a	50	101.61
1b	50	103.65
1c	50	103.77
2a	100	103.95
2b	100	105.69
2c	100	107.18
3a	125	104.73
3b	125	105.26
3c	125	105.64
Mean	104.61	
S	1.594	
RSD%	1.524	
CI	[103.38 – 105.84]	

Specificity

Based on the chromatograms without (Figure 5.8) and with (Figure 5.9) internal standard and the mass spectrometric data (not shown), one can conclude that the method is specific.

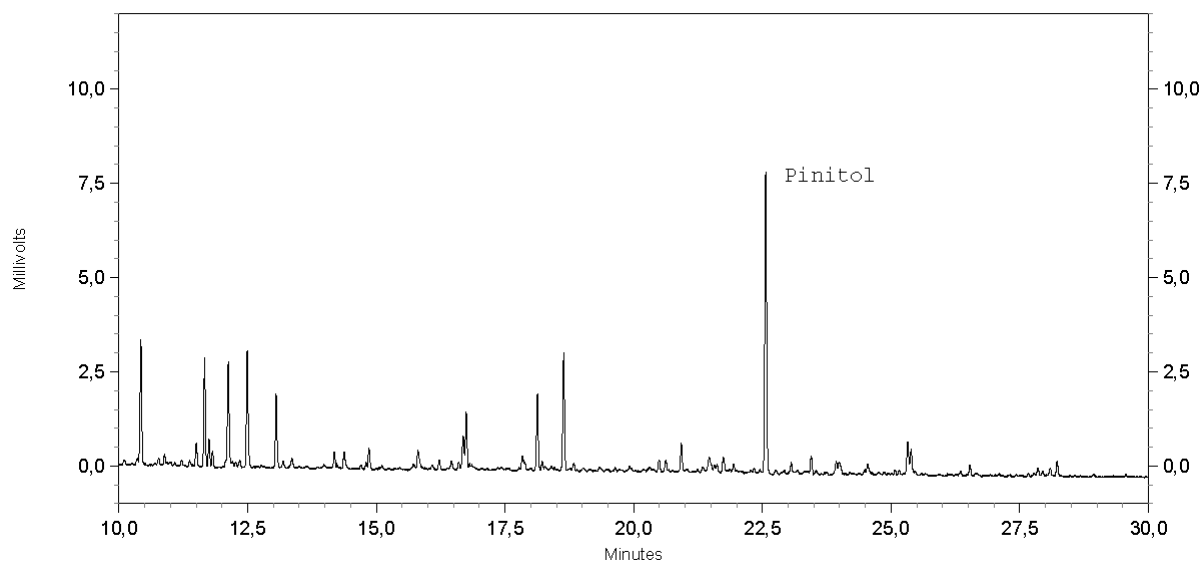


Figure 5.8 Chromatogram of a decoction of *D. adscendens* without internal standard.

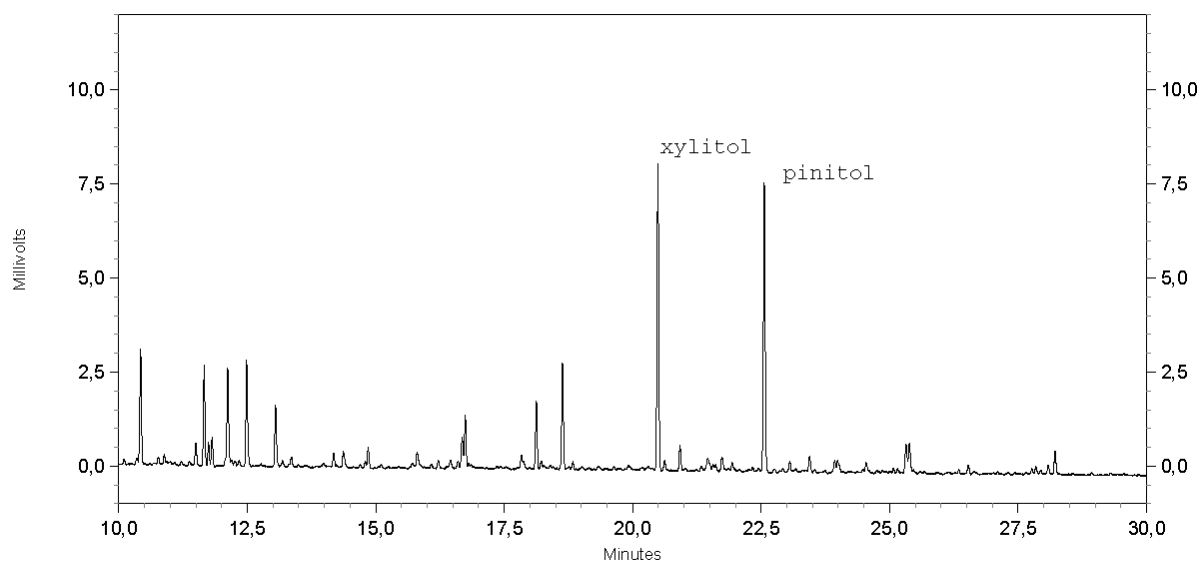


Figure 5.9 Chromatogram of a decoction of *D. adscendens* with internal standard (xylitol).

5.2.3.4 Food supplements and decoctions

The method was used as such to screen some different food supplements and different plant parts or decoctions, as described above, for their amount of D-pinitol.

The results of the analysis are shown in Table 5.5. In the drinkable solution, 2.12 mg/mL D-pinitol was found. The second and third food supplement contained 1.82 mg/capsule and 3.45 mg/capsule, respectively. Considering the amount of extract per capsule and the weight of the capsules, an

extract containing 0.91% of D-pinitol was used for supplement 2 and an extract containing 1.39% of D-pinitol, was used for the preparation of supplement 3. In the fourth food supplement, the highest amount of D-pinitol was found, namely 30.16 mg/capsule. The extract used contained 6.70% of D-pinitol. The latter food supplement contained 3.14 mg/capsule. The label did not indicate the amount of extract used for the preparation, but only the amount of *D. adscendens*, without further specification.

Table 5.5 Food supplements (FS): Pharmaceutical form, labeled content, recommended dose and amount of pinitol in the different food supplements and the used extracts.

FS	Pharmaceutical form	Labeled content	Recommended dose	Pinitol content solution or capsule	Pinitol content extract
1	Liquid dosage form solution	<i>D. adscendens</i> decoction 93%	2 x 10 mL /day	1.97 mg/mL	-
2	Solid dosage form capsules	200 mg <i>D. adscendens</i> extract	1 to 2 capsules/day	1.82 mg/capsule	0.91%
3	Solid dosage form capsules	200 mg <i>D. adscendens</i> extract	1 to 4 capsules/day	3.45 mg/capsule	1.39%
4	Solid dosage form capsules	450 mg <i>D. adscendens</i> extract	3 x 1 capsule/day	30.16 mg/capsule	6.70%
5	Solid dosage form capsules	2.5 g <i>D. adscendens</i>	2 x 2 capsules/day	3.14 mg/capsule	-

When looking at the amount of D-pinitol per capsule, the most relevant parameter for the patient, one can see that there is a substantial difference between the five investigated food supplements. For example, the amount of D-pinitol in food supplements 2 and 4 differs with almost a factor 17. Because the amount of D-pinitol in the used extracts also differed a lot (supplements 2, 3, and 4), one can presume that there was an enormous difference in D-pinitol content in the raw plant material, which could be influenced by many factors, for example, the origin, harvesting time, soil quality, storage conditions etc. or that there was a substantial difference in the extraction method, which could lead to lower or higher yields of D-pinitol.

The amount of D-pinitol in leaves was 0.65% for the additional batch from Ghana and 2.74% for batch B, 7.44% in twigs, and 3.96% in roots. A higher amount of D-pinitol could be obtained by using the twigs only, but the separation of leaves and twigs is time-consuming and causes an additional

cost regarding the industrial preparation of the decoction. A fresh batch of decoction (Batch B) prepared with 3 L, 2 L and 1 L water (per portion of 200 g) yielded 5.61, 5.77 and 6.22% of D-pinitol respectively, showing that the extraction of D-pinitol from the fresh plant material was complete.

5.2.4 Conclusion

A GC analysis method to quantify D-pinitol in a decoction of *D. adscendens* has been developed and validated. This was necessary since, although several analysis methods were available for the quantification of D-pinitol in different matrices, no methods were available for a decoction of *D. adscendens*. In addition, only one of all these methods, i.e. the method developed by Lein et al.⁴⁸ was partly validated. The extraction procedure was thoroughly evaluated for this specific matrix and the derivatization procedure was optimized. The calibration model was linear and the precision was acceptable. The accuracy ranged from 103.38% to 105.84%. Since no level dependency was revealed in the recovery testing and in the precision on different levels, it could be concluded that the extraction conditions are suitable and there is no loss of D-pinitol during the analysis. The method can be used to quantify D-pinitol in decoctions, used in *in vivo* experiments, or to screen food supplements. For the five food supplements that were investigated in this work, a substantial difference in the amount of D-pinitol could be seen, which has major implications for the posology of different supplements. For industrial purposes, the most efficient production method would be the preparation of a decoction of leaves and twigs, also found to be used traditionally, using 5 L of water for each kg of dried plant material.

5.3 Antihepatotoxic activity of a quantified *Desmodium adscendens* decoction and D-pinitol against chemically-induced liver damage in rats*

5.3.1 Introduction

Liver diseases are a serious health problem throughout the world. The liver is an important organ involved in the detoxification of many xenobiotic substances. Liver damage can be chemically induced, mostly by the generation of reactive species, including free radicals. If internal defense mechanisms fail, jaundice, cirrhosis and fatty liver may result. Only a few drugs are available to protect the liver against or to cure it of chemically-induced damage. The best-known example is silymarin, the flavanolignan mixture obtained from *Silybum marianum* (Asteraceae) or milk thistle.⁵⁵ With respect to the hepatoprotective activity, the *in vitro* free-radical scavenging activity of five medicinal plants from Ghana, including *D. adscendens*, was evaluated by Gyamfi et al.⁵⁶, but only *Thonningia sanguinea* was found to scavenge the 2,2-diphenyl-1-picrylhydrazyl (DPPH) radical. However, a patent has been taken on the use of *Desmodium*, especially *D. adscendens*, in the treatment of viral or chemically-induced hepatitis.¹⁷ Here, the protective and curative effect of this decoction, in which D-pinitol was quantified, and of pure D-pinitol, against liver damage induced by various chemicals in rats, is reported.

5.3.2 Materials and methods

5.3.2.1 Plant material and preparation of the decoction

Batch A (A1 and A2) and batch B as described in part 5.2 (5.2.2.1) were used. D-pinitol was quantified in the lyophilized aqueous decoction of *D. adscendens* by a validated GC-FID method, as described above. Batch A1 was found to contain 0.59% D-pinitol (or 0.64%, dry weight), batch A2 1.99% (or 2.05% dry weight), and batch B 5.55% (or 5.70%, dry weight).

*Published: Magielse, J.; Arcoraci, T.; Breynaert, A.; van Dooren, I.; Kanyanga, C.; Fransen, E.; Van Hoof, V.; Vlietinck, A.; Apers, S.; Pieters, L.; Hermans, N. Antihepatotoxic activity of a quantified *Desmodium adscendens* decoction and D-pinitol against chemically-induced liver damage in rats. *J. Ethnopharmacol.* **2013**, *146*, 250-256. Contribution: preparation of decoction and quantification of D-pinitol.

5.3.2.2 *General experimental procedures*

Experimental procedures as described by Magielse et al.²⁴ were used. Briefly, the protective effect against D-galactosamine-induced and chronic ethanol-induced liver damage, as well as the curative effect against D-galactosamine-induced liver damage and acute acetaminophen-induced hepatotoxicity, were investigated. Animals were treated with D-pinitol (95%) and silymarin (from Sigma-Aldrich), used as positive control, and with a decoction of *D. adscendens* prepared as described in 5.3.2.1. For the evaluation of the protective effect, the treatment was administered before liver damage was induced, whereas, for the evaluation of the curative effect, the treatment was started after liver damage was induced.

5.3.3 **Results and discussion**

5.3.3.1 *Protective effect against acute D-galactosamine-induced liver damage*

24 h after galactosamine injection no significant decrease could be observed for any treatment with regard to the aspartate aminotransferase (AST) and alkaline phosphatase (ALP) levels. However, there was a significant decrease of the alanine aminotransferase (ALT) level for both *Desmodium* groups (equivalent to 5 mg/kg and 20 mg/kg D-pinitol), the D-pinitol group and the silymarin group. 48 h after galactosamine-injection, the effects were more pronounced: a significant decrease of AST and ALT (but not ALP) was observed for both *Desmodium* groups, D-pinitol as well as silymarin. It appeared that even the lowest dose of *Desmodium* decoction (equivalent to 5 mg/kg D-pinitol) was more active as (AST) or similar to (ALT) 20 mg/kg D-pinitol or 20 mg/kg silymarin. No significant difference in effect was observed between D-pinitol and silymarin, both at a dose of 20 mg/kg. The effect of treatment with *Desmodium* decoction at a dose equivalent to 5 mg/kg D-pinitol was not significantly different ($P > 0.05$) from treatment with the dose equivalent to 20 mg/kg. No effect on serum ALP level was observed.

5.3.3.2 *Curative effect against chronic D-galactosamine-induced liver damage*

No curative effect of D-pinitol could be observed during this experiment.

5.3.3.3 *Curative effect against acute acetaminophen-induced hepatotoxicity*

No curative effect of D-pinitol or the standardized extract could be observed during this experiment.

5.3.3.4 Protective effect against chronic ethanol-induced liver damage

None of the treated groups showed a significantly decreased ALT or AST level compared to the hepatotoxic group. With respect to mortality of animals in the different treatment groups, an extensive dropout was observed in the untreated hepatotoxic group, whereas survival in the *Desmodium* group equivalent to 10 mg/kg D-pinitol, was better. Statistical analysis of survival data showed a significant difference in survival rate between the control and the hepatotoxic group ($p < 0.01$), and a trend towards significance ($p = 0.06$) between the *Desmodium* group equivalent to 10 mg/kg D-pinitol and the untreated hepatotoxic group. No statistical difference of the *Desmodium* group equivalent to 2 mg/kg D-pinitol, D-pinitol group (10 mg/kg) or silymarin group (20 mg/kg) with the hepatotoxic group was observed.

5.3.4 Conclusions

Based on these observations, it could be concluded that the aqueous decoction of *D. adscendens* and D-pinitol showed a hepatoprotective effect in rats against acute liver damage caused by D-galactosamine and that the effect of the *D. adscendens* decoction is at least in part due to the presence of D-pinitol. A significant protective effect of *D. adscendens* decoction was already observed at a dose containing 5 mg/kg D-pinitol and was more active (based on AST levels) or comparably active (based on ALT levels) as pure D-pinitol at a concentration of 20 mg/kg. The effect of the *Desmodium adscendens* decoction did not significantly increase when a higher concentration (corresponding to 20 mg/kg D-pinitol) was used and probably the maximal effect had already been achieved at a dose equivalent to 5 mg/kg D-pinitol. Therefore, the hepatoprotective effect of *D. adscendens* can be partially ascribed to D-pinitol but there is a possible synergistic effect of other constituents of the decoction, which explains the higher or comparable effect at a lower dose.

With respect to chronic ethanol administration, a protective trend was detected with *D. adscendens* in a dose equivalent to 10 mg/kg D-pinitol. No curative effect of D-pinitol on liver damage caused by chronic administration of D-galactosamine could be demonstrated, nor of a *Desmodium adscendens* decoction (in a dose equivalent to 10 mg/kg D-pinitol) after acute administration of acetaminophen.

5.4 Phytochemical analysis

5.4.1 Introduction

In vivo experiments (part 5.3) showed a significant liver-protective effect of a *D. adscendens* decoction. The hepatoprotective effect of *D. adscendens* can be partially ascribed to D-pinitol, but there is a possible synergistic effect of other constituents of the decoction, which explains the higher or comparable effect at a lower dose. For this reason, further phytochemical research was envisaged to characterize other constituents present in the decoction. As described in the introduction, some flavonoids were already isolated from *D. adscendens* and in addition, commercially available food supplements are standardized on vitexin. Therefore, after a general screening, the focus was mainly on the characterization of flavonoids. Their characterization was done by subsequent fractionation, isolation, and structure elucidation. The decoction was fractionated using flash chromatography and constituents from a flavonoid-rich fraction were isolated using repeated semi-preparative HPLC. Because only the major flavonoid was isolated in a sufficient amount for NMR analysis, also HPLC-SPE was used in order to isolate the minor constituents, but also in this way, insufficient amounts were obtained. In addition to NMR analysis, MS and MS/MS analysis was performed. In this way, the minor compounds were characterized and their identity was confirmed by using reference and surrogate standards.

5.4.2 Materials and methods

5.4.2.1 Quick screening by HPLC-UV and TLC

As a starting point, a quick screen for constituents described in literature and mentioned on the label of some food supplements (i.e. flavonoids, *vide supra*) was done by HPLC-DAD and TLC. For the detection of flavonoids, 100 mg of the sample was dissolved in 20.0 mL methanol 50% and sonicated for 15 min. After cooling down, the sample was brought to 25.0 mL with 50% methanol. 5.0 mg vitexin as standard was dissolved in 10.0 mL methanol and 3.0 mL of this solution was transferred into a 20.0 mL volumetric flask and was brought to volume with methanol 50%. Both solutions were filtered through a Nylon syringe filter (0.25 μm). Samples were analyzed on a Grace Smart RP-18 column (4.6 x 250 mm, 5 μm) with 0.5% (v/v) phosphoric acid in methanol 5% (v/v) as mobile phase A and acetonitrile as mobile phase B using the following gradient: 0 min – 10% B; 2 min – 10% B; 25

min – 25% B; 35 min – 85% B; 37 min – 10% B at a flow rate of 1 mL/min, UV-detection was done at 350 nm. Based on literature data, the decoction was compared with different polyphenolic standards: caffeic acid, chlorogenic acid, catechin, gallic acid, apigenin, genistein, hyperoside, isovitexin, kaempferol, naringenin, orientin, quercetin, quercetin-3-*O*-glucoside, quercetrin, rutin, and vitexin. For screening of saponins, the TLC method described by Pothier et al.³ was used, with soyasaponin I, II and III as standards. Briefly, samples were applied on a silica gel 60 F₂₅₄ plate and developed with a chloroform/methanol/water (60:40:10) mixture. Detection was performed after spraying with the anisaldehyde-sulfuric acid reagent and heating to 115 °C.

5.4.2.2 Optimization of chromatographic parameters for flavonoid isolation and analysis

Different columns and organic modifiers were used in order to obtain the best separation of flavonoids in the sample. A Grace Smart RP-18 column (250 x 4.6 mm; 5 µm), a Lichrospher 100 RP-18 (250 x 4; 5 µm), an Apollo C18 column (250 x 4.6 mm; 5 µm), an Econosphere C18 (250 x 4.6 mm; 5 µm) and a Luna C18 (2) column (250 x 4.6 mm; 5 µm) were evaluated in combination with acetonitrile or methanol as modifier. At the end of the practical work of this thesis, a newer column type based on fused core technology, a Kinetex EVO C18 column (250 x 4.6 mm, 5 µm) was also screened.

5.4.2.3 Compound isolation and structure elucidation

Column chromatography

To obtain pure compounds from the decoction of *D. adscendens*, it was first subjected to column chromatography using a Reveleris Flash Chromatography system equipped with a Reveleris silica column (80 g, 40 µm). A gradient starting with 100% ethyl acetate going to 100% methanol in 14 min was used to elute the compounds. Every fraction contained 22 mL. Detection was done by UV at 254 nm and 360 nm and by ELSD. Additionally, all fractions were monitored by TLC. Every fraction was applied on a normal phase TLC plate (20 x 20 cm, silica gel 60 F₂₅₄), and subsequently the plate was developed with EtOAc/CH₃COOH/HCOOH/H₂O (100:11:11:26), sprayed with NEU-reagent and a PEG 400 solution, and heated to 105 °C. Based on the observed TLC pattern, similar fractions were combined.

Semi-preparative LC

An enriched flavonoid fraction, obtained by normal phase flash chromatography, was separated by repeated semi-preparative HPLC. An AutoPurification™ system from Waters with DAD and TQD mass analyzer was used. Fractions were separated using a Luna C18 (2) column (250 x 10 mm, 5 μm).

The following gradient was used: solvent A: 0.1% FA; solvent B: ACN, 0 min – 15% B, 5 min – 15% B, 39 min – 23% B, 43 min – 0% B, 45 min – 0% B, 47 min – 15% B, 55 min – 15% B. The flow rate was 3 mL/min. Detection was done by DAD at 210 nm, 254 nm, 330 nm and 360 nm and by MS. A full scan in the negative ion mode ranging from m/z 200 to 800 was performed and fraction collection was done for all peaks with m/z 593, 563, 431 and 327 in the negative ion mode, the major signals showing a UV spectrum typical for flavonoids. The injection volume was 600 μL and the concentration of the flavonoid fraction was 20 mg/mL.

HPLC-SPE

Four different fractions, obtained by normal phase flash chromatography, were separated by an Agilent 1200 HPLC using a Luna C18 (2) column (250 x 4.6 mm, 5 μm). UV-detection was done at 330 nm. Trapping of the analytes was performed with an online SPE system Prospekt 2. HySphere™ Resin GP cartridges were used, after conditioning with methanol and equilibrating with water. To increase the concentration of the compound, the HPLC run was repeated and the same compounds were trapped several times on the same cartridge (multi-trapping). After trapping, the cartridges were dried with N₂ and compounds were eluted with CD₃CN into an NMR tube (3 mm).

NMR analysis

¹H, ¹³C-NMR and 2D-NMR (¹H-¹H COSY, ¹H-¹³C HSQC, ¹H-¹³C HMBC) spectra of the isolated compounds were recorded on a Bruker DRX 400 instrument equipped with a z-gradient 5 mm dual probe and a 3 mm broadband inverse probe using standard Bruker pulse sequences. All samples were dissolved in either CD₃OD, 99.5% D or CD₃CN 99.8% D. Chemical shifts are given in δ and coupling constants (J) in Hz.

LC-MS analysis

LC-MS analysis of a solution (50% methanol) of the decoction of *D. adscendens* (10 µg/mL) was performed employing a Surveyor LC system coupled to an LXQ linear ion trap and a Thermo Hypersil Gold column (150 x 2.1 mm, 3 µm). The flow rate was 0.2 mL/min, and the solvent program was as follows: solvent A: 0.1% FA; solvent B: ACN; 0 min – 5% B, 5 min – 5% B, 30 min – 23% B, 35 min – 100% B, 45 min – 100% B, 47 min – 5% B, 55 min – 5% B. The injection volume was 10 µL. Spectra were recorded in the (-)-ESI mode. Tune conditions were as follows: sheath gas flow: 50 arbitrary units; auxiliary gas flow: 5 arbitrary units; source voltage: 4.0 kV; ion transfer tube temperature: 350 °C; and capillary voltage: -34 V. Mass spectral data were recorded in full scan mode in the mass range m/z 50–1000. For MSⁿ experiments an isolation width of 2 Da was used and a normalized collision energy of 35% was applied. All data were acquired and processed using Xcalibur software, version 2.0.

In addition, a solution of the decoction of *D. adscendens* (200 µg/mL) was compared with a solution of a *Passiflora incarnata* extract (200 µg/mL). *P. incarnata* is known to contain a high amount of flavone C-glycosides and therefore it was used as a surrogate standard to confirm our findings since commercial reference standards are very costly. The same apparatus and a Luna C18 (2) column (250 x 4.6 mm, 5 µm) were used. The flow rate was 1 mL/min using a splitter, and the solvent program was as follows: solvent A: 0.1% FA; solvent B: ACN + 0.1% FA; 0 min – 5% B, 5 min – 5% B, 30 min – 23% B, 35 min – 100% B, 45 min – 100% B, 47 min – 5% B, 55 min – 5% B. The injection volume was 10 µL. Spectra were recorded in both (-)-ESI and (+)-ESI mode. Tune conditions were as follows: sheath gas flow: 50 arbitrary units; auxiliary gas flow: 5 arbitrary units; source voltage: 4.0 kV; ion transfer tube temperature: 350 °C; and capillary voltage: -34 V and 14 V, respectively. Mass spectral data were recorded in full scan mode in the mass range m/z 115 – 1000. For MSⁿ experiments an isolation width of 2 Da was used and a normalized collision energy of 35% was applied. All data were acquired and processed using Xcalibur software, version 2.0.

Analysis on an LC-MSD ion trap with ESI and HP Chemstation software was performed in both positive and negative ion mode using the Luna C18 (2) column (250 x 4.6 mm, 5 µm). The flow rate was 1 mL/min and the solvent program was as follows: solvent A: 0.1% FA; solvent B: ACN + 0.1% FA; 0 min – 5% B, 5 min – 10% B, 80 min – 50% B, 85 min – 100% B, 88 min – 100% B, 91 min – 5% B, 95 min – 5% B. The injection volume was 20 µL. The capillary voltage was set at 1500 V, the

accumulation time at 25 ms and the averages at 4 (i.e. the amount of scans leading to a single spectrum at a designated retention time).

An extract of *D. adscendens* was analyzed and compared with an extract of *Passiflora incarnata* dry extract by means of UPLC-HRMS as described by De Paepe et al.⁵⁷ and by means of LC-MS using an LXQ linear ion trap and Luna C18 (2) column with the abovementioned parameters.

All product ions were labeled according to the nomenclature of Domon and Costello⁵⁸, with product ions $^{k,l}X_j$, Y_j , and Z_j being product ions containing the intact aglycone. Superscripts k and l indicate the cleavages in the sugar molecule and subscript j indicates the number of the interglycosidic bond that is broken, starting from the aglycone. For di-C-glycosides, subscripts H and P indicate a hexose and a pentose.

5.4.2.4 Total flavonoid content of five food supplements containing *D. adscendens* and different plant parts

The flavonoid content was quantified for the samples described in 5.2.2.1. They were dissolved in a volume of methanol 50% equal to 80% of the volume of the measuring flask and sonicated for 15 min. After cooling down the sample was brought to the end volume with methanol 50%. 5.27 mg vitexin as standard was dissolved in 20.0 mL methanol and 4.0 mL of this solution was transferred into a 20.0 mL volumetric flask and was brought to volume with methanol 50%. An additional dilution was made from this solution by transferring 800 μ L to 2.0 mL methanol 50%. Sample solutions were centrifuged for 5 min at 1760 g (3000 rpm) and analyzed in triplicate by an Agilent 1200 HPLC using a Kinetex EVO C18 column (250 x 4.6 mm, 5 μ m). The following gradient was used: solvent A: 0.1% FA; solvent B: ACN, 0 min – 15% B, 5 min – 15% B, 39 min – 23% B, 55 min – 0% B, 57 min – 0% B, 59 min – 15% B, 67 min – 15% B. The flow rate was 0.4 mL/min. Detection was done by DAD at 210 nm, 254 nm, 330 nm, 334 nm, and 355 nm.

5.4.3 Results and discussion

5.4.3.1 Quick screening by HPLC-UV and TLC

The decoction appeared to be rich in flavonoids, more in particular flavone derivatives, based on the UV absorption maxima at 270 and 334 nm (Figure 5.10).^{23,59-60} In addition, compounds with a UV spectrum typical for phenolic acids were present (Figure 5.11). Typical purple-blue spots were visible

in the upper half of the TLC plate where also the soyasaponin standards eluted. Since the *in vivo* study showed that the decoction prevented D-galactosamine-induced liver damage, this work focused on the isolation and identification of the flavonoids present in *D. adscendens*, a class of natural products which are generally known to have anti-oxidative properties (free radical scavenging).⁶¹

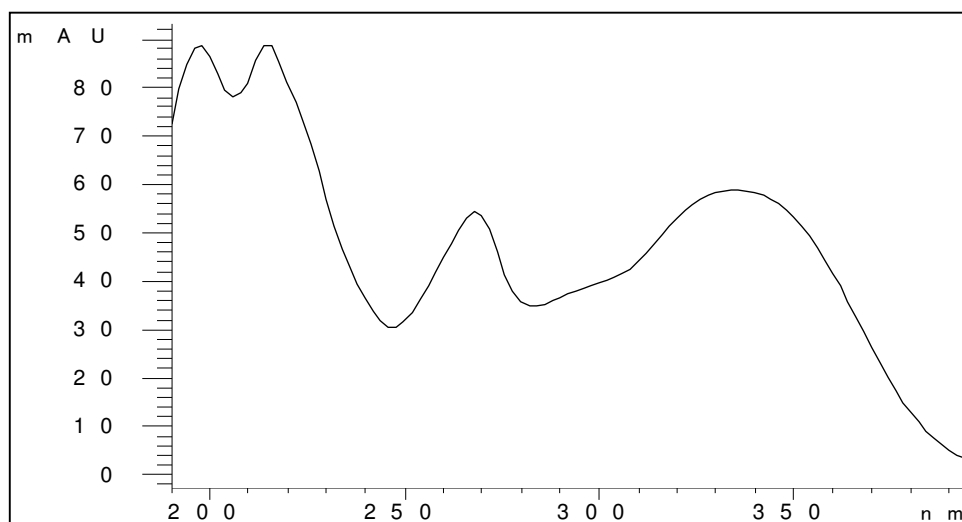


Figure 5.10 UV spectrum of the main flavonoid.

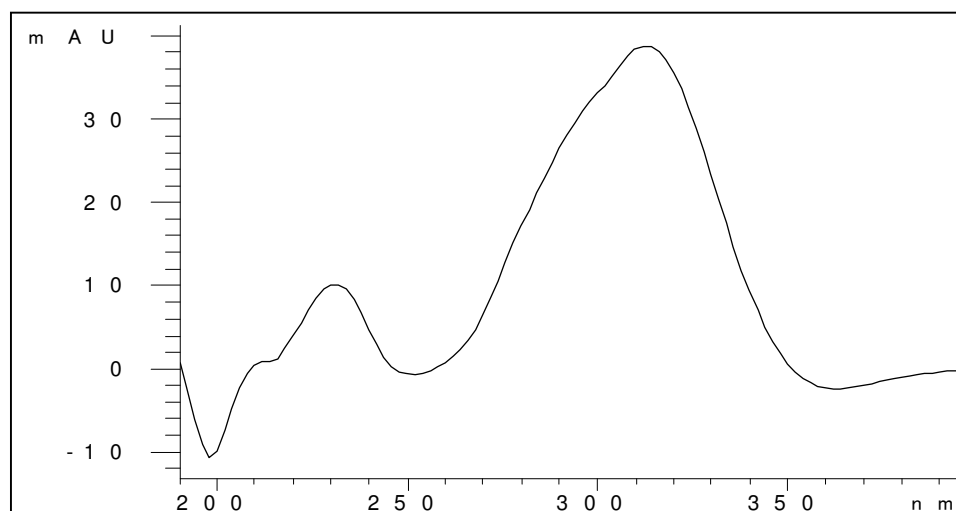


Figure 5.11 UV spectrum of the main phenolic acid.

5.4.3.2 Optimization of chromatographic parameters for flavonoid isolation and analysis

The separation of the flavonoids was hard to achieve, probably because of their structural similarity. The chromatograms with the best separation for each column are shown in Figure 5.12 at a wavelength of 330/334 nm so that the phenolic acids present in the decoction were also visible. It is

clear that the Luna C18 (2) and Kinetex column are the most suitable columns giving both acceptable separation with nice peak forms. The Purospher STAR, Grace Smart, and Econosphere column showed far less separation. For all further isolation purposes, a Luna C18 (2) column (250 x 10 mm, 5 μ m) was used with water + 0.1% FA (A) and ACN (B) as mobile phases and following gradient: 0 min – 15% B; 5 min – 15% B; 39 min – 23% B; 43 min – 100% B; 45 min – 100% B; 47 min – 15% B; 55 min – 15% B. The flow was 1 mL/min. No semi-preparative Kinetex EVO column was available in the laboratory at that time. For analytical purposes, both the Luna C18 (2) and Kinetex EVO columns were used based on their availability at the respective time point of the work. An analytical Kinetex EVO column (250 x 4.6 mm, 5 μ m) was used for quantification of flavonoids in different *Desmodium* samples.

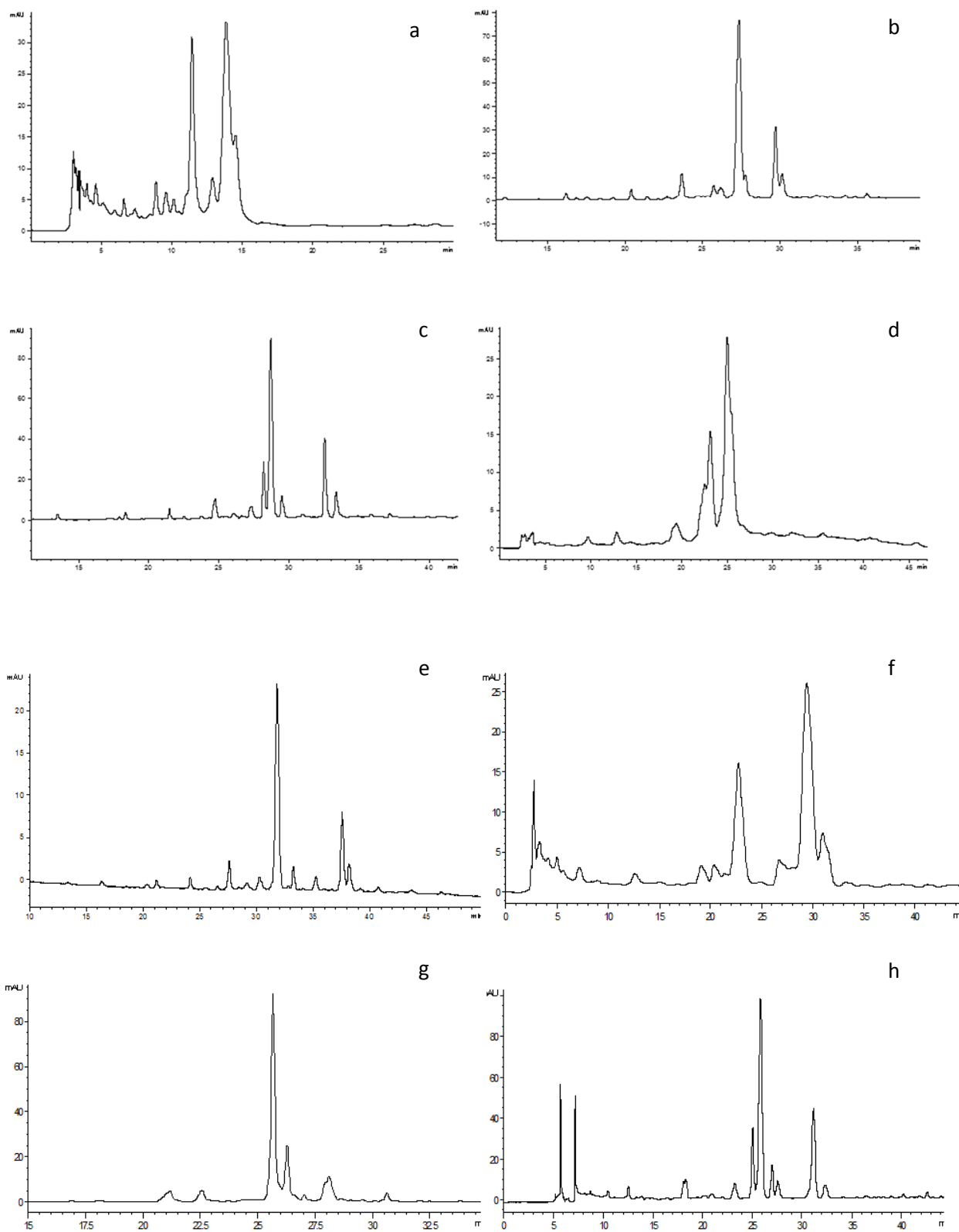


Figure 5.12 Chromatograms of the decoction of *D. adscendens* with detection at 330/334 nm. a. Grace smart C18 column; b. Lichrospher RP-18 column; c. Luna C18 column; d. Econospher C18 column; e. Apollo C18 column; f. Purospher STAR C18 column; g. NH₂ column; h. Kinetex EVO column.

5.4.3.3 Isolation and structure elucidation

Flash chromatography

The fractions obtained by flash chromatography together with the crude extract (CE) and two standards rutin and quercetin were analyzed by TLC and the results are shown below (Figure 5.13). The number of each fraction is written below. The greenish-yellow spots are flavones and the blue spots are phenolic acids. A crude separation of flavonoids and phenolic acids was achieved. Flavonoids started to show up in fraction 12. Before this fraction only rather lipophilic compounds which were of no interest in this context were eluted from the column. A nice lowering of the retardation factor (Rf) was seen for the flavonoids over time, although some flavones tended to co-elute. From fraction 25 some phenolic acids started to elute too. The fractions which contained flavonoids (fraction 12-23) were combined to prepare a flavonoid-enriched fraction that can be processed by semi-preparative LC.

The flash chromatography process was repeated and fractions were analyzed by both TLC and HPLC. Fractions with a similar HPLC profile were combined and in this way four combined fractions were obtained: 23 mg of fraction 1, 43 mg of fraction 2, 322 mg of fraction 3 and 301 mg of fraction 4 of which the HPLC chromatograms are shown in Figures 5.14, 5.15, 5.16 and 5.17, respectively.

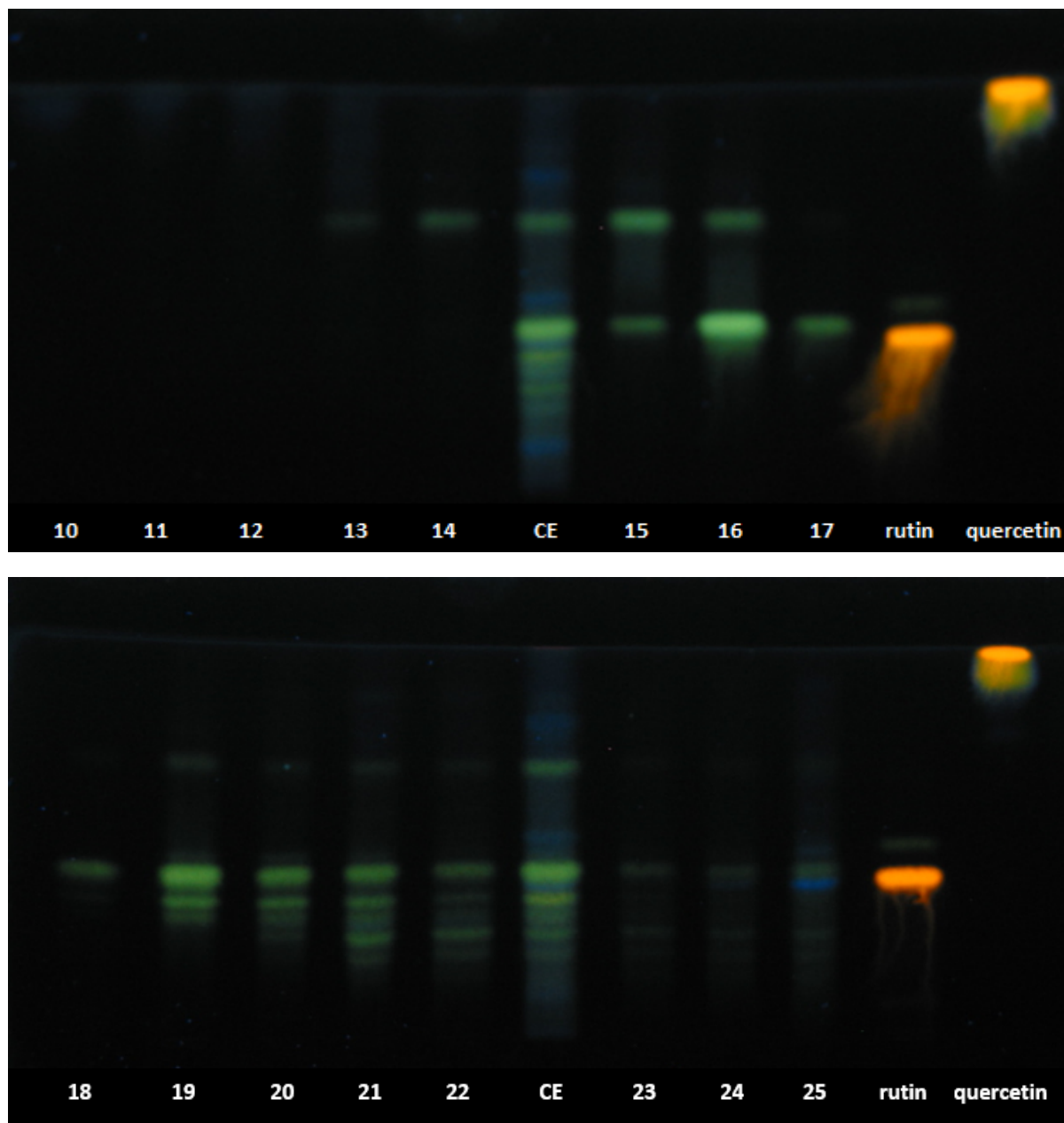


Figure 5.13 TLC chromatogram of fractions obtained by flash chromatography.

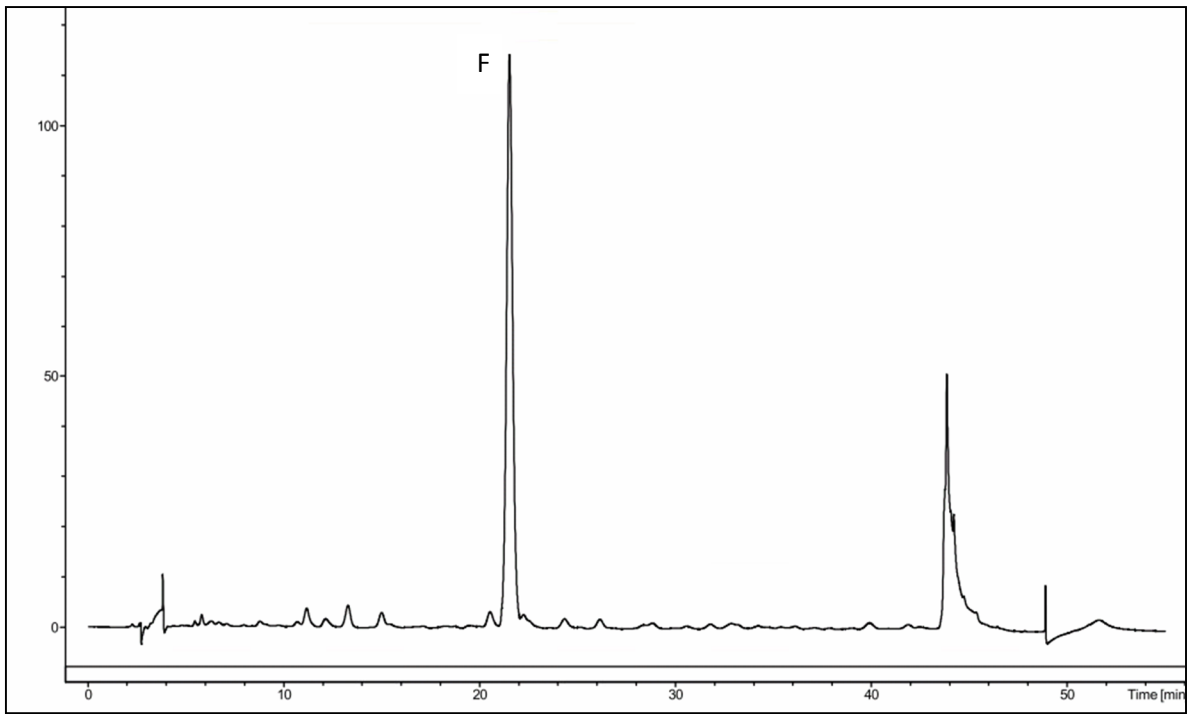


Figure 5.14 Chromatographic profile of fraction 1.

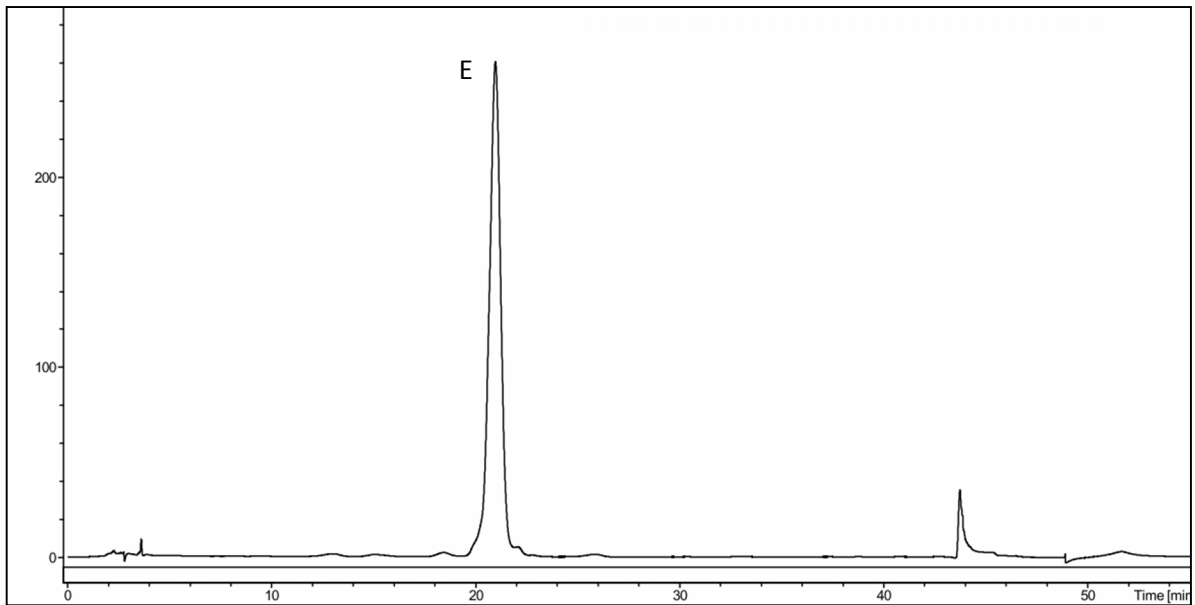


Figure 5.15 Chromatographic profile of fraction 2.

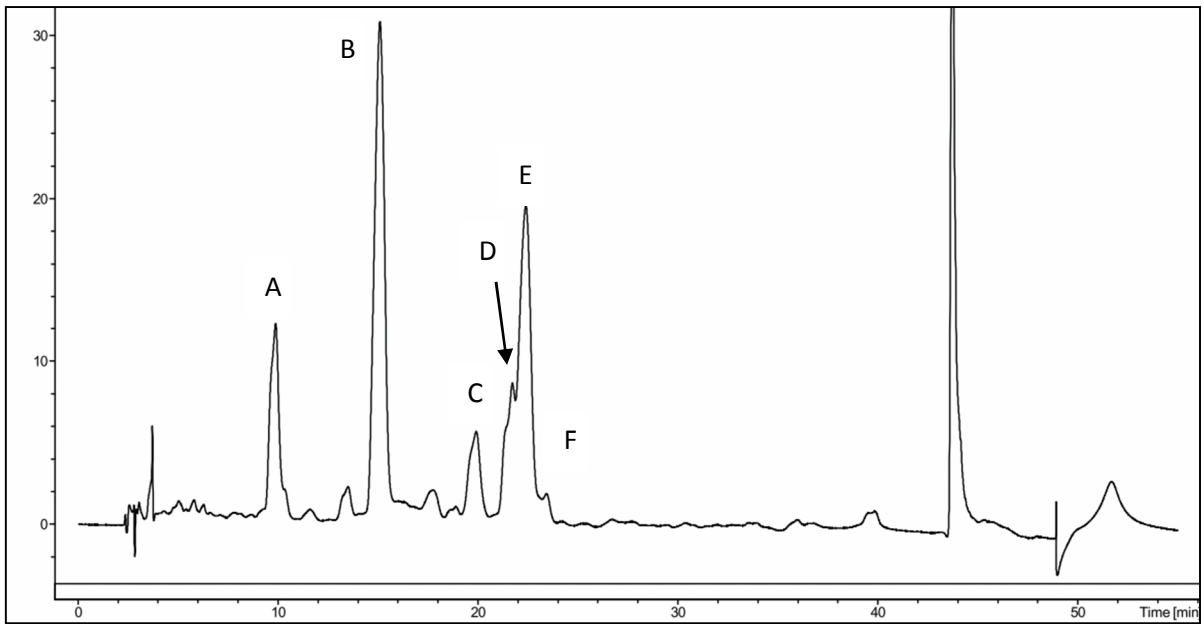


Figure 5.16 Chromatographic profile of fraction 3.

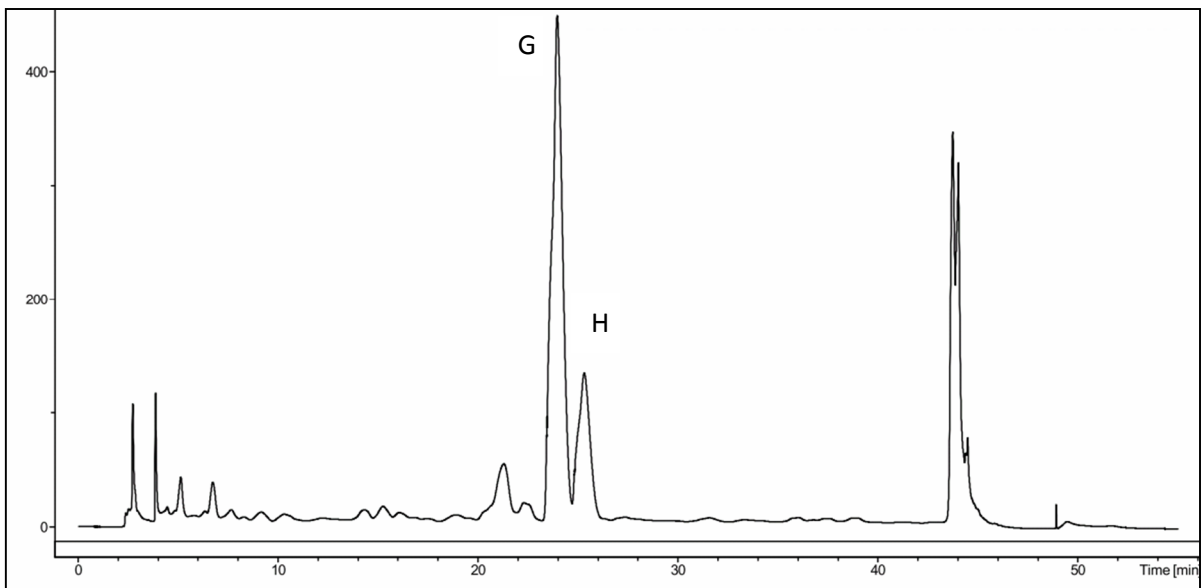


Figure 5.17 Chromatographic profile of fraction 4.

Fraction 1 contained a flavonoid, indicated as peak F; fraction 2 contained a flavonoid indicated as peak E; fraction 3 contained, in addition to peak E and F, some minor flavonoids indicated as A, B, C, and D; and fraction 4 contained two phenolic acids, indicated as G and H.

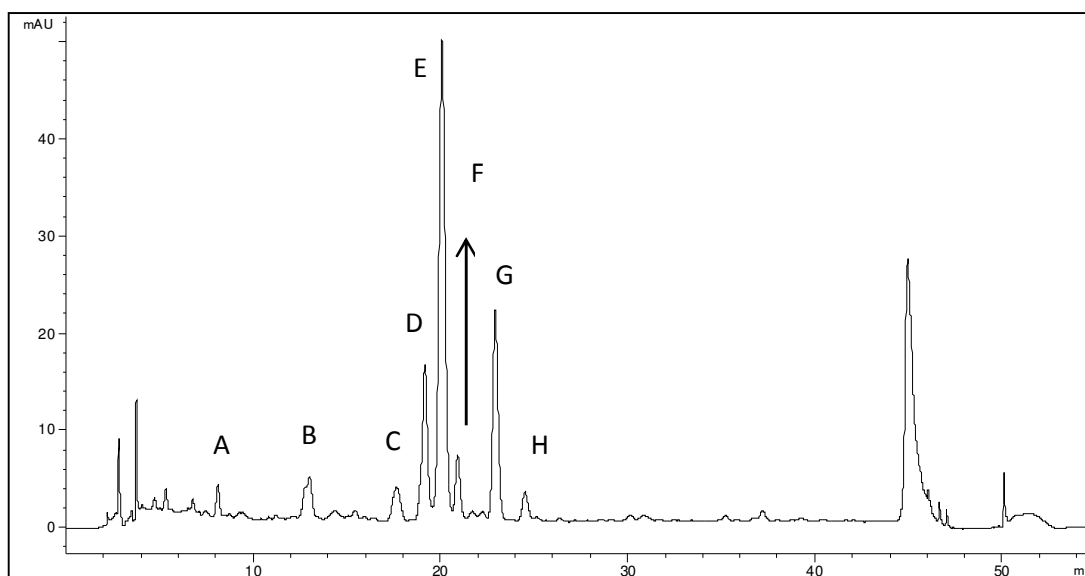


Figure 5.18 Chromatogram of the crude extract. Flavonoid peaks are indicated as A, B, C, D, E and F; phenolic acids as G and H.

Semi-preparative HPLC and HPLC-SPE-NMR

The yield after semi-preparative HPLC isolation was 1.1 mg for peak F, 5.6 mg for peak E, 0.9 mg for peak A, 1.9 mg for B and also for C, and 1.6 mg for peak D.

During HPLC-SPE one peak was trapped for fraction 1 and 2, four peaks for fraction 3, and two peaks for fraction 4. All trapped peaks were analyzed first by $^1\text{H-NMR}$.

NMR and MS analysis

Compounds isolated with semi-preparative LC

$^1\text{H-NMR}$ from all compounds obtained by semi-preparative LC indicated that most of them were not pure and consisted of more than one flavonoid. This was evident from the signals of the C-5 OH observed in the region δ 12-13. When two peaks are visible, probably more than one component is present and the sample is a mixture. In addition, most of the compounds were too low in concentration to obtain a good signal-to-noise ratio. Only compound **E** (Figure 5.19) was isolated as a pure compound giving a good $^1\text{H-NMR}$ spectrum (Figure 5.20). For this compound $^{13}\text{C-NMR}$ (Figure 5.21), DEPT-90, DEPT-135 and 2D experiments (DQF-COSY (Figure 5.22), HSQC (Figure 5.23) and HMBC (Figure 5.24)) were recorded. The $^{13}\text{C-NMR}$ spectrum confirmed the hypothesis that this compound was a flavone as previously deduced from the UV spectrum. The characteristic shift of δ 102.2, typical for the C-3 of a flavone, confirmed this (Table 5.6). Two doublets at δ 7.98 ($J = 8.4$ Hz)

and δ 6.91 ($J = 8.4$ Hz) pointed to a para-disubstituted B ring. HMBC correlations between H-6 and C-5, C-7, C-8 and C-10 and between Glc H-1 and C-8, C-9 and C-10 indicated a glycosylation at C-8. From these results, apigenin could be identified as the aglycone. Based on the typical chemical shifts of the sugar moieties, they could be identified as glucose and xylose. Glucose was directly attached to the C-8 of the aglycone as can be observed in the HMBC spectrum by the correlation between Glc H-1 and C-8. Correlations in the HMBC and COSY spectrum showed that xylose was attached to glucose by a 1 \rightarrow 2 glycosidic bond. These results suggested compound E to be 2''-O-xylosyl-vitexin, shown in Figure 5.19.⁶²

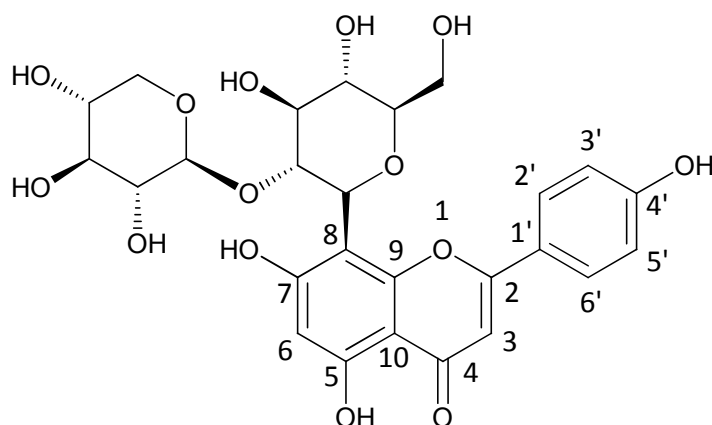


Figure 5.19 Structure of compound E, 2''-O-xylosyl-vitexin.

Table 5.6 ¹H-NMR and ¹³C-NMR assignments of compound E, 2''-O-xylosyl-vitexin.

position	δ_c (ppm)	δ_H (ppm), mult, J (Hz)
1		
2	163.5	
3	102.2	6.71
4	181.7	
5	160.5	13.10 (OH)
6	98.5	6.18
7	161.3	
8	103.7	
9	156.6	
10	106.2	
1'	121.4	
2', 6'	128.7	7.98 (d, $J = 8.4$ Hz)
3', 5'	115.9	6.91 (d, $J = 8.4$ Hz)
4'	161.4	

Table 5.6 continued ¹H-NMR and ¹³C-NMR assignments of compound E, 2''-O-xylosyl-vitexin.

position	δ_c (ppm)	δ_H (ppm), mult, J (Hz)
Glc		
1	71.5	4.79 (d, $J = 10.2$ Hz)
2	81.7	3.24
3	78.3	3.46
4	70.2	3.42
5	80.8	4.06
6	61.0	3.73, 3.54
Xyl		
1	105.7	3.86 (d, $J = 7.3$ Hz)
2	73.6	2.75
3	75.8	2.84
4	69.3	2.95
5	65.4	3.07, 2.33

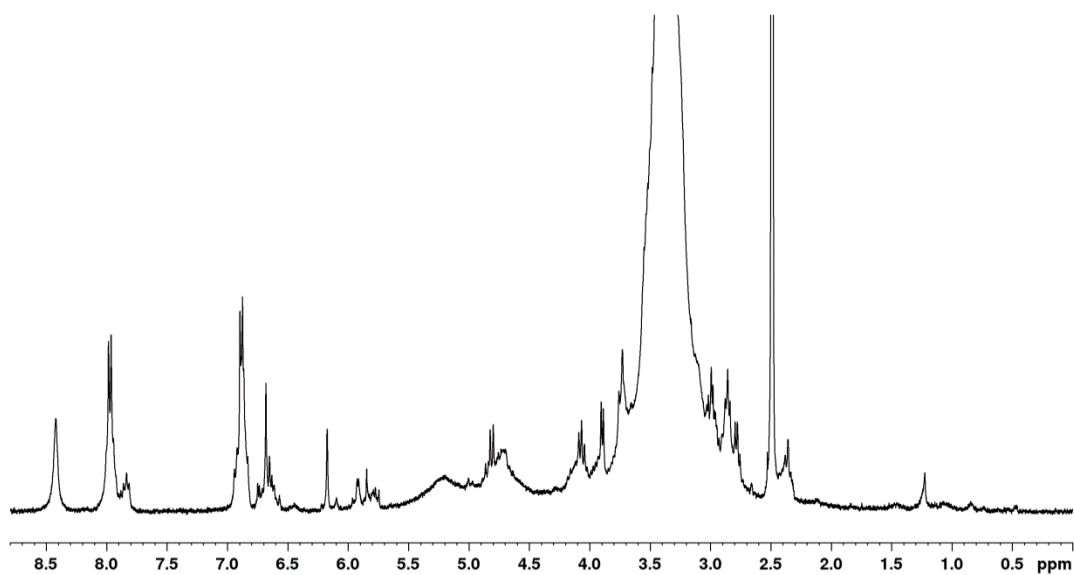


Figure 5.20 ¹H-NMR spectrum of compound E, 2''-O-xylosyl-vitexin.

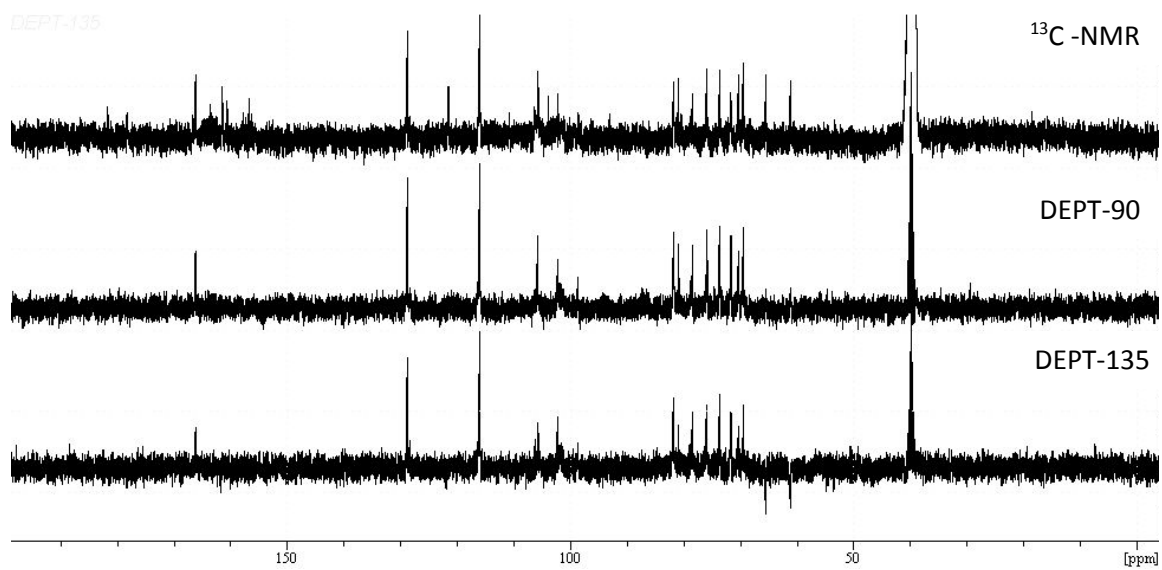


Figure 5.21 ^{13}C -NMR, DEPT-135 and DEPT-90 spectra of compound E, 2''-O-xylosyl-vitexin.

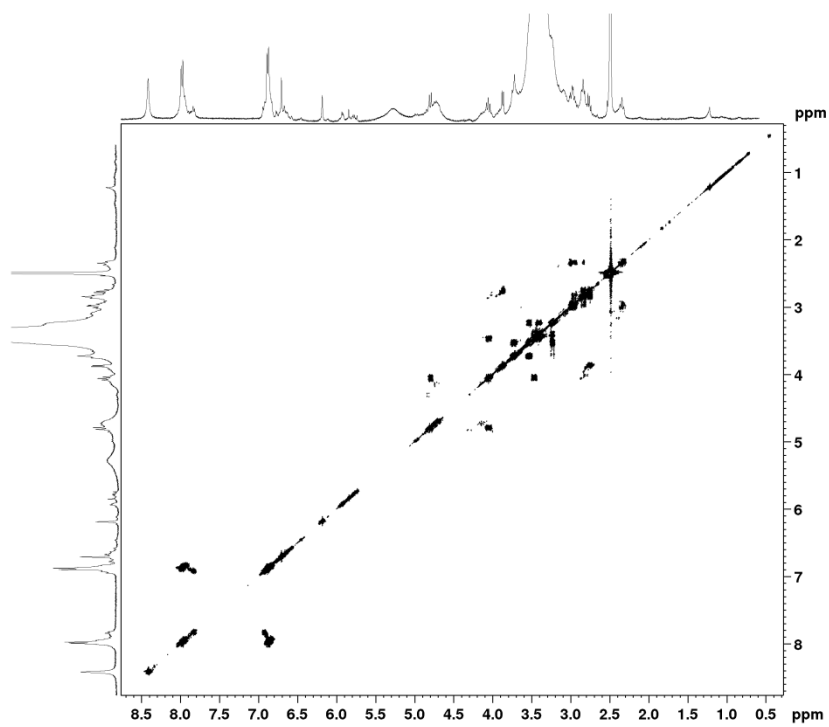


Figure 5.22 DQF-COSY spectrum of compound E, 2''-O-xylosyl-vitexin.

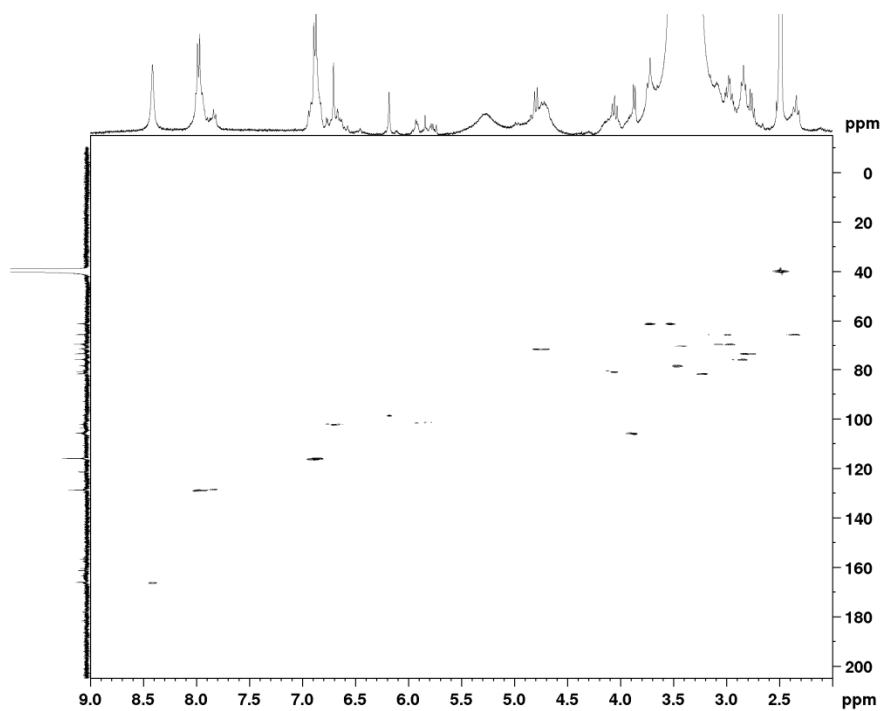


Figure 5.23 HSQC spectrum of compound E, 2''-O-xylosyl-vitexin.

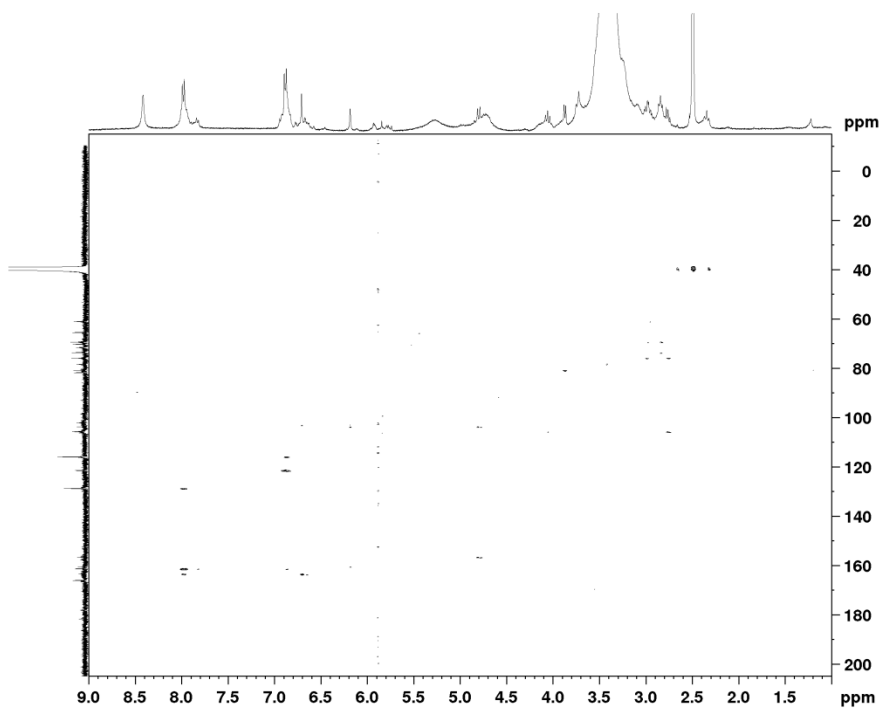


Figure 5.24 HMBC spectrum of compound E, 2''-O-xylosyl-vitexin.

MS analysis of compound **E** showed a deprotonated molecule at m/z 563 $[M-H]^-$ and MS^2 analysis of this ion resulted in product ions at m/z at 443, 413, 341, 311, and 293 (Figure 5.25). Internal cleavage of a saccharidic unit resulted in a small $^{0,2}X_0^-$ ion at m/z 443, which suggested the presence of a C-glycosidic bond. This product ion indicated that the second sugar moiety was bound at O-2 of the first sugar moiety.⁶³ The presence a Z_1^- ion, an intense signal at m/z 413 $[M-150-H]^-$, formed by the loss of a pentose moiety, is characteristic for an O-glycosidic bond between the pentose and the other sugar moiety and is characteristic for a 1→2 glycosidic bond as was already suggested.⁶³⁻⁶⁶ A scheme of the formation of these product ions is given in Figure 5.26. The formation of product ions at m/z 293 $[Ag + 41-18-H]^-$, at m/z 311 $[Ag + 41-H]^-$ and at m/z 341 $[Ag + 71-H]^-$ are indicative for apigenin as aglycone. MS^3 analysis of the most abundant ion in MS^2 (Z_1^-) resulted in a product ion at m/z 293. This product ion was also observed when MS^3 analysis of m/z 443 ($^{0,2}X_0^-$ ion) was performed, in addition to an ion at m/z 311, formed by the loss of the pentose moiety, which confirmed the presence of a 1→2 glycosidic bond.^{63,67}

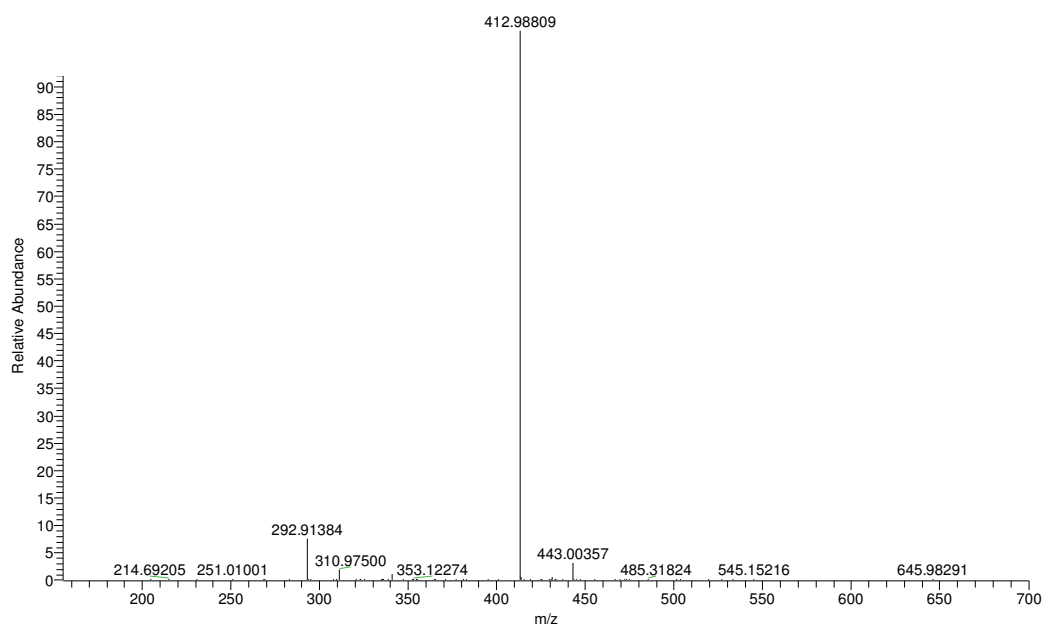


Figure 5.25 MS^2 spectra of compound **E**, 2''-O-xylosyl-vitexin in the negative ion mode.

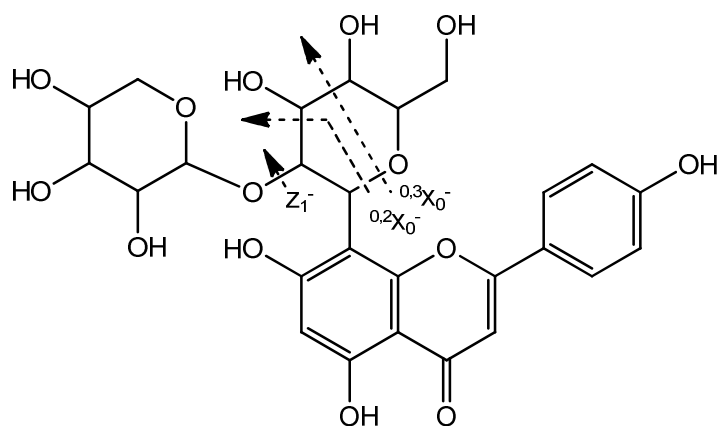


Figure 5.26 Fragmentation of compound E, 2''-O-xylosyl-vitexin in the negative ion mode.

Product ions generated in the positive ion mode were present at m/z 547, 445, 433, 415, 397, 367, 337, and 313 (Figure 5.27). The first product ion can be explained by the loss of one molecule of water. Internal cleavage of a saccharidic unit resulted in a small $^{0,2}X_0^+$ ion at m/z 445, which suggested the presence of a C-glycosidic bond. The most abundant product ion Y_1^+ at m/z 433 which is formed by the loss of 132 u indicated an O-glycosidic bond. The formation of these product ions is depicted in Figure 5.28. Subsequent losses of molecules of water gave rise to product ions at m/z 415 and 397, whereas the formation of a $^{0,2}X_0^+$ fragment resulted in an ion at m/z 313. An internal cleavage of the hexose moiety resulted in the formation of a $^{0,2}X_0^+$ fragment which together with a $^{0,2}X_1^+$ or $^{0,3}X_1^+$ fragment and loss of a water molecule led to product ions at m/z 337 and 367.

MS³ analysis of m/z 433 (Y_1^+ ion) led to product ions at m/z 337, 367 and 313 corresponding to the formation of a $^{0,4}X_0^+$ ion and the loss of two molecules of water, a $^{2,3}X_0^+$ ion and the loss of two molecules of water, and a $^{0,2}X_0^+$ ion, respectively, whereas MS³ analysis of the $^{0,2}X_0^+ - H_2O$ ion led to $^{0,4}X_1^+$ and $^{0,3}X_1^+$ ion, both with the loss of a molecule of water (m/z 379 and 349) and a Z_1^+ ion at m/z 295. These findings were in accordance with the NMR results and therefore compound E was identified as 2''-O-xylosyl-vitexin.

This was the first time that 2''-O-xylosyl-vitexin was isolated from *D. adscendens*. This finding was confirmed afterwards by Zielinska et al.²⁰, who found this compound in an ethanolic extract (60%) of leaves of *D. adscendens*. Previously, it was also isolated from roots of *D. trifolium*.⁶⁸

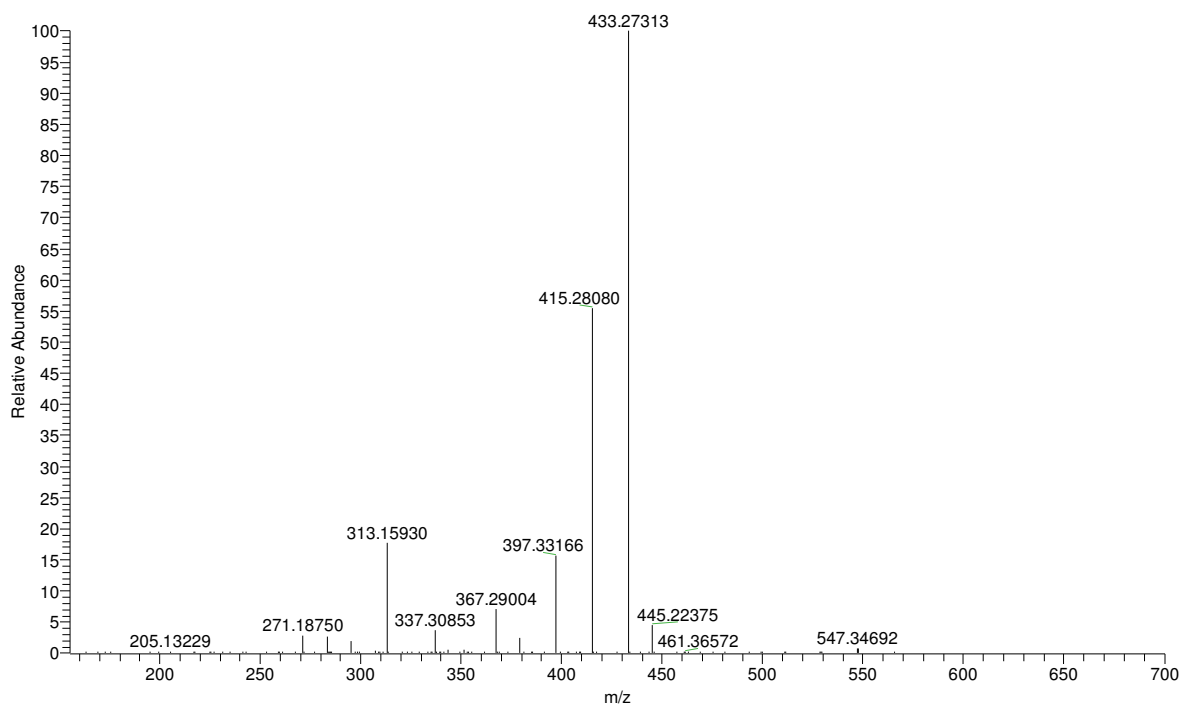


Figure 5.27 MS² spectra for compound E, 2''-O-xylosyl-vitexin in positive mode.

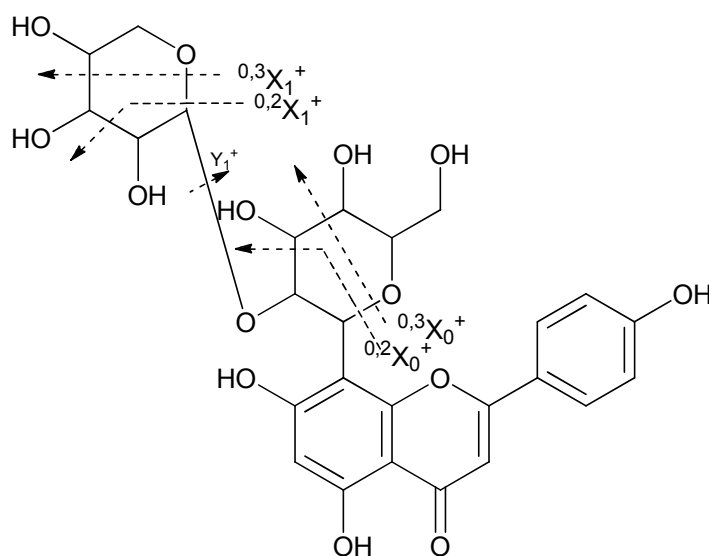


Figure 5.28 Formation of product ions for compound E, 2''-O-xylosyl-vitexin in the positive ion mode.

In order to obtain larger amounts of pure compounds and thus cleaner spectra, another isolation technique was used as described above.

Compounds isolated by HPLC-SPE

HPLC-SPE-NMR only resulted in interpretable proton NMR spectra for compounds **E** and **G**. For the other compounds, concentrations were again too low. NMR analysis was done by means of DQF-COSY, HSQC, and HMBC. The spectra of compound **E** from fraction 2 confirmed the previous experiments. This compound was already identified as vitexin-2-*O*-xyloside by NMR after semi-preparative HPLC. Compound **G** (Figure 5.29) was not a flavonoid but was the most abundant phenolic acid appearing in the chromatogram of the crude decoction of *D. adscendens*. In the ¹H-NMR spectrum (Figure 5.30) two doublets were present at δ 7.51 ($J = 8.6$ Hz) and 6.84 ($J = 8.6$ Hz) (Table 5.7). This AA'BB' spin system is typical for a 1,4-substituted aromatic ring and the signals showed cross-peaks with each other in COSY (Figure 5.31). These signals were assigned to H-2'/H-6' and H-3'/H-5', respectively. In addition, two other coupled doublets ($J = 16.0$ Hz) were present at δ 7.68 and δ 6.36, and were attributed to two olefinic protons.⁶⁹ The coupling constant of 16 Hz suggested an *E*-configuration.⁷⁰⁻⁷¹ In the COSY spectrum, these two signals were correlated with each other and were assigned as H-7' and H-8'. In the region from δ 2.5 to 6, three doublets of doublets were visible at respectively δ 5.4, δ 2.93 and δ 2.87 indicating that every proton had two other neighboring protons. Typical geminal coupling constants of H-3a and H-3b suggested that they were both attached to the same carbon atom ($J = 16.6$ Hz) and have another proton on the adjacent carbon (vicinal $J = 7.9$ Hz and 4.7 Hz). The two vicinal coupling constants with H-2 and cross-peaks from both H-3a and H-3b with H-2 in COSY confirmed these findings. MS analysis of this compound showed a deprotonated molecule at m/z 279 [M-H]⁻. This compound was identified as 2-*O*-(*E*-coumaroyl)-malic acid (Figure 5.29) and the abovementioned results were in accordance with literature.⁷²

Table 5.7 ¹H-NMR and ¹³C-NMR assignments of compound G, 2-*O*-(*E*-coumaroyl)-malic acid.

position	δ_{H} (ppm), mult., J (Hz)
1	
2	5.40, dd, $J = 7.9$ Hz, 4.7 Hz
3a	2.93, dd, $J = 16.6$ Hz, 4.7 Hz*
3b	2.87, dd, $J = 16.6$ Hz, 7.9 Hz*
4	
1'	-
2'/6'	7.51, d, $J = 8.6$ Hz
3'/5'	6.84, d, $J = 8.6$ Hz
4'	-
7'	7.68, d, $J = 16.0$ Hz
8'	6.36, d, $J = 16.0$ Hz

*Signals could be interchangeable

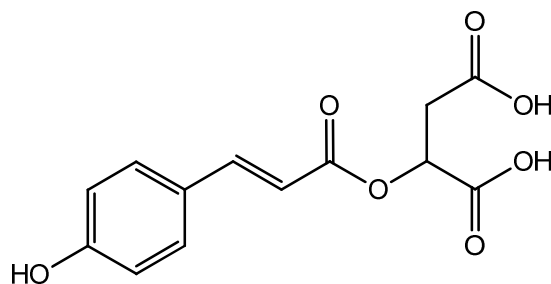


Figure 5.29 Compound G, 2-*O*-(*E*-coumaroyl)-malic acid.

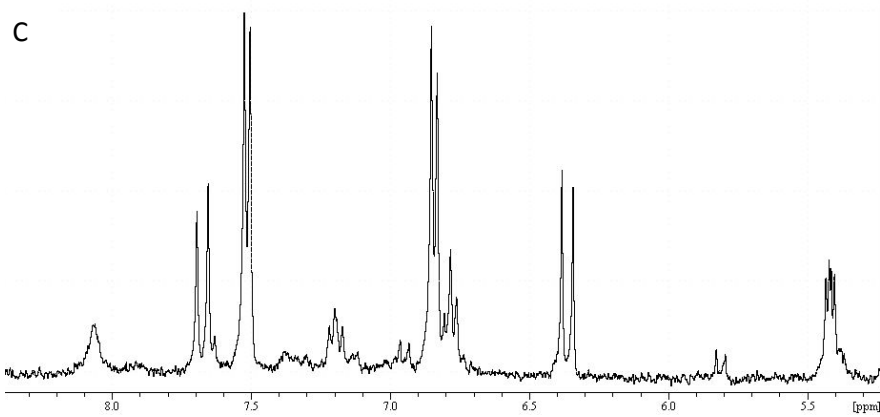
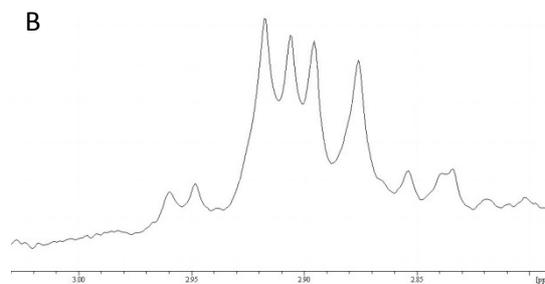
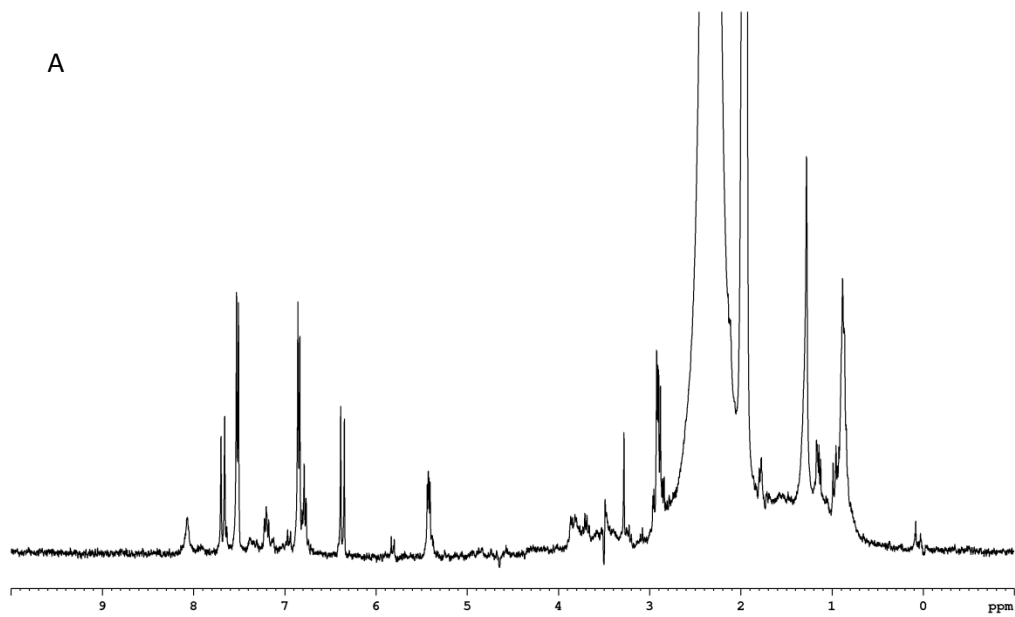


Figure 5.30 A: $^1\text{H-NMR}$ spectrum of compound G, 2-*O*-(*E*-coumaroyl)-malic acid; B close-up (2.8 – 3 ppm) of A; C: close up (5.3 – 8.3 ppm) of A.

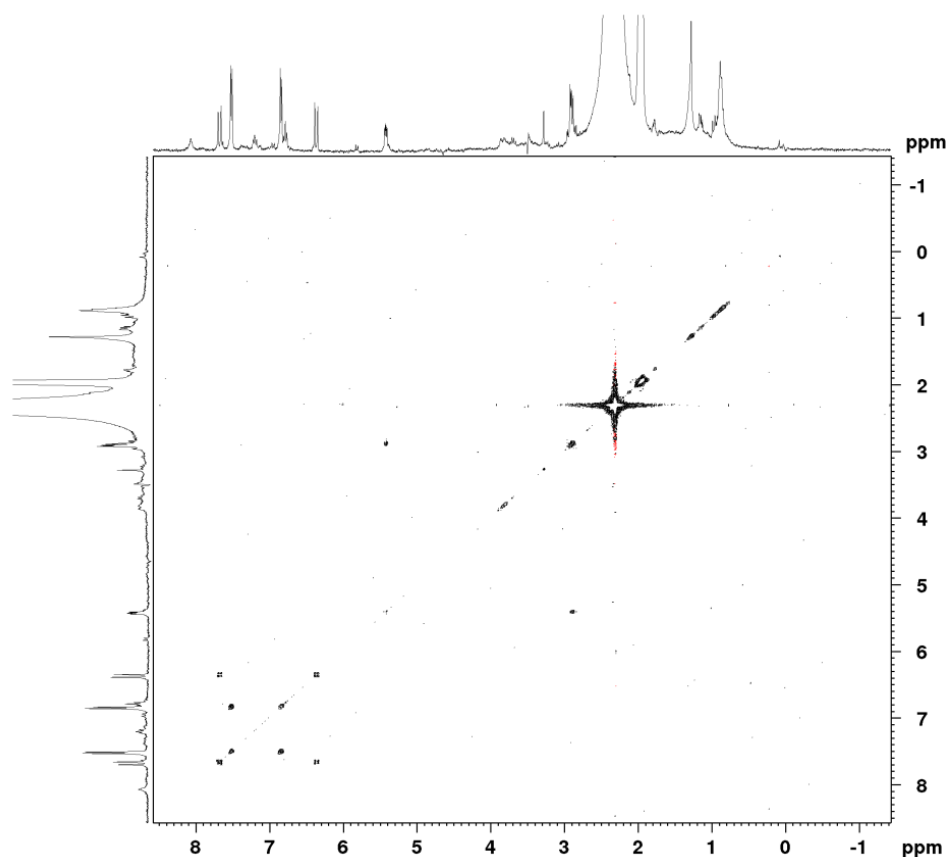


Figure 5.31 DQF-COSY spectrum of compound G, 2-O-(*E*-coumaroyl)-malic acid.

Compounds elucidated with HPLC-MS

In addition to NMR, also MS and MS/MS experiments were carried out. Experiments on an LC-MSD ion trap equipped with DAD made it easier to select the peaks of interest. Peaks with a typical flavonoid UV spectrum were selected for MSⁿ experiments to obtain fragmentation patterns. Experiments were performed with both an LC-MSD ion trap and an LC-LXQ linear ion trap. Figure 5.32 shows the chromatogram recorded at 334 nm, which is the absorption maximum of flavones. The peaks marked with a black arrow were selected for MSⁿ experiments and showed ions at *m/z* of 431, 563 or 593 in the negative ion mode, and at *m/z* 433, 565 or 595 in the positive ion mode.

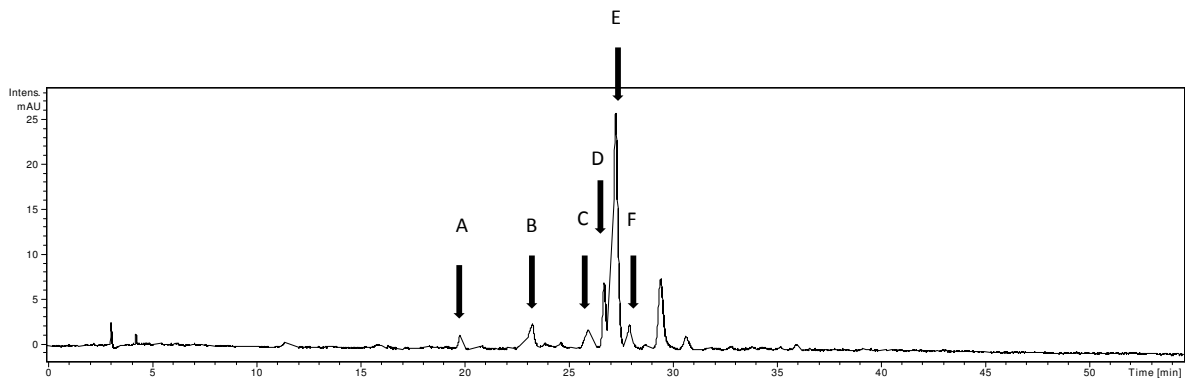


Figure 5.32 UV chromatogram of a decoction of *D. adscendens* at 334 nm obtained with the HPLC-DAD-ion trap.

These experiments resulted in an MS/MS chromatogram as shown in Figures 5.33 and 5.34 (obtained with HPLC-MS using the LXQ linear ion trap). In addition to the major peaks, a lot of smaller peaks can be seen in addition to the peaks visible with UV detection because of the higher sensitivity of the mass spectrometric detector.

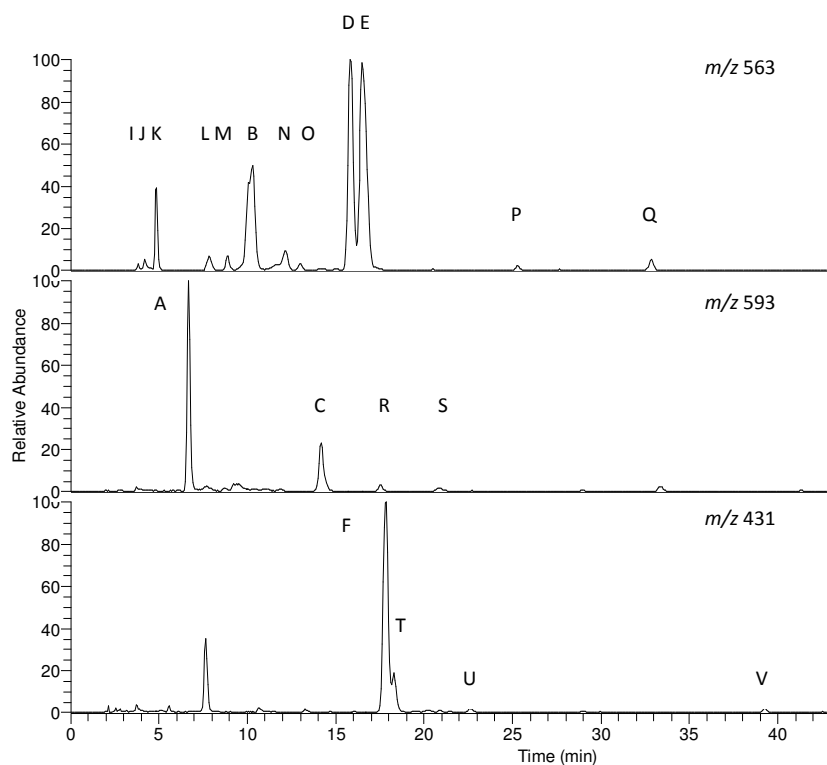


Figure 5.33. MS/MS chromatogram of m/z 563, m/z 595 and m/z 431 in the negative ion mode.

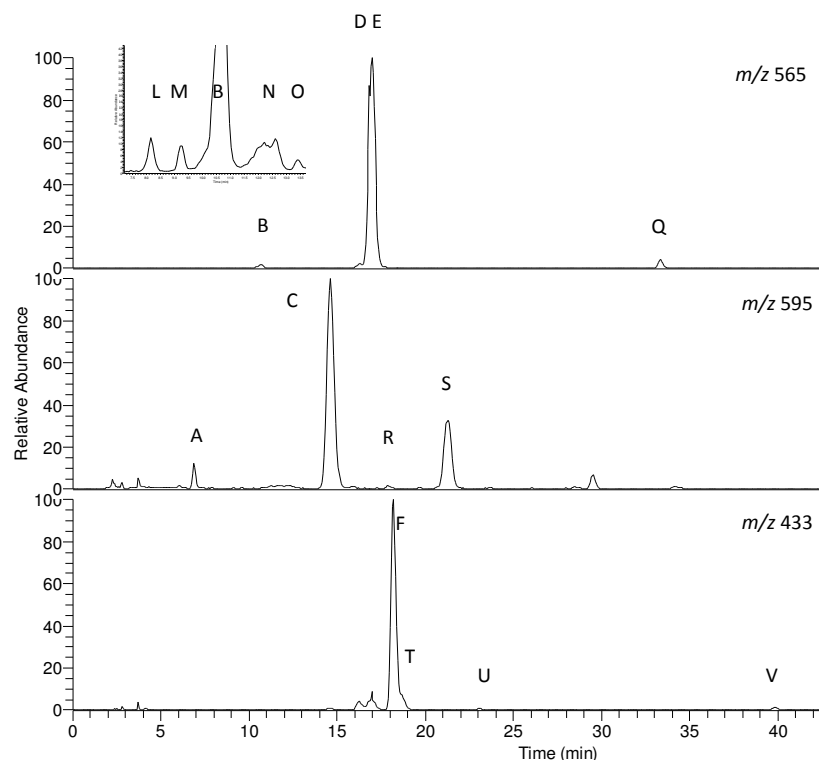


Figure 5.34 MS/MS chromatogram of m/z 565, m/z 595 and m/z 433 in the positive ion mode.

Since different attempts to isolate the minor flavonoids were not successful and standard material from the suspected flavonoid molecules (schaftoside, isoschaftoside, vicenin-1, and vicenin-2) were too expensive, the crude extract of *D. adscendens* was also compared with an extract of *Passiflora incarnata* known to contain C-glycosides of apigenin.

Compounds I, J, and K showed a deprotonated molecule at m/z 563 $[M-H]^-$. MS² analysis of these compounds resulted in similar product ion spectra shown in Figure 5.35. Product ions at m/z 501, 461 and 419 were formed by the loss of 62 u, 102 u, and 144 u, respectively. The formation of these product ions formed in the negative ion mode suggested the presence of a 3-hydroxymethyl glutaryl moiety as described by Di Donna, Pereira, and Barreca.⁷³⁻⁷⁵ In the positive ion mode, a product ion at m/z 433 was formed by the loss of 132 u which suggested that a pentose unit was present. MS³ analysis of the product ion at m/z 419 resulted in product ions at m/z 401, 391, 293 and 287, which could be explained by the loss of a water molecule $[M-144-18-H]^+$, the loss of CO $[M-144-28-H]^+$, the loss of a pyranone unit $[M-144-126-H]^+$, and the loss of a pentose moiety $[M-144-132-H]^+$. The accurate mass of the most abundant compound was m/z 563.1623 $[M-H]^+$ suggesting a molecular formula of $C_{23}H_{32}O_{16}$ with an error of 0.954 ppm. Because of the low intensity, due to the low

concentration of these compounds in the extract, their UV spectrum was not clear, but examining these data, it was obvious that they were not flavonoids. Based on these results compounds **I-K** were tentatively identified as 3-hydroxymethylglutaryl, pentosyl-hexosyl-pyranones.

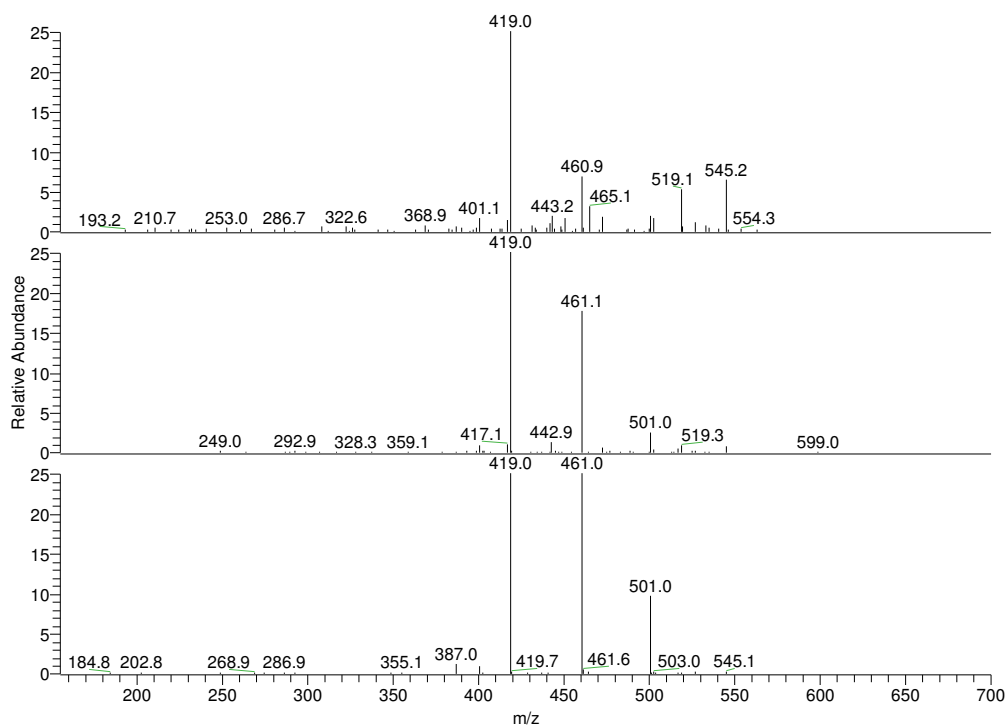


Figure 5.35 MS² spectra of compounds I-K.

Compounds **L**, **M**, **B1**, **B2**, **N** and **O** all showed a deprotonated molecule at m/z 563 $[M-H]^-$ like compounds **I-K** but the product ion spectra were totally different. MS^2 analysis of compounds **B1**, **B2** and **L** to **O** resulted in similar product ion spectra with product ions at m/z 545, 503, 485, 473, 455, 443, 425, 413, 383 and 353 in the negative ion mode (Figure 5.36). The product ion at m/z 545 is formed by the loss of a water molecule $[M-18-H]^-$. Product ions at m/z 503, 473 and 443, a $^{0,3}X_P^-$ ion, $^{0,2}X_P^-$ ion or a $^{0,3}X_H^-$ ion, and a $^{0,2}X_H^-$ ion, respectively, resulted from cross-ring cleavages of saccharidic residues. These cross-ring cleavages are typical for flavonoid C-glycosides (Figure 5.37).^{63,66,76}

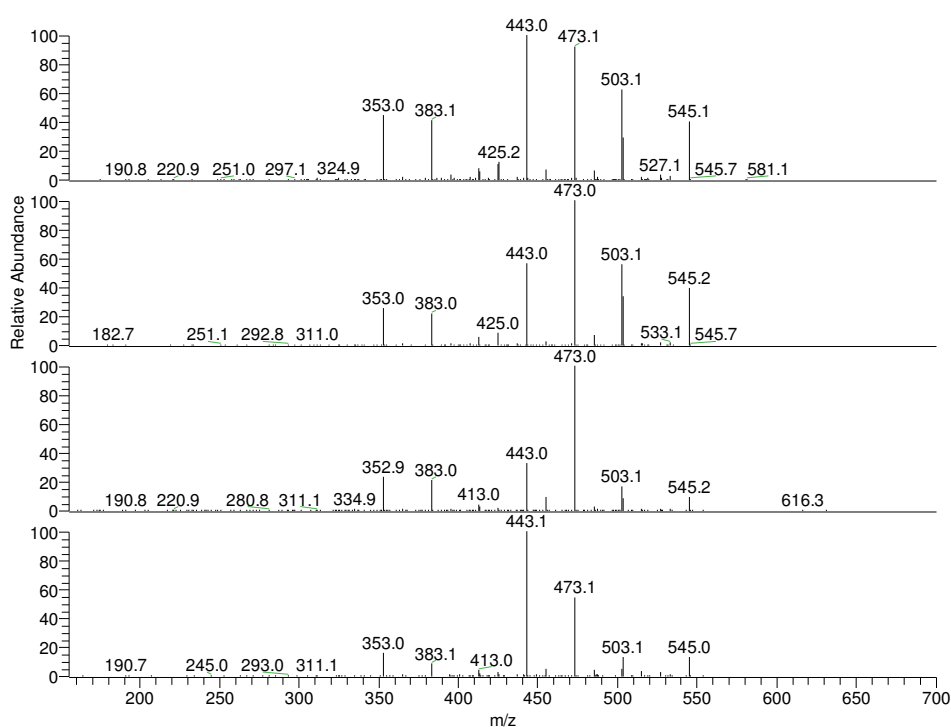


Figure 5.36 MS^2 spectra of compounds **L**, **M**, **O**, and **P**.

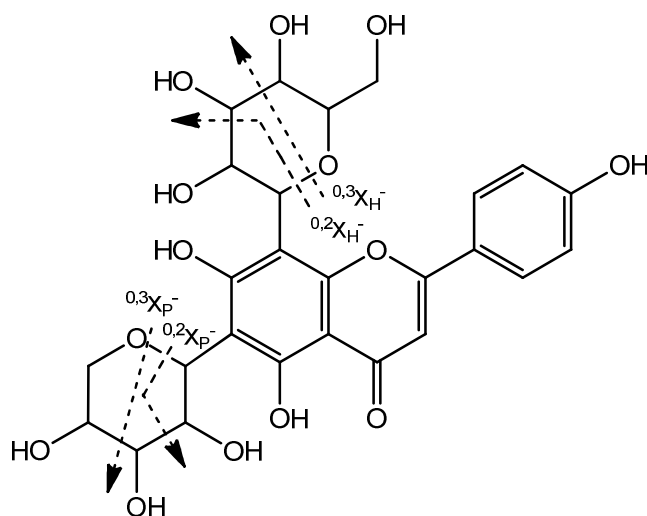


Figure 5.37 Cross-ring cleavages in compound B2 in the negative ion mode.

Subsequent losses of water gave rise to product ions at m/z 485, 455, and 425. The product ion at m/z 413 was obtained by $^{0,3}X_{P/H}^-$ cross-ring cleavages. The formation of product ions at m/z 383 [Ag+113-H] $^-$ and 353 [Ag+83-H] $^-$ revealed the nature of the aglycone to be apigenin with di-C substitution.⁶⁴ An explanation of all product ions is given in Table 5.8. When a closer look is taken at the peak at R_t 10.2 min, it is clear that this peak consisted of two non-separated peaks due to two co-eluting compounds (Figure 5.38). This was also confirmed by examining the MS² spectrum of the first and the last parts of the peak, which gave the same product ions but with totally different relative abundances (Figure 5.39). MS³ analysis of $^{0,2}X_{P/H}^-$ and $^{0,3}X_{P/H}^-$ product ions resulted in product ions which were also formed by cross-ring cleavages and confirmed the presence of two sugar moieties attached to apigenin by a C-glycosidic bond (Table 5.9).

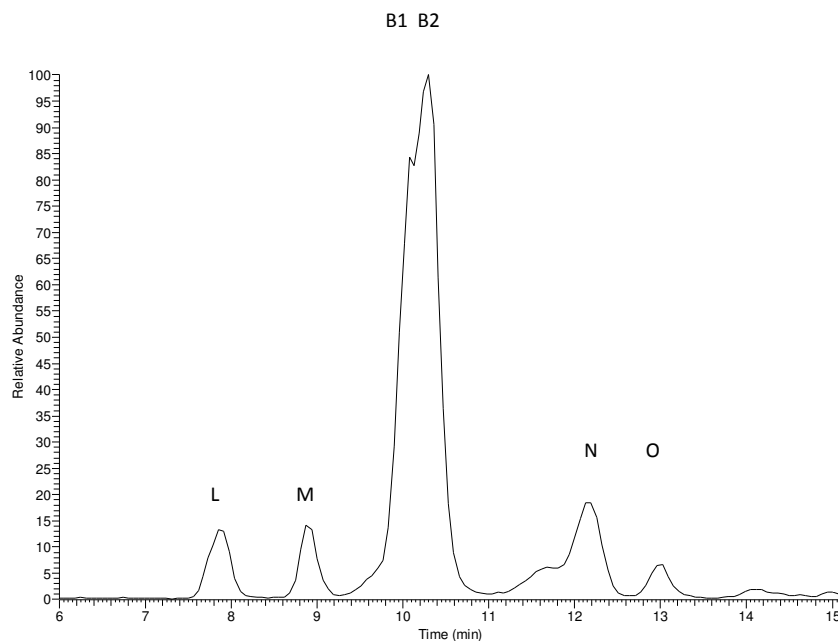


Figure 5.38 MS² chromatogram of compounds B1, B2, and L-O. The largest peak is that from B1 and B2.

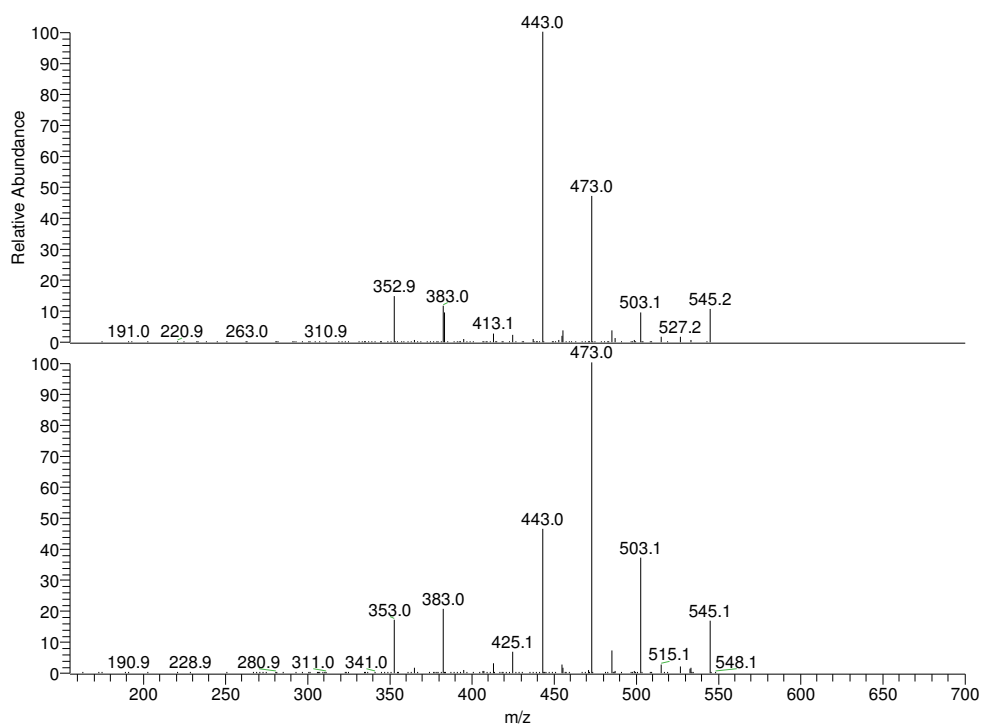


Figure 5.39 MS² spectra of compounds B1 and B2 in the negative ion mode.

In the positive mode, the loss of one, two, three or four molecules of water was observed giving rise to product ions at m/z 547, 529, 511, and 493 (Figure 5.40). The following product ions at m/z 499, 481, 475 and 457 corresponded to a $^{0,4}X_p^+$ ion followed by the loss of two or three water molecules, and a $^{0,2}X_p^+$ ion as such and followed by the loss of a water molecule, whereas the product ions at m/z

469, 451, 445 and 427 arose from the same type of cross-ring cleavage fragments but of a hexose unit instead of a pentose unit. The formation of product ions at m/z 409 and 415 could be explained by a $^{0,2}X_H^+$ ion followed by the loss of two molecules of water and a $^{0,3}X_P^+$ ion together with a $^{0,3}X_H^+$ ion. The loss of one and two molecules of water gave rise to ions at m/z 397 and 379, respectively. An overview of all cross-ring cleavages is given in Figure 5.41 and Table 5.8. This confirmed the findings in the negative ion mode.

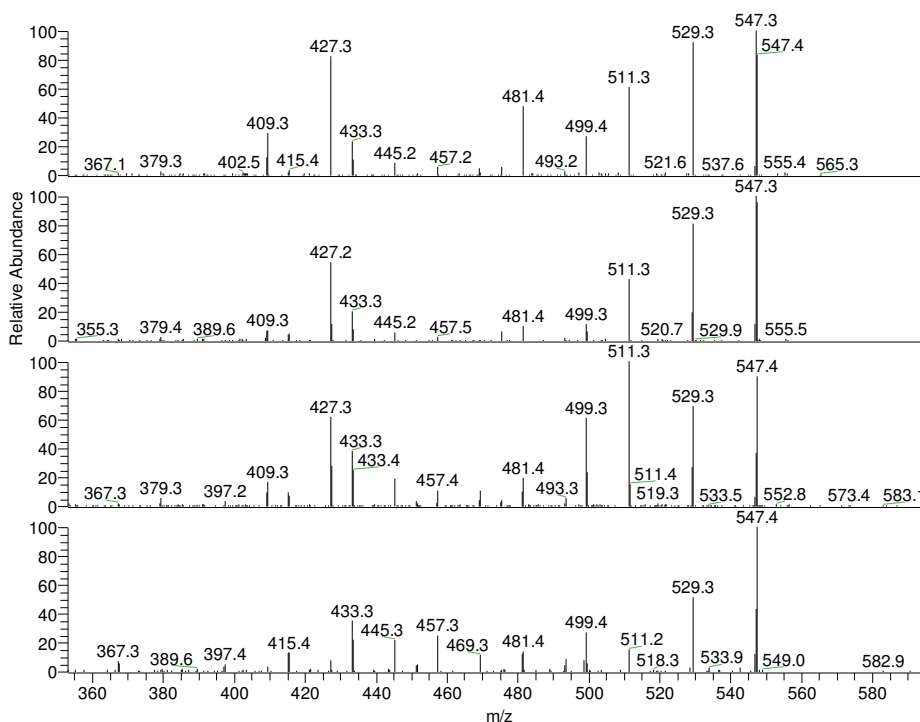


Figure 5.40 MS² spectra of compounds L, M, N and O in the positive ion mode.

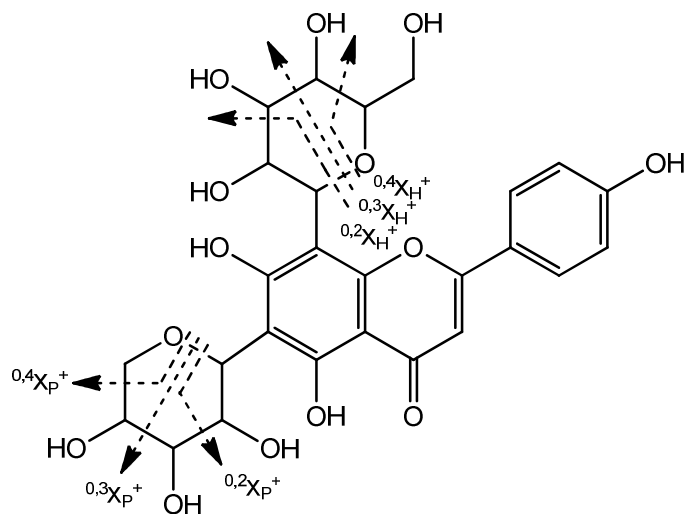


Figure 5.41 Cross-ring cleavages in compound B2 in the positive ion mode.

The MS² spectrum taken from the first part and the last part of the peak at R_t 10.2 min gave the same product ions but with totally different relative abundances, which was also seen in the negative ion mode (Figure 5.42).

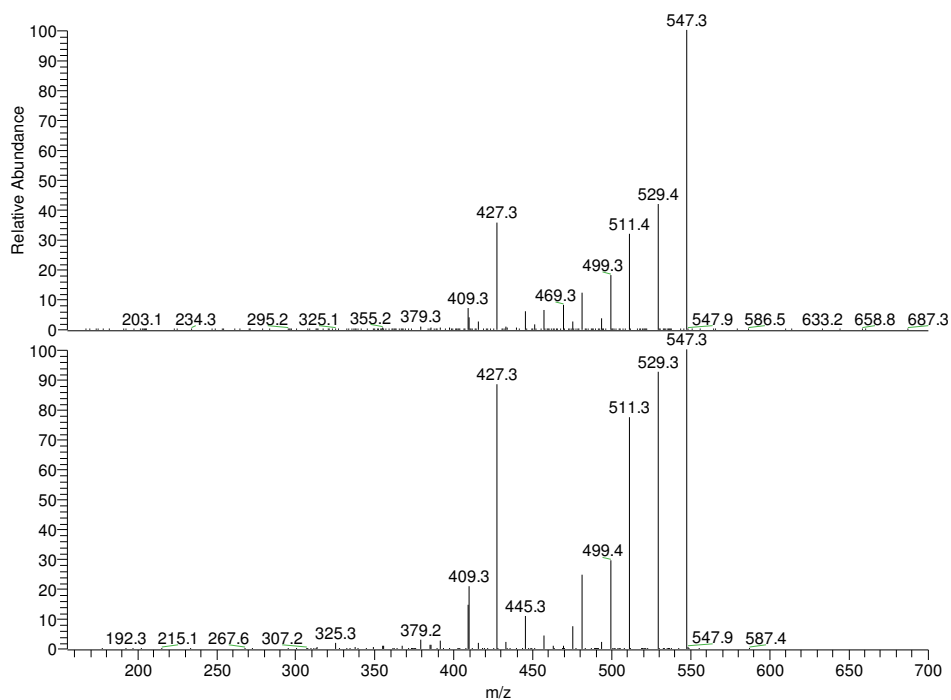


Figure 5.42 MS² spectra of compounds B1 and B2 in the positive ion mode.

MS³ analysis of the ^{0,2}X_p⁺- H₂O product ion resulted in product ions which were also formed by cross-ring cleavages, confirming the presence of di-C-glycosides of apigenin. A full overview is given in Table 5.9.

After comparison with an extract of *Passiflora incarnata* and literature, compounds **B1** and **B2** could be identified as schaftoside and isoschaftoside (Figure 5.43), which were also isolated from other *Desmodium* species, namely *D. styracifolium* and *D. uncatum*.^{59,60,63-65,68,77-82}

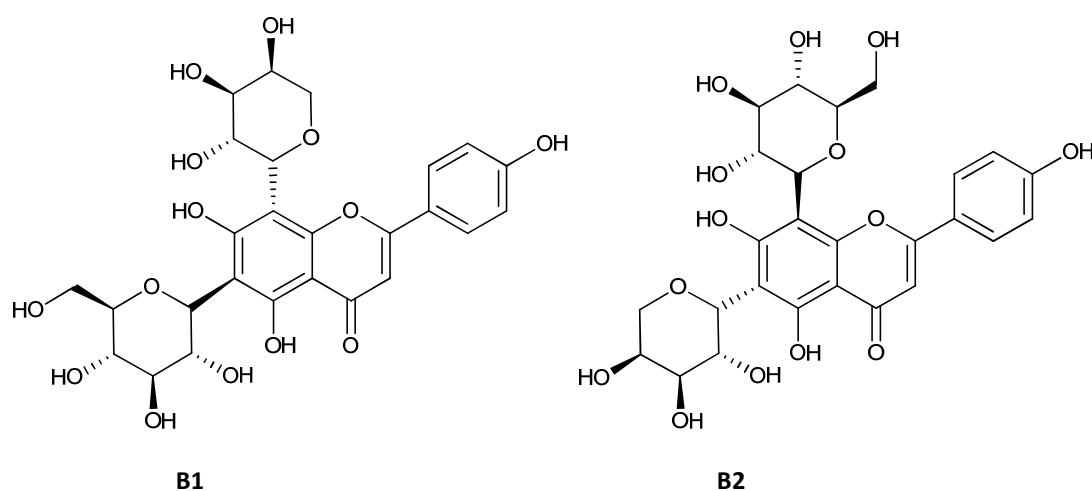


Figure 5.43 Structure of compounds B1, schaftoside and B2, isoschaftoside.

Compounds **L**, **M**, **N** and **O** (Figure 5.38) were elucidated as apigenin di-C-glycosides, more specifically x-C-pentosyl-x-C-hexosyl-apigenin derivatives, and possibly two of these compounds are vicenin-1 and vicenin-3, already found in aerial parts of *D. styracifolium*.^{68,83}

Table 5.8 Product ions formed for compounds B1, B2, and O-L.

Product ion m/z - negative ion mode

545	[M-H-18] ⁻ Loss of water molecule
503	[M-H-60] ⁻ ^{0,3} X ⁻ fragment of a pentose
485	[M-H-60-18] ⁻ ^{0,3} X ⁻ fragment of a pentose and additional loss of water molecule
473	[M-H-90] ⁻ ^{0,2} X ⁻ fragment of a pentose or a ^{0,3} X ⁻ fragment of a hexose
455	[M-H-90-18] ⁻ ^{0,2} X ⁻ fragment of a pentose or a ^{0,3} X ⁻ fragment of a hexose and additional loss of a water molecule
443	[M-H-120] ⁻ ^{0,2} X ⁻ fragment of a hexose
425	[M-H-120-18] ⁻ ^{0,2} X ⁻ fragment of a hexose and additional loss of a water molecule
413	[M-H-60-90] ⁻ ^{0,3} X ⁻ fragment of a pentose and a ^{0,3} X ⁻ fragment of a hexose
383	[M-H-90-90] ⁻ ^{0,2} X ⁻ fragment of a pentose and a ^{0,3} X ⁻ fragment of a hexose, Ag + 113
353	[M-H-90-120] ⁻ ^{0,2} X ⁻ fragment of a pentose and a ^{0,2} X ⁻ fragment of a hexose, Ag + 83

Table 5.8 continued

Product ion m/z - positive ion mode

547	$[M+H-18]^+$ Loss of one molecule of water
529	$[M+H-18-18]^+$ Loss of two molecules of water
511	$[M+H-18-18-18]^+$ Loss of three molecules of water
499	$[M+H-30-18-18]^+$ $^{0,4}X^+$ fragment of a pentose and additional loss of two molecules of water
493	$[M+H-18-18-18-18]^+$ Loss of four molecules of water
481	$[M+H-30-18-18-18]^+$ $^{0,4}X^+$ fragment of a pentose and additional loss of three molecules of water
475	$[M+H-90]^+$ $^{0,2}X^+$ fragment of a pentose
469	$[M+H-60-18-18]^+$ $^{0,4}X^+$ fragment of a hexose and additional loss of two molecules of water
457	$[M+H-90-18]^+$ $^{0,2}X^+$ fragment of a pentose and additional loss of a water molecule
451	$[M+H-60-18-18-18]^+$ $^{0,4}X^+$ fragment of a hexose and additional loss of three molecules of water
445	$[M+H-120]^+$ $^{0,2}X^+$ fragment of a hexose
427	$[M+H-120-18]^+$ $^{0,2}X^+$ fragment of a hexose and additional loss of a water molecule
415	$[M+H-60-90]^+$ $^{0,3}X^+$ fragment of a pentose and a $^{0,3}X^+$ fragment of a hexose
409	$[M+H-120-18-18]^+$ $^{0,2}X^+$ fragment of a hexose and additional loss of two water molecules
397	$[M+H-60-90-18]^+$ $^{0,3}X^+$ fragment of a pentose and a $^{0,3}X^+$ fragment of a hexose and additional loss of a water molecule
379	$[M+H-90-60-18-18]^+$ $^{0,3}X^+$ fragment of a hexose and $^{0,3}X^+$ fragment of a pentose and additional loss of two water molecule

Compounds **D**, **P** and **Q** also showed the same deprotonated molecule as compound **E**, elucidated as 2''-*O*-xylosyl vitexin, at m/z 563 $[M-H]^-$ and MS^2 analysis of them resulted in a similar product ion spectrum for each compound (Figure 5.44). The same product ions were formed as for compound **E**. MS^3 analysis of the most abundant ion in MS^2 (Z_1^-) resulted in a product ion at m/z 293 which also was found for compound **E**.

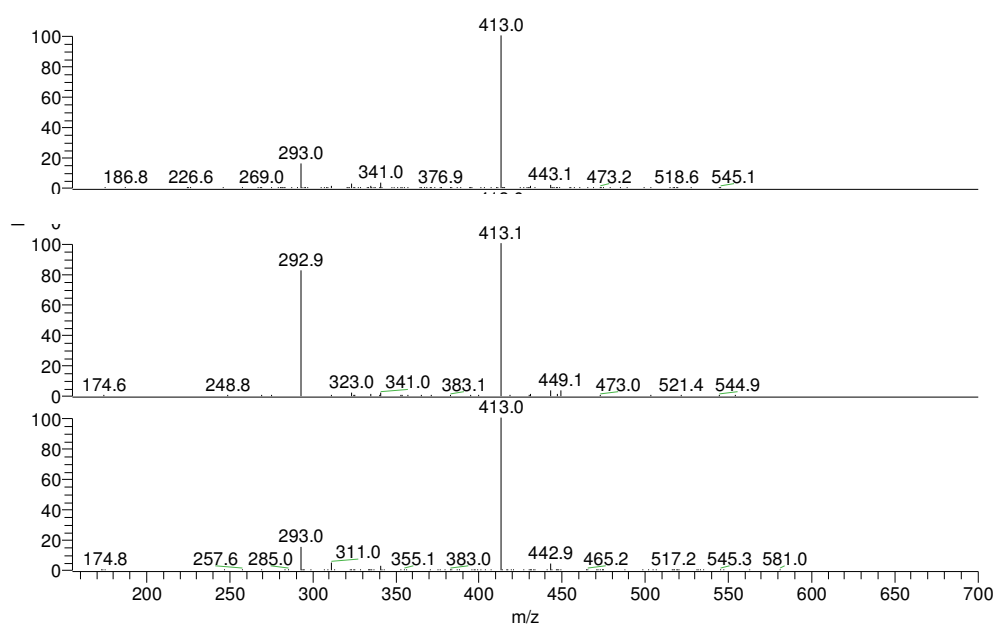


Figure 5.44 MS^2 spectra of compound **D**, **P** and **Q** in the negative mode.

In the positive ion mode, also the same product ions were present as for compound **E** (Figure 5.45). MS^3 analysis led to the same product ions as for compound **E**. These findings led to the characterization of compounds **D**, **P** and **Q** (Figures 5.33 and 5.34) as 2-*O*-pentosyl-*x*-*C*-hexosyl-apigenin isomers such as compound **E**, already identified as 2''-*O*-xylosyl-vitexin.⁷⁴ The exact binding position of the pentose and hexose is not known and the identity of the sugars stays unclear. Although some research was done in order to distinguish between 6-*C* and 8-*C* isomers, this is still highly dependent on the apparatus and settings used and can only be done when isomers co-exist.^{63,84,85} In addition, literature on this topic is rather limited. One of these compounds could be 2''-*O*-xylosyl-isovitexin as described by Zielinska et al.²⁰

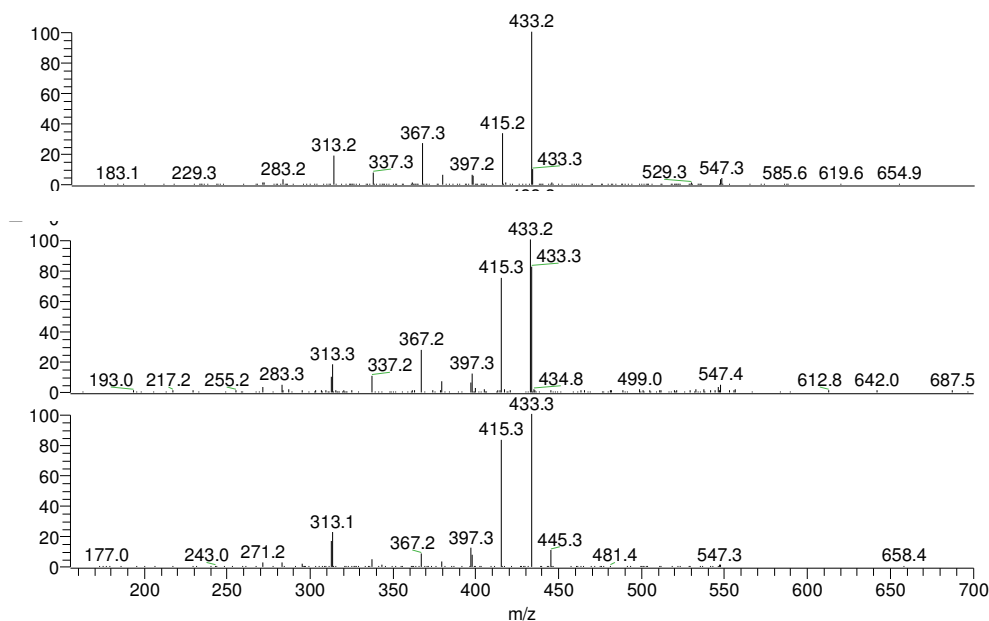


Figure 5.45 MS² spectra for compounds D, P, and Q in the positive mode.

Compound A (Figures 5.33 and 5.34) showed a deprotonated molecule at m/z 593 [M-H]⁻ and a protonated molecule at m/z 595 [M+H]⁺. MS² experiments showed some similar product ions as found for compound L to O (Figures 5.46 and 5.47). The loss of a water molecule (loss of 18 u) resulted in a product ion at m/z 575, the loss of 90 u and 120 u resulted in the formation of diagnostic product ions at m/z 503 (^{0,3}X_H⁻ ion) and 473 (^{0,2}X_H⁻ ion), which suggested two hexose moieties attached to the aglycone by a C-C binding. Product ions at m/z 383 [Ag+113-H]⁻ and m/z 353 [Ag+83-H]⁻ suggested apigenin as aglycone with di-C glycosylation.^{61,62} MS³ analysis of the diagnostic ions resulted in ^{0,2}X_H⁻ and ^{0,3}X_H⁻ ions at m/z 383 and 353.

MS² of m/z 595 [M+H]⁺ resulted in product ions at m/z 577, 559, 541 and 529 formed by the loss of one, two or three water molecules or by the loss of two water molecules and a CH₂O molecule, respectively. A ^{0,2}X_H⁺ product ion at m/z 475 was formed. Loss of a water molecule resulted in an ion at m/z 457. Small ion peaks at m/z 499 and m/z 481 were due to the formation of a ^{0,4}X_H⁺ ion and the loss of two and three molecules of water. MS³ of m/z 457 resulted in the loss of water molecules (m/z 439 and 421) and a CH₂O and H₂O molecule (m/z 409) and formation of ^{0,2}X_H⁺ (m/z 337) and ^{0,4}X_H⁺-H₂O (m/z 379) ions. These findings together with those in the negative ion mode confirmed a di-C-hexosyl-apigenin as structure. Through comparison with an extract of *Passiflora incarnata* and

literature, compound **A** could be identified as vicenin-2 (Figure 5.48), which was already isolated from *D. styracifolium*.^{59,64-66,75,77,80-84,86}

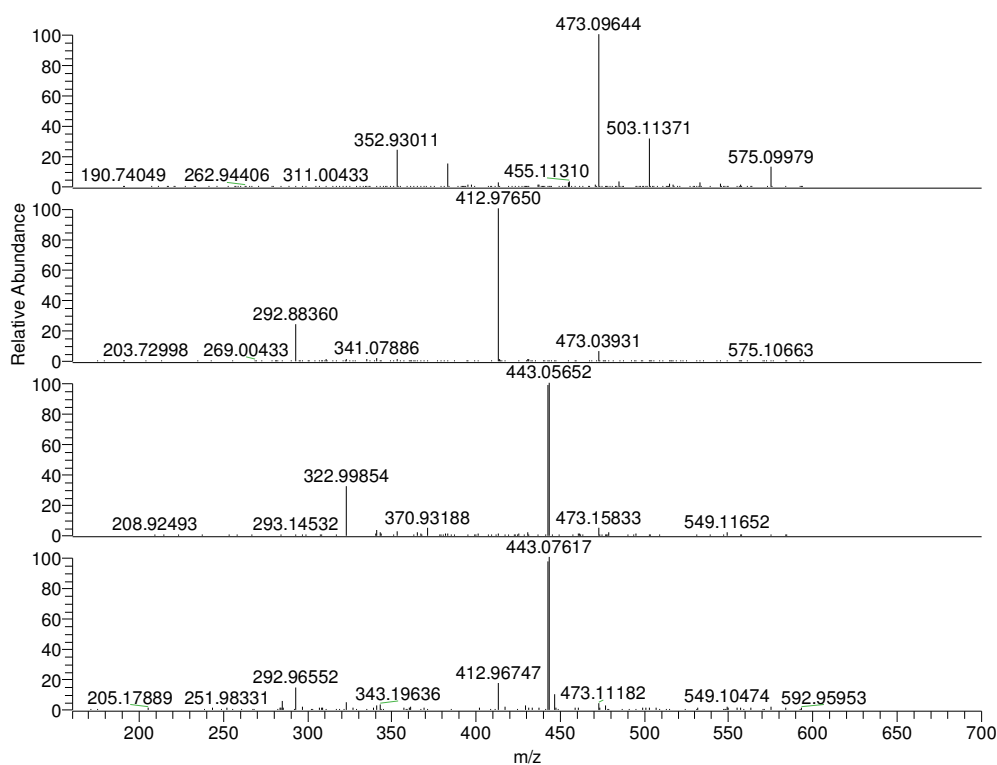


Figure 5.46 MS² spectra of compounds **A**, **C**, **R** and **S** in the negative ion mode.

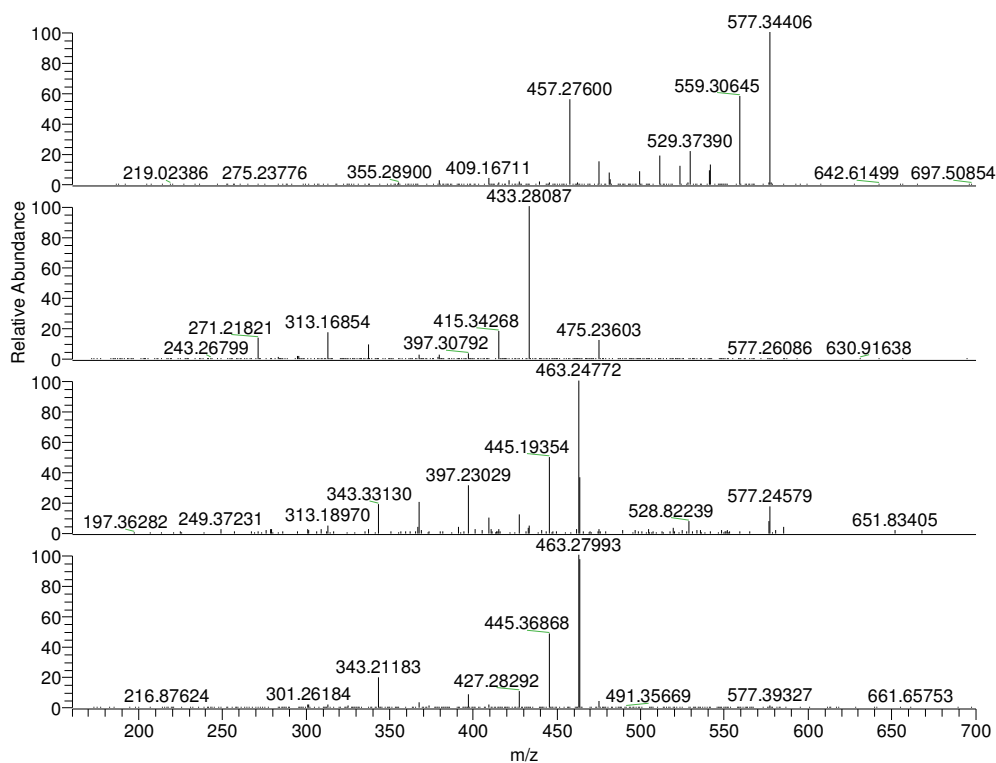


Figure 5.47 MS² spectra for compounds **A**, **C**, **R** and **S** in the positive ion mode.

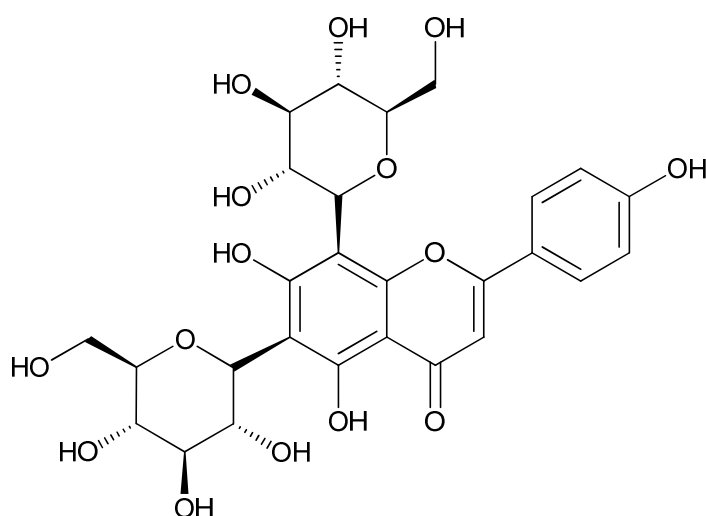


Figure 5.48 Structure of compound A, vicenin-2.

Compound C also showed a deprotonated molecule at m/z 593 $[M-H]^-$ and a protonated molecule at m/z 595 $[M+H]^+$. The product ion Z_1^- at m/z 413 is due to the loss of 180 u, which suggested the presence of a hexose. Also a $^{0,2}X_0^-$ product ion at m/z 473 as well as a $^{0,2}X_0^+$ product ion at m/z 475 was formed. This ion was also compatible with a hexose and pointed to a C-glycosidic bond. The presence of these ions suggested a 1→2 binding. A product ion at m/z 293 $[Ag+41-18-H]^-$ was indicative for apigenin as an aglycone. In the positive ion mode, the most abundant ion in MS^2 was found at m/z 433 (Y_1^+) $[M-162+H]^+$ which was indicative for the loss of a hexose moiety bound by an O-glycosidic binding. The subsequent loss of one molecule of water gave rise to a product ion at m/z 415, whereas the formation of a $^{0,2}X_0^+$ ion resulted in an ion at m/z 313. An internal cleavage of the O-glycosylated sugar moiety resulted in the formation of a $^{0,2}X_1^+$ ion which together with a $^{0,2}X_0^+$ ion and loss of a water molecule led to the product ion at m/z 337. Formation of an ion at m/z 271 confirmed the finding that the aglycone was apigenin.⁷⁴ MS^3 of m/z 433 resulted in multiple water losses (m/z 415, 397, and 379), loss of two water molecules and one or two CH_2O molecules (m/z 367 and 337) and a $^{0,2}X_0^+$ ion (m/z 313). The formation of a $^{0,2}X_0^+$ ion combined with the loss of a water molecule or a CH_2O molecule resulted in ion peaks at m/z 295 and 283.

This compound was characterized as an x-O-hexosyl-x-C-hexosyl-apigenin, and tentatively identified as 2''-O-glucosylvitexin (Figure 5.49), also isolated from the roots of *D. trifolium*.⁶⁸

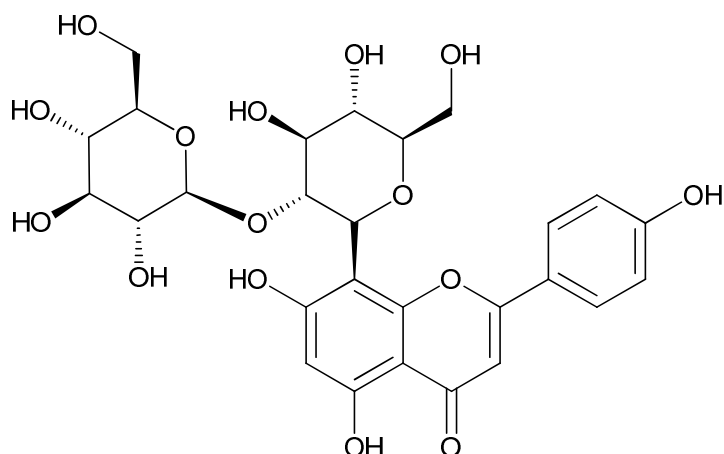


Figure 5.49 structure of compound C, tentatively identified as 2''-O-glucosyl-vitexin.

Compounds **R** and **S** both showed a deprotonated molecule at m/z 593 $[M-H]^-$ and a protonated molecule at 595 $[M+H]^+$ and produced product ions at m/z 473, 433, 371 and 323 in the negative ion mode (Figure 5.46). The most abundant ion was found at m/z 443, being a Z_1^- ion typical for a pentose and an *O*-glycosidic bond. A smaller ion at m/z 473 corresponds to a $^{0,2}X_0^-$ product ion which indicated a *C*-glycosidic bond. Product ions at m/z 323 and 371 could be explained by $[Ag+41-18-H]^-$ and $[Ag+71-H]^-$ and were indicative for methyl luteolin.^{23,63,74} The ion at m/z 323 was also obtained when MS³ analysis of m/z 433 (Z_1^-) was done. In the positive ion mode, the most abundant peak in MS² was found at m/z 463 (Y_1^+) $[M-132+H]^+$, which was indicative of the loss of a pentose moiety bound by an *O*-glycosidic binding (Figure 5.47). The subsequent loss of a molecule of water gave rise to a product ion at m/z 445, whereas the formation of a $^{0,2}X_0^+$ ion resulted in an ion at m/z 343. An internal cleavage of the sugar moiety of *C*-glycosylation resulted in the formation of a $^{0,2}X_0^+$ ion which together with a $^{0,2}X_1^+$ or $^{0,3}X_1^+$ ion and loss of a water molecule led to product ions at m/z 367 and 397. MS³ of m/z 463 (Y_1^+) resulted in multiple water losses (m/z 445, 427 and 409), loss of two water molecules and one or two CH_2O molecules (m/z 397 and 367) and a $^{0,2}X_0^+$ ion (m/z 343). The formation of a $^{0,2}X_0^+$ ion combined with the loss of a CH_2O molecule resulted in an ion at m/z 313. These compounds could be tentatively identified as 2-*O*-pentosyl-*x-C*-hexosyl-methyl luteolin.^{63,74} This is the first time that *O,C*-glycosides of luteolin were found in *D. adscendens*. Biaocchi et al.²³ described the presence of a 5-*O*-glycoside, a 7-*O*-glycoside, and di-*C*-glycosides of luteolin in *D. adscendens*, and Ma et al.⁸⁷ found a 6-*C*-glucosyl-luteolin in *D. styracifolium*.

Compound **F** and **T** were already identified as vitexin and isovitexin, respectively, after spiking with a standard solution (Figure 5.50). MS and MS² experiments, showing a deprotonated molecule at m/z 431 [M-H]⁻ and a protonated molecule 433 [M+H]⁺ and the formation of a ^{0,2}X₀⁻ and ^{0,3}X₀⁻ ion together with a ^{0,2}X₀⁺ and ^{0,4}X₀⁺-H₂O ion confirmed these findings (Figures 5.51 and 5.52). Also, MS³ findings (Table 5.9) were in accordance with these findings and literature.^{4,23}

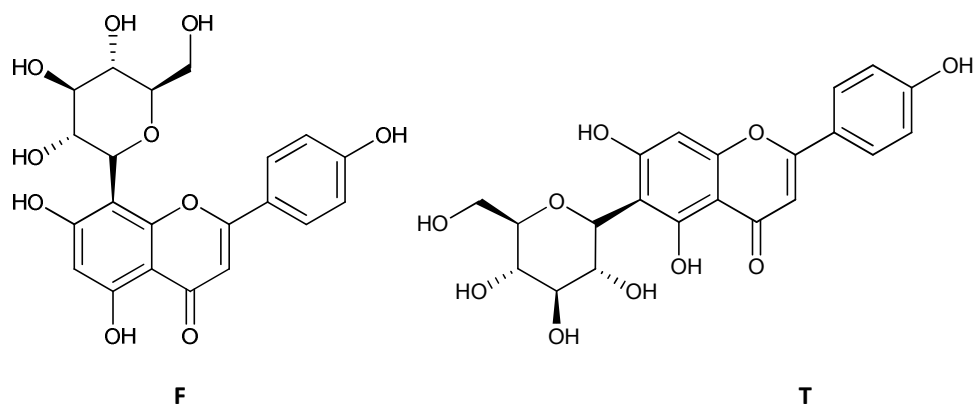


Figure 5.50 Structure of compound **F**, vitexin and compound **T**, isovitexin.

Compound **U**, showing the same deprotonated molecule and protonated molecule in the negative and the positive ion mode, respectively, as compounds **F** and **T**, was tentatively identified as x-O-hexosyl-apigenin because of the presence of product ions at m/z 269 [M-162-H]⁻ and 271 [M-162+H]⁺ (Figure 5.51 and Figure 5.52). Spiking with apigenin-7-O-glucoside revealed that the hexose in compound **U** was not attached in 7 position.

Since all results of compound **V** were similar to those found for compound **F** and **T**, it was concluded that compound **V** was another apigenin-C-hexoside (Figure 5.51 and Figure 5.52).

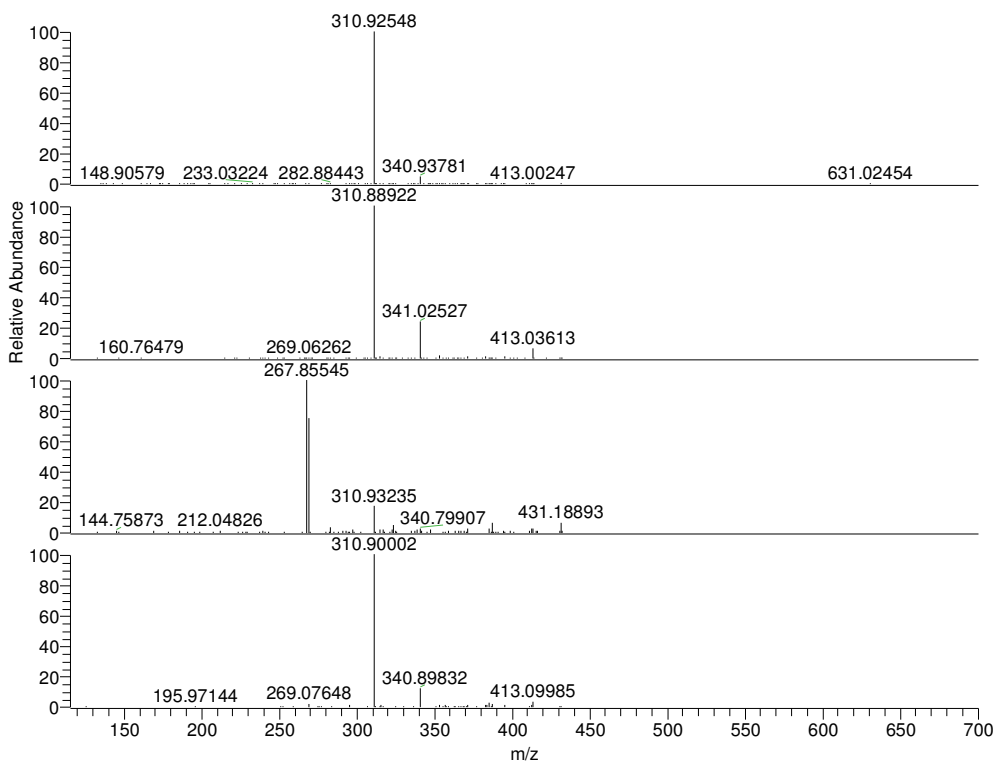


Figure 5.51 MS² spectra of compounds F, T, U and V in the negative ion mode.

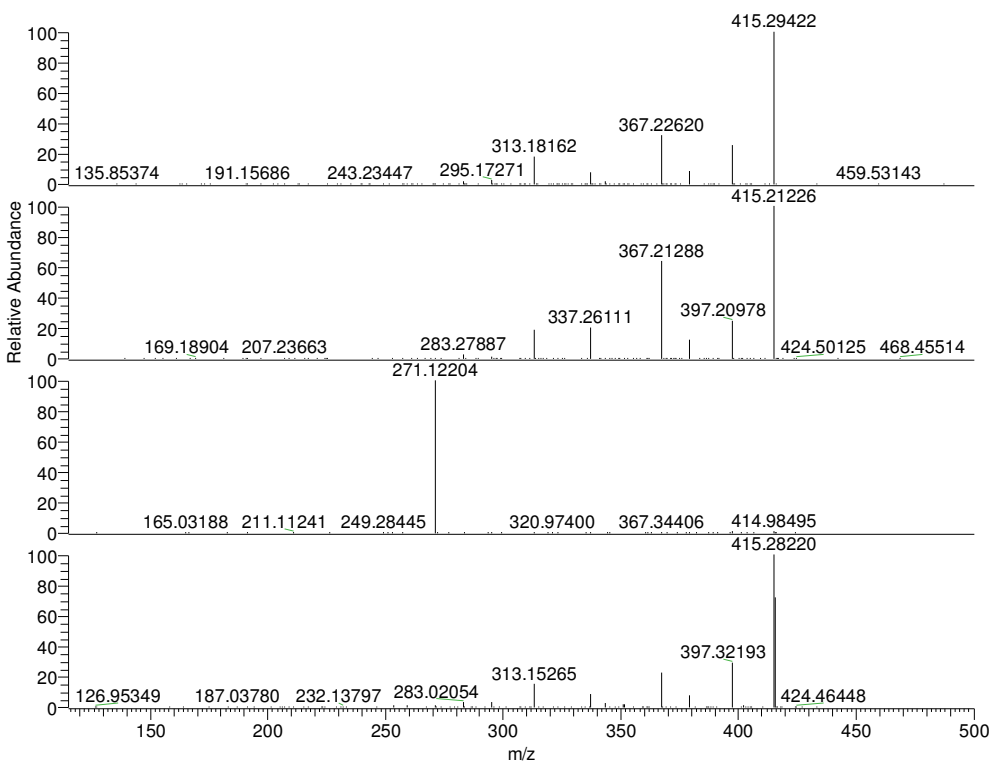


Figure 5.52 MS² spectra of compounds F, T, U and V in the positive ion mode.

Additional screening for known compounds by LC-HRMS

Analysis with high resolution mass spectrometry showed the presence of minor compounds described in literature like x-O-pentosyl-x-C-hexosyl-kaempferol or x-O-pentosyl-x-C-hexosyl-luteolin (HRMS $[M-H]^-$ = 579.1356, M = C₂₆H₂₈O₁₅ 0.927 ppm) (MS² analysis resulted in product ions at *m/z* 459, 429, 357, 327, and 285) and rhamnosyl-pentosyl-apigenin (HRMS $[M-H]^-$ = 577.1570, M = C₂₇H₃₀O₁₄ 0.76 ppm) (MS² analysis resulted in product ions at *m/z* 413 and 293) and luteolin or kaempferol O- and C-hexosides (HRMS $[M-H]^-$ = 447.0937, M = C₂₁H₂₀O₁₁ 1.482 ppm) (MS² analysis resulted in product ions at *m/z* 379 and 285).²³

Also, the presence of soyasaponins was confirmed by HRMS analysis. In addition to soyasaponins I and III, dehydrosoyasaponin I was present in the decoction. In the positive ion mode dimethyltryptamine, an alkaloid, was found as described in literature.^{4,13,23}

Table 5.9 Overview of MS, MS² and MS³ experiments. Compounds with the same molecular mass are put together in ascending retention time order.

Compound	[M-H] ⁻ /[M+H] ⁺	MS ²	MS ³	elucidation
I	563/565	501;461;419/433	419→401;391;293	(3-hydroxymethyl glutaryl, pentosyl)-hexosyl-pyranones
J	563/565	501;461;419/433	419→401;391;293	
K	563/565	501;461;419/433	419→401;391;293	
L	563/565	545;503;485;473;455;443;425;413;383;353/547; 529;511;493;499;481;475;457;469;451;445;427; 409;415;397;379	443→425;383;353 473→455;413;383;353 503→485;473;413;383 427→409;391;379;349;337 ;325;295	x-C-pentosyl-x-C-hexosyl-apigenin derivative
M	563/565	545;503;485;473;455;443;425;413;383;353/547; 529;511;493;499;481;475;457;469;451;445;427; 409;415;397;379	443→425;383;353 473→455;413;383;353 503→485;473;413;383 427→409;391;379;349;337 ;325;295	x-C-pentosyl-x-C-hexosyl-apigenin derivative
B1	563/565	545;503;485;473;455;443;425;413;383;353/547; 529;511;493;499;481;475;457;469;451;445;427; 409;415;397;379	443→425;383;353 473→455;413;383;353 503→485;473;443;413;383 427→409;391;379;349;337 ;325;295	Schaftoside
B2	563/565	545;503;485;473;455;443;425;413;383;353/547; 529;511;493;499;481;475;457;469;451;445;427; 409;415;397;379	443→425;383;353 473→455;413;383;353 503→485;473;443;413;383 427→409;391;379;349;337 ;325;295	Isoschaftoside
N	563/565	545;503;485;473;455;443;425;413;383;353/547; 529;511;493;499;481;475;457;469;451;445;427; 409;415;397;379	443→425;383;353 473→455;413;383;353 503→485;473;443;413;383 427→409;391;379;349;337 ;325;295	x-C-pentosyl-x-C-hexosyl-apigenin derivative

Table 5.9 continued Overview of MS, MS² and MS³ experiments. Compounds with the same molecular mass are put together in ascending retention time order.

Compound	[M-H] ⁻ /[M+H] ⁺	MS ²	MS ³	elucidation
O	563/565	545;503;485;473;455;443;425;413;383;353/547; 529;511;493;499;481;475;457;469;451;445;427; 409;415;397;379	443→425;383;353 473→455;413;383;353 503→485;473;443;413;383 427→409;391;379;349;337 ;325;295	x-C-pentosyl-x-C-hexosyl- apigenin derivative
D	563/565	443;413;341;311;293/547;445;433;415;397;367; 337;313	413→293 443→311;293 433→415;397;379;367;337 ;313;295;283 427→409;391;379;349;325 ;307;295	2''-O-pentosyl-x-C-hexosyl- apigenin derivative
E	563/565	443;413;341;311;293/547;445;433;415;397;367; 337;313	413→293 443→425;311;293 433→415;397;379;367;337 ;313;295;283 427→409;379;349;337;325 ;313;307;295;283	2''-O-xylosyl-vitexin
P	563/565	443;413;341;311;293/547;445;433;415;397;367; 337;313	433→415;397;379;367;337 ;313;295;283	x-O-pentosyl-x-C-hexosyl- apigenin derivative
Q	563/565	443;413;341;311;293/547;445;433;415;397;367; 337;313	433→415;379;367;337;313 ;295;283 427→409;379;367;349;337 ;313;283	x-O-pentosyl-x-C-hexosyl- apigenin derivative
A	593/595	575;503;473;383;353/577;559;541;529;475;457; 499;481	503→485;413;383 473→455;383;353 457→439;421;409;379;337 ;325;307	Vicenin-2

Table 5.9 continued Overview of MS, MS² and MS³ experiments. Compounds with the same molecular mass are put together in ascending retention time order.

Compound	[M-H] ⁻ /[M+H] ⁺	MS ²	MS ³	elucidation
C	593/595	475;473;413;293/433;415;337;313;271	413→293 433→415;397;379;367;337 ;313;295;283	2''-O-hexosyl-x-C-hexosyl- apigenin derivative
R	593/595	473;433;371;323/463;445;397;367;343	443→323 463→445;427;409;397;367 ;343;313	2''-O-pentosyl-x-C-hexosyl methyl luteoline derivative
S	593/595	473;433;371;323/463;445;397;367;343	443→323/463→445;427;3 97;343	2''-O-pentosyl-x-C-hexosyl methyl luteoline derivative
F	431/433	341;311/415;397;379;367;337;313	341→323;311;283;281;269 ;247;179 311→283	Vitexin
T	431/433	341;311/415;397;379;367;337;313	341→323;311;283;281;269 ;247;179 311→283	Isovitexin
U	431/433	269/271	341→323;281 311→283;267	x-O-hexosyl-x-C-apigenin
V	431/433	341;311/415;397;379;367;337;313	341→323;311;283;281;269 ; 179 311→283	x-C-hexosyl-apigenin

5.4.3.4 Total flavonoid content of five food supplements containing *D. adscendens* and of different plant parts

The flavonoid content of the samples (5.2.2.1) was determined as described in 5.4.2.4. The results of the analysis are shown in Table 5.10.

Table 5.10 Overview of flavonoid content of food supplements and different plant parts.

	Flavonoid content
Food supplement 1 (drinkable solution)	0.46 mg/mL
Food supplement 2 (capsules)	0.39 mg/capsule
Food supplement 3 (capsules)	0.99 mg/capsule
Food supplement 4 (capsules)	2.88 mg/capsule
Food supplement 5 (capsules)	0.61 mg/capsule
Decoction batch A1	0.91%
Decoction batch A2	n.a.*
Decoction of twigs	0.57%
Decoction of leaves (batch B)	1.97%
Decoction of leaves (additional batch Ghana)	1.35%
Decoction of roots	0.16%
Decoction batch B (extraction solvent 3L)	0.99%
Decoction batch B (extraction solvent 2L)	0.46%
Decoction batch B (extraction solvent 1L)	0.36%

* no more decoction left for analysis

The same trend as for the D-pinitol content of the five food supplements was obvious. The amount of flavonoids ranged from 10% to 30% of the D-pinitol content. As described for D-pinitol, there is a substantial difference between the five investigated food supplements, but this difference was smaller. For food supplement 1 and 4, the flavonoid content was stated on the label. In the fourth food supplement, the highest amount of flavonoids was found, namely 2.88 mg/capsule. Only 30% of its stated content was found. For supplement 1, the drinkable solution, 98.4% of its stated content was found.

For the different plant parts investigated, the leaves showed the highest flavonoid content, whereas in the roots, only a very low amount of flavonoids was found. A fresh batch of decoction (Batch B) prepared with 3 L, 2 L and 1 L of water yielded 0.99%, 0.46% and 0.36% flavonoids, respectively,

showing that the extraction of flavonoids from the fresh plant material was not complete, certainly not for the decoctions prepared with 1 and 2 L of water. Typically, a decoction prepared as described in 5.2.2.1 yielded about 1% of flavonoids.

5.4.4 Conclusions

Phytochemical analysis of a decoction of *D. adscendens* revealed the presence of a significant amount of flavonoids, more specifically flavone-*O*-glycosides and flavone-*C*-glycosides. Vitexin-2''-*O*-xyloside and 2-*O*-(*E*-coumaroyl)-malic acid were isolated and identified for the first time in *D. adscendens*. Their structure elucidation was performed by thorough investigation of NMR and mass spectra. Isoschaftoside, schaftoside and vicenin-2 were found to be present by comparison with a surrogate standard.

5.5 Biological activity and metabolism

5.5.1 Introduction

5.5.1.1 General introduction

Although some pharmacological studies were performed for *D. adscendens*, no studies about the bioavailability and metabolism of the decoction exist at the moment. In addition, the information about the fate of the constituents, such as D-pinitol and flavone-C-glycosides present in the decoction, in the gastro-intestinal tract are scarce. Therefore, D-pinitol, vitexin and a flavonoid-rich fraction of a decoction of *D. adscendens* were investigated *in vitro* using a gastro-intestinal dialysis model (GIDM) with a colonic phase.

The *in vivo* study (part 5.3) suggested that in addition to D-pinitol some other constituents contribute to the hepatoprotective effect and further phytochemical research proved the presence of flavonoids in the decoction, which could be responsible for the synergistic effect seen in the study. In addition, some authors described the antioxidative activity of *D. adscendens*.^{19,20} Therefore, and based on the traditional use of *D. adscendens* for the management of anti-inflammatory disorders and hepatitis and the hepatoprotective and antidiabetic activity of D-pinitol, it was decided to evaluate the ability of a decoction of *D. adscendens* to inhibit the formation of advanced glycation end products (AGEs). The formation of AGEs is associated with various diseases, such as diabetes, and their formation includes oxidation reactions which lead to many reactive intermediates.⁸⁸⁻⁹⁰ In this way, a decoction of *D. adscendens* could possibly inhibit the formation of AGEs.

5.5.1.2 Metabolization

Before a drug reaches its target tissue or organ, it travels through the gastro-intestinal tract and needs to be absorbed to reach the blood. The stability of a test compound in the gastro-intestinal tract and its absorption can be evaluated *in vitro* using models which simulate the gastro-intestinal tract, *in vivo* using animal models, or by human studies. Since the latter option is time-consuming and quite costly, *in vitro* models are frequently used.⁹¹ Models which predict the effect of the gastro-intestinal tract can roughly be divided into two types, namely static models and dynamic models. In the former models, the amount of enzymes, salts and digested materials is kept constant, while this is not the case for dynamic models where there is a continuous change to mimic the physiological

conditions of the gastro-intestinal tract. At the moment, most of the models used belong to the static type and only a limited number of dynamic models are operated today. Furthermore, the compartments of the gastro-intestinal tract (oral cavity, stomach, small intestine, large intestine) that are included can be different, giving rise to a high number of models.⁹¹ Hence, the comparison of studies using a different type of model can be rather difficult. For the *in vitro* evaluation of absorption, different models are used such as *in silico* models and physicochemical methods, where the latter only have a low predictive value. Furthermore, brush border membrane vesicles, artificial membranes, isolated intestinal cells, everted intestinal sacs, Caco-2 cell systems, Using chambers, and *in situ* intestinal perfusion models are described for the prediction of the intestinal absorption of drugs. All these models have their specific strengths and limitations, as discussed in depth by Deferme et al.⁹², as for example the limited viability of used cells or tissue or the fact that artificial membranes only predict a part of the absorption process, mostly passive transport. Although the *in situ* perfusion model mimics the *in vivo* situation the best, surgery on animals is needed and this model is time-consuming. Hence, it is rather not used for high throughput screening.

Generally, when flavonoid glycosides enter the gastro-intestinal tract they can be deglycosylated in part by enzymes in the small intestine with the formation of their aglycones, which are subsequently absorbed and subjected to phase I and II metabolization in the intestine and liver. The formed metabolites are released in the bile and reach the colon together with remaining flavonoid glycosides, such as C-glycosides, where they are hydrolyzed by the colon microbiota before absorption or further degraded into small phenolic acids.⁹³⁻⁹⁵ This is all well studied for flavonoid O-glycosides, while much less is known for flavonoid C-glycosides. Findings in literature concerning their fate in the gastro-intestinal tract are sometimes contradictory. Generally, the existing studies show a low bioavailability for vitexin derivatives and other C-glycosides. Liang et al.⁷⁷ found that vitexin-2''-O-rhamnoside (VOR) and vitexin-2''-O-glucoside (VOG) were absorbed in rats, but the absorption was poor. *In vitro* evaluation of the absorption of VOR was carried out by Xu et al.⁹⁶ and they concluded that the major route of absorption was passive diffusion and that absorption enhancement was achieved by co-administration of P-glycoprotein (P-gp) inhibitors. These findings were confirmed in an *in vivo* study in rats.^{87,97} Also for vitexin-4''-O-glucoside, a low bioavailability was found due to significant hepatic and intestinal first-pass effects and to the possible contribution of CYP3A and P-gp efflux.⁹⁸ While Gouvea et al.⁹⁹ showed that vicenin-2 was not absorbed using

Caco-2 cells, *in situ* single pass experiments showed that this compound could be absorbed in the small intestine of rats.^{99,100} Some human intestinal bacterial strains have been found which are able to deglycosylate some flavonoid C-glycosides. Xu et al.¹⁰¹ found that *Enterococcus sp.* 45 was able to transform orientin (8-C-luteolin) into the aglycone luteolin, whereas Braune et al.¹⁰² observed deglycosylation of homoorientin and isovitexin by *Eubacterium cellulosolvens*. Their isomers orientin and vitexin were resistant; this was also observed by Kim et al.¹⁰³, who found some *Lactococcus sp.* and *Enterococcus sp.* which were able to deglycosylate isoflavone-C-glycosides. Therefore, it could be concluded that the ability to deglycosylate flavonoid C-glycosides depends on the bacterial flora of each person.

5.5.1.3 Advanced glycation end products

AGEs are formed by the reaction of a reducing sugar and the amino group of a protein. This reaction is also known as the Maillard reaction, which consists of two phases. In the initial reversible phase, a Schiff base is formed and a rearrangement of the imine via a 1,2-eneaminol gives rise to an aminoketose which is better known as an Amadori product. In the latter stage, the Amadori product is further transformed by a number of oxidation, dehydrogenation, cyclization and condensation reactions (Hodge pathway) into advanced glycation end products. During these reactions, many intermediate products are formed including the very reactive α -dicarbonyl intermediates, such as glyoxal and methylglyoxal, and in some of these reactions transition metal ions are involved. In addition, Schiff base rearrangements (Nakimi pathway) and auto-oxidative degradation of sugars (Wolff pathway) also lead to the formation of AGE precursors. The AGEs formed can be fluorescent products, such as versperlysine and pentosidine, or non-fluorescent such as carboxymethyl-lysine.

The formation of AGEs leads to the loss of function of target proteins and these products are associated with various diseases, such as diabetes, where the high blood sugar concentration will give rise to the formation of AGEs, which are associated with complications such as diabetic nephropathy, retinopathy, and neuropathy. Other diseases where AGEs play an important role are atherosclerosis, Alzheimer's and Parkinson's disease, while high serum levels of AGEs were found in hepatocellular carcinoma, cystic fibrosis, multiple sclerosis, and schizophrenia. Interaction of AGEs with AGEs receptors (RAGEs) results in inflammation via increased gene transcription and a cascade of cytokines and chemokines.⁸⁸⁻⁹⁰

Prevention of AGEs formation has been reported for aminoguanidine, pyridoxine, metformin and pioglitazone, and also for angiotensin-converting enzyme blockers, angiotensin receptor blockers, aspirin, and pentoxifylline. Aminoguanidine was found to catch reactive intermediates, while pyridoxine inhibits oxidation, catches reactive oxygen species, (di)carbonyl intermediates or metal chelates. In addition, antioxidants and metal chelators were found to inhibit glycation. Already formed Amadori products can be deglycated by amadoriase enzymes and α -dicarbonyl cross-links can be broken by some products such as phenacylthiazolium bromide. Many natural compounds and plants showed an AGE formation inhibitory activity *in vitro* and a correlation with their antioxidative and radical scavenging activity. *In vitro* anti-AGEs activity was already proven for some flavonoid C-glycosides, such as vicenin-2, apigenin, vitexin, isovitexin and puerarin, by different researchers.¹⁰⁴⁻¹⁰⁷ For some natural compounds and extracts, such as procyanidin B2, pinocembrin, and grape skin, AGEs inhibition was observed in animal studies.⁹⁰

Although many products with AGEs inhibitory activity are known, until today no registered drug is on the market for this purpose, mostly because of the side effects of the drugs. Therefore, the search for AGE-inhibitors with a better activity profile is still going on.

The first evaluation of possible AGE inhibitory activity can be done by a battery of *in vitro* tests such as the bovine serum albumin (BSA)-glucose assay as described by Vinson and Howard¹⁰⁸, the colorimetric nitrobleutetrazolium assay measuring the formation of fructosamine, which is an Amadori product, and the spectrophotometric determination of the amount of α -dicarbonyl products using the Girard T reagent.

5.5.2 Materials and methods

5.5.2.1 Gastro-intestinal dialysis model

Metabolization experiments were carried out on D-pinitol (50 mg) and vitexin (5 mg)(pure standards) and on a flavonoid fraction of *Desmodium adscendens* (28 mg).

For the *in vitro* experiments, a blank and three samples were used. To a given amount of sample, 47 mL of water was added and the pH was adjusted to 2.5 using 6 M HCl. After 15 min, the pH was adjusted until 2 with 6 M HCl. To this solution, 3 mL of pepsin solution (16% m/v in 0.1 M HCl) was added and the samples were placed in a shaking hot water bath (120 strokes/min) for one hour at 35-37 °C. In this way, the stomach was mimicked. The stomach phase was poured into the dialysis

cell (Amicon stirred cells equipped with a dialysis membrane) and 50 mL of water was added together with a tubular dialysis membrane (bag) filled with 985 μL , 1005 μL and 1265 μL of NaHCO_3 , respectively. The blank was prepared in the same way as the samples but without adding test compound. All four dialysis cells were attached in parallel to a system that feeds the cells with either water or gas (N_2) to mimic the transport mechanism of water from plasma into the chyme in humans. The dialysate was collected in small plastic jars. This part together with the colonic phase was executed in an anaerobic globe-box. After 30 min of dialysis, 15 mL of a pancreatin – bile solution (0.4% m/v pancreatin and 0.4% m/v bile in 0.1 M NaHCO_3) was added and dialysis was done for one hour. The dialysate was collected. This phase mimicked the small intestine. The fluid that remained in the dialysis cells is called the retentate. It was stored at 4 °C overnight and a small sample (1 mL) was taken for further analysis. To the retentate of the dialysis cells containing the blank, sample 1 and sample 2, 50 mL of a fecal suspension (10^8 CFU/mL) was added. To the third cell containing sample, only 50 mL of WCB medium was added, so no colonic bacteria were present to metabolize the compounds. The pH was adjusted to 5.8-6 with 1 M HCl and all the dialysis cells were connected to the dialysis system. Dialysis was performed for 2 hours at different time points (0, 5, 23 and 25 h for standard compounds and at 0, 3, 21, 27, 45, 51 and 69 h for the flavonoid-rich fraction of *D. adscendens*). After every 2 hours of dialysis, a sample from the retentate was taken and the dialysis jars were renewed. The dialysate was lyophilized and the retentate was stored at -80 °C and centrifuged (8 min, 17970 g – 14000 rpm) before analysis.

5.5.2.2 Analysis

Vitexin and *D. adscendens* samples were analyzed by LC-UV and LC-MS and D-pinitol samples were analyzed by means of GC-FID and GC-MS. Before analysis with LC-MS, samples were prepared by the procedure described by Rechner et al.¹⁰⁹ In brief, a C18 cartridge was washed with 3 mL of methanol and conditioned with 6 mL of water/methanol/acetic acid (94:5:1). Thereafter, the sample was applied onto the cartridge and the cartridge was washed again with 6 mL of water/methanol/acetic acid (94:5:1) to remove salts. The polyphenols were eluted with 12 mL of methanol, the eluate was concentrated, and a ½ dilution with water was prepared before analysis. The optimal HPLC method was used as described in 5.4.3.2. Parameters for MS were: sheath gas flow 65 arbitrary units; auxiliary gas flow 14 arbitrary units; sweep gas flow 3 arbitrary units; the source voltage was 4 kV;

the capillary temperature was 350 °C and the capillary voltage was -3 V. GC analysis was performed with the analysis method described in 5.2.2.4. A total ion chromatogram (TIC) was recorded followed by single ion monitoring (SIM) of ions at m/z 305, 318, 260, 217, and 147. Spectra of blank solutions were compared with spectra of solutions of either standard or the flavonoid fraction. Samples taken at all time points for standards and at time points 0, 21, 45 and 69h were analyzed.

5.5.2.3 Advanced glycation end products

BSA-glucose assay

This assay is based on the formation of fluorescent AGEs by reaction of BSA with glucose. Pure compounds, vitexin and D-pinitol and a lyophilized decoction of *D. adscendens* were evaluated for their AGEs inhibition activity using the BSA-glucose assay based on the method described by Vinson and Howard.¹⁰⁸ Aminoguanidine and quercetin were used as positive controls. Pure compounds were dissolved in DMSO and the decoction of *Desmodium adscendens* was dissolved in 90% buffer solution (50 mM sodium phosphate buffer pH 7.4 containing 0.02% NaN₃) and 10% DMSO. The latter mixture was sonicated for one hour and centrifuged for 5 min at 1760 *g* (3000 rpm). Stock solutions were diluted using DMSO to obtain the following final concentrations: 4-200 µg/mL for vitexin, 100-400 µg/mL for D-pinitol, 5-20 µg/mL for aminoguanidine, and 1-10 µg/mL for quercetin. The supernatant of the decoction was diluted using 90% buffer solution and 10% DMSO so that the final concentration ranged from 50 to 1000 µg/mL. Test solutions were prepared by combining 180 µL of the BSA solution (10 mg/mL in buffer solution) with 180 µL of the glucose solution (500 mM in buffer solution) and 40 µL of the sample solutions. Blanks were prepared by using DMSO or a solution of 90% buffer solution and 10% DMSO instead of sample solutions. All test solutions were prepared in duplo: one series was incubated at 37 °C (formation of AGEs) and the other series was stored at 4 °C for one week (no formation of AGEs = blank). After incubation 150 µL of the solutions was pipetted into a 96-well plate and the fluorescence intensity of the reaction products (AGEs) formed was measured using a Tecan spectrophotometer. Measurements were performed at room temperature at λ_{exc} 370 and λ_{em} 440 nm for vesperlysines and λ_{exc} 335 and λ_{em} 380 nm for pentosidines. The % inhibition is calculated using the following formula:

$$\% \text{ inhibition} = \frac{[(\text{BSA} + \text{glc})_{37^\circ\text{C}} - (\text{BSA} + \text{glc})_{4^\circ\text{C}}] - [(\text{BSA} + \text{glc} + \text{sample})_{37^\circ\text{C}} - (\text{BSA} + \text{glc} + \text{sample})_{4^\circ\text{C}}]}{[(\text{BSA} + \text{glc})_{37^\circ\text{C}} - (\text{BSA} + \text{glc})_{4^\circ\text{C}}]} \times 100$$

(BSA + glc)_{37 °C} : formation of AGEs

(BSA + glc)_{4 °C} : no formation of AGEs/ correction for autofluorescence of BSA and possible formation of fluorescent BSA-glucose complexes

(BSA + glc + sample)_{37 °C} : inhibition of AGEs formation by sample

(BSA + glc + sample)_{4 °C} : no formation of AGEs/ correction for autofluorescence of BSA, sample and possible formation of complexes between products

Fructosamine assay

This colorimetric assay is based on the reduction of nitrobleutetrazolium (NBT) by fructosamine in alkaline conditions. The formation of reduced NBT can be measured spectrophotometrically at 530 nm.

Pure compounds (vitexin, D-pinitol, aminoguanidine, and quercetin), a lyophilized decoction of *D. adscendens*, and a flavonoid-rich fraction were evaluated for their inhibitory activity on fructosamine formation. Pure compounds were dissolved in DMSO; the decoction of *Desmodium adscendens* and the flavonoid-rich fraction were dissolved in 90% buffer solution (50 mM sodium phosphate buffer pH 7.4 containing 0.02% NaN₃) and 10% DMSO. The decoction was sonicated for one hour and centrifuged for 5 min at 1760 g (3000 rpm). Stock solutions were diluted using DMSO to obtain the following final concentrations: 25-125 µg/mL for vitexin, 100-1000 µg/mL for D-pinitol, 5-150 µg/mL for aminoguanidine, and 1-100 µg/mL for quercetin. The supernatant of the decoction and flavonoid-rich fraction were diluted using 90% buffer solution and 10% DMSO so that the final concentrations ranged from 200 to 1400 µg/mL and 25-250 µg/mL, respectively. Test solutions were prepared in the same way as for the BSA-glucose assay described above. The solutions were incubated at 37 °C for one week. 40 µL of the test solutions were combined with 160 µL of a 300 µM NBT solution (dissolved in 100 mM sodium phosphate buffer pH 10.35) in a 96-well plate and the absorption was measured with a Tecan spectrophotometer at 37 °C at 530 nm during 30 min.

5.5.3 Results

5.5.3.1 Gastro-intestinal dialysis model

Vitexin

During the whole experiment, vitexin was detected in the dialysate. No difference between the chromatograms of the blank or samples was detected at any of the different time points. Because metabolites can be formed in very small amounts, a specific search for possible metabolites such as 4-hydroxyphenylacetic acid, 4-hydroxybenzoic acid and 3-(4-hydroxyphenyl)-propionic acid was performed, but none of those metabolites was formed. This means that vitexin, a C-glycoside of apigenin, is quite stable during the passage in the gastro-intestinal dialysis model. The amount of vitexin absorbed during the duodenal phase could not be determined since only a few percentages of the starting amount of vitexin was recovered. This could be due to degradation during the time before analysis since this experiment was performed after the qualitative LC-MS analysis described above, or due to adsorption onto the dialysis membranes.

Flavonoid fraction

The flavonoid fraction (Figure 5.53) contained the same main flavonoids as the crude extract (phytochemical analysis Figure 5.33) and were given the same numbers to identify them. Two flavonoids showed a deprotonated molecule at m/z of 593 $[M-H]^-$ and were previously identified as vicenin-2, a di-C-hexosyl-apigenin (compound **A** - $R_t = 8.42$ min) and x-O-hexosyl-x-C-hexosyl-apigenin (compound **C** - $R_t = 17.64$ min). Four flavonoids showed a deprotonated molecule at m/z 563 $[M-H]^-$ and were identified as x-C-pentosyl-x-C-hexosyl-apigenin and x-O-pentosyl-x-C-hexosyl-apigenin isomers (compounds **B1** and **B2**, **D** and **E** - $R_t = 13.27$ min, 19.31 min and 20.10 min) of which compound **E** was fully characterized as 2''-O-xylosyl-vitexin and compounds **B1** and **B2** were identified as schaftoside and isoschaftoside, respectively. One flavonoid produced a deprotonated molecule at m/z 431 $[M-H]^-$, which was identified as vitexin (compound **F** - $R_t = 21.04$ min).

After 2 h of incubation in the colon compartment and dialysis, none of the flavonoid peaks had diminished, taking into account that the intensities of all peaks from the cells with colon bacteria were similar to those of the cell with only flavonoid fraction and no bacteria, which means that no metabolization had occurred yet (Figure 5.54).

After 21 h, compound **C** was not visible anymore, whereas, compound **A** was still present. The ratio of compounds **B1/B2** (sum peak), **D** and **E** was changed at this time point, more specifically compound **D** had decreased. This effect was more pronounced after 45 h and at the end of the experiment, this peak was almost not visible anymore. At the third and fourth collection time point, i.e. after 45 and 69 h the ratio between compounds **B1/B2** (sum peak) and **E** became more distinctive meaning, that also the latter compound was metabolized by the colon bacteria. Since the peak intensity of compounds **B1/B2** (sum peak) was still the same with and without bacteria at the end of the experiment, this compound was considered stable, which was also the case for compound **A**. These findings indicate that most probably only the O-glycosidic bonds of the O,C-glycoside derivatives of vitexin were metabolized by the colon bacteria. Some of those compounds seemed to be more susceptible to metabolization since they were almost fully metabolized at the end of the experiment, as observed for compound **D**, or were already fully converted after some hours, as was the case for compound **C**. This could also be concentration dependent. Apart from all peaks disappearing, some peaks emerged during the experiment, being vitexin and another peak with a deprotonated molecule at m/z 431 $[M-H]^-$, which was identified as isovitexin, which means that in addition to vitexin derivatives, some isovitexin glycosides may be present as well.

In addition, a specific search for possible metabolites such as apigenin, 4-hydroxyphenylacetic acid, 4-hydroxybenzoic acid and 3-(4-hydroxyphenyl)-propionic acid was performed, but none of those metabolites were formed.¹⁰² This means that all vitexin, initially present and originating from the metabolization of vitexin glycosides, is quite stable during the passage in the gastro-intestinal dialysis model. This is in accordance with previously reported data (*vide supra*).

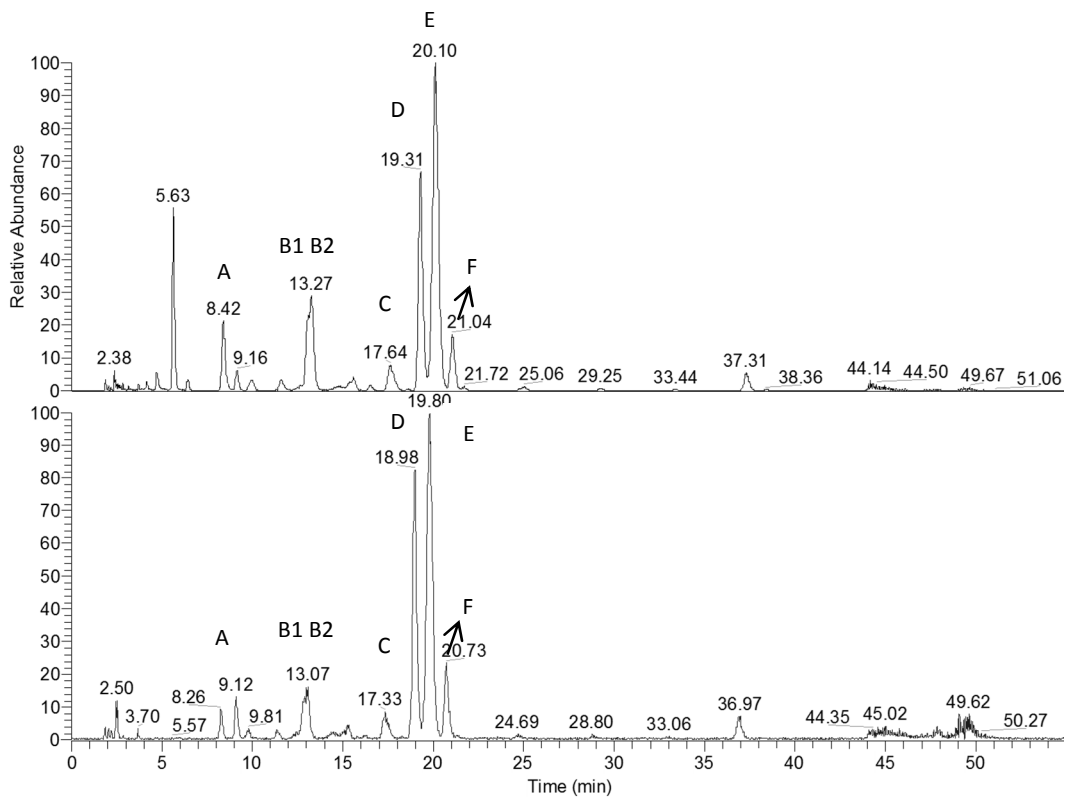


Figure 5.53 Upper chromatogram: profile of flavonoids in the crude extract of *D. adscendens*; lower chromatogram: flavonoid profile of the flavonoid-rich fraction.

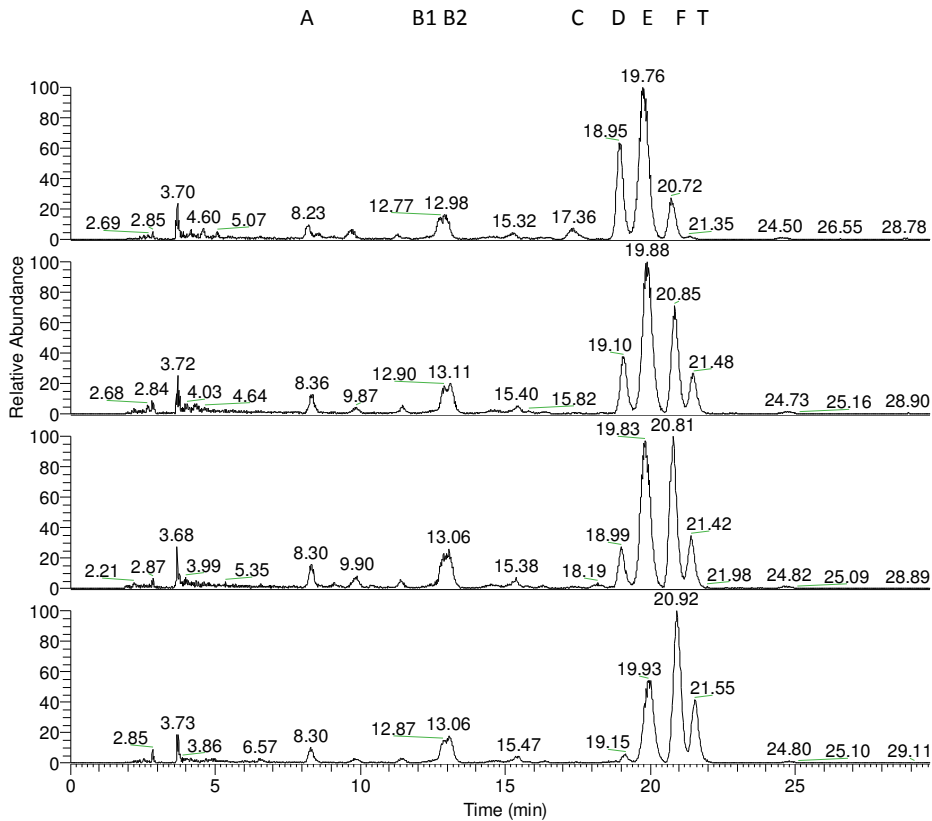


Figure 5.54 Flavonoid profile of the flavonoid-rich fraction during the colonic phase after 0, 21, 45, and 69 h.

D-pinitol

GC-FID quantification of the lyophilized dialysate showed that 27% of D-pinitol was present and therefore 73 % was available for the colonic phase of the experiment. Qualitative analysis by GC-MS of all dialysis samples, both from D-pinitol and from the extract, showed that D-pinitol was still present at the end of the experiment and no *D-chiro*-inositol was formed. Thus, D-pinitol appeared to be stable in the gastric phase and small intestine, as well as in the colonic phase. This is in accordance with literature data, where D-pinitol is found in blood of humans after oral intake of D-pinitol.^{24,33}

5.5.3.2 Advanced glycation end products

BSA-glucose assay

Results are shown in Table 5.11 and Figure 5.55. Results for aminoguanidine were in agreement with literature.¹¹⁰ A difference between the IC₅₀ value for vesperlysine AGEs and pentosidine AGEs was observed and could be explained by the reaction of aminoguanidine with dicarbonyl intermediates with the formation of triazines, which show similar photophysical behavior as the vesperlysine-like AGEs. Fluorescence values for vitexin and quercetin blanks decreased with increasing concentration, suggesting that vitexin and quercetin quenched the fluorescence. This effect was observed for both vesperlysine and pentosidine measurements performed at λ_{exc} 370 and λ_{em} 440 nm, and λ_{exc} 335 and λ_{em} 380 nm, respectively. For quercetin this effect was minimal (vesperlysines) and therefore almost no effect on the IC₅₀ value was expected. The IC₅₀ seemed to be in accordance with literature.¹¹¹ These quenching phenomena were described for quercetin and rutin. The formation of flavonoid-BSA complexes lies at the basis of fluorescence quenching, which can be both dynamic and static in nature and therefore temperature dependent.^{111,112} Because of this temperature dependency, the quenching effects cannot be compensated by using a blank at 4 °C, as was done in our experiments. A better way to compensate for fluorescence quenching can be the subtraction of fluorescence values of both BSA + sample and glucose + sample, incubated at 37 °C instead of 4 °C, from the fluorescence value of BSA + glucose + sample.

For D-pinitol, no dose-dependent effect could be determined and no significant inhibition of AGEs was observed. The decoction of *Desmodium adscendens* showed higher fluorescence intensity with increasing concentrations in the vesperlysine test, an effect better known as autofluorescence, but this was not observed in the pentosidine test. This effect is compensated by using blanks containing

BSA, glucose and the sample incubated at 4 °C, so that the autofluorescence of the sample is taken into account. The IC₅₀ value of the decoction of *D. adscendens* was 11 mg/mL and 7.4 mg/mL for the vesperlysine and pentosidine tests, respectively, which was much higher than the IC₅₀ values of the extracts evaluated by Séro et al.¹¹⁰ Since this assay has many drawbacks and disadvantages such as interference of natural products due to autofluorescence or fluorescence quenching, another assay based on the reducing properties of fructosamine in alkaline environment was performed, i.e. the fructosamine assay, but none of the tested samples were able to inhibit the formation of fructosamine.

Table 5.11 IC₅₀ values of the BSA-glucose experiment.

	IC ₅₀ value (mg/mL)	IC ₅₀ value (mg/mL)
	vesperlysines	pentosidines
Aminoguanidine	3.2	0.20
Vitexin	-	-
Quercetin	0.09	-
D-pinitol	> 4	> 4
<i>Desmodium adscendens</i> decoction	11	7.4

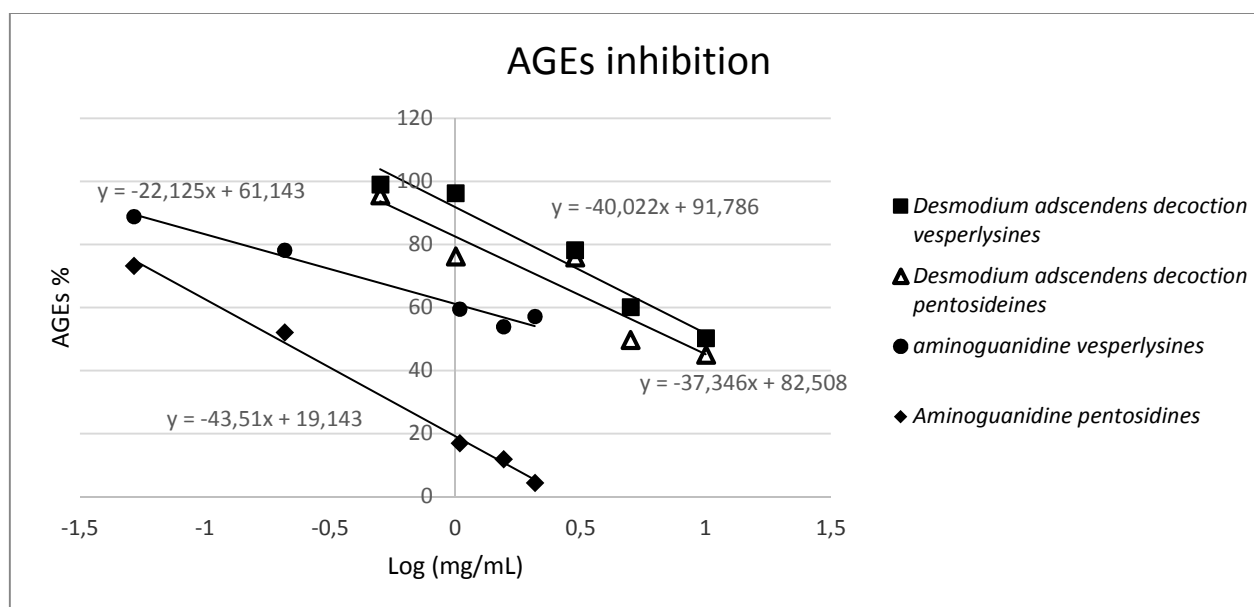


Figure 5.55 AGEs inhibition of *D. adscendens* and aminoguanidine.

5.5.4 Conclusions

Investigations using the gastro-intestinal dialysis model resulted in valuable information concerning absorption and stability. Vitexin, glycosides of vitexin and isovitexin, and D-pinitol were found to be absorbed during the small intestinal phase of the model. Since this model only mimics absorption by passive diffusion, no information about absorption by active transport or enzymatic phenomena taking place in the brush borders of the small intestine was obtained. In addition, passive diffusion through the dialysis membrane of polar compounds may not reflect passive diffusion in the gastro-intestinal tract, which requires more lipophilic properties. Hence, no full absorption profile was obtained in this way. During the colonic phase, vitexin and C-glycosides thereof were found to be stable throughout their passage in the simulated gastro-intestinal tract. Only the O-glycosidic bonds of O,C-glycosides of vitexin or isovitexin were hydrolyzed. This was confirmed by the absence of phenolic acids or C-deglycosylated aglycones, products of the colonic metabolism of flavonoids. An *in vitro* BSA-glucose test indicated a very weak anti-glycation activity of a decoction of *D. adscendens*, with IC₅₀ values three to thirty times higher than those of aminoguanidine.

References

1. Rastogi, S.; Pandey, M. M.; Rawat, A. K. An ethnomedicinal, phytochemical and pharmacological profile of *Desmodium gangeticum* (L.) DC. and *Desmodium adscendens* (Sw.) DC. *J. Ethnopharmacol.* **2011**, *136* (2), 283-296.
2. HEAR PIER pacific islands ecosystems at risk *Desmodium adscendens* <http://www.hear.org/pier/>. (accessed 2010).
3. Agrolinkfito <http://www.agrolink.com.br/agrolinkfito/secure/ProblemaDetalhe.aspx?p=125> (accessed may 2016)
4. Pothier, J.; Ragot, J.; Galand, N. Planar chromatographic study of flavonoids and soyasaponins for validation of fingerprints of *Desmodium adscendens* of different origin. *J. Planar Chromatogr. - Mod. TLC.* **2006**, *19* (109), 191-194.
5. N'gouemo, P.; Baldy-Moulinier, M.; Nguemby-Bina, C. Effects of an ethanolic extract of *Desmodium adscendens* on central nervous system in rodents. *J. Ethnopharmacol.* **1996**, *52* (2), 77-83.
6. Ampofo, O. Plants that heal. *Magazine of the WHO* **1977**, 5.
7. Addy, M. E.; Awumey, E. M. K. Effects of the extracts of *Desmodium adscendens* on anaphylaxis. *J. Ethnopharmacol.* **1984**, *11* (3), 283-292.
8. Addy, M. E.; Dzandu, W. K. Dose-response effects of *Desmodium adscendens* aqueous extract on histamine response, content and anaphylactic reactions in the guinea pig. *J. Ethnopharmacol.* **1986**, *18* (1), 13-20.
9. Addy, M. E.; Burka, J. F. Effect of *Desmodium adscendens* fractions on antigen- and arachidonic acid-induced contractions of guinea pig airways. *Can. J. Physiol. Pharmacol.* **1988**, *66* (6), 820-825.
10. Addy, M. Several chromatographically distinct fractions of *Desmodium adscendens* inhibit smooth muscle contractions. *Int. J. Crude Drug Res.* **1989**, *27* (2), 81-91.
11. Addy, M. E.; Burka, J. F. Effect of *Desmodium adscendens* fraction 3 on contractions of respiratory smooth muscle. *J. Ethnopharmacol.* **1990**, *29* (3), 325-335.
12. Addy, M. E.; Schwartzman, M. L. An extract of *Desmodium adscendens* inhibits NADPH-dependent oxygenation of arachidonic acid by kidney cortical microsomes. *Phytother. Res.* **1992**, *6* (5), 245-250.
13. Addy, M. Some secondary plant metabolites in *Desmodium adscendens* and their effects on arachidonic acid metabolism. *Prostaglandins, Leukotrienes Essent. Fatty Acids* **1992**, *47*, 85-91.
14. McManus, O. B.; Harris, G. H.; Giangiacomo, K. M.; Feigenbaum, P.; Reuben, J. P.; Addy, M. E.; Burka, J. F.; Kaczorowski, G. J.; Garcia, M. L. An activator of calcium-dependent potassium channels isolated from a medicinal herb. *Biochemistry* **1993**, *32* (24), 6128-6133.
15. Irie-N'guessan, G.; Champy, P.; Kouakou-Siransy, G.; Koffi, A.; Kablan, B. J.; Leblais, V. Tracheal relaxation of five Ivorian anti-asthmatic plants: role of epithelium and K(+) channels in the effect of the aqueous-alcoholic extract of *Dichrostachys cinerea* root bark. *J. Ethnopharmacol.* **2011**, *138* (2), 432-438.
16. Barreto, G. S. Effect of butanolic fraction of *Desmodium adscendens* on the anococcygeus of the rat. *Braz. J. Biol.* **2002**, *62* (2), 223-230.

17. Tubéry, P.; Tubéry, A. Use of *Desmodium* in the treatment of hepatitis, and medicaments thereof. Patent EP0309342 (A1), 1989.
18. Nyarko, A. K.; Asare-Anane, H.; Ofosuhene, M.; Addy, M. E. Extract of *Ocimum canum* lowers blood glucose and facilitates insulin release by isolated pancreatic beta-islet cells. *Phytomedicine*. **2002**, *9* (4), 346-351.
19. Muanda, F. N.; Bouayed, J.; Djilani, A.; Yao, C.; Soulimani, R.; Dicko, A. Chemical composition and cellular evaluation of the antioxidant activity of *Desmodium adscendens* leaves. *J. Evidence-Based Complementary Altern. Med.* **2011**, Article ID620862.
20. Zielinska-Pisklak, M. A.; Kaliszewska, D.; Stolarczyk, M.; Kiss, A. K., Activity-guided isolation, identification and quantification of biologically active isomeric compounds from folk medicinal plant *Desmodium adscendens* using high performance liquid chromatography with diode array detector, mass spectrometry and multidimensional nuclear magnetic resonance spectroscopy. *J. Pharm. Biomed. Anal.* **2015**, *102*, 54-63.
21. François, C.; Fares, M.; Baiocchi, C.; Maixent, J. Safety of *Desmodium adscendens* extract on hepatocytes and renal cells. Protective effect against oxidative stress. *J. Intercult. Ethnopharmacol.* **2015**, *4* (1), 1-5.
22. Gyamfi, M.; Yonamine, M.; Aniya, Y. Free-radical scavenging action of medicinal herbs from Ghana *Thonningia sanguinea* on experimentally-induced liver injuries. *Gen. Pharmacol.* **1999**, *32* (6), 661-667.
23. Baiocchi, C.; Medana, C.; Giancotti, V.; Aigotti, R.; Dal Bello, F.; Massolino, C.; Gastaldi, D.; Grandi, M. Qualitative characterization of *Desmodium adscendens* constituents by high-performance liquid chromatography-diode array ultraviolet-electrospray ionization multistage mass spectrometry. *Eur. J. Mass Spectrom.* **2013**, *19* (1), 1-15.
24. Magielse, J.; Arcoraci, T.; Breynaert, A.; van Dooren, I.; Kanyanga, C.; Fransen, E.; Van Hoof, V.; Vlietinck, A.; Apers, S.; Pieters, L.; Hermans, N. Antihepatotoxic activity of a quantified *Desmodium adscendens* decoction and D-pinitol against chemically-induced liver damage in rats. *J. Ethnopharmacol.* **2013**, *146* (1), 250-256.
25. Sivakumar, S.; Subramanian, P. Pancreatic tissue protective nature of D-pinitol studied in streptozotocin-mediated oxidative stress in experimental diabetic rats. *Eur. J. Pharmacol.* **2009**, *622* (1-3), 65-70.
26. Zhou, Y.; Park, C.; Cho, C.; Song, Y. Protective effect of pinitol against D-galactosamine-induced hepatotoxicity in rats fed on a high-fat diet. *Biosci., Biotechnol., Biochem.* **2008**, *72* (7), 1657-1666.
27. Bhat, K.; Shah, B.; Gupta, K.; Pandey, A. Semi-synthetic analogs of pinitol as potential inhibitors of TNF- α cytokine expression in human neutrophils. *Bioorg. Med. Chem. Lett.* **2009**, *19* (7), 1939-1943.
28. Choi, M.; Lee, W.; Kwon, E.; Kang, M.; Lee, M. Effect of soy pinitol on the proinflammatory cytokines and scavenger receptors in oxidized low-density lipoprotein-treated THP-1 macrophages. *J. Med. Food* **2007**, *10* (2), 351-357.
29. Do, G.; Choi, M.; Kim, H.; Woo, M.; Lee, M.; Jeon, S. Soy pinitol acts partly as an insulin sensitizer or insulin mediator in 3T3-L1 preadipocytes. *Genes Nutr.* **2008**, *2* (4), 359-364.

30. Lee, J.; Jung, I.; Jeong, Y.; Lee, C.; Shin, Y.; Lee, S.; Suh, D.; Yoon, M.; Lee, K.; Choi, Y.; Chung, H.; Park, Y. D-pinitol inhibits Th1 polarization via the suppression of dendritic cells. *Int. Immunopharmacol.* **2007**, *7* (6), 791-804.
31. Yap, A.; Nishiumi, S.; Yoshida, K.; Ashida, H. Rat L6 myotubes as an in vitro model system to study GLUT4-dependent glucose uptake simulated by inositol derivatives. *Cytotechnology* **2007**, *55* (2-3), 103-108.
32. Sethi, G.; Ahn, K.; Sung, B.; Aggarwal, B. Pinitol targets nuclear factor-kB activation pathway leading to inhibition of gene products associated with proliferation, apoptosis, invasion and angiogenesis. *Mol. Cancer Ther.* **2008**, *7* (6), 1604-1614.
33. Campbell, W.; Haub, M.; Fluckey, J.; Ostlund, R.; Thyfault, J.; Morse-Carrithers, H.; Hulver, M.; Birge, Z. Pinitol supplementation does not affect insulin-mediated glucose metabolism and muscle insulin receptor content and phosphorylation in older humans. *Human Nutrition and Metabolism* **2004**, *134* (11), 2998-3003.
34. Davis, A.; Christiansen, M.; Horowitz, J.; Klein, S.; Hellerstein, M.; Ostlund, R. Effect of pinitol treatment on insulin action in subjects with insulin resistance. *Diabetes Care* **2000**, *23* (7), 1000-1005.
35. Bates, S.; Jones, R.; Bailey, C. Insulin-like effect of pinitol. *Br. J. Pharmacol.* **2000**, *130* (8), 1944-1948.
36. Geethan, P.; Prince, P. Antihyperlipidemic effect of D-pinitol on streptozotocin-induced diabetic wistar rats. *J. Biochem. Mol. Toxicol.* **2008**, *22* (4), 220-224.
37. Kim, J.; Shin, J.; Shin, D.; Kim, S.; Park, S.; Park, R.; Park, S.; Kim, Y.; Shin, Y. Synergistic anti-inflammatory effects of pinitol and glucosamine in rats. *Phytother. Res.* **2005**, *19* (12), 1048-1051.
38. Kim, M.; Yoo, K.; Kim, J.; Seo, Y.; Ha, B.; Kho, J.; Shin, Y.; Chung, C. Effect of pinitol on glucose metabolism and adipocytokines in uncontrolled type 2 diabetes. *Diabetes Res. Clin. Pract.* **2007**, *77S*, 247-251.
39. Singh, R.; Pandey, B.; Tripathi, M.; Pandey, V. Anti-inflammatory effect of (+)-pinitol. *Fitoterapia* **2001**, *72* (2), 168-170.
40. Belgian Center for Pharmaceutical Center. <http://www.bcfi.be/nl/start> (accessed May, 2016)
41. Pharmacopendium Plus. <http://www.farmacopendium.be/farma/> (accessed May, 2016)
42. Shin, Y.; Jeon, J.; Kim, J. Use of pinitol or chiro-inositol for protecting the liver. Patent US2007098826 (A1). 2007.
43. Garland, S.; Goheen, S.; Donald, P.; McDonald, L.; Campbell, J. Application of derivatization gas chromatography/mass spectrometry for the identification and quantification of pinitol in plant roots. *Anal. Lett.* **2009**, *42*, 2096-2015.
44. Murakeözy, E.; Smirnoff, N.; Nagy, Z.; Tuba, Z. Seasonal accumulation pattern of pinitol and other carbohydrates in *Limonium gmelini* subsp. *hungarica*. *J. Plant. Physiol.* **2002**, *159*, 485-4902.
45. Obendorf, R.; Sensenig, E.; Wu, J.; Ohashi, M.; O'Sullivan, T.; Kosina, S.; Schnebly, S. Soluble carbohydrates in mature soybean seed after feeding D-chiroinositol, myo-inositol, or D-pinitol to stem-leaf-pod explants of low raffinose, low-stachyose lines. *Plant Sci.* **2008**, *175* (5), 650-655.

46. Sanz, M.; Martinez-Castro, I.; Moreno-Arribas, M. Identification of the origin of commercial enological tannins by the analysis of monosaccharides and polyalcohols. *Food Chem.* **2008**, *111* (3) 778-783.
47. Sanz, M.; Sanz, J.; Martinez-Castro, I. Presence of some cyclitols in honey. *Food Chem.* **2004**, *84* (1), 133-135.
48. Lein, S.; Van Boven, M.; Holser, R.; Decuyper, E.; Flo, G.; Lievens, S.; Cokelaere, M. Simultaneous determination of carbohydrates and simmondsins in jojoba seed meal (*Simmondsia chinensis*) by gas chromatography. *J. Chromatogr. A* **2002**, *977* (2), 257-264.
49. Qiu, W.; Wang, Z.; Nie, W.; Guo, Y.; Huang, L. GC-MS Determination of Sucralose in Splenda. *Chromatographia* **2007**, *66* (11), 935-939.
50. Lee, J.; Chung, B. C. Simultaneous measurement of urinary polyols using gas chromatography/mass spectrometry. *J. Chromatogr.; Anal. Technol. Biomed. Life Sci.* **2006**, *831* (1-2), 126-31.
51. Medeiros, P.; Simoneit, B. Analysis of sugars in environmental samples by gas chromatography-mass spectrometry. *J. Chromatogr. A* **2007**, *1141* (2), 271-278.
52. Corradini, C.; Cavazza, A.; Bignardi, C. High-performance anion-exchange chromatography coupled with pulsed electrochemical detection as a powerful tool to evaluate carbohydrates of food interest: principles and applications. *Int. J. Carbohydr. Chem.* **2012**, *13*, Article ID 587564.
53. Yang, N.; Ren, G. Determination of D-chiro-inositol in tartary buckwheat using high-performance liquid chromatography with an evaporative lightscattering detector. *J. Agric. Food Chem.* **2008**, *56* (3), 757-760.
54. Bauer, H.; Claeys, M.; Vermeylen, R.; Schueller, E.; Weinke, G.; Berger, A.; Puxbaum, H. Arabitol and mannitol as tracers for the quantification of airborne fungal spores. *Atmos. Environ.* **2008**, *42* (3), 588-593.
55. Shaker, E.; Mahmoud, H.; Mnaa, S. Silymarin, the antioxidant component and *Silybum marianum* extracts prevent liver damage. *Food Chem. Toxicol.* **2010**, *48* (3), 803-806.
56. Wallace, T. C.; Giusti, M. M., Extraction and normal-phase HPLC-fluorescence-electrospray MS characterization and quantification of procyanidins in cranberry extracts. *J. Food Sci.* **2010**, *75* (8), C690-696.
57. De Paepe, D.; Servaes, K.; Noten, B.; Diels, L.; De Loose, M.; Van Droogenbroeck, B.; Voorspoels, S. An improved mass spectrometric method for identification and quantification of phenolic compounds in apple fruits. *Food Chem.* **2013**, *136* (2), 368-375.
58. Domon, B.; Costello, C. E., A systematic nomenclature for carbohydrate fragmentations in fab-ms ms spectra of glycoconjugates. *Glycoconjugate J.* **1988**, *5* (4), 397-409.
59. Piccinelli, A. L.; Mesa, M. G.; Armenteros, D. M.; Alfonso, M. A.; Arevalo, A. C.; Campone, L.; Rastrelli, L. HPLC-PDA-MS and NMR characterization of C-glycosyl flavones in a hydroalcoholic extract of *Citrus aurantifolia* leaves with antiplatelet activity. *J. Agric. Food Chem.* **2008**, *56* (5), 1574-1581.
60. Negri, G.; de Santi, D.; Tabach, R. Chemical composition of hydroethanolic extracts from *Siparuna guianensis*, medicinal plant used as anxiolytics in Amazon region. *Braz. J. Pharmacog.* **2012**, *22* (5), 1024-1034.

61. Rice-Evans, C.; Packer, L. *Flavonoids in health and disease*. Marcel Dekker: New York, USA, 2003; p 467.
62. Compagnone, R. S.; Suarez, A. C.; Leitao, S. G.; Delle Monache, F. Flavonoids, benzophenones and a new euphane derivative from *Clusia columnaris* Engl. *Braz. J. Pharmacog.* **2008**, *18* (1), 6-10.
63. Ferreres, F.; Gil-Izquierdo, A.; Andrade, P. B.; Valentao, P.; Tomas-Barberan, F. A. Characterization of C-glycosyl flavones O-glycosylated by liquid chromatography-tandem mass spectrometry. *J. Chromatogr. A* **2007**, *1161* (1-2), 214-23.
64. Ferreres, F.; Silva, B. M.; Andrade, P. B.; Seabra, R. M.; Ferreira, M. A. Approach to the study of C-glycosyl flavones by ion trap HPLC-PAD-ESI/MS/MS: Application to seeds of quince (*Cydonia oblonga*). *Phytochem. Anal.* **2003**, *14* (6), 352-359.
65. Sakalem, M.; Negri, G.; Tabach, R. Chemical composition of hydroethanolic extracts from five species of the *Passiflora* genus. *Braz. J. Pharmacog.* **2012**, *22* (6), 1219-1232.
66. Cuyckens, F.; Claeys, M., Mass spectrometry in the structural analysis of flavonoids. *J. Mass Spectrom.* **2004**, *39* (1), 1-15.
67. Vukics, V.; Guttman, A. Structural characterization of flavonoid glycosides by multi-stage mass spectrometry. *Mass Spectrom. Rev.* **2010**, *29* (1), 1-16.
68. Ma, X. Q.; Zheng, C. J.; Hu, C. L.; Rahman, K.; Qin, L. P. The genus *Desmodium* (Fabaceae)-traditional uses in Chinese medicine, phytochemistry and pharmacology. *J. Ethnopharmacol.* **2011**, *138* (2), 314-332.
69. Tanahashi, T.; Shimada, A.; Nagakura, N.; Inoue, K.; Ono, M.; Fujita, T.; Chen, C. C. Structure elucidation of 6 acylated iridoid glucosides from *Jasminum hemsleyi*. *Chem. Pharm. Bull.* **1995**, *43* (5), 729-733.
70. Shaker, K. H.; Dockendorff, K.; Bernhardt, M.; Seifert, K. A new triterpenoid saponin from *Ononis spinosa* and two new flavonoid glycosides from *Ononis vaginalis*. *Z. Naturforsch., B: J. Chem. Sci.* **2004**, *59* (1), 124-128.
71. Kuczkowiak, U.; Petereit, F.; Nahrstedt, A. Hydroxycinnamic acid derivatives obtained from a commercial *Crataegus* extract and from authentic *Crataegus* spp. *Sci. Pharm.* **2014**, *82* (4), 835-846.
72. Kim, H. K.; Choi, Y. H.; Verpoorte, R. NMR-based metabolomic analysis of plants. *Nat. Protoc.* **2010**, *5* (3), 536-549.
73. Di Donna, L.; De Luca, G.; Mazzotti, F.; Napoli, A.; Salerno, R.; Taverna, D.; Sindona, G. Statin-like principles of bergamot fruit (*Citrus bergamia*): isolation of 3-hydroxymethylglutaryl flavonoid glycosides. *J. Nat. Prod.* **2009**, *72* (7), 1352-1354.
74. Pereira, O. R.; Silva, A. M. S.; Domingues, M. R. M.; Cardoso, S. M. Identification of phenolic constituents of *Cytisus multiflorus*. *Food Chem.* **2012**, *131* (2), 652-659.
75. Barreca, D.; Bellocco, E.; Caristi, C.; Leuzzi, U.; Gattuso, G. Distribution of C- and O-glycosyl flavonoids, (3-hydroxy-3-methylglutaryl)glycosyl flavanones and furocoumarins in *Citrus aurantium* L. juice. *Food Chem.* **2011**, *124* (2), 576-582.
76. Plazonic, A.; Bucar, F.; Males, Z.; Mornar, A.; Nigovic, B.; Kujundzic, N. Identification and quantification of flavonoids and phenolic acids in burr parsley (*Caucalis platycarpos* L.), using high-performance liquid

- chromatography with diode array detection and electrospray ionization mass spectrometry. *Molecules* **2009**, *14* (7), 2466-2490.
77. Raffaelli, A.; Moneti, G.; Mercati, V.; Toja, E. Mass spectrometric characterization of flavonoids in extracts from *Passiflora incarnata*. *J. Chromatogr. A* **1997**, *777* (1), 223-231.
 78. Kite, G. C.; Porter, E. A.; Denison, F. C.; Grayer, R. J.; Veitch, N. C.; Butler, I.; Simmonds, M. S. Data-directed scan sequence for the general assignment of C-glycosylflavone O-glycosides in plant extracts by liquid chromatography-ion trap mass spectrometry. *J. Chromatogr. A* **2006**, *1104* (1-2), 123-131.
 79. Liang, M.; Xu, W.; Zhang, W.; Zhang, C.; Liu, R.; Shen, Y.; Li, H.; Wang, X.; Wang, X.; Pan, Q.; Chen, C. Quantitative LC/MS/MS method and *in vivo* pharmacokinetic studies of vitexin rhamnoside, a bioactive constituent on cardiovascular system from hawthorn. *Biomed. Chromatogr.* **2007**, *21* (4), 422-429.
 80. World Health Organization. WHO monographs on selected medicinal plants - Volume 3.
 81. Li, Q. M.; Vandenhoevel, H.; Delorenzo, O.; Corthout, J.; Pieters, L. A. C.; Vlietinck, A. J.; Claeys, M. Mass-spectral characterization of c-glycosidic flavonoids isolated from a medicinal plant (*Passiflora incarnata*). *J. Chromatogr., Biomed. Appl.* **1991**, *562* (1-2), 435-446.
 82. Geiger, H.; Markham, K. R. The C-glycosylflavone pattern of *Passiflora incarnata* l. *Z. Naturforsch., C: J. Biosci.* **1986**, *41* (9-10), 949-950.
 83. Zhang, Y. Q.; Luo, J. G.; Han, C.; Xu, J. F.; Kong, L. Y. Bioassay-guided preparative separation of angiotensin-converting enzyme inhibitory C-flavone glycosides from *Desmodium styracifolium* by recycling complexation high-speed counter-current chromatography. *J. Pharm. Biomed Anal.* **2015**, *102*, 276-281.
 84. Cao, J.; Yin, C. L.; Qin, Y.; Cheng, Z. H.; Chen, D. F. Approach to the study of flavone di-C-glycosides by high performance liquid chromatography-tandem ion trap mass spectrometry and its application to characterization of flavonoid composition in *Viola yedoensis*. *J. Mass Spectrom.* **2014**, *49* (10), 1010-1024.
 85. Guo, X. F.; Yue, Y. D.; Tang, F.; Wang, J.; Yao, X.; Sun, J. A comparison of C-glycosidic flavonoid isomers by electrospray ionization quadrupole time-of-flight tandem mass spectrometry in negative and positive ion mode. *Int. J. Mass Spectrom.* **2013**, *333*, 59-66.
 86. Endale, A.; Kammerer, B.; Gebre-Mariam, T.; Schmidt, P. C. Quantitative determination of the group of flavonoids and saponins from the extracts of the seeds of *Glinus lotoides* and tablet formulation thereof by high-performance liquid chromatography. *J. Chromatogr. A* **2005**, *1083* (1-2), 32-41.
 87. Ma, L. Y.; Liu, R. H.; Xu, X. D.; Yu, M. Q.; Zhang, Q.; Liu, H. L. The pharmacokinetics of C-glycosyl flavones of Hawthorn leaf flavonoids in rat after single dose oral administration. *Phytomedicine* **2010**, *17* (8-9), 640-645.
 88. Rempel, L. C. T.; Finco, A. B.; Maciel, R. A. P.; Bosquetti, B.; Alvarenga, L. M.; Souza, W. M.; Pecoits, R.; Stingen, A. E. M. Effect of PKC-beta signaling pathway on expression of MCP-1 and VCAM-1 in different cell models in response to advanced glycation end products (AGEs). *Toxins* **2015**, *7* (5), 1722-1737.

89. Vistoli, G.; De Maddis, D.; Cipak, A.; Zarkovic, N.; Carini, M.; Aldini, G. Advanced glycoxidation and lipoxidation end products (AGEs and ALEs): an overview of their mechanisms of formation. *Free Radic. Res.* **2013**, *47*, 3-27.
90. Sadowska-Bartosz, I.; Bartosz, G. Prevention of protein glycation by natural compounds. *Molecules* **2015**, *20* (2), 3309-3334.
91. Alminger, M.; Aura, A. M.; Bohn, T.; Dufour, C.; El, S. N.; Gomes, A.; Karakaya, S.; Martinez-Cuesta, M. C.; McDougall, G. J.; Requena, T.; Santos, C. N. *In vitro* models for studying secondary plant metabolite digestion and bioaccessibility. *Compr. Rev. Food Sci. Food Saf.* **2014**, *13* (4), 413-436.
92. Deferme, S.; Annaert, P.; Augustijns, P. *In vitro* screening models to assess intestinal drug absorption and metabolism. In *Drug absorption studies: In situ, in vitro and in silico models*, Ehrhardt, C., Ed. Springer: New York, 2008; p 34.
93. Thilakarathna, S. H.; Rupasinghe, H. P. Flavonoid bioavailability and attempts for bioavailability enhancement. *Nutrients* **2013**, *5* (9), 3367-3387.
94. Hollmann, P. Absorption, bioavailability, and metabolism of flavonoids. *Pharmaceutical Biology* **2004**, *42* (s1), 74-83.
95. Manach, C.; Scalbert, A.; Morand, C.; Rémésy, C.; Jiménez, L. Polyphenols: food sources and bioavailability. *Am. J. Clin. Nutr.* **2004**, *79* (5), 727-747.
96. Xu, Y. A.; Fan, G.; Gao, S.; Hong, Z. Assessment of intestinal absorption of vitexin-2''-O-rhamnoside in hawthorn leaves flavonoids in rat using *in situ* and *in vitro* absorption models. *Drug development and industrial pharmacy* **2008**, *34* (2), 164-170.
97. Lu, D.; Zhang, W.; Zou, H.; Xue, H.; Yin, J.; Chen, Y.; Ying, X.; Kang, T. Bioavailability of vitexin-2''-O-rhamnoside after oral co-administration with ketoconazole, verapamil and bile salts. *Lat. Am. J. Pharm.* **2013**, *32* (8), 1218-1223.
98. Chen, Y.; Zhang, W.; Li, D.; Ai, J.; Meng, Y.; Ying, X.; Kang, T. Hepatic and gastrointestinal first-pass effects of vitexin-4''-O-glucoside in rats. *J. Pharm. Pharmacol.* **2013**, *65* (10), 1500-1507.
99. Gouvea, D. R.; de Barros Bello Ribeiro, A.; Thormann, U.; Lopes, N. P.; Butterweck, V. Evaluation of intestinal permeability of vicenin-2 and lychnopholic acid from *Lychnophora salicifolia* (Brazilian arnica) using Caco-2 cells. *J. Nat. Prod.* **2014**, *77* (3), 464-471.
100. Buqui, G. A.; Sy, S. K. B.; Merino-Sanjuan, M.; Gouvea, D. R.; Nixdorf, S. L.; Kimura, E.; Derendorf, H.; Lopes, N. P.; Diniz, A. Characterization of intestinal absorption of C-glycoside flavonoid vicenin-2 from *Lychnophora ericoides* leaves in rats by nonlinear mixed effects modeling. *Braz. J. Pharmacog.* **2015**, *25* (3), 212-218.
101. Xu, J.; Qian, D.; Jiang, S.; Guo, J.; Shang, E. X.; Duan, J. A.; Yang, J. Application of ultra-performance liquid chromatography coupled with quadrupole time-of-flight mass spectrometry to determine the metabolites of orientin produced by human intestinal bacteria. *J. Chromatogr. B, Anal. Technol. Biomed. Life Sci.* **2014**, *944*, 123-127.
102. Braune, A.; Blaut, M. Intestinal bacterium *Eubacterium cellulosolvens* deglycosylates flavonoid C- and O-glucosides. *Appl. Environ. Microbiol.* **2012**, *78* (22), 8151-8153.

103. Kim, M.; Lee, J.; Han, J. Deglycosylation of isoflavone C-glycosides by newly isolated human intestinal bacteria. *J. Sci. Food Agric.* **2015**, *95* (9), 1925-1931.
104. Islam, M. N.; Ishita, I. J.; Jung, H. A.; Choi, J. S. Vicenin 2 isolated from *Artemisia capillaris* exhibited potent anti-glycation properties. *Food Chem. Toxicol.* **2014**, *69*, 55-62.
105. Choi, J. S.; Islam, M. N.; Ali, M. Y.; Kim, E. J.; Kim, Y. M.; Jung, H. A. Effects of C-glycosylation on anti-diabetic, anti-Alzheimer's disease and anti-inflammatory potential of apigenin. *Food Chem. Toxicol.* **2014**, *64*, 27-33.
106. Peng, X. F.; Zheng, Z. P.; Cheng, K. W.; Shan, F.; Ren, G. X.; Chen, F.; Wang, M. F. Inhibitory effect of mung bean extract and its constituents vitexin and isovitexin on the formation of advanced glycation endproducts. *Food Chem.* **2008**, *106* (2), 475-481.
107. Kim, J. M.; Lee, Y. M.; Lee, G. Y.; Jang, D. S.; Bae, K. H.; Kim, J. S. Constituents of the roots of *Pueraria lobata* inhibit formation of advanced glycation end products (AGEs). *Arch. Pharm. Res.* **2006**, *29* (10), 821-825.
108. Vinson, J. A.; Howard, T. B. Inhibition of protein glycation and advanced glycation end products by ascorbic acid and other vitamins and nutrients. *J. Nutr. Biochem.* **1996**, *7* (12), 659-663.
109. Rechner, A. Colonic metabolism of dietary polyphenols: influence of structure on microbial fermentation products. *Free Rad. Biol. Med.* **2004**, *36* (2), 212-225.
110. Sero, L.; Sanguinet, L.; Blanchard, P.; Dang, B. T.; Morel, S.; Richomme, P.; Seraphin, D.; Derbre, S. Tuning a 96-well microtiter plate fluorescence-based assay to identify AGE inhibitors in crude plant extracts. *Molecules* **2013**, *18* (11), 14320-14339.
111. Papadopoulou, A.; Green, R. J.; Frazier, R. A. Interaction of flavonoids with bovine serum albumin: A fluorescence quenching study. *J. Agric. Food Chem.* **2005**, *53* (1), 158-163.
112. Liu, E. H.; Qi, L. W.; Li, P. Structural relationship and binding mechanisms of five flavonoids with bovine serum albumin. *Molecules* **2010**, *15* (12), 9092-9103

Chapter 6

HERNIARIA HIRSUTA

6.1 General introduction

6.1.1 *Herniaria hirsuta*

Herniaria hirsuta L. (Caryophyllaceae) is a small herb which occurs in the Mediterranean region, North Africa, and in parts of Central Europe. It has a 10 cm long, terete, multi-branched stem, which bears obovate, opposite stipules of 7 cm long, which are sparsely ciliate at the margins and membranous. The small green yellowish flowers are grouped in axillary clusters with 5 to 10 flowers per cluster. Each flower consists of five elliptical sepals, five petals, five filaments, and an achene with a style (Figure 6.1). The stems, leaves, and flowers of *Herniaria hirsuta* are green-grayish and pubescent, in contrast with those of *Herniaria glabra* which are almost glabrous and vivid green.^{1,2}

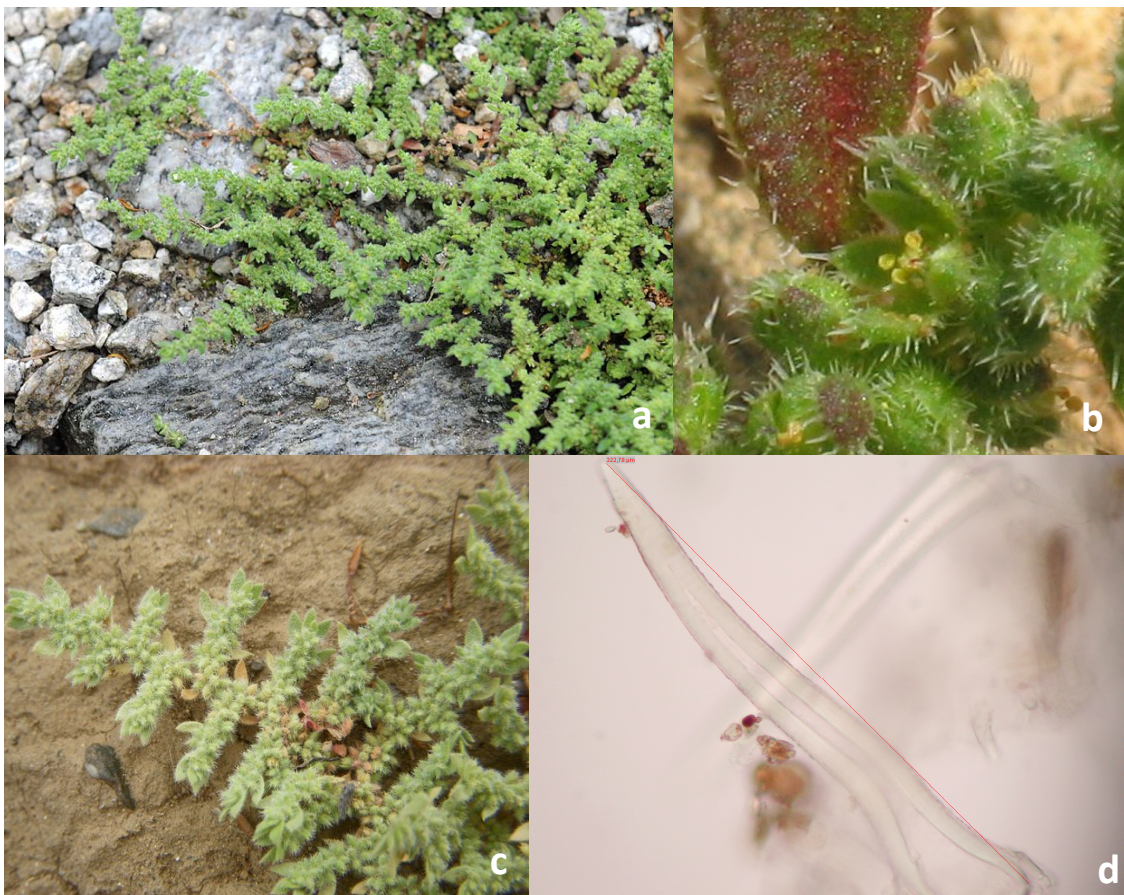


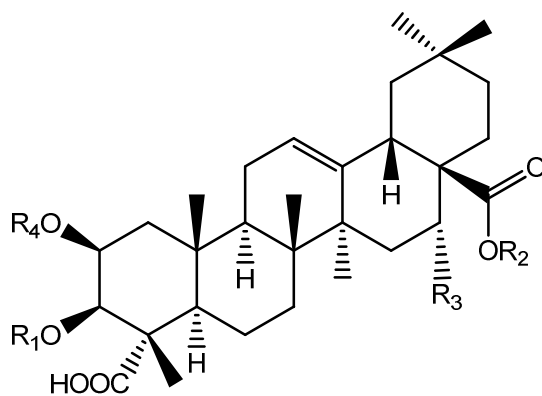
Figure 6.1 a) *Herniaria hirsuta* L.; b) detail of flowers; c) detail of a branch; d) hair - microscopic analysis.³⁻⁵

Besides the fact that an infusion of either *H. hirsuta* L. (hairy rupturewort), *H. glabra* L. (smooth rupturewort) or *H. fontanesii* J. Gay is well known in Moroccan folk medicine for the treatment of biliary dyskinesia, (uro)lithiasis or as a diuretic, some ethnobotanical surveys proved the traditional

use of *H. hirsuta* in Jordan, Palestine, Bosnia-Herzegovina and Mallorca for the treatment of bladder and prostate disorders, as a renal lithotriptic and bronchodilator.⁶⁻¹⁵

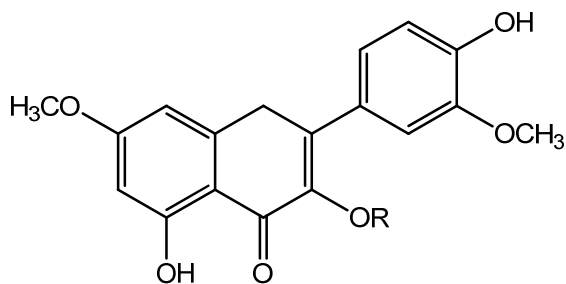
Some phytochemical research on these species revealed the presence of several saponins, flavonoids, and coumarins. While *H. fontanesii* was reported to contain herniariasaponins A-D, which are bidesmosidic triterpenoid saponins, two monodesmosidic derivatives of medicagenic acid, herniariasaponins E and F, were isolated from the aerial parts of *H. hirsuta*, and several mono- and bidesmosidic medicagenic acid derivatives, named herniariasaponins 1-7, were isolated from *H. glabra*.^{10,11,16-21} All of them contain medicagenic acid or 16-hydroxymedicagenic acid as aglycone (Figure 6.2).

Herniariae herba was reported to contain quercetin- and isorhamnetin-derivatives such as narcissin and rutin.^{1,22} In addition, narcissin (isorhametin-3-*O*-rutinoside) was isolated from *Herniaria glabra*. Isorhamnetin 3-[3'''-feruloylrhamnosyl-(1→6)-galactoside], isorhamnetin 3-robinobioside and catechin were reported in *Herniaria fontanesii* and rhamnazin 3-rutinoside (Figure 6.3) was found in *Herniaria ciliolata*.^{23,24} Herniarin (Figure 6.4) and umbelliferone were found as the major coumarins.²⁵



	R1	R2	R3	R4
Herniariasaponin A	Rha 1→4 GlcA	Rha 1→2 (Rha 1→3) Xyl 1→2 Fuc	H	H
Herniariasaponin B	Rha 1→4 GlcA	Rha 1→2 (Rha 1→3) Xyl 1→2 Fuc	OH	H
Herniariasaponin C	Rha 1→2 GlcA	Rha 1→2 (Rha 1→3) 4-AcFuc	H	H
Herniariasaponin D	Rha 1→2 GlcA	Rha 1→2 (Rha 1→3) Fuc	H	H
Herniariasaponin E	H	Xyl 1→4 Rha 1→2 (Glc 1→6) Glc	H	Ac
Herniariasaponin F	H	Xyl 1→4 Rha 1→2 (Rha 1→4 Glc 1→6) Glc	H	H
Herniariasaponin 1	GlcA	Glc 1→3 Rha 1→2 3,4-diAcFuc	H	H
Herniariasaponin 2	H	Rha 1→4 Glc 1→6 (Glc 1→2) Glc	H	Ac
Herniariasaponin 3	GlcA	Glc 1→3 Rha 1→2 (Glc 1→3) 4-AcFuc	H	H
Herniariasaponin 4	H	Rha 1→4 Glc 1→6 (Glc 1→2) Glc	H	H
Herniariasaponin 5	GlcA	Glc 1→3 Rha 1→2 (Api 1→3) 4-AcFuc	OH	H
Herniariasaponin 6	H	Rha 1→4 Glc 1→6 (AcGlc 1→2) Glc	H	H
Herniariasaponin 7	GlcA	Glc 1→3 Rha 1→2 (Api 1→3) 4-AcFuc	H	H

Figure 6.2 Overview of herniariasaponins found in *H. glabra*, *H. hirsuta*, and *H. fontanesii*.



R = Rha 1→6 Glu

Figure 6.3 Rhamnazin 3-rutinoside.

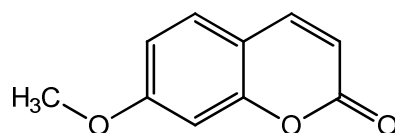


Figure 6.4 Herniarin.

6.1.2 Kidney stones and gallstones

Urinary and biliary stones have a relatively high prevalence of about 10-12% and 10-20%, respectively, in Western society, and constitute a major health problem. In addition, the recurrence rate is rather high.²⁶⁻³¹

Kidney stones can be divided into different classes according to their content. The most prevalent type of kidney stones are calcium stones, from which roughly 80% consists of calcium oxalate and 20% of calcium phosphate. The pathophysiology is complex and multicausal including low urine volume, high urinary levels of calcium, uric acid and oxalate, low urinary citric acid levels, and abnormal urinary pH values. Hypercalciuria, caused by increased intestinal calcium absorption, increased release of calcium from bones and decreased renal reabsorption, is the most prevalent abnormality observed in patients suffering from calcium kidney stones. Other less prevalent stones include uric acid stones, cystine stones, and infectious stones. The treatment of urolithiasis is focused on interventional procedures, such as extracorporeal shock wave lithotripsy, ureteroscopy or percutaneous nephrolithotomy on the one hand, and prophylactic, dissolution and medical expulsion therapy on the other hand. Various drugs are used in these therapies, such as thiazide diuretics, potassium citrate, allopurinol, UroPhos-K (a slow-release potassium phosphate preparation), sodium bicarbonate, D-penicillamine, acetohydroxamic acid, Tham E (an alkalinizing irrigant), alpha-blockers, calcium-channel blockers, and corticosteroids. However, many of these drugs cause severe side effects and up till today no drugs are available for clinical therapy, especially for the prevention and the recurrence of stones.³²⁻³⁴ Teas containing *Herniariae herba*, which can contain *H. glabra* and *H. hirsuta*, are known in Europe, especially in Austria, for the treatment of urological problems.^{35,36} In Italy, a combinational food supplement containing *Herniaria* is available under the name Renalit-Combi Colic.³⁵ Mechanistic research on *Herniaria hirsuta*, traditionally used for the treatment of kidney stones, showed its ability to reduce the size of calcium oxalate stones in nephrolithic rats treated with *Henriaria hirsuta*. Small calcium oxalate dihydrate crystals were formed instead of large

calcium oxalate monohydrate crystals. In addition, in the treated group the deposition of calcium oxalate was limited compared to the control group. The formation of smaller crystals could be beneficial since they are more easily excreted.^{6,7} Later on, it was demonstrated by bioguided fractionation that a fraction rich in saponins was responsible for the abovementioned effects.³⁷

Gallstones are classified into three types: cholesterol gallstones, containing more than 70% cholesterol, pigment gallstones, which consist mainly of calcium bilirubinate and contain only 30% cholesterol or less, and mixed gallstones which have a cholesterol content between 30% and 70%. In developed countries the majority of gallstones consists mainly of cholesterol.^{28,38,39} Risk factors for development of gallstones are obesity, hypercholesterolemia, diabetes mellitus, hyperinsulinemia, metabolic syndrome, low physical activity, rapid weight loss and a high-fat diet, in addition to unmodifiable factors such as ethnicity, female gender, age, and heredity.^{29,40,41} The pathophysiology of these stones is complex and multiple factors are involved. Hypersecretion of cholesterol into bile, leading to supersaturation of bile is a prerequisite for the formation of gallstones. Other factors including gallbladder hypomotility, gallbladder inflammation, hypersecretions of mucin, rapid-phase transitions of cholesterol, genetic factors such as the expression of multiple *Lith* genes and increased intestinal absorption of cholesterol have their specific role in the formation of gallstones.⁴⁰⁻⁴³ Normally, cholesterol is solubilized in mixed micelles together with bile acids and phospholipids. With increasing cholesterol levels in bile, phase separation from micelles occurs and unilamellar and multilamellar vesicles are formed. From these vesicles, liquid cholesterol crystals are formed which can then turn into plate-like cholesterol monohydrate crystals (solid crystals). Aggregation and agglomeration of the plate-like crystals will eventually lead to macroscopic gallstones.⁴⁰⁻⁴³ The cornerstone of the treatment of gallstone disease consists almost exclusively of cholecystectomy and endoscopic or medical treatment of complications and the use of drugs is still limited. Cholecystectomy, although an established procedure, still carries a small but existent complication rate, especially when performed in an acute setting.^{28,43,44} Some 20% of patients continue to suffer from pain after cholecystectomy, and symptomatic therapy with analgesics (non-steroidal anti-inflammatory drugs (NSAIDs), narcotic analgesics) is designated. Medical dissolution therapy with ursodeoxycholic acid (UDCA), mainly based on resolving the cholesterol supersaturation of the bile, is an alternative for patients experiencing moderate symptoms due to small radiolucent cholesterol gallstones.^{39,43} The main drawbacks of this treatment are its low efficacy (40%), slowness in action,

and the possibility of stone recurrence.⁴⁵ The use of drugs influencing hepatic synthesis and/or secretion of cholesterol-like statins, and/or intestinal absorption of cholesterol, like ezetimibe, might be able to influence the formation of cholesterol gallstones and promote the dissolution of gallstones. These drugs are currently not used against gallstones and to prove the efficacy of the latter, rather expensive drugs in the treatment of cholelithiasis, still long-term well-designed experimental studies should be performed.^{43,46} Because many synthetic chemical drugs show side effects, there is an increasing public interest in natural medicines. On the internet, some poorly characterized products and some homeopathic drugs against cholelithiasis are advertised. However, currently, no herbal medicinal products, for which the efficacy against cholelithiasis has been proven, are available. An infusion of *H. hirsuta* would be a valuable candidate since the efficacy of this plant species against cholelithiasis was already proven in an *in vivo* study in dogs.⁴⁷ This study and an earlier study demonstrated a reduced secretion of biliary cholesterol and a rapid dissolution of human gallstones consisting of cholesterol implemented into the gallbladder of dogs.^{8,47} However, the efficacy and use of a standardized extract against cholelithiasis have never been investigated. This work aims to initiate the development of a new herbal medicinal product for the treatment of gallstones. Therefore, the following workflow was adopted. First, the characterization of the extract was achieved by isolation and identification of the major phytochemical constituents. An analytical method for quantification of these constituents was developed and validated in order to standardize the extract and as such to ensure a consistent high-quality product and thus a reproducible therapeutic effect from one batch to another and to meet the quality demands of herbal medicinal products. In addition, *Herniaria spp.* samples from different regions were screened using this method. Finally, the *in vivo* effect of the standardized extract of the plant on the level of cholesterol in the bile of dogs receiving a cholesterol-rich diet was investigated. In addition, the genotoxicity was evaluated. Because of its established traditional use in Morocco and in European countries, and the absence of reported toxicity in folk medicine and in the *in vivo* experiments, an extract of *Herniaria hirsuta* can be considered as non-toxic according to the legislation on herbal medicinal products (traditional use). However, since pharmacovigilance and long-standing use cannot be used as evidence for the absence of genotoxic risks, the genotoxicity must be evaluated according to the European guideline on the assessment of genotoxicity of herbal substances/preparations. The basic

requirement is to assess genotoxicity in a bacterial reverse mutation test using a test battery of different bacterial strains (Ames test) (EMEA/HMPC/107079/2007).⁴⁸

6.2 Saponins and flavonoids from an infusion of *Herniaria hirsuta**

6.2.1 Introduction

Since an infusion of *H. hirsuta* has a proven efficacy against urolithiasis and cholelithiasis, this part focuses on the phytochemical characterization of the main constituents of this infusion using semi-preparative HPLC, mass spectrometry and NMR, finally aiming at the development of a standardized extract that can be used in the treatment and prophylaxis of stone diseases.

6.2.2 Materials and methods

6.2.2.1 Plant material

Aerial parts from *Herniaria hirsuta* were collected in d'Oujda, Morocco. A voucher specimen of the plant is kept at the Muséum National d'Histoire Naturelle -Institut Scientifique-Université Mohamed V Agdal – (Reference number: 5902). The material was air dried. The aqueous infusions of *Herniaria hirsuta* were prepared from 80 g in 4 L of boiling water for 30 min with continuous stirring.⁸ The infusions were cooled, portions were combined, filtered, and lyophilized. Typically, 100 g of plant material yielded about 15 g lyophilizate.

6.2.2.2 General experimental procedures

Column chromatography

To obtain pure compounds from *H. hirsuta*, the infusion was first subjected to column chromatography. The separation was performed using a Gilson[®] 306-pump coupled to a normal phase GraceResolv[®] column (150 g, 40 – 63 µm) and the sample was applied on top (7.3 g). Elution of the column was performed subsequently with dichloromethane, ethyl acetate, and methanol. Fractions were collected in volumes of 30 mL. Subsequently, reversed phase flash chromatography was carried out using a Reveleris Flash Chromatography system equipped with a Reveleris C18 column (40 g, 40 µm). Compounds were eluted with water and methanol using the following gradient: solvent A: H₂O; solvent B: methanol, 5% B for 8 min – from 5% to 100% B in 82 min – 100% B for 5 min; fractions of 25 mL were collected. All fractions were monitored by TLC. Every fraction

*Published: van Dooren, I.; Foubert, K.; Bijttebier, S.; Theunis, M.; Velichkova, S.; Claeys, M.; Pieters, L.; Exarchou, V.; Apers, S. Saponins and flavonoids from an infusion of *Herniaria hirsuta*. *Planta Med.* DOI <http://dx.doi.org/10.1055/s-0042-118710>.

was applied on a normal phase – TLC plate (20 x 20 cm, silica gel 60 F₂₅₄), and subsequently the plate was developed with the organic phase of a *n*-BuOH – CH₃COOH – H₂O (13:3:5) mixture, sprayed with anisaldehyde-sulphuric acid reagent and heated to 105 °C. Based on the observed TLC pattern, similar fractions were combined.

Semi-preparative HPLC

Fraction 1A (eluted with 90% ethyl acetate and 10% methanol, 78.8 mg), and fraction 1B (eluted with 30% ethyl acetate and 70% methanol, 255.6 mg), obtained by normal phase chromatography, and fractions 2C-2J (eluted with a gradient of water and methanol see below), obtained with reversed phase chromatography, were separated by repeated semi-preparative HPLC. An Agilent 1200 Series HPLC with DAD and a Gilson 322 HPLC with UV detection were used for the isolation of the flavonoids. Saponins were isolated using an AutoPurification™ system from Waters with DAD and a Micromass Quattro micro TQD mass analyzer. Fractions were separated using an Apollo® column (250 x 10 mm, 5 µm). Separation was optimized for all fractions and the following gradients were applied: solvent A: H₂O + 0.05% FA; solvent B: methanol + 0.05% FA, gradient fraction 1A: from 50% to 70% B in 20 min – from 70% to 95% in 2 min; gradient fraction 1B: from 15% to 67% B in 45 min – from 67% to 100% B in 1 min; fractions C-J: 60% B for 5 min – from 60% to 100% B in 30 min – 100% B for 3 min – from 100% to 60% B in 1 min – 60% B for 5 min. Flow rate for all gradients: 3 mL/min; detection: at 210 nm and 320 nm; injection volume: fraction 1A and 1B: 450 µL, fraction 2C, 2F, 2G and 2H: 600 µL, fraction 2D, 2E, 2I and 2J: 300 µL; concentration, fractions 1A: 10 mg/mL and 1B: 30 mg/mL; fractions 2C-2J: 1.8-10 mg/mL.

Structure elucidation

LC-MS analysis of the infusion of *H. hirsuta* (10 mg/mL, 80% methanol) was performed employing a Surveyor LC-LXQ system equipped a Grace Smart column (250 x 4 mm, 5 µm). The flow rate was 1.0 mL/min and a splitter was used. UV detection was carried out at 210, 254, 300 and 320 nm and the solvent program was as follows: solvent A: H₂O + 0.05% FA; solvent B: methanol + 0.05% FA; from 5% to 100% B in 60 min – stay at 100% during 2 min. The injection volume was 20 µL. The experimental data were recorded in the (-)-ESI mode using following conditions: sheath gas flow: 65 arbitrary units;

auxiliary gas flow: 14 arbitrary units; source voltage: 4.0 kV; ion transfer tube temperature: 350 °C; and capillary voltage: -10 V. Mass spectral data were recorded using data-dependent scanning in the mass range m/z 150–1800. For MSⁿ experiments, an isolation width of 2 Da was used and normalized collision energy of 35% was applied. All data were acquired and processed using Xcalibur software, version 2.0.

Accurate mass measurements were carried out using an Orbitrap mass spectrometer (Q Exactive™) equipped with an Ion Max™ ESI source in negative ion mode. Chromatographic parameters were used as described in De Paepe et al.⁴⁹

To obtain information about the identity of the sugar moieties of the two main saponins, GC–MS analysis was performed. The compounds were hydrolyzed in basic and acidic conditions. For basic hydrolysis, a 5% potassium hydroxide solution was added to the sample (compound **1**: 1.27 mg + 6.4 mL 5% KOH solution, compound **2**: 1.49 mg + 7.5 mL 5% KOH solution) and refluxed for 2 h. The solution was brought to pH 6 with 1M HCl and extracted 3 times with 10 mL of *n*-butanol. Both butanol and water phases were evaporated and redissolved in 3 mL methanol and water, respectively, and centrifuged for 5 min at 2397g (3500 rpm). Both phases were analyzed by direct infusion on an LXQ linear ion trap. Clean-up of the water phase was done by using a Strata-X (33u polymeric reversed phase, 30 mg/mL) SPE column, using 10% of methanol as elution solvent to obtain the cleaved sugar chain from the ester linkage. To both the glycan part obtained after alkaline hydrolysis and the pure saponin (1.02 mg) 1 mL TFA (2M) was added and samples were kept in an oven at 120 °C for 5 h.

Samples obtained from both alkaline and acid hydrolysis and all reference monosaccharides (D-ribose, L-rhamnose monohydrate, L-arabinose, L-xylose, D-glucuronic acid, D-glucose, D-fructose, L-fucose, D-galactose, D-mannose (100 µg)) were treated with pyridine and the trimethylsilylation reagent (BSTFA + 1% TMCS) and heated for 1 h at 70 °C. All samples were analyzed according to Medeiros and Simoneit⁵⁰ employing a Voyager GC–MS with Trace 2000 GC and an Alltech Heliflex AT-5 ms capillary column with a length of 30 m, an internal diameter of 0.25 mm, and a film thickness of 0.25 µm. The carrier gas He was used at a constant flow rate of 1.3 mL/min, the injector and MS source temperature were maintained at 200 °C and 230 °C, respectively. The temperature program was as follows: start at 65 °C – hold on 65 °C for 2 min – temperature increase of 6 °C/min till 300 °C – hold on 300 °C for 15 min. The mass spectrometer was operated with an electron ionization energy

of 70 eV. Chromatograms were recorded using selected ion monitoring (SIM), looking for prominent mass peaks at m/z 204 and 217. About 1 μL of every sample was analyzed with a split ratio of 8. All data were recorded and processed using Xcalibur software, version 1.0. The monosaccharide units present in the hydrolyzed sample were elucidated by means of the retention time of the reference sugars. The absolute configuration was determined based on their most abundant configuration in nature. The retention times of the sugars (α ; β) were as follows: D-ribose (20.00 min; 20.24 min), L-rhamnose monohydrate (19.53 min; 20.72 min), L-arabinose (19.28 min; 19.85 min), L-xylose (21.08 min; 22.02 min), D-glucuronic acid (25.67 min; 26.52 min), D-glucose (24.29 min; 25.80 min), D-fructose (22.76 min; 22.94 min), L-fucose (20.24 min; 20.99 min), D-galactose (23.73 min; 24.49 min), D-mannose (23.25 min; 24.91 min), D-galacturonic acid (25.34 min; 26.38 min).

NMR spectra were recorded in $\text{DMSO-}d_6$ (flavonoids) and $\text{methanol-}d_4$ (saponins) on a Bruker DRX-400 instrument, operating at 400 MHz for ^1H and at 100 MHz for ^{13}C . Chemical shifts are expressed in ppm and coupling constants (J) in Hz.

The specific rotation was determined in a Jasco P-2000 digital polarimeter.

6.2.3 Results and discussion

6.2.3.1 Isolation

Normal phase flash chromatography of 7.3 g of the dry residue after lyophilization of the infusion of *H. hirsuta* resulted in two fractions of 78 mg (1A) and 310 mg (1B), respectively (Figure 6.5). Semi-preparative HPLC of fraction 1A resulted in the isolation of compound **5** (1.36 mg), whereas semi-preparative HPLC of fraction 1B resulted in the isolation of compound **3** (3.5 mg) and **4** (1.9 mg). Fractions 2C-J (3.0 - 38.0 mg), obtained after reversed flash chromatography, yielded compound **1** (9.0 mg) and compound **2** (25.5 mg).

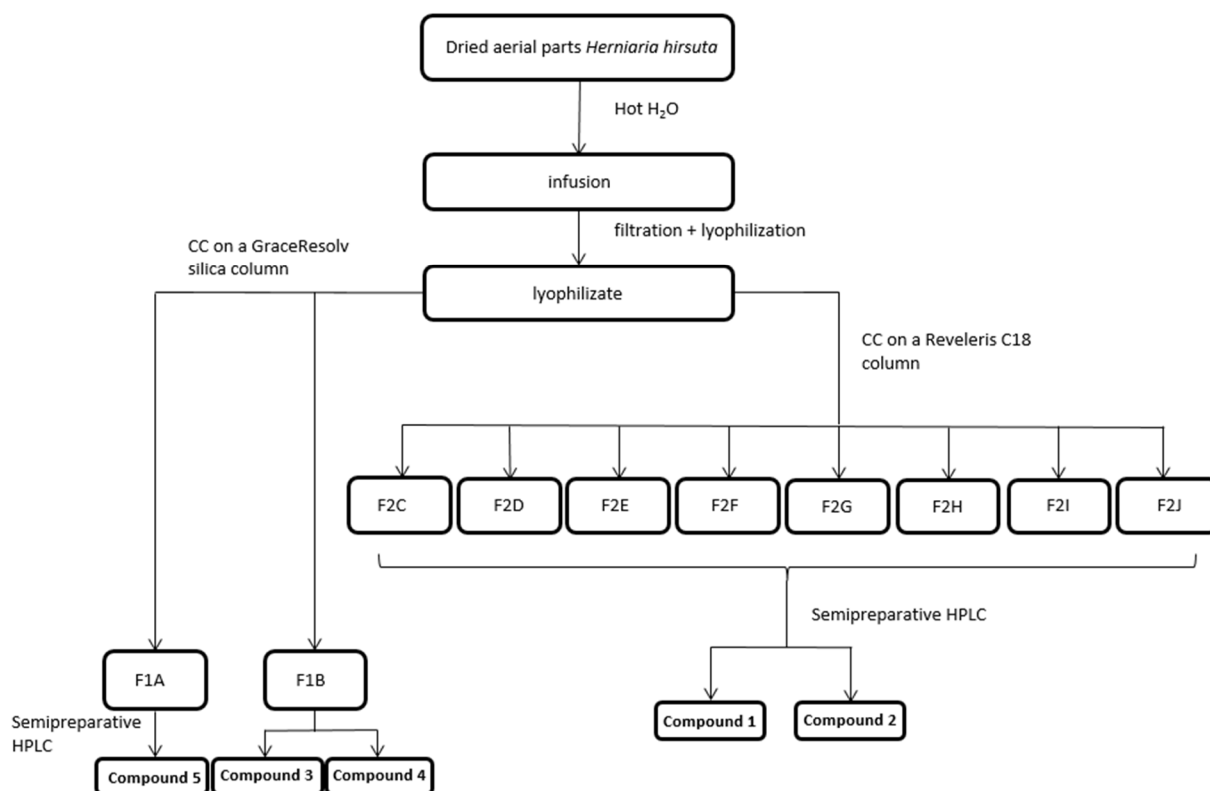


Figure 6.5 Extraction scheme for saponins and flavonoids from an infusion of *H. hirsuta*.

6.2.3.2 Structure elucidation

Compound **1** (Figure 6.14) was obtained as a white amorphous powder. The UV spectrum of compound **1** showed an absorbance maximum at 194 nm and $[\alpha]^{20}_D$ was 0.99 (3.5 g/L, MeOH). The HR-ESI-MS mass spectrum showed a deprotonated molecule at m/z 1103.5289 $[M-H]^-$ and supported a molecular formula of $C_{53}H_{84}O_{24}$. The ESI-mass spectrum of **1** exhibited a deprotonated molecule at m/z 1103 $[M-H]^-$. The fragmentation pattern is depicted in Figure 6.15. The m/z 1103 MS^2 product ion spectrum resulted in ions at m/z 1085 $[M-H-18]^-$, 971 $[M-H-132]^-$, 941 $[M-H-162]^-$ and 923 $[M-H-180]^-$, due to the loss of a molecule of water (18 u), a pentose unit (132 u), a hexose unit (162 u) and a hexose unit and a molecule of water (180 u), respectively. The product ion at m/z 501 $[M-H-162-132-162-146]^-$ attributed to the loss of two hexoses, a pentose unit and a deoxyhexose unit (602 u) together with product ions formed at m/z 483 $[Aglycone-H-18]^-$ and 439 $[Aglycone-H-18-44]^-$ are characteristic for medicagenic acid as an aglycone.⁵¹ The MS^3 product ion spectrum of m/z 971 $[M-H-132]^-$ resulted in ions at m/z 809 $[M-H-162]^-$ due to the loss of a hexose moiety, whereas MS^3 analysis of m/z 941 $[M-H-162]^-$ resulted in a product ion peak at m/z 747 $[M-H-132-18-44]^-$ due to the loss of a pentose moiety together with a water and carbon dioxide molecule. The formation of these latter

MS³ product ions together with the MS² spectra indicated that both residues were in a terminal position, suggesting the presence of a branched sugar chain.

The monosaccharides obtained after alkaline and acidic hydrolysis of compound **1** were identified as D-glucose, D-xylose and L-rhamnose by comparison with GC-MS.⁵⁰

The ¹H-NMR (Figure 6.6) and ¹³C-NMR (Figure 6.7) spectra of the aglycone part of compound **1** displayed six tertiary methyl signals at δ 0.80 (H-26), 0.91 (H-29), 0.94 (H-30), 1.16 (H-27), 1.291 (H-25) and 1.33 (H-24) giving correlations in HSQC with δ 18.3 (C-26), 33.7 (C-29), 24.4 (C-30), 26.4 (C-27), 17.9 (C-25) and 13.3 (C-24), an olefinic proton at δ 5.29 (H-12), two olefinic carbons at δ 123.7 (C-12) and 145.0 (C-13) and two oxygen bearing methine protons at δ 3.98 (H-3) and 4.08 (H-2) (Table 1). Furthermore, a downfield shifted signal at δ 182.4 (C-23) and an upfield shifted carbon signal at 178.2 (C-28) suggested the presence of a carboxylic acid and ester function, respectively. Thorough 1D (Figures 6.6 – 6.9) and 2D (Figures 6.10 – 6.13) NMR spectroscopic analysis confirmed the structure of the aglycone to be medicagenic acid (2 β ,3 β -dihydroxyolean-12-ene-23,28-dioic acid). These findings are in accordance with the results obtained with ESI-MS experiments and with previously published data.^{16,17,37,52} The presence of an upfield shifted carbon signal (C-28) at δ 178.2 suggested compound **1** to be a monodesmosidic saponin. Four anomeric proton signals at δ 5.44 (d, J = 1.5 Hz) (Rha H-1), 5.38 (d, J = 7.6 Hz) (Glcl H-1), 4.42 (d, J = 7.6) (Xyl H-1) and 4.34 (d, J = 7.7) (Glcll H-1) displaying correlations in the HSQC spectrum with four anomeric carbon signals at δ 101.3 (Rha C-1), 95.2 (Glcl C-1), 107.6 (Xyl C-1) and 104.9 (Glcll C-1), respectively, evidenced the presence of four sugar moieties. The complete assignment of the monosaccharides residues was performed by COSY, TOCSY, HSQC and HMBC experiments, further described in depth, and GC-MS analysis. This led to the identification of two β -D-glucopyranose moieties (Glcl and Glcll), a β -D-xylopyranose (Xyl) and a α -L-rhamnopyranose unit (Rha). The β -anomeric configuration of the glucopyranosyl and xylopyranosyl moiety and the α -anomeric configuration of the rhamnosyl moiety were confirmed by the specific J_{H_1, H_2} coupling constants of 7-8 Hz and 1.5 Hz, respectively. The α -anomeric configuration was confirmed by comparison with the ¹³C NMR values of methyl α -L-rhamnoside and methyl β -L-rhamnoside published by Agrawal et al.⁵³

Linkages between both the aglycone and sugar units were mainly achieved by HMBC and are shown in Figure 6.16. A cross-peak in the HMBC spectrum between the anomeric proton of Glcl (δ 5.38) and

the quaternary carbon at δ 178.2 (C-28) indicated that GlcI was linked to the C-28 position of the aglycone. This ester linkage was confirmed by the upfield shifted C-28 signal and by the downfield shift of the ^{13}C -NMR peak at δ 95.2 ppm (GlcI C-1).^{10,16,17,20} The HMBC spectrum also showed long-range C-H correlations between δ 76.7 (GlcI C-2) and δ 5.38 (GlcI H-1) and δ 5.44 (Rha H-1), and between δ 95.2 (GlcI C-1) and δ 3.62 (GlcI H-2). Other cross-peaks were present between GlcI C-2 at δ 76.7 and GlcI H-3 at δ 3.56, between GlcI C-3 at δ 79.4 and GlcI H-2 at δ 3.62, between GlcI C-3 at δ 79.4 and GlcI H-4 at δ 3.47, and between GlcI C-4 at δ 69.7 and H-3 at δ 3.56. Starting from the anomeric proton, the signals in the COSY and TOCSY spectra confirmed these findings and revealed the position of GlcI H-5 at δ 3.49 with a cross-peak in HSQC (GlcI C-5 at δ 77.8). TOCSY correlations were observed from δ 5.39 (GlcI H-1) to δ 3.76 (GlcI H-6a) and δ 4.10 (GlcI H-6b), and the latter signals were correlated in the HSQC spectrum with a ^{13}C -NMR signal at δ 69.7, assigned to the sixth carbon of this sugar moiety. These data together with GC-MS data allowed identifying this monosaccharide as β -D-glucose (GlcI). A second monosaccharide moiety was found to be attached to GlcI by a 1 \rightarrow 2 linkage evidenced by long-range correlations between δ 101.3 (Rha C-1) and δ 3.62 (GlcI H-2) and between δ 76.7 (GlcI C-2) and δ 5.44 (Rha H-1), as already mentioned above. The HMBC and COSY/TOCSY spectra revealed the other positions of this second sugar moiety. HMBC long-range correlations were present between Rha C-4 (δ 84.9) and Rha H-6 (δ 1.285), Rha H-2 (δ 3.95) and Rha H-3 (δ 3.845) and between Rha C-5 (δ 68.97) and Rha H-6 (δ 1.285). A typical Rha C-6 signal, a methyl at δ 17.5 corresponding in HSQC to a doublet at δ 1.285 in ^1H NMR, suggested the presence of a rhamnosyl moiety. The downfield shifted signal of Rha C-4 revealed the next binding position. This finding was confirmed by the presence of long-range correlations in the HMBC spectrum between Xyl C-1 (δ 107.6) and Rha H-4 (δ 84.9) and between Rha C-4 (δ 84.9) and an anomeric proton Xyl H-1 (δ 4.42). Other correlations in the HMBC spectrum were present between Xyl C-1 (δ 107.6) and Xyl H-2 (δ 3.181) and Xyl H-5b (δ 3.178), between Xyl C-2 (δ 76.4) Xyl and H-3 (δ 3.31), Xyl C-3 (δ 78.5) and Xyl H-2 (δ 3.181) and between Xyl C-4 (δ 71.3) and Xyl H-3 (δ 3.31). This monosaccharide was identified as β -D-xylose. The presence of a downfield-shifted carbon signal of GlcI at C-6 indicated that in addition to the α -L-rhamnopyranosyl moiety another sugar unit was attached. An HMBC correlation between δ 62.9 (GlcI C-6) and the anomeric proton GlcII H-1 at δ 4.34 evidenced the 1 \rightarrow 6 linkage of GlcII to GlcI.

The anomeric proton was correlated in HSQC to a carbon signal at δ 104.9 and an HMBC long-range correlation between GlcII C-2 at δ 3.20 (HSQC to δ 75.3) and this proton was present. A cross-peak in COSY between GlcII H-2 (δ 3.20) and δ 3.37 revealed the GlcII H-3 to be at δ 3.37, which was confirmed by long-range correlations in the HMBC spectrum (GlcII C-2 at δ 75.3 to GlcII H-3 at δ 3.37 and GlcII C-3 at δ 78.1 to GlcII H-2 at δ 3.20). A cross-peak from GlcII C-4 at δ 71.7 to GlcII H-3 at δ 3.37 and from GlcII C-5 at δ 78.1 to GlcII H-4 at δ 3.30 together with a TOCSY cross-peak between GlcII H-1 at δ 4.34 and GlcII H-5 at δ 3.24 allowed to assign GlcII C-4 to the signal at δ 71.7 (HSQC – δ 3.30) and GlcII C-5 at δ 78.1 (HSQC - δ 3.24). In the HMBC spectrum, a cross-peak was observed between GlcII C-5 at δ 78.1 and one of the protons of GlcII H-6 at δ 3.850. TOCSY spectra confirmed the protons at GlcII H-6 to be located at δ 3.67 and δ 3.850 correlating with GlcII C-6 at δ 62.9 in HSQC. Together with GC-MS data, this monosaccharide moiety was identified as β -D-glucose. Briefly, the HMBC cross-peaks at $\delta_{\text{H}}/\delta_{\text{C}}$ 5.44 (Rha H-1)/76.7 (GlcI C-2), 4.42 (Xyl H-1)/84.9 (Rha C-4), and 4.34 (GlcII H-1)/69.7 (GlcI C-6) suggested the sequence of the oligosaccharide moiety at C-28 to be [β -D-xylopyranosyl-(1 \rightarrow 4)- α -L-rhamnopyranosyl-(1 \rightarrow 2)]- $[\beta$ -D-glucopyranoside-(1-6)]- β -D-glucopyranoside. Therefore, compound **1** could finally be elucidated as 28-O- $[\beta$ -D-xylopyranosyl-(1 \rightarrow 4)- α -L-rhamnopyranosyl-(1 \rightarrow 2)]- $[\beta$ -D-glucopyranoside-(1-6)]- β -D-glucopyranosyl)-medicagenic acid, for which the name herniariasaponin G was adopted (Figures 6.14, 6.15, and 6.16).

Table 6.1 $^1\text{H-NMR}$ and $^{13}\text{C-NMR}$ assignments of compounds **1** and **2**.

Aglycone	(1)		Aglycone	(2)	
	δ_{C} (ppm)	δ_{H} (ppm), mult., J (Hz)		δ_{C} (ppm)	δ_{H} (ppm), mult., J (Hz)
1	45.8	2.11, 1.221, m	1	45.1	2.10, 1.25, m
2	72.2	4.08, m	2	71.0	4.31, d ($J = 2.3$) or br s
3	76.6	3.98, d (3.8)	3	86.7	4.07, m
4	54.3		4	53.6	
5	53.0	1.586, m	5	53.3	1.59, m
6	22.2	1.65, 1.17, m	6	21.8	1.57, 1.20, m
7	33.9	1.49, 1.38, m	7	34.0	1.51, 1.38, m
8	41.2		8	41.2	
9	49.9	1.585, m	9	49.8	1.58, m
10	37.6		10	37.6	

Table 6.1 continued ¹H-NMR and ¹³C-NMR assignments of compounds 1 and 2.

Aglycone	(1)		Aglycone	(2)	
	δ_c (ppm)	δ_H (ppm), mult., <i>J</i> (Hz)		δ_c (ppm)	δ_H (ppm), mult., <i>J</i> (Hz)
11	24.8	2.02, 1.93, m	11	24.1	2.05, 1.62, m
12	123.7	5.29, t (3.2)	12	123.8	5.27, t (3.4)
13	145.0		13	144.8	
14	43.3		14	43.3	
15	29.4	1.55, 1.219, m	15	29.2	1.63, 1.197, m
16	24.1	2.06, 1.63, m	16	24.8	1.99, 1.91, m
17	50.2		17	48.1	
18	42.9	2.82, dd (14.0, 3.8)	18	43.1	2.83, dd (14.0, 4.0)
19	47.5	1.715, 1.14, m	19	47.4	1.73, 1.14, m
20	31.7		20	31.7	
21	35.0	1.40, 1.23, m	21	35.0	1.39, 1.23, m
22	33.2	1.723, 1.57, m	22	33.2	1.76, 1.57, m
23	182.4		23	182.4	
24	13.3	1.33, s	24	13.9	1.39, s
25	17.9	1.291, s	25	17.3	1.27, s
26	18.3	0.80, s	26	17.9	0.80, s
27	26.4	1.16, s	27	26.5	1.17, s
28	178.2		28	178.2	
29	33.7	0.91, s	29	33.6	0.91, s
30	24.4	0.94, s	30	24.3	0.93, s
GlcI			GlcA		
1	95.2	5.38, d (7.6)	1	105.09	4.39, d (<i>J</i> = 7.6)
2	76.7	3.62, m	2	75.9	3.39, m
3	79.4	3.56, m	3	82.7	3.55, m
4	71.1	3.47, m	4	72.3	3.51, m
5	77.8	3.49, m	5	76.6	3.71, m
6	69.7	4.10, 3.76 d (10.8); dd (11.8; 4.92)	6	175.7	

Table 6.1 continued ¹H-NMR and ¹³C-NMR assignments of compounds 1 and 2.

Aglycone	(1)		Aglycone	(2)	
	δ_c (ppm)	δ_H (ppm), mult., J (Hz)		δ_c (ppm)	δ_H (ppm), mult., J (Hz)
Rha			RhaI		
1	101.3	5.44, br s (1.5)	1	102.4	5.19, br s ($J = 1.1$)
2	72.0	3.95, m	2	72.5	3.92, m
3	72.4	3.845, m	3	72.4	3.70, m
4	84.9	3.51, m	4	74.3	3.36, m
5	68.9	3.82, m	5	69.9	4.07, m
6	17.5	1.285, s	6	18.0	1.23, s
Xyl			Fuc		
1	107.6	4.42, d (7.6)	1	95.4	5.35, d ($J = 8.2$)
2	76.4	3.181, m	2	74.9	3.82, m
3	78.5	3.31, m	3	76.6	3.71, m
4	71.3	3.45, m	4	73.8	3.57, m
5	67.4	3.84, 3.178, m	5	72.8	3.69, m
GlcII			6	16.7	1.22, s
1	104.9	4.34, d (7.7)	RhaII		
2	75.3	3.20, m	1	101.5	5.37, br s ($J = 1.2$)
3	78.1	3.37, m	2	72.1	4.088, m
4	71.7	3.30, m	3	81.6	3.84, m
5	78.1	3.24, m	4	79.2	3.65, m
6	62.9	3.850, 3.67, m	5	68.8	3.86, m
			6	18.6	1.24, s
			Api		
			1	112.0	5.24, d ($J = 3.8$)
			2	78.3	4.03, d ($J = 3.9$)
			3	80.2	
			4	74.9	4.091, m/ 3.76, d ($J = 9.7$)
			5	65.2	3.58, s

Table 6.1 continued ¹H-NMR and ¹³C-NMR assignments of compounds 1 and 2.

(1)		(2)			
Aglycone	δ_c (ppm)	δ_H (ppm), mult., J (Hz)	Aglycone	δ_c (ppm)	δ_H (ppm), mult., J (Hz)
Xyl					
		1	105.12	4.63, d ($J = 7.7$)	
		2	75.3	3.33, m	
		3	88.2	3.47, m	
		4	70.2	3.59, m	
		5	66.7	3.90, m/3.20, m	
Glc					
		1	105.3	4.58, d ($J = 7.8$)	
		2	75.5	3.35, m	
		3	77.8	3.46, m	
		4	78.3	3.34, m	
		5	71.6	3.30, m	
		6	62.8	3.88, m/3.66, m	

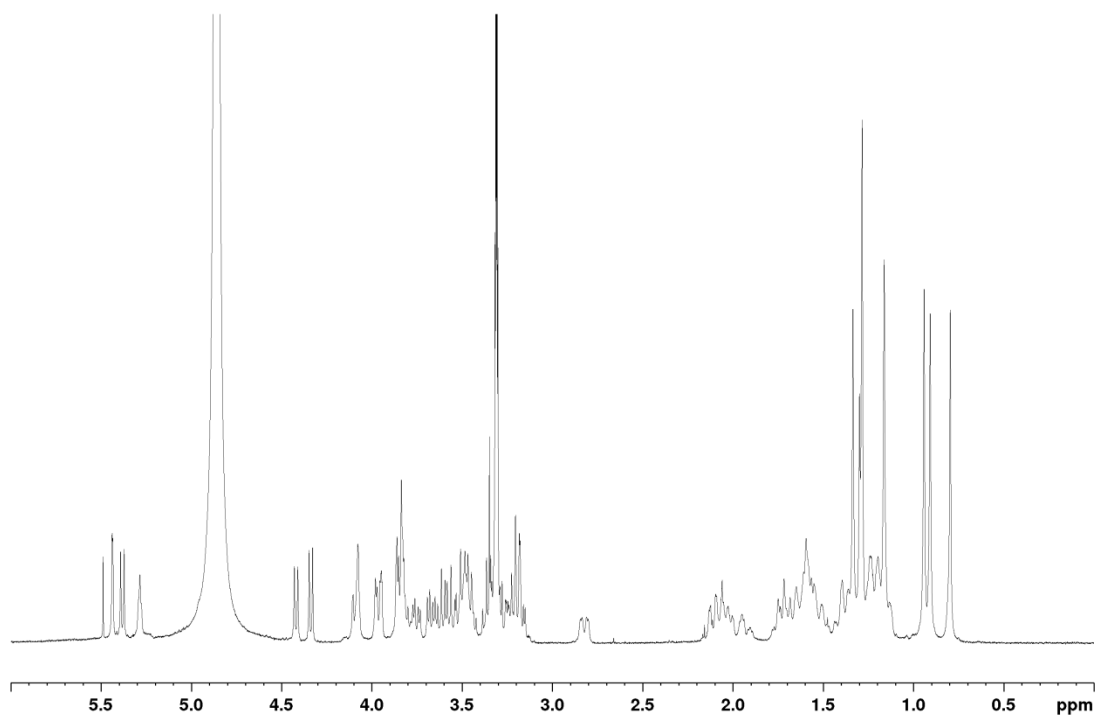


Figure 6.6 ¹H-NMR spectrum of compound 1.

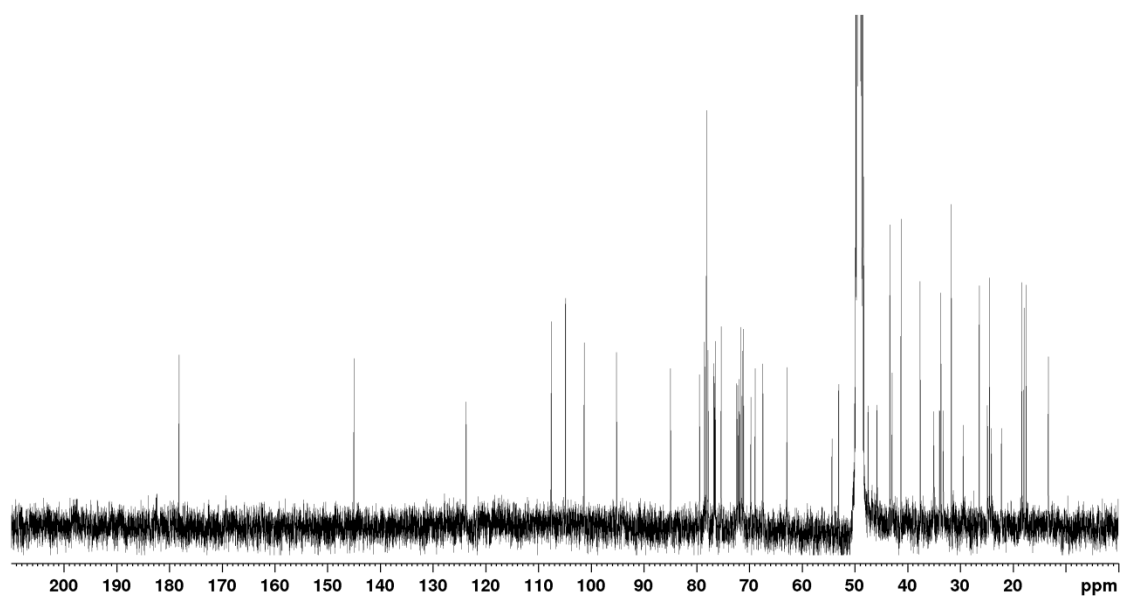


Figure 6.7 ^{13}C NMR spectrum of compound 1.

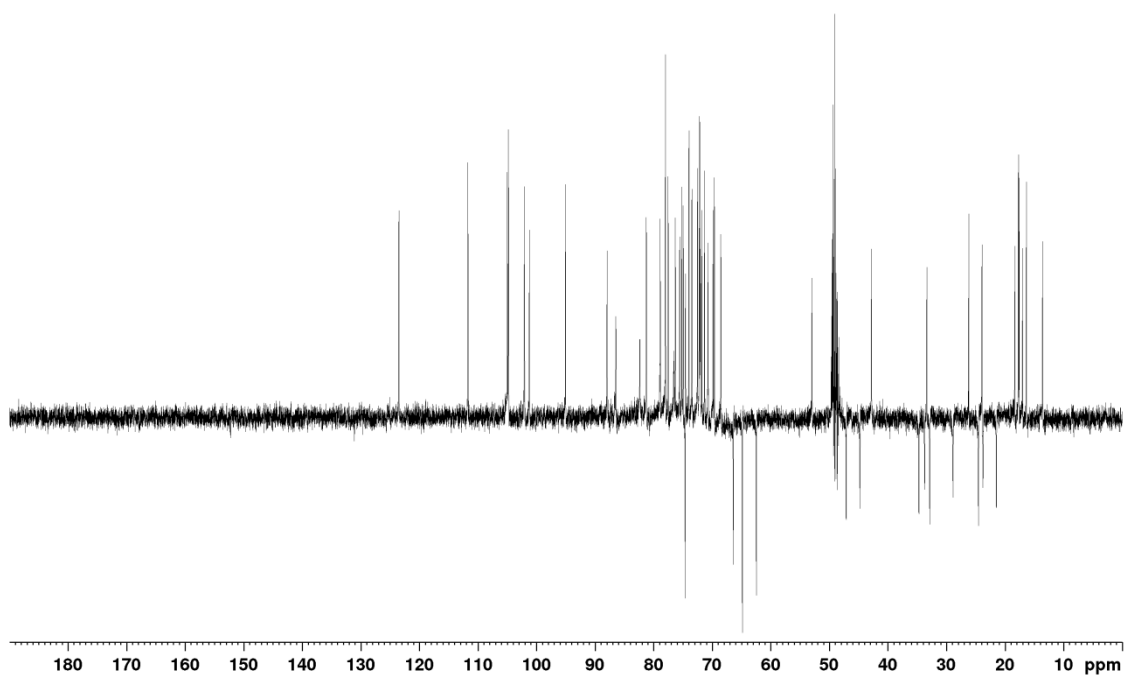


Figure 6.8 DEPT-135 spectrum of compound 1.

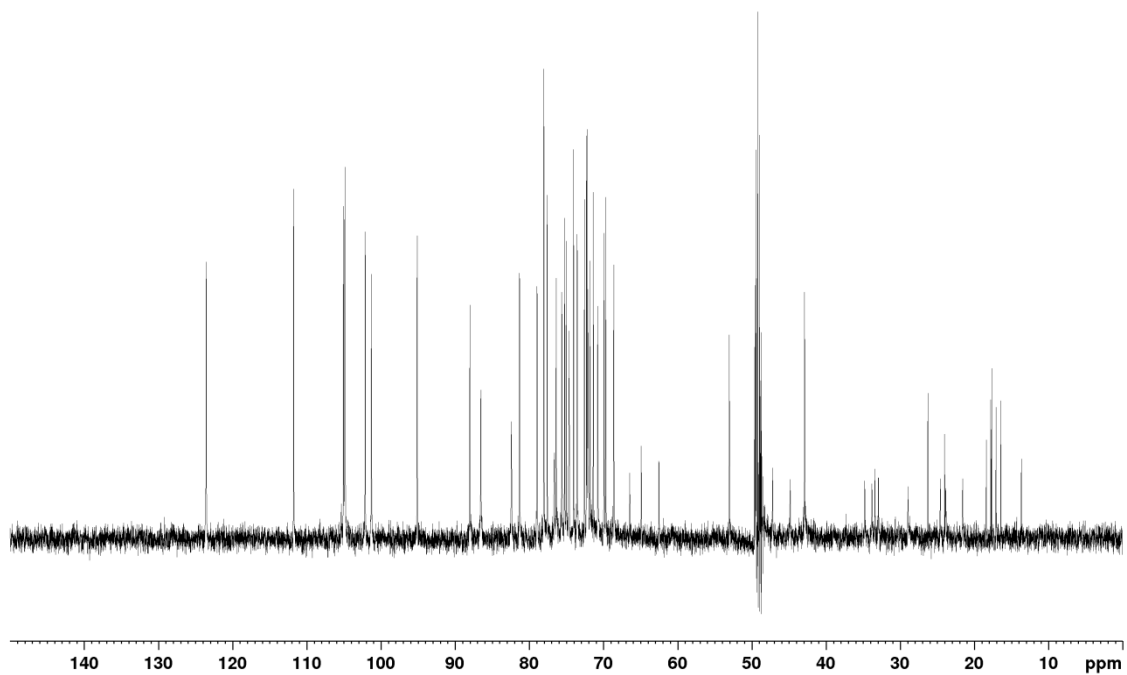


Figure 6.9 DEPT-90 spectrum of compound 1.

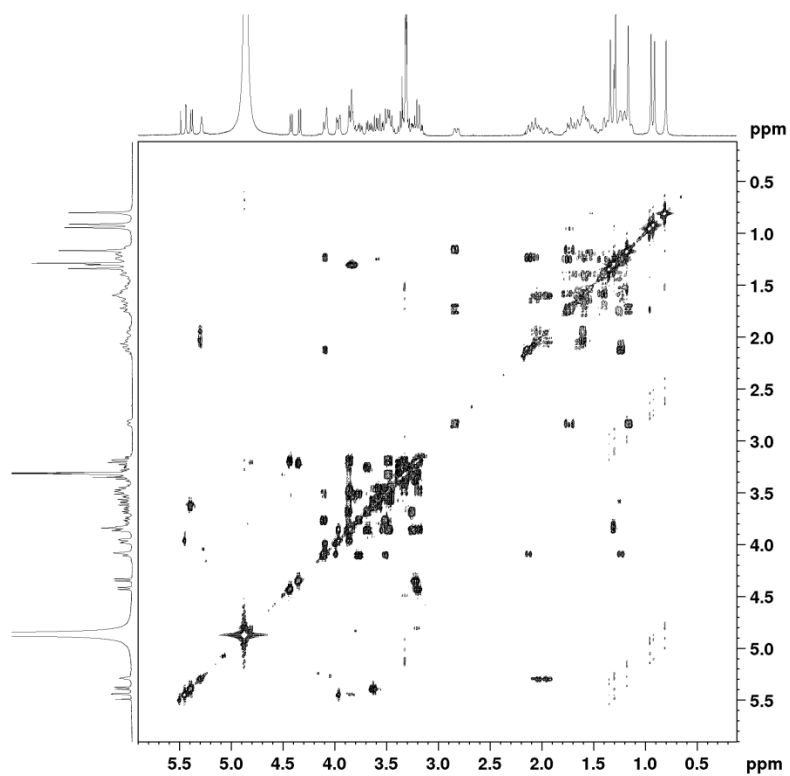


Figure 6.10 COSY spectrum of compound 1.

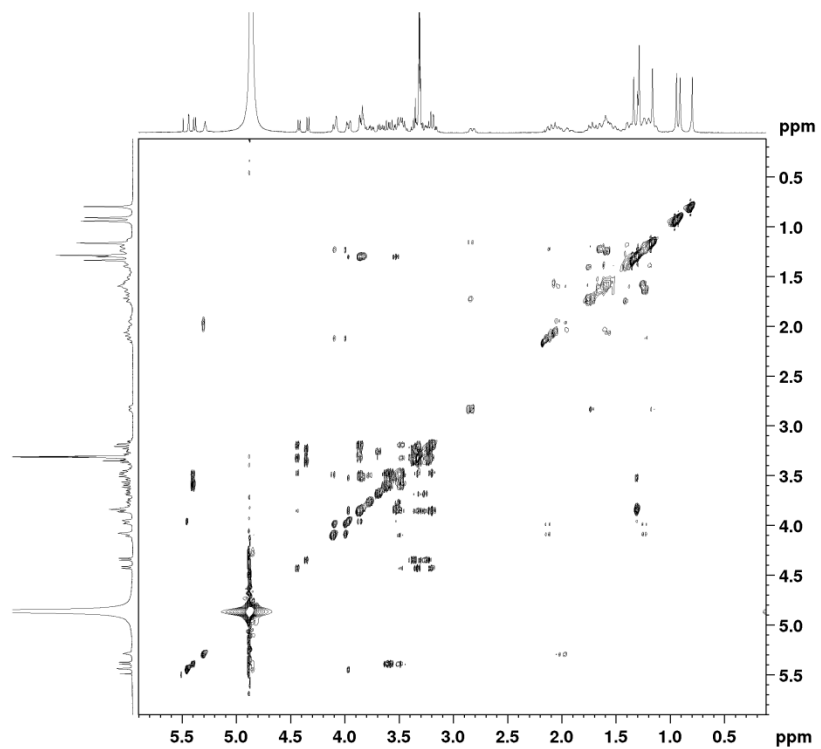


Figure 6.11 TOCSY spectrum of compound 1.

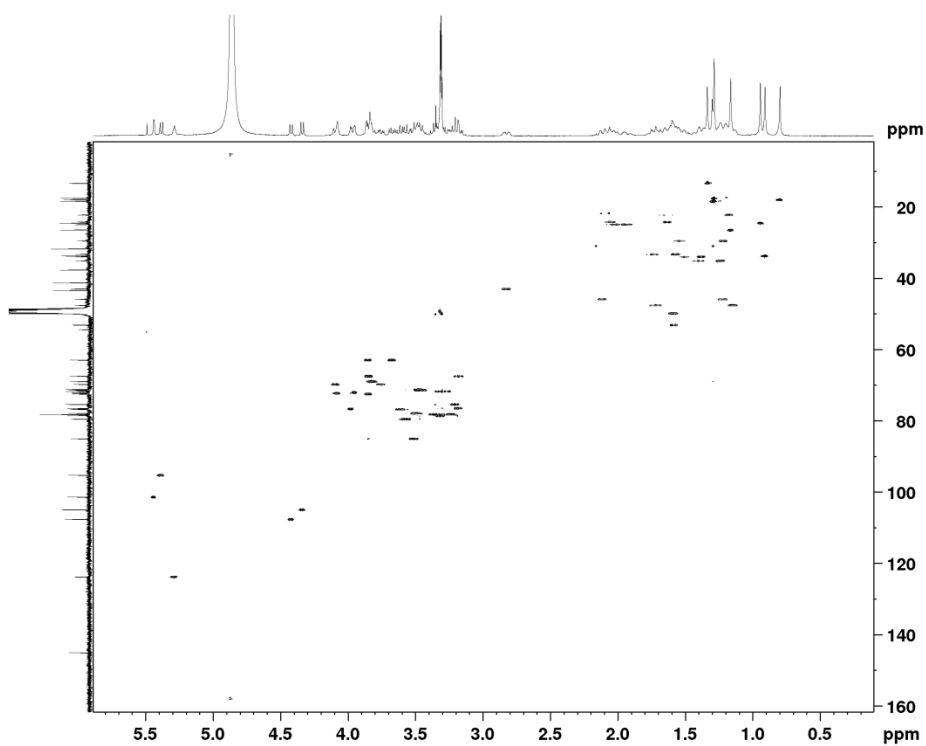


Figure 6.12 HSQC spectrum of compound 1.

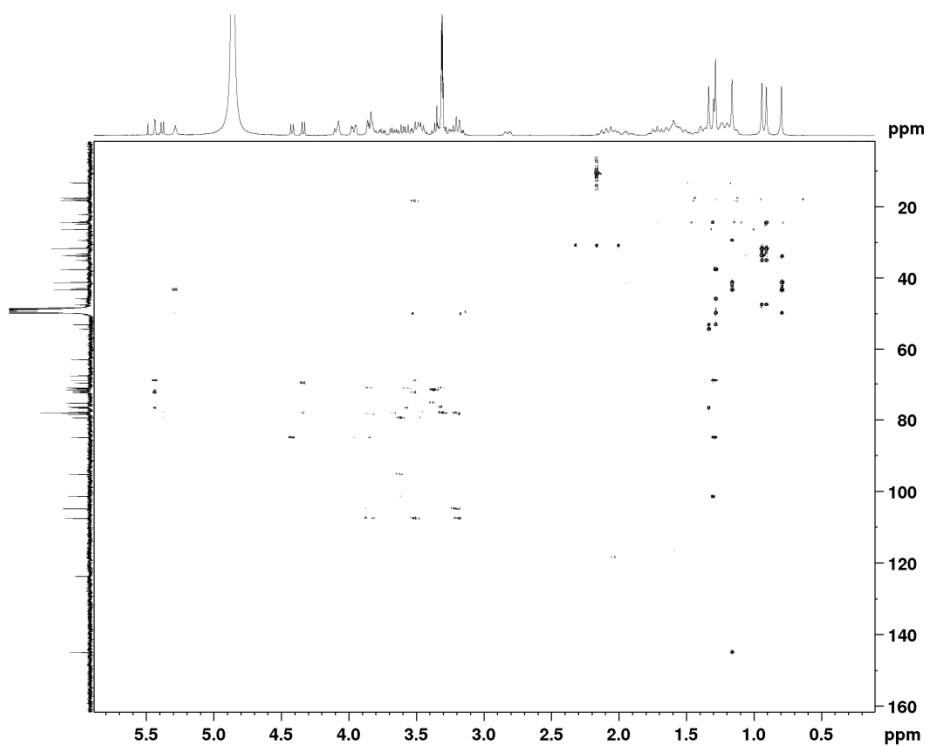


Figure 6.13 HMBC spectrum of compound 1.

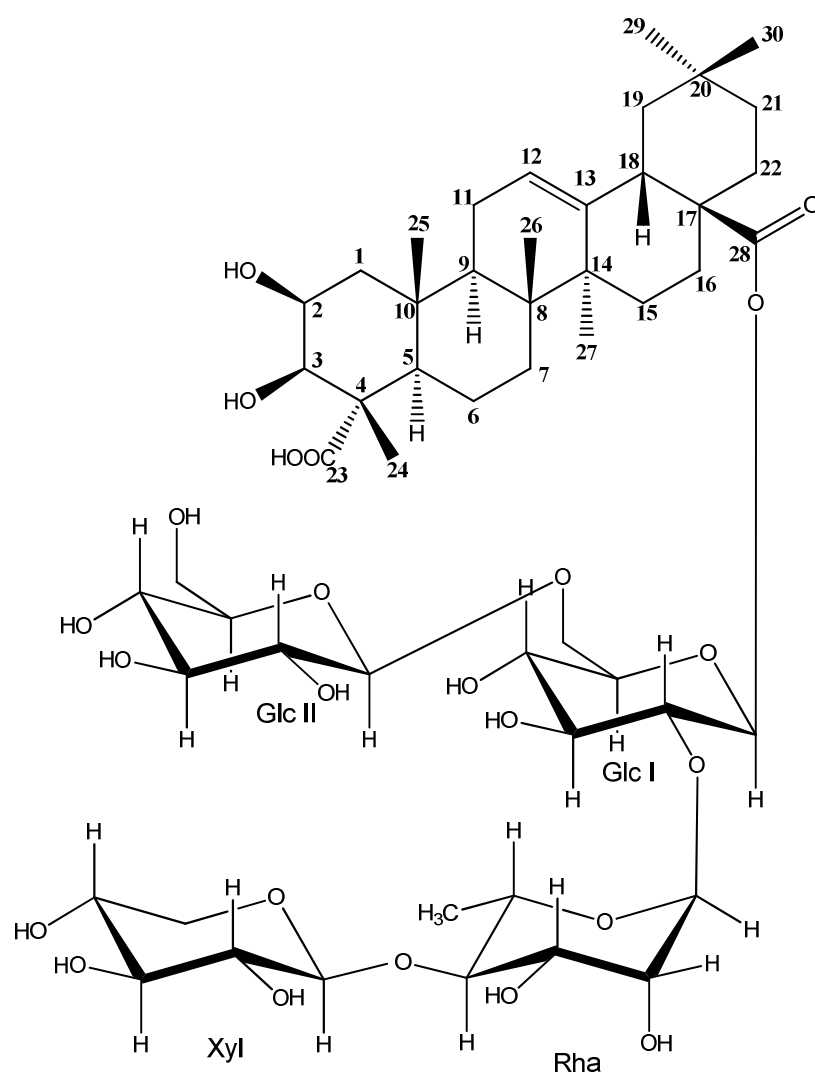


Figure 6.14 Structure of compound 1.

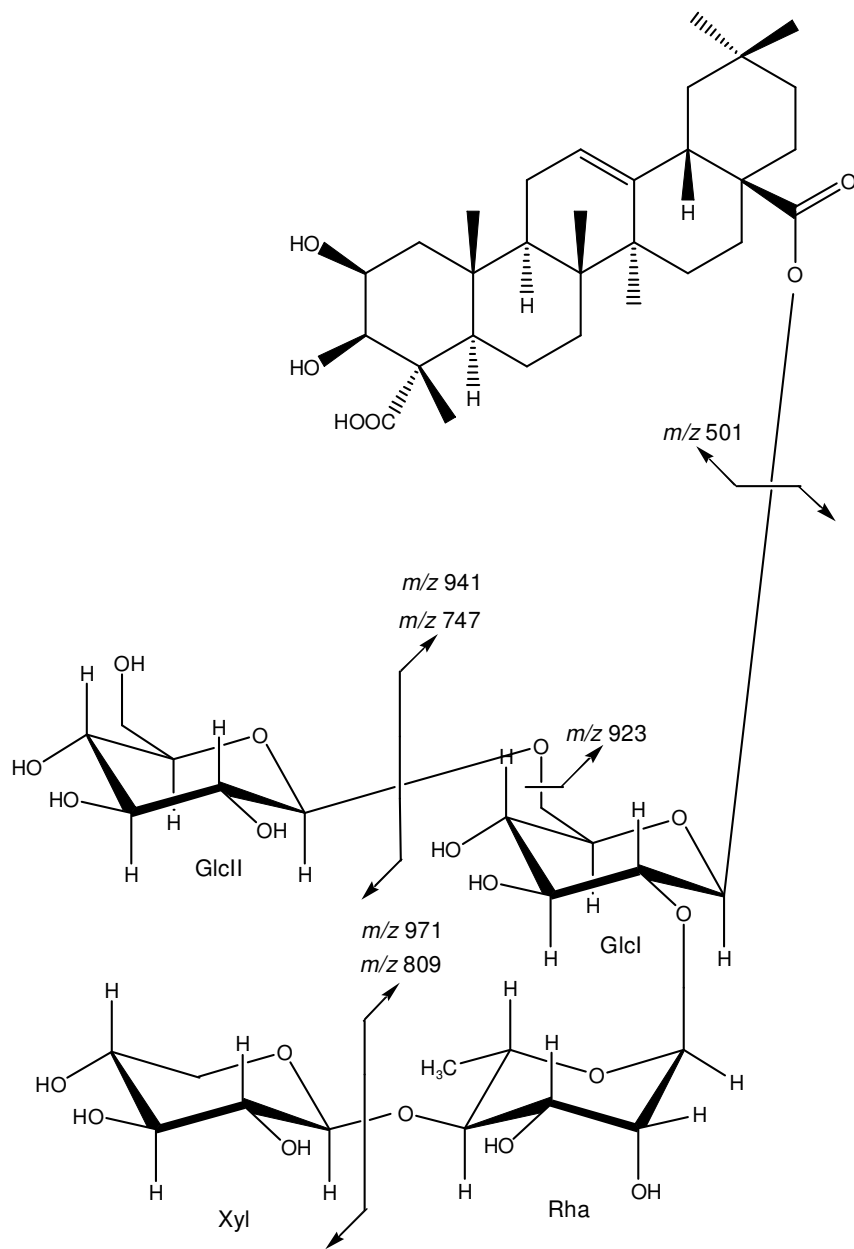


Figure 6.15 Scheme of MS² and MS³ analysis of compound 1.

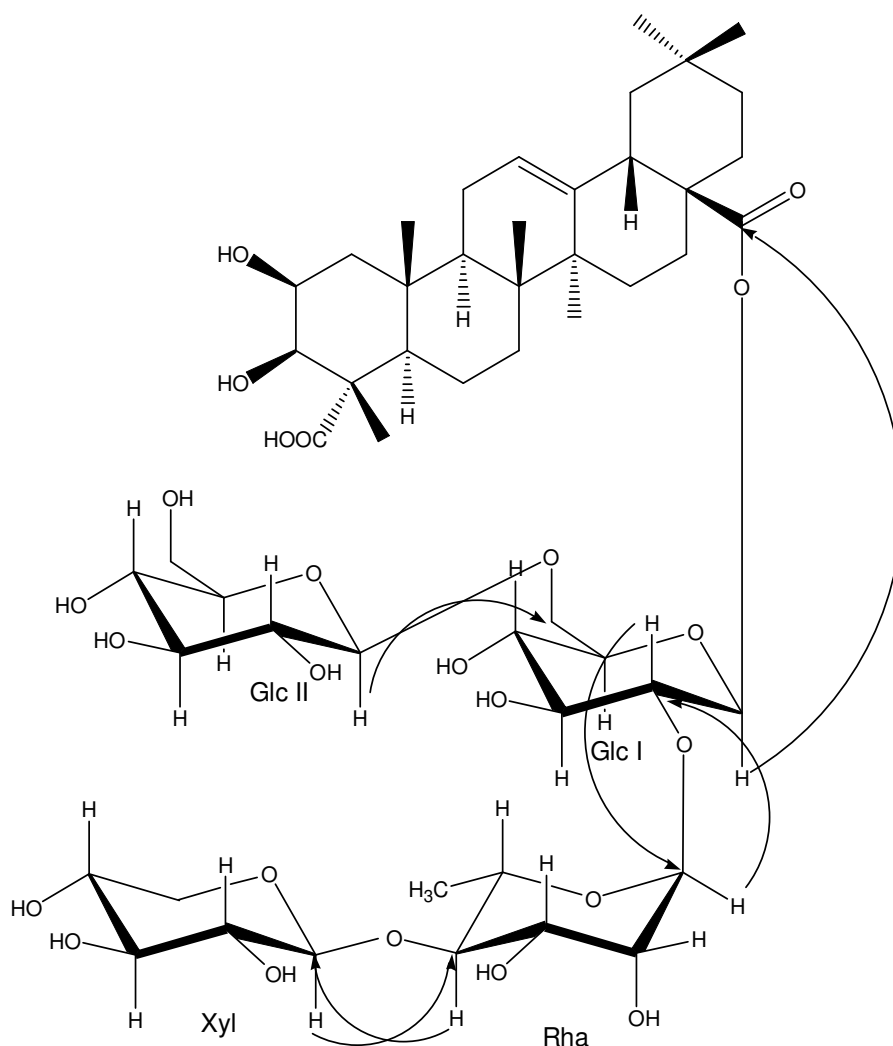


Figure 6.16 Important HMBC correlations of the sugar part of compound 1.

Compound **2** (Figure 6.25) was obtained as a white amorphous powder. The UV spectrum of compound **2** showed an absorbance maximum at 196 nm and $[\alpha]_D^{20}$ was -35.34 (3.0 g/L, MeOH). The HR-ESI-mass spectrum showed a deprotonated molecule at m/z 1541.6649 $[M-H]^-$ and supported a molecular formula of $C_{70}H_{110}O_{37}$. ESI-MS of **2** exhibited a deprotonated molecule at m/z 1541 $[M-H]^-$. The fragmentation pattern is depicted in Figure 6.26. The MS^2 product ion spectrum of m/z 1541 resulted in ions at m/z 1523 $[M-H-18]^-$, 1395 $[M-H-146]^-$ and 1379 $[M-H-162]^-$, which indicated the presence of a terminal deoxyhexose and hexose moiety. Other product ions were generated at m/z 1219 $[M-H-146-176]^-$, 1201 $[M-H-146-176-18]^-$, 1157 $[M-H-146-176-18-44]^-$, 1087 $[M-H-146-176-132]^-$, 1057 $[M-H-146-176-162]^-$, 925 $[M-H-146-176-162-132]^-$, 823 $[M-H-162+132+132+146+146]^-$ and 717 $[162+132+132+146+146-H]^-$. The MS^3 product ion spectrum of m/z 1395 $[M-H-146]^-$ resulted in ions at m/z 1377 $[M-H-H_2O]^-$, 1219 $[M-H-176]^-$ and 1157 $[M-H-176-18-44]^-$, suggesting a hexuronic moiety

attached to a terminal deoxyhexose unit. MS³ analysis of m/z 1219 [M-H-146-176]⁻ resulted in product ions at m/z 1201 [M- H-H₂O]⁻, 1087 [M-H-132]⁻, 1057 [M-H-162]⁻, 925 [M-H-162-132]⁻, 717 [162+132+132+146+146-H]⁻, 501 [M-H-146-176-162-132-132-146-146]⁻ and 483 [Aglycone-H-H₂O]⁻. MS³ analysis of m/z 1087 [M-H-146-176-132]⁻ resulted in product ions at m/z 1069 [M-H-H₂O]⁻, 925 [M-H-162]⁻ and 501 [M-H-146-176-162-132-132-146-146]⁻, whereas MS³ analysis of m/z 1057 [M-H-146-176-162]⁻ resulted in product ions at m/z 925 [M-H-132]⁻, 647 [M-H-146-176-162-132-132-146]⁻, 629 [M-H-146-176-162-132-132-146-18]⁻, and 501 [M-H-146-176-162-132-132-146-146]⁻. The formation of product ions m/z 1087 and m/z 1057, formed by the loss of a pentose and a hexose residue, respectively, together with their MS³ spectra, showing a loss of a hexose for the ion at m/z 1087 and a loss of a pentose for the ion at m/z 1057, indicated that both residues are in a terminal position, suggesting that the sugar chain was most probably branched. The MS³ product ion spectrum of m/z 925 revealed peaks at m/z 501 [M-H-146-176-162-132-132-146-146]⁻ and 483 [Aglycone-H-H₂O]⁻.

GC-MS analysis of the trimethylsilylated monosaccharides obtained after alkaline hydrolysis followed by an acidic hydrolysis of the sugar chain, which has been removed, resulted in the identification of D-glucose, D-xylose, D-fucose, and L-rhamnose. An additional peak, later on identified by ¹H-NMR and ¹³C-NMR as apiose, was present at a retention time that was different from those of the standards used. This sugar chain was attached to the aglycone by an ester linkage since only these bonds are cleaved after alkaline hydrolysis. After acid hydrolysis, L-rhamnose and D-glucuronic acid were identified as sugar moieties being attached to the aglycone by an O-heterosidic bond.

¹H-NMR and ¹³C-NMR chemical shifts of the aglycone part of compound **2** are shown in Table 1 and were similar to those of compound **1** indicating that the same aglycone was present. The presence an upfield shifted carbon signal and a deshielded carbon signal at δ 178.2 (C-28) and δ 86.7 (C-3), respectively, suggested compound **2** to be a bidesmosidic saponin.

Seven anomeric proton signals (Figure 6.17) at δ 5.37 (d, J = 1.2 Hz) (Rh_{all} H-1), δ 5.35 (d, J = 8.2 Hz) (Fuc H-1), δ 5.24 (d, J = 3.8) (Api H-1), δ 5.19 (d, J = 1.1 Hz) (Rh_{al} H-1), δ 4.63 (d, J = 7.7) (Xyl H-1), δ 4.58 (d, J = 7.8) (Glc H-1) and δ 4.39 (d, J = 7.6 Hz) (GlcA H-1) displaying correlations in the HSQC spectrum (Figure 6.23) with seven anomeric carbon signals (Figures 6.18 – 6.20) at δ 101.5 (Rh_{all} C-1), 95.4 (Fuc C-1), 112.0 (Api C-1), 102.4 (Rh_{al} C-1), 105.2 (Xyl C-1), 105.3 (Glc C-1) and 105.09 (GlcA C-1), respectively, evidenced the presence of seven sugar moieties. The complete assignment of the

monosaccharides residues was performed by COSY (Figure 6.21), TOCSY (Figure 6.22), HSQC (Figure 6.23) and HMBC (Figure 6.24) experiments, discussed further in depth, and GC-MS analysis, leading to the identification of a β -D-glucopyranose moiety (Glc), a β -D-xylopyranose (Xyl), two α -L-rhamnopyranose moieties (RhaI and RhaII), a β -D-apiofuranosyl moiety (Api), and a β -D-fucopyranosyl moiety (Fuc). The β -anomeric configuration of the glucopyranosyl, xylopyranosyl, apiofuranosyl, fucopyranosyl and glucopyranosyl moiety was confirmed by the large $J_{H1, H2}$ coupling constants between 7 and 8 Hz. The coupling constants of 1.1-1.2 Hz confirmed the α -anomeric configuration of the rhamnopyranosyl moiety. The α -anomeric configuration was confirmed by comparison with the ^{13}C NMR values of methyl α -L-rhamnoside and methyl β -L-rhamnoside published by Agrawal et al.⁵³

Linkages between both the aglycone and sugar units were mainly achieved by HMBC and are shown in Figure 6.27. A cross-peak in the HMBC spectrum from C-3 of the aglycone at δ 86.7 to the anomeric proton at δ 4.39 (GlcA H-1) indicated the linkage position of the β -D-glucuronic acid moiety. GlcA H-1 (δ 4.39) correlated in the HSQC spectrum with GlcA C-1 (δ 105.09). Via the COSY spectrum, GlcA H-2 could be found at δ 3.39 (correlated in HSQC to δ 75.9) and GlcA H-3 at δ 3.55 (correlated in HSQC to δ 82.7). These results were all confirmed by TOCSY. A correlation in the COSY spectrum between δ 3.51 and δ 3.71 was present and according to literature, these signals could be assigned to positions 4 and 5, respectively.⁵⁴ The downfield shifted signal of GlcA C-3 at δ 82.7 giving an HMBC correlation with the anomeric proton of RhaI at δ 5.19 suggested a substitution at this position. A COSY signal at δ 5.19 (RhaI H-1) and δ 3.92 (RhaI H-2) allowed to assign RhaI H-2 (δ 3.92), which is correlated in HSQC with δ 72.5 (RhaI C-2). A correlation from δ 3.92 (RhaI H-2) to δ 3.70 revealed RhaI H-3, correlated in HSQC with δ 72.4 (RhaI C-3). TOCSY cross-peaks confirmed RhaI H-2 and RhaI H-3. RhaI C-2 (δ 72.5) has long-range correlations in HMBC with RhaI H-1 at δ 5.19 and RhaI H-4 at δ 3.36, whereas RhaI C-3 (δ 72.4) showed a long-range correlation with RhaI H-4 at δ 3.36. The signal at δ 74.3 (RhaI C-4) (in the HSQC spectrum correlated with δ 3.36 (RhaI H-4)) from the fourth position was correlated in the HMBC spectrum with protons at positions 2, 3 and 6 of rhamnose. The signal at δ 69.9 showed HMBC long-range correlations with δ 5.19 (RhaI H-1), δ 3.36 (RhaI H-4) and δ 1.23 (RhaI H-6), and was assigned to RhaI C-5. All ^1H -NMR assignments were confirmed by TOCSY. The glycan part at C-3 was identified as α -L-rhamnopyranosyl-(1 \rightarrow 3)- β -D-glucuronopyranoside.

A deshielded signal of the anomeric proton of Fuc at δ 5.35 giving a correlation in the HSQC spectrum with a shielded anomeric carbon signal at δ 95.4 indicated the linkage of Fuc to the C-28 position of the aglycone through an ester linkage. An HMBC cross-peak between δ 5.35 (Fuc H-1) and δ 178.2 (C-28) confirmed this finding. A cross-peak in COSY from Fuc H-1 (δ 5.35) to Fuc H-2 (δ 3.82) and a long-range peak in the HMBC spectrum between δ 95.4 (Fuc C-1) and δ 3.82 (Fuc H-2) confirmed position 2. A correlation between Fuc H-2 (δ 3.82) and Fuc H-3 (δ 3.71) in COSY and between Fuc C-3 (δ 76.6) and Fuc H-2 in the HMBC spectrum revealed position 3. Other positions were elucidated by the presence of the HMBC spectrum correlations between Fuc C-2 (δ 74.9) and Fuc H-4 (δ 3.57), Fuc C-3 (δ 76.6) and Fuc H-4 (δ 3.57 ppm), and between Fuc C-4 at δ 73.8 and Fuc H-3 at δ 3.71 and Fuc H-5 at δ 3.69. COSY correlations between δ 3.71 (Fuc H-3) and δ 3.57 (Fuc H-4) and between δ 3.57 (Fuc H-4) and δ 3.69 (Fuc H-5), together with correlations in the TOCSY spectrum confirmed these findings. Correlations in the HMBC spectrum between both δ 72.8 (Fuc C-5) and δ 73.8 (Fuc C-4) and 1.22 suggested the presence of a CH₃ group. These findings, together with the coupling constant of the anomeric proton of 8.2 Hz and the results of GC-MS analysis, allowed to identify this sugar moiety as β -D-fucose. Long-range peaks in the HMBC spectrum between δ 101.5 (Rhall C-1) and δ 3.82 (Fuc H-2) and between the anomeric proton signal of Rhall at δ 5.37 and Fuc C-2 (δ 74.9) suggested a substitution at position 2 of Fuc with Rhall. The COSY spectrum showed a correlation between Rhall H-1 (δ 5.37) and Rhall H-2 at δ 4.088 and between Rhall H-2 (δ 4.088) and Rhall H-3 at δ 3.84. A cross-peak between Rhall C-5 (δ 68.8), Rhall C-3 (δ 81.6) and the anomeric proton and a weak cross-peak between Rhall C-2 (δ 72.1) and the anomeric proton confirmed positions 2, 3, and 5. The presence of two deshielded carbon signals of Rhall at C-3 (δ 81.6) and Rhall C-4 (δ 79.2) showing correlations with anomeric protons at δ 5.24 (Api H-1) and δ 4.63 (Xyl H-1), respectively, revealed a disubstitution of Rhall.

The anomeric proton at δ 5.24 was correlated in the HSQC spectrum to δ 112.0 (Api C-1). HMBC signals between Api C-1 and δ 4.03 (HSQC δ 78.3) and between δ 78.3 and δ 5.24 revealed position 2 to produce signals at δ 78.3 (Api C-2) and δ 4.03 (Api H-2). This was confirmed by the COSY spectrum. The signal at δ 80.2 showed no correlation with a proton in the HSQC spectrum, and the DEPT-135 (Figure 6.19) and DEPT-90 (Figure 6.20) spectra confirmed this to be a quaternary carbon peak. HMBC cross-peaks were observed from δ 80.2 to δ 5.24 (Api H-1), δ 4.091 (Api H-4a), δ 3.76 (Api H-4b), and δ 3.58 (Api H-5). The signal at δ 80.2 was assigned as Api C-3. A cross-peak between Api C-2

(δ 78.3) and δ 3.76 (Api H-4b), between Api C-1 at δ 112.0 and δ 3.76 (Api H-4b), and between Api C-4 (δ 74.9) and Api H-1 (δ 5.24) confirmed the position 4 to produce a doublet at δ 4.091 - 3.76 (HSQC - δ 74.9). Position 5 was found by examining cross-peaks from δ 65.2 (Api C-5) to δ 4.03 (Api H-2) and δ 4.091 (Api H-4a), from Api C-4 to δ 3.58 (Api H-5), and from Api C-2 to δ 3.58 (Api H-5). Api C-3 (δ 80.2) correlated in HMBC with Api H-5 (δ 3.58). These signals are characteristic for a β -D-apiose moiety.⁵⁵

The substitution at position 4 of Rhall was confirmed by the correlation between Xyl C-1 at δ 105.1 and Rhall H-4 at δ 3.65. A correlation in the COSY spectrum between Xyl H-1 (δ 4.63) and δ 3.33 revealed position 2. A cross-peak from Xyl C-3 at δ 88.2 correlated with δ 3.90 (Xyl H-5a) and δ 4.58 in the HMBC spectrum. This latter correlation indicated the binding with the next sugar. No further HMBC cross-peaks were visible. COSY and TOCSY confirmed Xyl H-2 and revealed the position of Xyl H-3, Xyl H-4, Xyl H-5a and Xyl H-5b being the peaks at δ 3.47, δ 3.59, δ 3.90, and δ 3.20. This sugar moiety was identified as β -D-xylose by GC-MS analysis.

A downfield shifted carbon signal of Xyl C-3 (δ 88.2) correlating with δ 3.90 (Xyl H-5a) and δ 4.58 (Glc H-1) in the HMBC spectrum indicated the next linkage position. This was confirmed by a cross-peak between Glc C-1 at δ 105.3 and Xyl H-3 at δ 3.47, indicating a 1 \rightarrow 3 linkage. A cross-peak in COSY between Glc H-1 at δ 4.58 and δ 3.35 (Glc H-2) revealed position 2. Cross-peaks from Glc C-3 at δ 77.8 to Glc H-2 and Glc H-4 at δ 3.35 and δ 3.34, respectively, and from Glc C-4 (δ 78.3) to Glc H-5 (δ 3.30) and Glc C-5 (δ 71.6) to H-3 (δ 3.46) in the HMBC spectrum, together with correlations in the COSY and TOCSY spectra, revealed the other positions of this sugar moiety, which could be identified as β -D-glucose. Briefly, the HMBC cross-peaks at $\delta_{\text{H}}/\delta_{\text{C}}$ 5.37 (Rhall H-1)/74.9 (Fuc C-2), 3.82 (Fuc H-2)/101.5 (Rhall C-1), 5.24 (Api H-1)/81.6 (Rhall C-3), 4.63 (Xyl H-1)/79.2 (Rhall C-4), and 3.65 (Rhall H-4)/105.1 (Xyl C-1) suggested the sequence of the oligosaccharide moiety at C-28 to be [β -D-glucopyranosyl-(1 \rightarrow 3)- β -D-xylopyranosyl-(1 \rightarrow 4)]- [β -D-apiofuranosyl-(1 \rightarrow 3)]- α -L-rhamnopyranosyl-(1 \rightarrow 2)- β -D-fucopyranoside. Therefore, compound **2** could finally be elucidated as 3-O-[α -L-rhamnopyranosyl-(1 \rightarrow 3)- β -D-glucuronopyranosyl]-28-O-[[β -D-glucopyranosyl-(1 \rightarrow 3)- β -D-xylopyranosyl-(1 \rightarrow 4)]- [β -D-apiofuranosyl-(1 \rightarrow 3)]- α -L-rhamnopyranosyl-(1 \rightarrow 2)- β -D-fucopyranosyl]-medicagenic acid, for which the name herniariasaponin H has been adopted (Figures 6.25, 6.26, and 6.27).

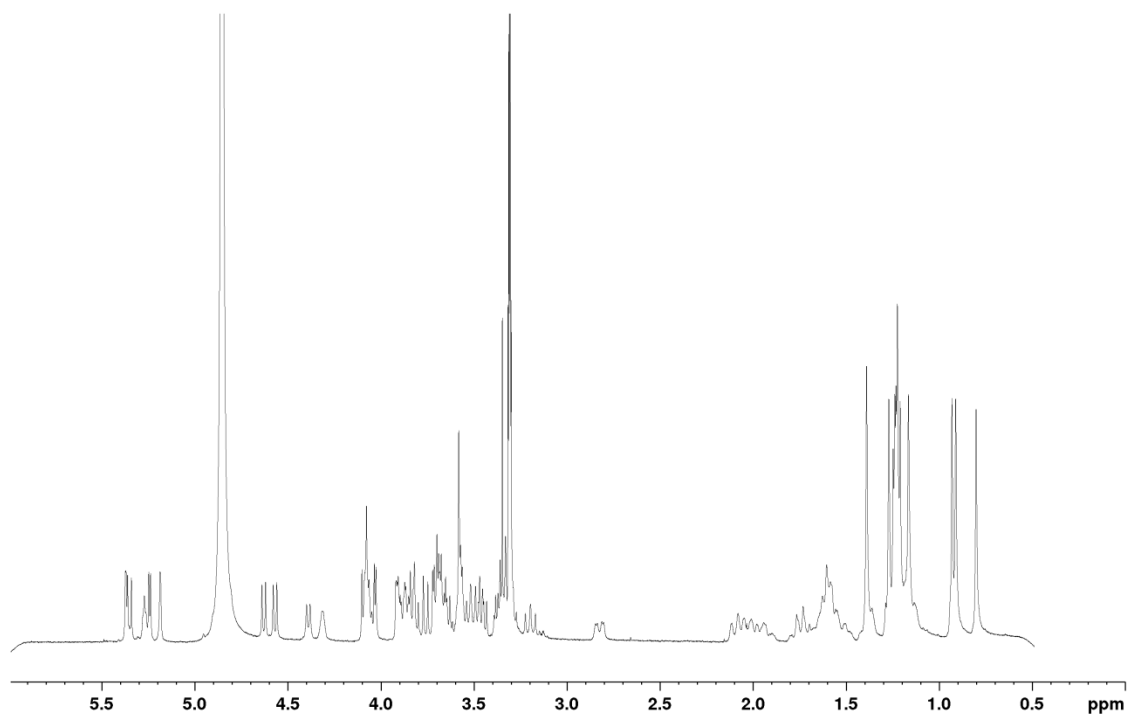


Figure 6.17 ^1H -NMR spectrum of compound 2.

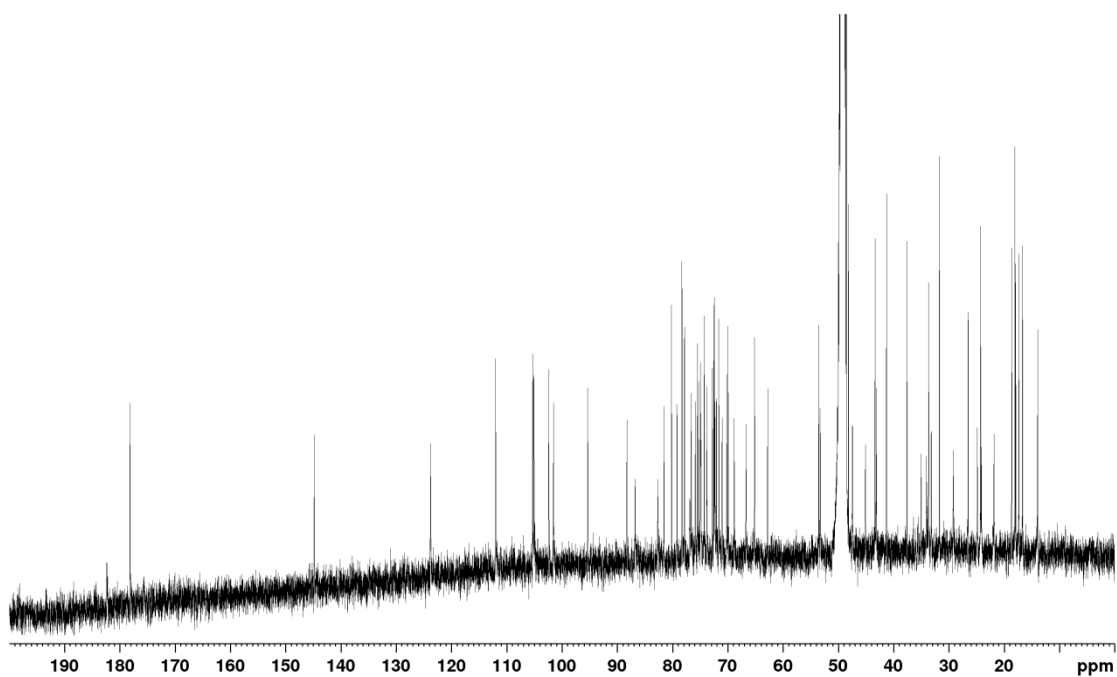


Figure 6.18 ^{13}C -NMR spectrum of compound 2.

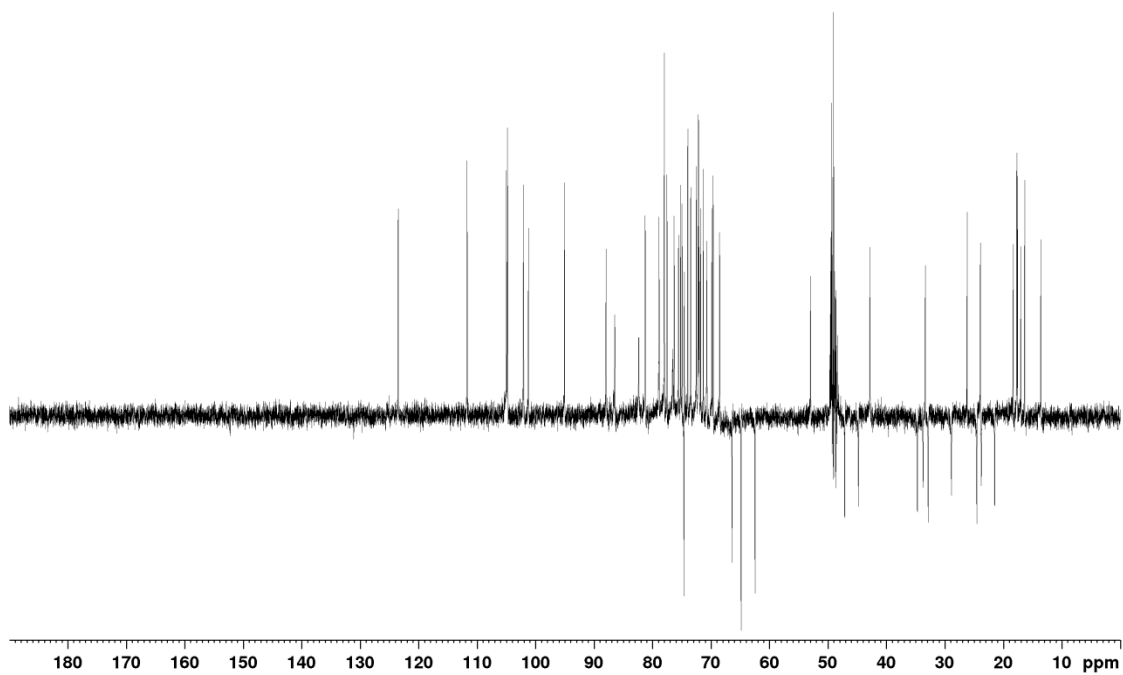


Figure 6.19 DEPT-135 spectrum of compound 2.

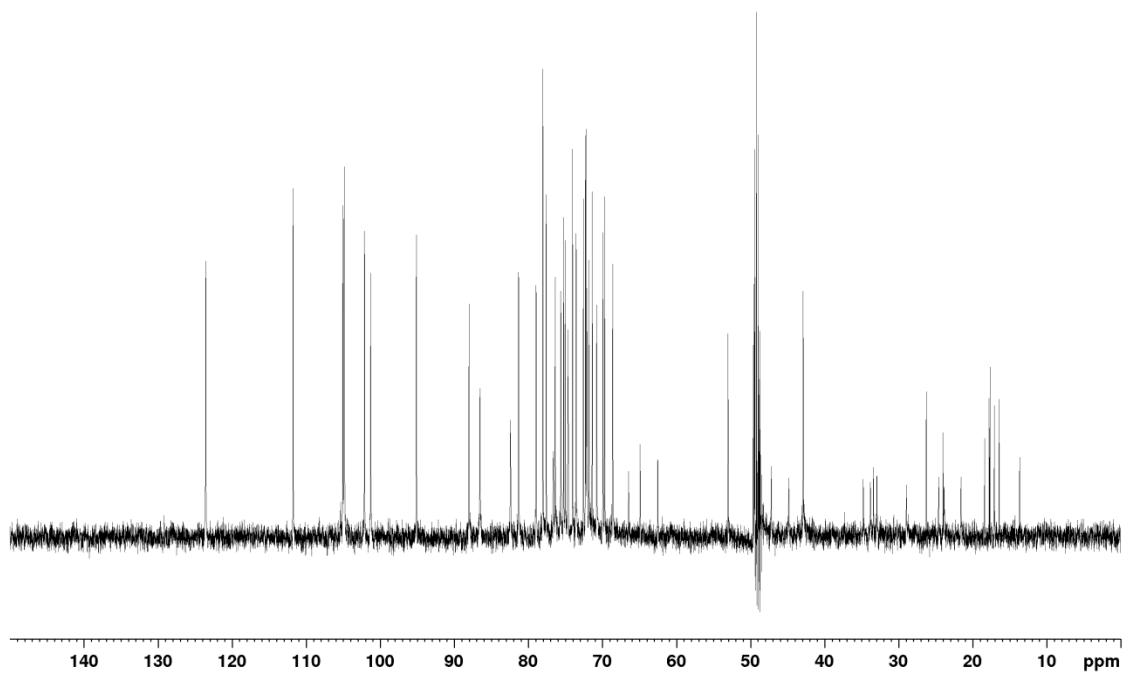


Figure 6.20 DEPT-90 spectrum of compound 2.

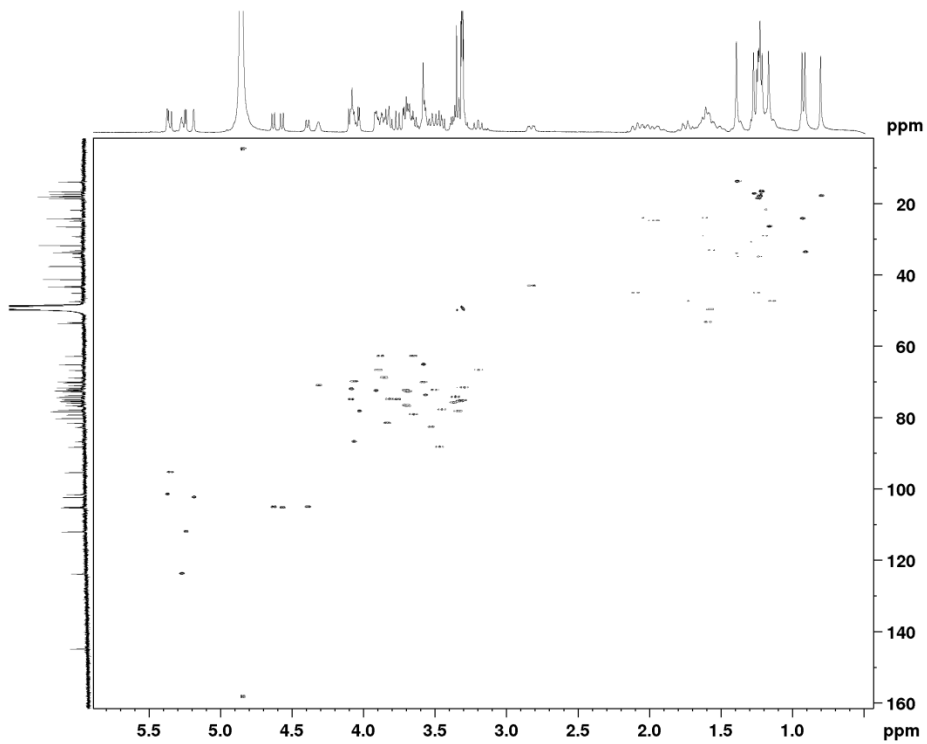


Figure 6.23 HSQC spectrum of compound 2.

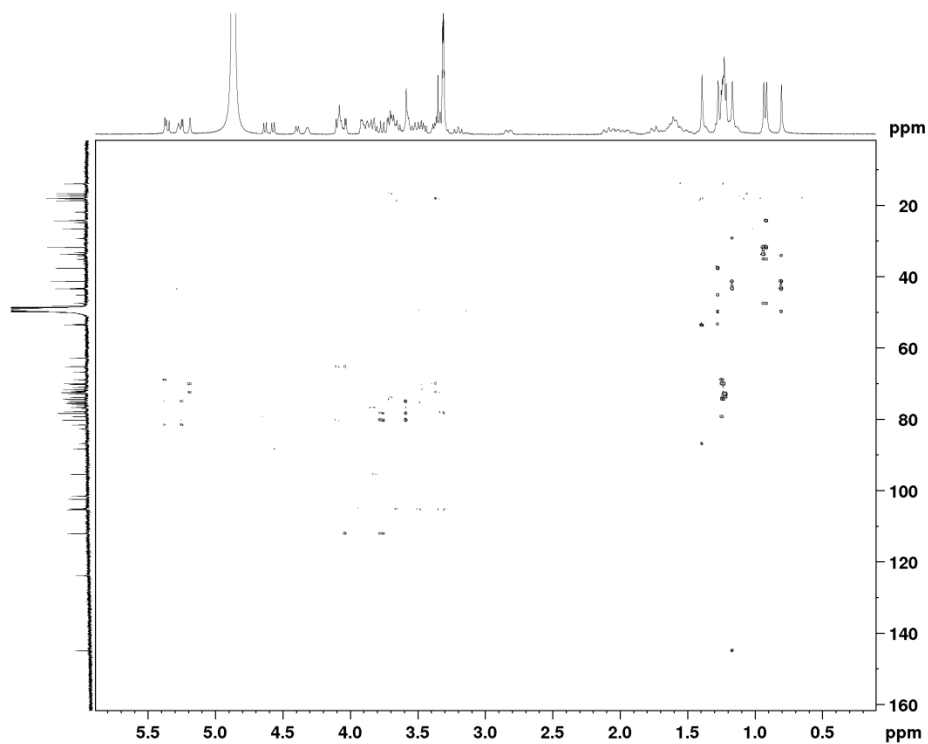


Figure 6.24 HMBC spectrum of compound 2.

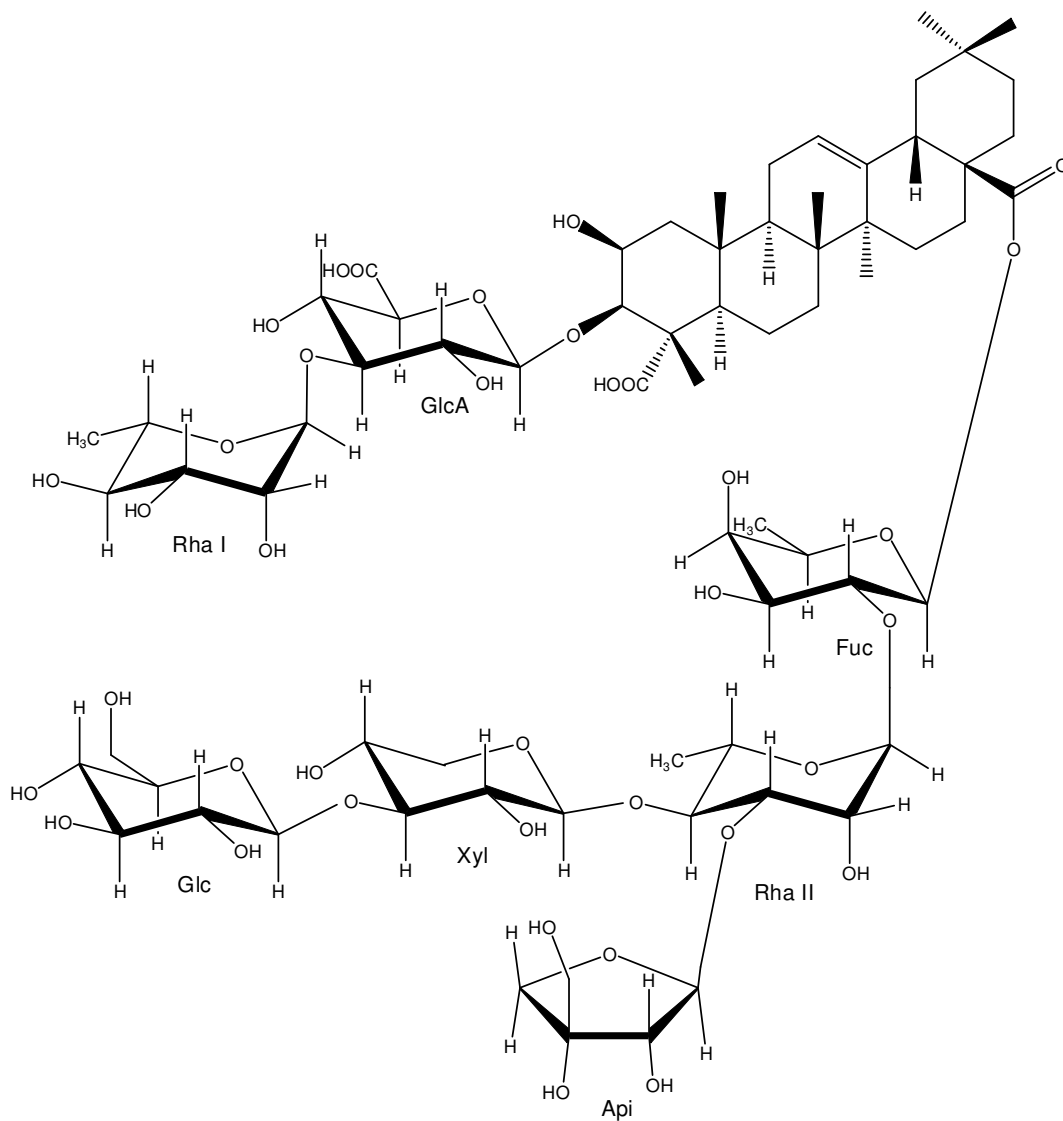


Figure 6.25 Structure of compound 2.

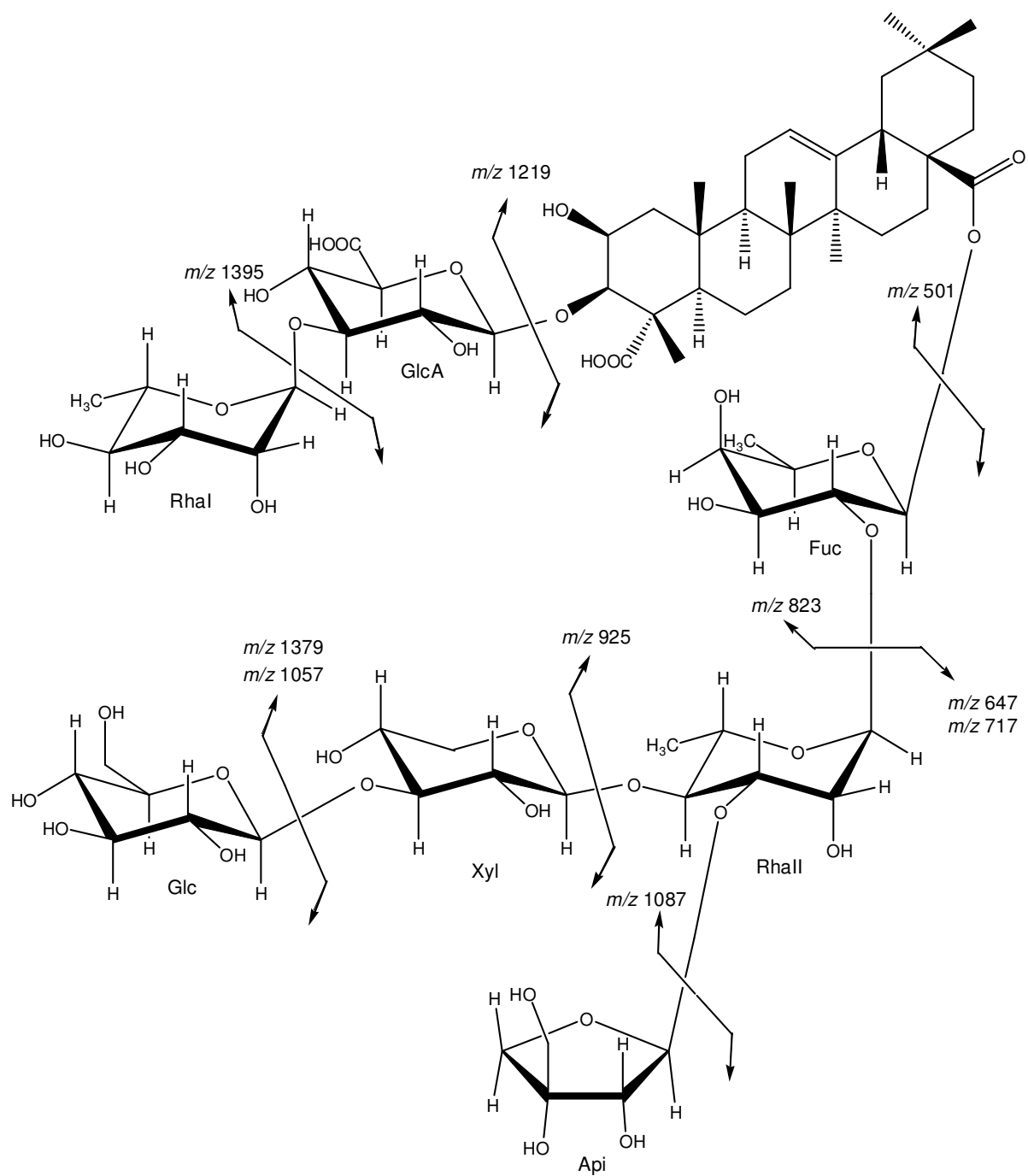


Figure 6.26 MS² and MS³ analysis of compound 2.

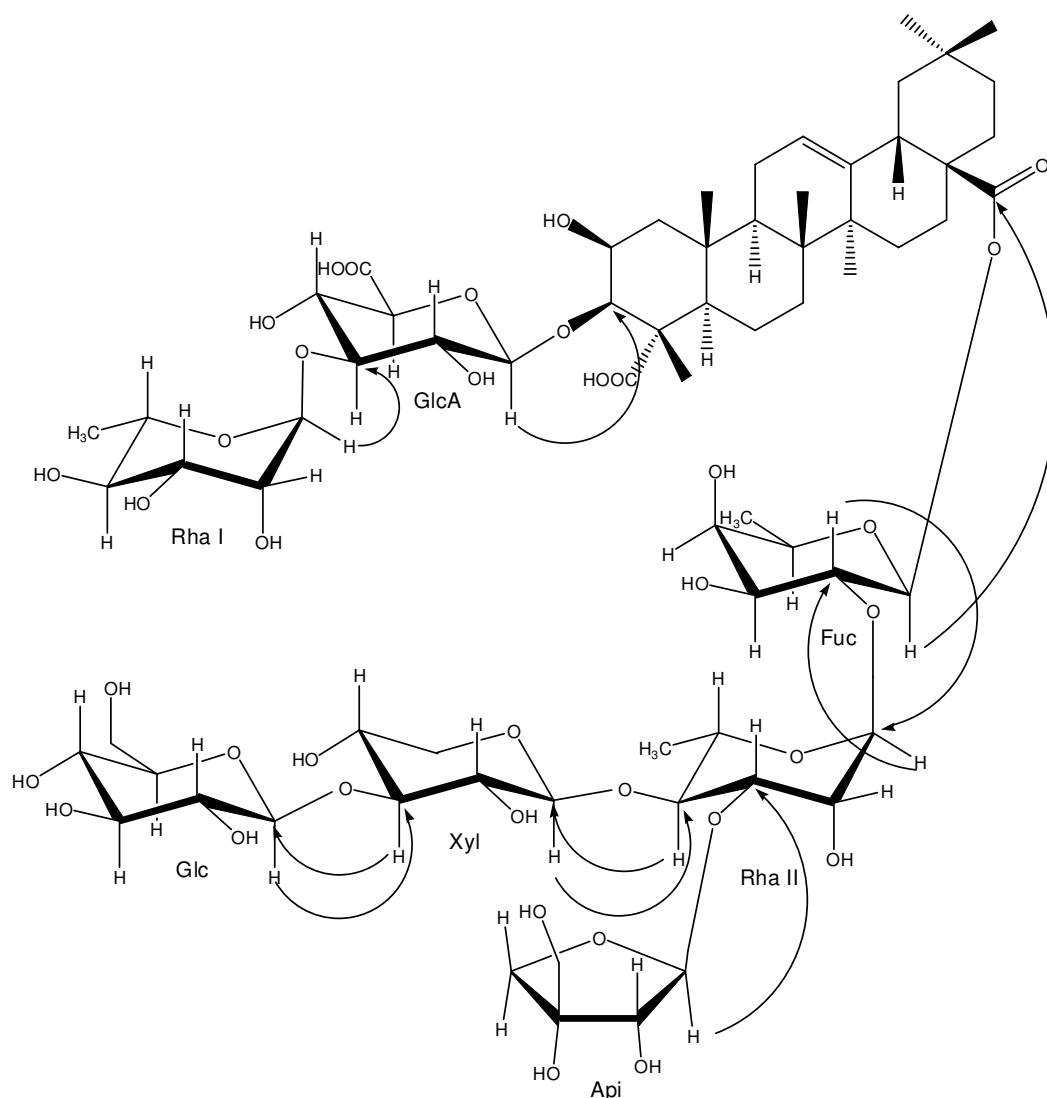


Figure 6.27 Important HMBC correlations of the sugar part of compound 2.

In addition, three known flavonoids were isolated from the infusion of *H. hirsuta* (compounds 3-5). The UV spectrum of compound 3 exhibited two absorbance maxima at 256 nm and 355 nm and a shoulder at 270 nm, which are all typical for flavon-3-ols.⁵⁶ Compound 3 showed a deprotonated molecule at m/z 623 $[M-H]^-$. The m/z 623 MS^2 product ion spectrum resulted in an ion at m/z 301 $[M-H-322]^-$, which was formed by the loss of a hexuronic acid residue (176 u) and a deoxyhexose residue (146 u). 1H -NMR and ^{13}C -NMR shifts are shown in Table 6.2 and were indicative of a quercetin aglycone with two sugar moieties, due to the presence of two anomeric protons at δ 5.67 (d, $J = 7.6$ Hz) and 5.07 (d, $J = 2.0$ Hz). The anomeric proton at δ 5.67, coupled with a carbon at δ 132.9 (C-3) in the HMBC spectrum, indicated that the sugar moiety was directly attached to the aglycone at C-3. A cross-peak in the HMBC spectrum between GlcA H-5 at δ 3.42 (HSQC correlation with GlcA C-5 at δ

77.0) and a signal at δ 172.5 (GlcA C-6, COOH) suggested a glucuronyl moiety. A correlation between GlcA H-2 (δ 3.51) and Rha C-1 (δ 100.6) together with the downfield shifted GlcA C-2 indicated a 1 \rightarrow 2 interglycosidic linkage. A signal at δ 17.2, characteristic for a methyl group, corresponding in the HSQC spectrum to a doublet at δ 0.78 (CH₃), suggested a rhamnosyl moiety in a terminal position. The UV, MS and NMR data confirmed compound **3** as quercetine-3-*O*-(2''-*O*- α -L-rhamnopyranosyl)- β -D-glucuronopyranoside (C₂₇H₂₈O₁₇), shown in Figure 6.35. These data are in accordance with Felser et al.⁵⁷

Table 6.2 ¹H-NMR and ¹³C-NMR assignments of compound **3**.

(3)		
Aglycone	δ_c (ppm)	δ_H (ppm), mult., <i>J</i> (Hz)
1	-	
2	156.3	
3	132.9	
4	177.2	
5	161.2	
6	98.7	6.35, s
7	164.2	
8	93.6	6.43, s
9	156.25	
10	103.9	
1'	121.1	
2'	116.4	7.61, s
3'	144.9	
4'	148.4	
5'	114.9	6.83-6.81, d, (<i>J</i> = 8.4)
6'	121.5	7.57-7.55, dd, (<i>J</i> = 7.7)
GlcA		
1	98.7	5.67-5.66, d, (<i>J</i> = 7.6)
2	77.4	3.51, m
3	74.8	3.41, m
4	71.9	3.34, m
5	77.0	3.42, m
6	172.5	
Rha		
1	100.6	5.07, s

Table 6.2 continued ¹H-NMR and ¹³C-NMR assignments of compound 3.

(3)

Aglycone	δ_c (ppm)	δ_H (ppm), mult., J (Hz)
2	70.7	3.75, m
3	70.7	3.47, m
4	71.9	3.13, m
5	68.3	3.71, m
6	17.2	0.78, s

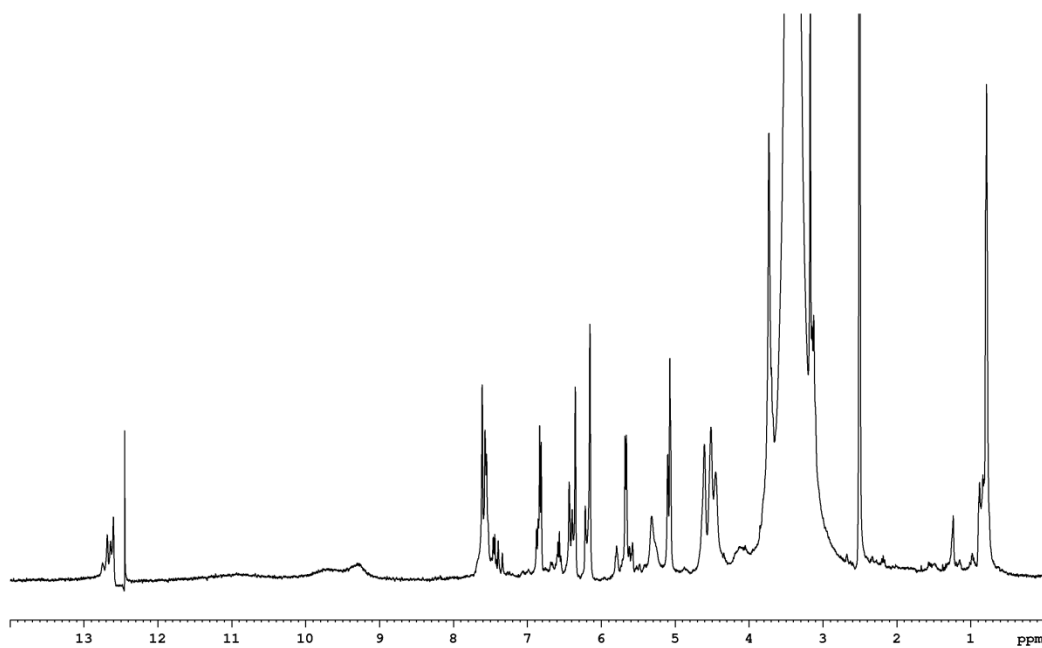


Figure 6.28 ¹H-NMR spectrum of compound 3.

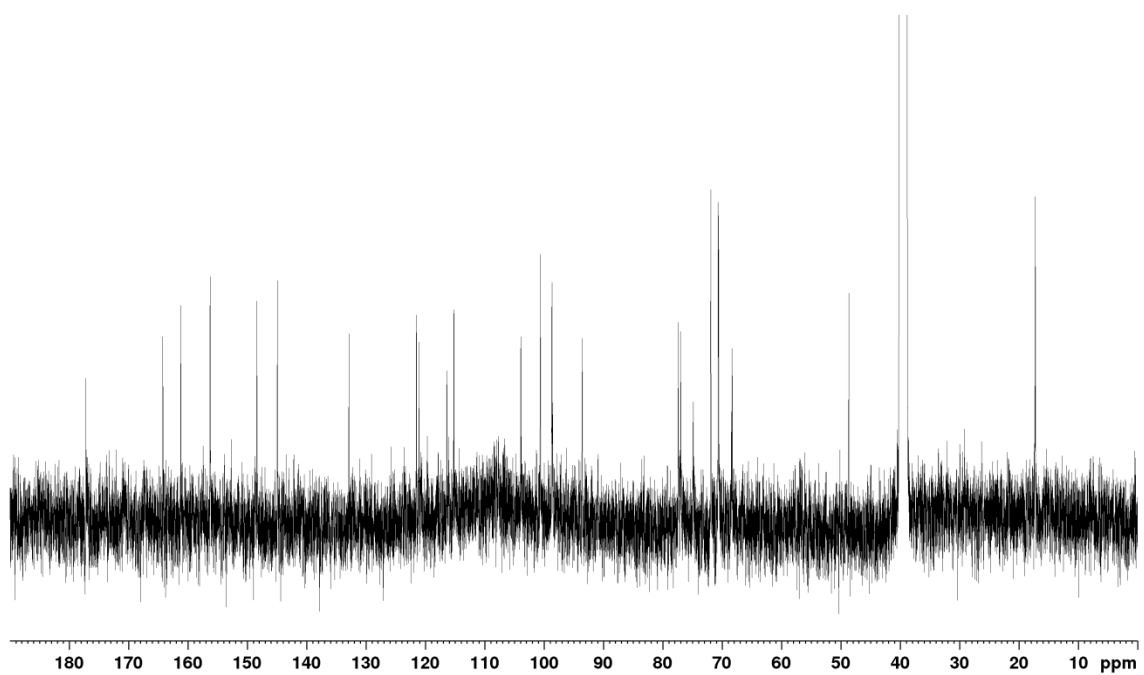


Figure 6.29 ¹³C-NMR spectrum of compound 3.

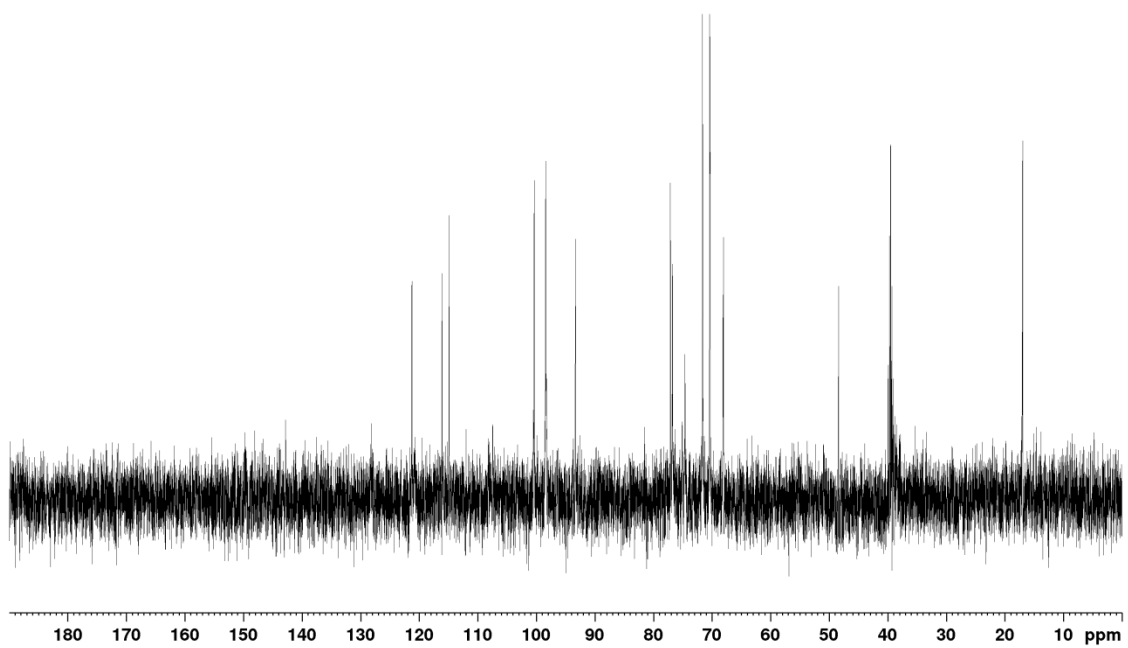


Figure 6.30 DEPT-135 spectrum of compound 3.

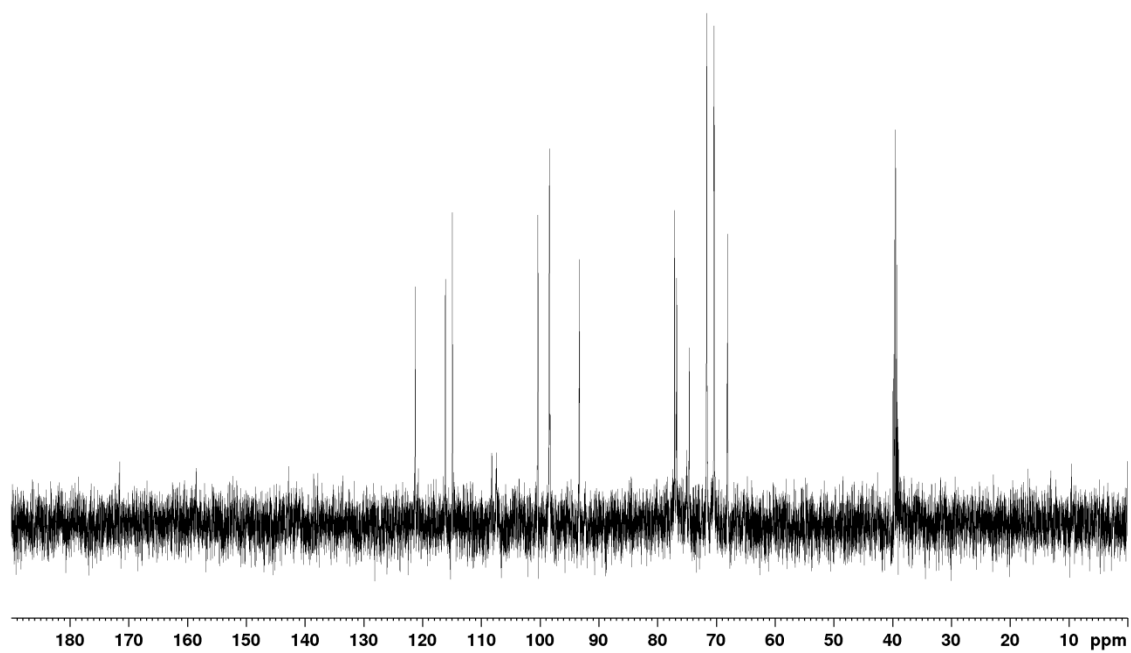


Figure 6.31 DEPT-90 spectrum of compound 3.

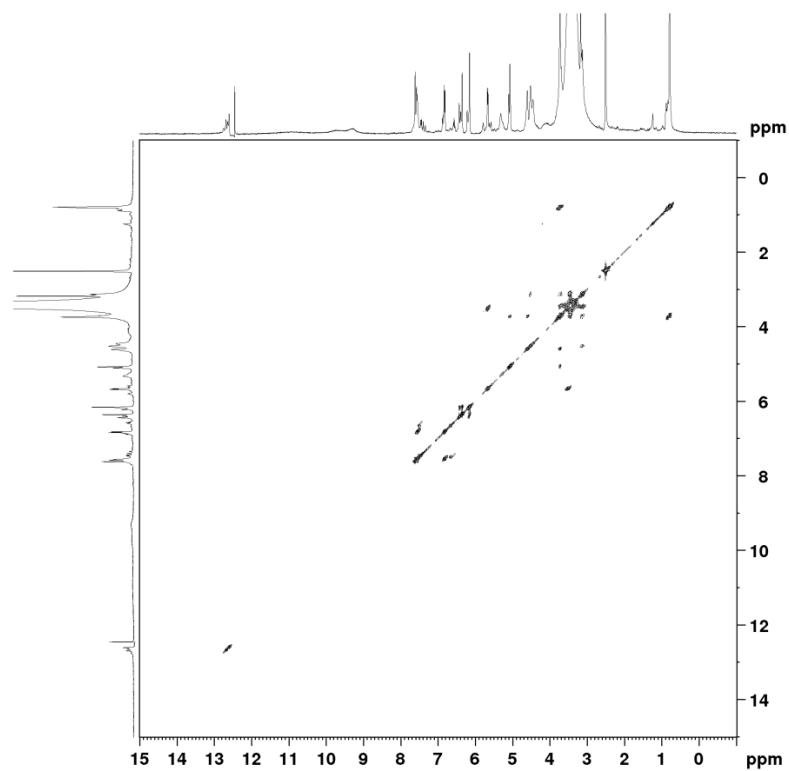


Figure 6.32 COSY spectrum of compound 3.

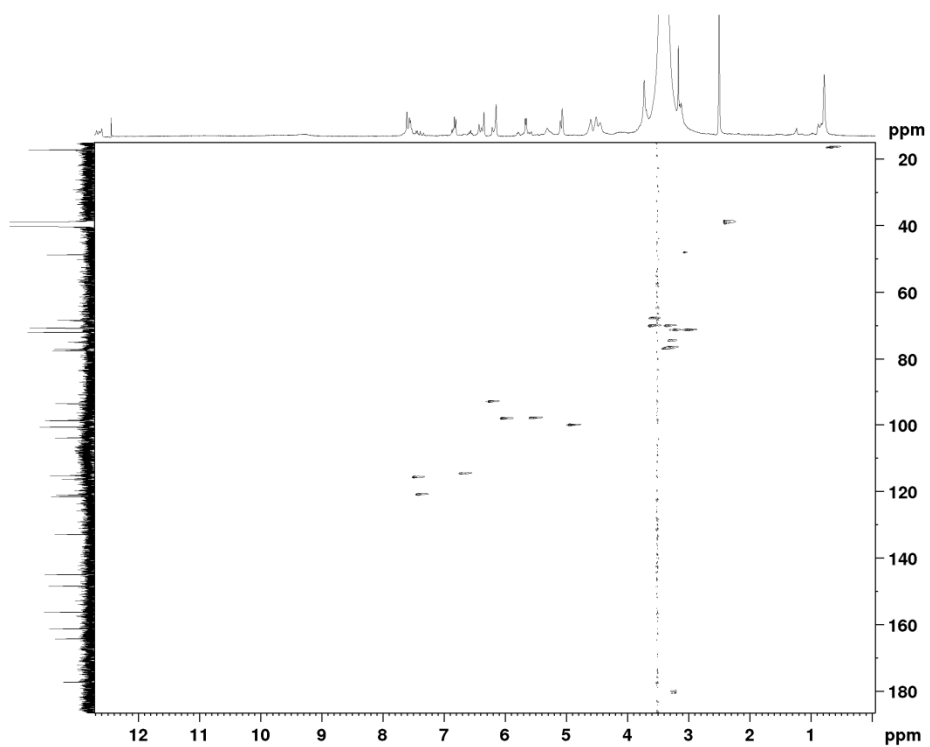


Figure 6.33 HSQC spectrum of compound 3.

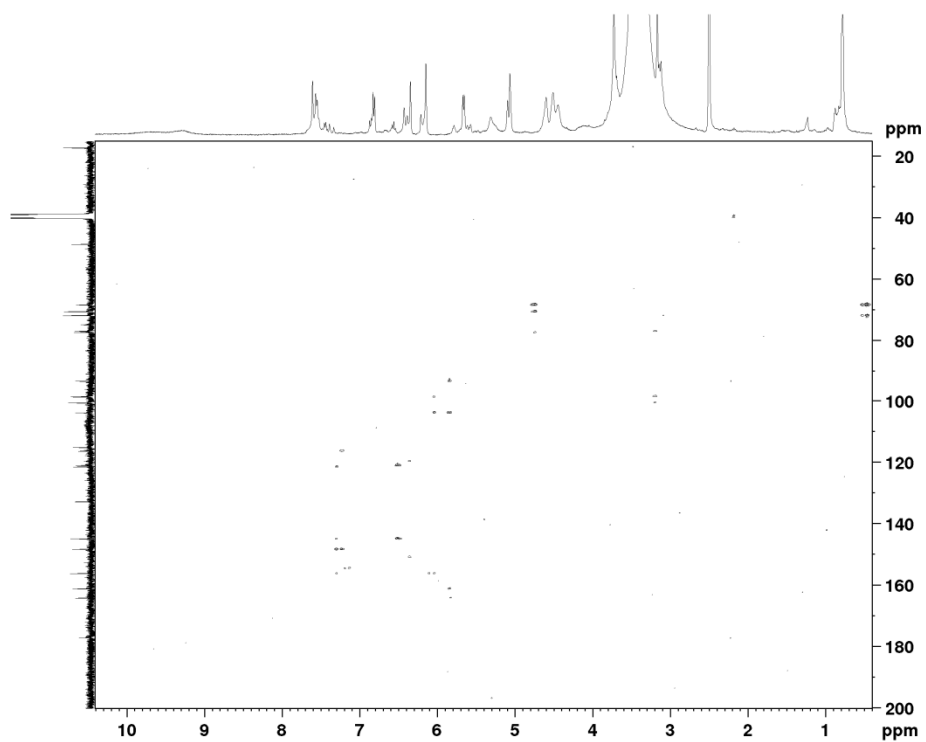


Figure 6.34 HMBC spectrum of compound 3.

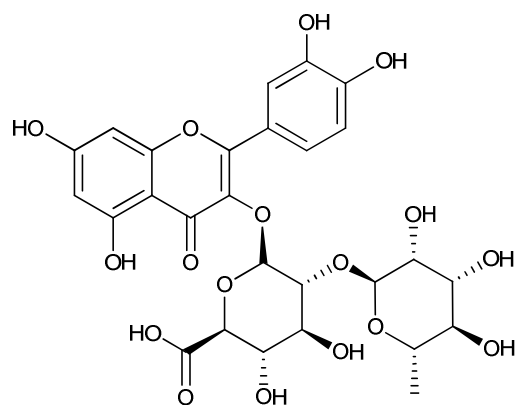


Figure 6.35 Structure of compound 3.

The UV spectrum of compound 4 exhibited two absorbance maxima at 256 nm and 355 nm and a shoulder at 270 nm, which are all typical for flavon-3-ols.²⁵ Compound 4 showed a deprotonated molecule at m/z 609 $[M-H]^-$. The m/z 609 MS^2 product ion spectrum resulted in an ion at m/z 301 $[M-H-308]^-$, which was formed by the loss of a hexose residue (162 u) and a deoxyhexose residue (146 u). 1H -NMR shifts were indicative of a quercetin aglycone with two sugar moieties. The 1H -NMR spectrum was identical to that of a rutin standard. HPLC analysis of the crude extract spiked with a standard solution of rutin confirmed the identity of compound 4 ($C_{27}H_{30}O_{16}$) as rutin (Figure 6.36).²²

The UV spectrum of compound 5 was also typical for flavon-3-ols, as described for compound 3 and compound 4.²⁵ Compound 5 showed a deprotonated molecule at m/z 623 $[M-H]^-$. The m/z 623 MS^2 product ion spectrum resulted in an ion at m/z 315, which was 14 u higher than the quercetin aglycone and indicated a methoxyl instead of a hydroxyl substitution of the aglycone. 1H -NMR shifts were indicative of an isorhamnetin aglycone with two sugar moieties. The 1H -NMR spectrum was identical to that of a narcissin (isorhamnetin-3-*O*-rutinoside) standard. Spiking of the crude extract with a standard solution of narcissin confirmed the identity of compound 5 ($C_{28}H_{32}O_{16}$) (Figure 6.36).²²

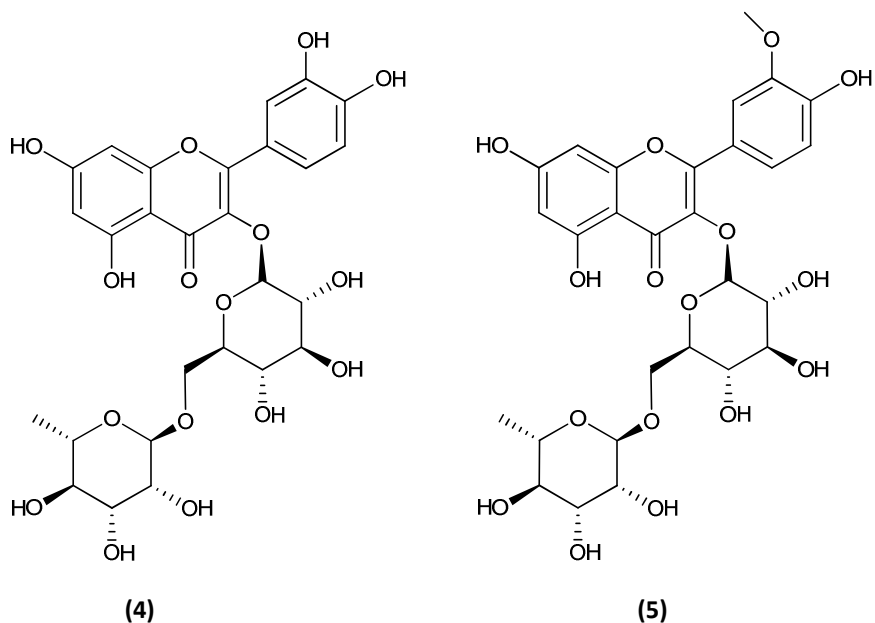


Figure 6.36 Structure of compounds 4 and 5.

6.2.3.3 Discussion

The majority of saponins of the Caryophyllaceae contains as aglycone gypsogenic acid, gypsogenin, or quillaic acid. Saponins containing medicagenic acid as aglycone, such as herniariasaponins, are less frequently found.⁵⁸ To the best of our knowledge, until now thirteen herniariasaponins have been reported, from which only two from *Herniaria hirsuta*, i.e. herniariasaponin E and herniariasaponin F.¹⁰ Other herniariasaponins were also found in other species: herniariasaponins A-D were already reported from *Herniaria fontanesii* and herniariasaponins **1-7** were found in *Herniaria glabra*.^{11,16-21} Compounds **1** and **2**, for which the name herniariasaponin G and H, respectively, has been adopted, are reported here for the first time from nature. Both compounds **1** and **2** have medicagenic acid as aglycone, which is, in addition to 16-hydroxymedicagenic acid, one of the two aglycones found in herniariasaponins. Compound **1** is a monodesmosidic saponin which differs from herniariasaponin E by the absence of an acetyl group in position 2 of the aglycone. Saponin **2** is a bidesmosidic saponin containing seven sugar moieties, one more than all other herniariasaponins found in nature, and is the largest herniariasaponin reported until now. It also contains apiose as a sugar moiety, which is present as well in herniariasaponins 5 and 7.

Herniariae herba was reported to contain quercetin- and isorhamnetin derivatives such as narcissin and rutin.^{1,22} In addition, narcissin (isorhamnetin-3-*O*-rutinoside) was isolated from *Herniaria glabra*, isorhamnetin 3-[3'''-feruloylrhamnosyl-(1→6)-galactoside], isorhamnetin 3-robinobioside and

catechin were discovered in *Herniaria fontanesii* and rhamnazin 3-rutinoside in *Herniaria ciliolate*.²³

To the best of our knowledge, this is the first time that quercetin-3-*O*-(2''-*O*- α -L-rhamnopyranosyl)- β -D-glucuronopyranoside was isolated from *Herniaria hirsuta*.

Compounds **1** – **5** isolated during the present work constitute the main peaks in the chromatographic profile of the infusion of *Herniaria hirsuta*.

6.3 Development and validation of an HPLC-UV method for the quantification of flavonoids and saponins in infusions of *Herniaria hirsuta* L.*

6.3.1 Introduction

The main compounds of an infusion of *Herniaria hirsuta* were elucidated as described in the previous part. In order to carry out qualitative *in vivo* experiments, a quantified extract of *H. hirsuta* with known levels of these flavonoids and saponins is needed, and, therefore, an analytical method should be developed and validated. Besides this, a validated method is required for batch controls in quality control.

6.3.2 Materials and methods

6.3.2.1 Plant material and infusion

The plant material and preparation of the infusion is described in 6.2.2.1.

6.3.2.2 Method development

For the optimization of the chromatographic conditions of the method several analytical columns and mobile phases were tested. A Luna C18 (2) column (4.6 x 250 mm, 5 µm), an Econosphere C18 column (4.6 x 250 mm, 5 µm) and an Apollo C18 column (4.6 x 250 mm, 5 µm) were compared. As mobile phases, water, methanol and acetonitrile with 0.05% formic acid were evaluated. For all solvent systems, the gradient was optimized to obtain an optimal analysis time with an acceptable resolution.

Different extraction parameters were evaluated in order to fully extract all compounds of interest from the lyophilized infusion. The extraction solvent composition (5%, 20%, 50%, and 80% methanol), sonication time (20 and 60 min) and number of extractions (1 – 3 times) were tested.

*Published: van Dooren, I.; Faouzi, M.E.A.; Foubert, K.; Theunis, M.; Pieters, L.; Cherrah, Y.; Apers, S. Cholesterol lowering effect in gall bladder of dogs by a standardized infusion of *Herniaria hirsuta* L. *J. Ethnopharmacol.* **2015**, *169*, 69-75.

6.3.2.3 Final method

As a final method the following procedure was performed. About 100 mg of the lyophilized infusion was accurately weighed in a measuring flask of 10.0 mL. Methanol 50% was added, the sample was ultrasonicated during 20 min, and the solution was filtered.

For the subsequent HPLC analysis, 50 μ L of the extraction solution was injected on an Apollo C18 column (4.6 mm x 250 mm, 5 μ m). A flow rate of 1 mL/min was chosen and the following gradient was used: mobile phase A: H₂O + 0.05% FA, B: methanol + 0.05% FA; gradient: 0 min – 5% B; 5 min – 5% B; 55 min – 100% B; 57 min – 100% B; 58 min – 5%B; 60 min – 5%B.

6.3.2.4 Method validation

The method was validated according to the ICH guidelines described in Chapter 4.^{59,60}

The calibration model of the two selected standards was investigated. Therefore, nine concentration levels of rutin (4.2 – 209.4 μ g/mL) and eight levels for α -hederacoside C (33.0 – 660.4 μ g/mL) were prepared. All solutions were analyzed in duplicate.

For the repeatability of the injection, one sample was analyzed 6 times. Also the repeatability and the intermediate precision were investigated. Therefore, six independently prepared samples (100%; 100 mg) were analyzed according to the above described method. The procedure was repeated on three different days. The intermediate precision on different concentration levels was determined by analyzing six samples weighing 50% of the normal mass (50 mg) and six samples weighing 150% of the normal mass (150 mg). A solution of both standards, used to determine the amount of flavonoids and saponins, expressed in %, was freshly prepared each day and analyzed twice, using the same HPLC method.

To investigate the accuracy of the method, a recovery experiment for both rutin and α -hederacoside was performed. To 50% of the infusion of *H. hirsuta* a known amount of rutin or α -hederacoside C was added until a total concentration of 100% of either rutin or the saponins. For both compounds the samples were prepared in triplicate according to the described procedure.

6.3.3 Results and discussion

6.3.3.1 Method development

Suitable standard compounds were selected for the quantification of the flavonoids as well as for the saponins. Rutin which is present in the infusion was chosen as a standard for the flavonoids. Since the saponins present in the infusion of *H. hirsuta* are not commercially available and their large scale isolation would be very time-consuming and expensive, which would in addition make the method not useful for other research groups, α -hederacoside C was selected. The extraction experiments showed that 50% (v/v) methanol gave the best results and was chosen as extraction solvent. The best resolution was obtained with the Apollo C18 column, using water and methanol with 0.05% formic acid as mobile phases (Figure 6.37). A gradient, starting with 5% methanol + 0.05% FA going to 100% methanol + 0.05% FA was used.

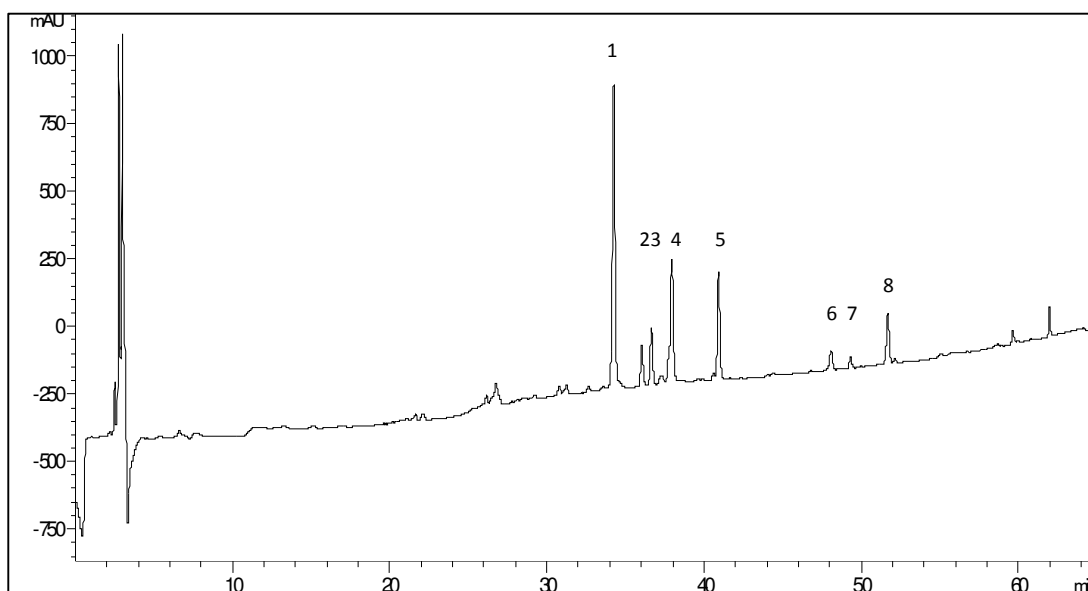


Figure 6.37 Chromatographic profile of *H. hirsuta* at 210 nm. Compounds 1-5 are flavonoids of which compound 1, 4 and 5 were elucidated in (6.2.3.2) as quercetin-3-*O*-(2''-*O*- α -L-rhamnopyranosyl)- β -D-glucuronopyranoside (1), rutin (4) and narcissin (5). Compounds 6-8 are saponins of which 7 and 8 were elucidated in (6.2.3.2) as 28-*O*-[[β -D-xylopyranosyl-(1 \rightarrow 4)- α -L-rhamnopyranosyl-(1 \rightarrow 2)]- β -D-glucopyranosyl-(1-6)]- β -D-glucopyranosyl]-medicagenic acid (7) and 3-*O*-[α -L-rhamnopyranosyl-(1 \rightarrow 3)]- β -D-glucuronopyranosyl]-28-*O*-[[β -D-glucopyranosyl-(1 \rightarrow 3)]- β -D-xylopyranosyl-(1 \rightarrow 4)]- β -D-apiofuranosyl-(1 \rightarrow 3)]- α -L-rhamnopyranosyl-(1 \rightarrow 2)]- β -D-fucopyranosyl]-medicagenic acid (8).

The calibration model of both compounds was investigated. The regression line was constructed, the equation was generated, and the correlation coefficient calculated. The slope and intercept were investigated with a Student t-test. The residuals were graphically evaluated. Also an ANOVA lack of fit test was performed. A visual inspection of the regression line and residuals plot showed that the

method was linear and homoscedastic (Figures 6.38, 6.39, and 6.40). The correlation coefficient was higher than 0.99. The slope of the regression line was significant and the intercept of the line did include the point (0,0) for rutin but not for α -Hederacoside C (Table 6.3). The F-value was smaller than the critical value for the ANOVA lack of fit test, meaning that there was no lack of fit for both calibration lines.

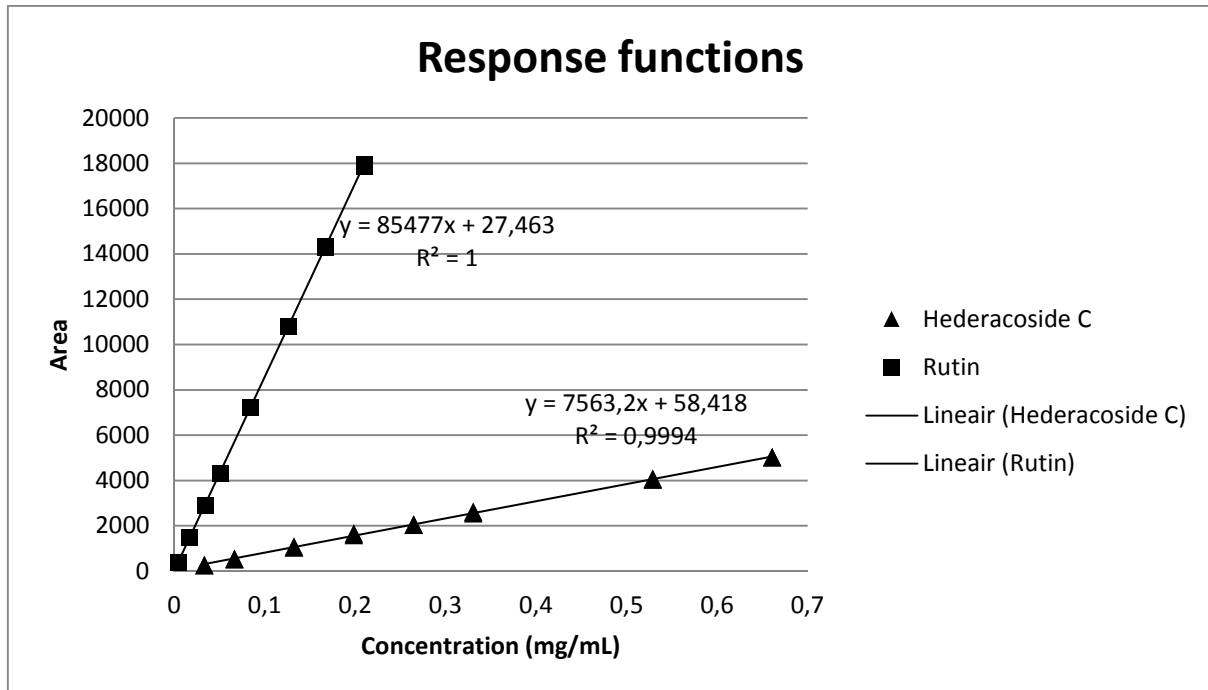


Figure 6.38 Response functions of rutin and hederacoside C.

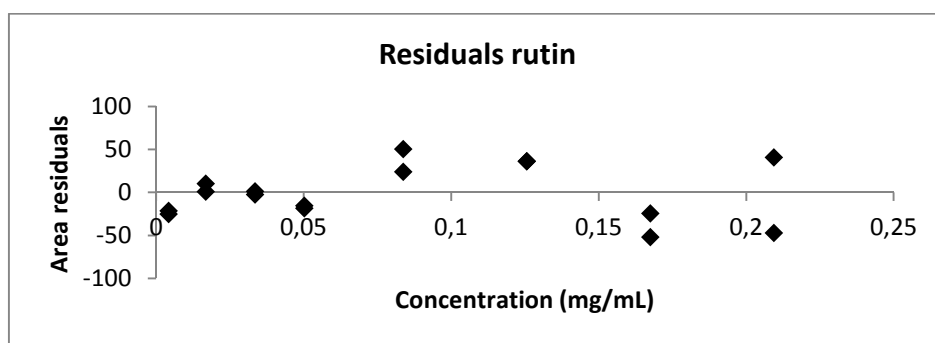


Figure 6.39 Residuals plot for rutin.

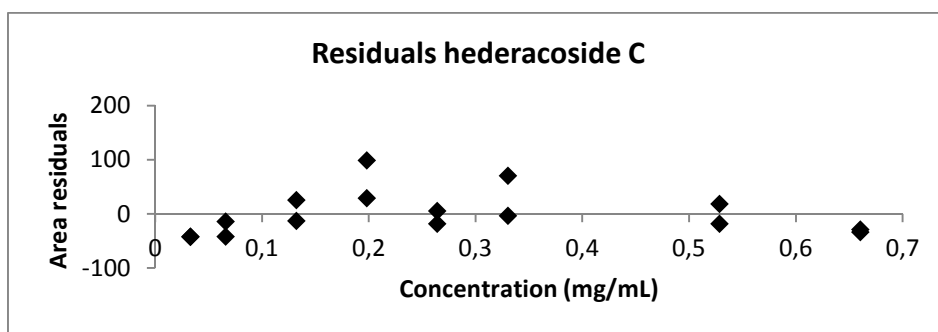


Figure 6.40 Residuals plot for hederacoside C.

Table 6.3 Regression analysis.

	Rutin	Hederacoside C
Correlation coefficient	1.0000	0.9997
Slope	7563.2	85476.7
Intercept	58.4	27.6
95% CI intercept	[20.67;96.16]	[-0.16;55.09]

For the investigation of the precision, the mean, the standard deviation and the RSD% were calculated for each day and each concentration level. The overall mean, standard deviation and RSD% were calculated for the three days and also for the three different concentration levels. All results are shown in Figures 6.41 and 6.42 and in Table 6.4. The repeatability and intermediate precision were evaluated by an ANOVA single factor test. For the repeatability, the within mean squares were used to calculate the standard deviation and RSD%. For the intermediate precision, the standard deviation was calculated using the following formula:

$$s = \sqrt{\frac{MS_{between} - MS_{within}}{n_j} + MS_{within}}$$

Before performing the ANOVA single factor, a Cochran test was done. The calculated Cochran value was smaller than the critical C-value, as well as for different days as for the different concentration levels, implying that the variances are not significantly different and an ANOVA single factor could be carried out.

For the interday precision, the calculated and theoretical F-values are presented in Table 6.4. Though for most of the flavonoids and for the saponins, there is a significant effect of the factor day and/or factor concentration, the precision of the method is acceptable taking into account the complexity of

the analysis. The RSD_{between} for the determination of flavonoids is smaller than 3%, more specifically, 1.72%, 2.02%, 1.95%, 2.66%, 256%, and 1.81%. $RSD\%_{\text{between}}$ values for saponins ranged from 3.13% to 14.54%. Saponins are detected at a wavelength of 210 nm causing higher variation in results, especially when the concentration is low, which is the case for one of them. Therefore, only the total content of saponins can be determined with an acceptable RSD_{between} (3.13%).

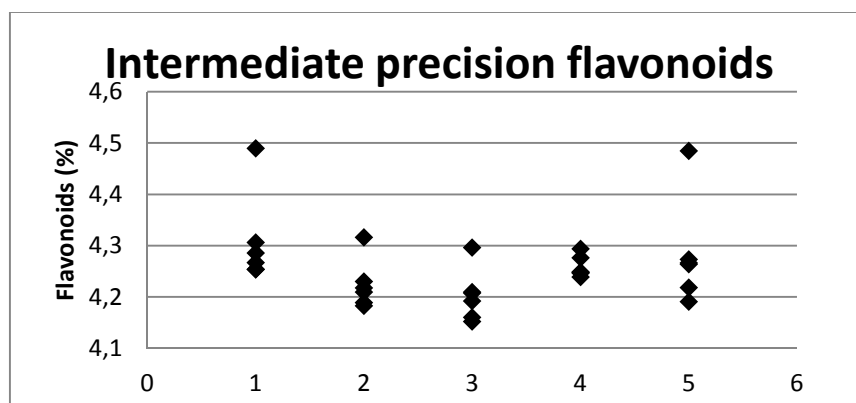


Figure 6.41 Results from intermediate precision for flavonoids: 1 = concentration level 50%; 2 = concentration level 100%, day 1; 3 = concentration level 100%, day 2; 4 = concentration level 100%, day 3; 5 = concentration level 150%.

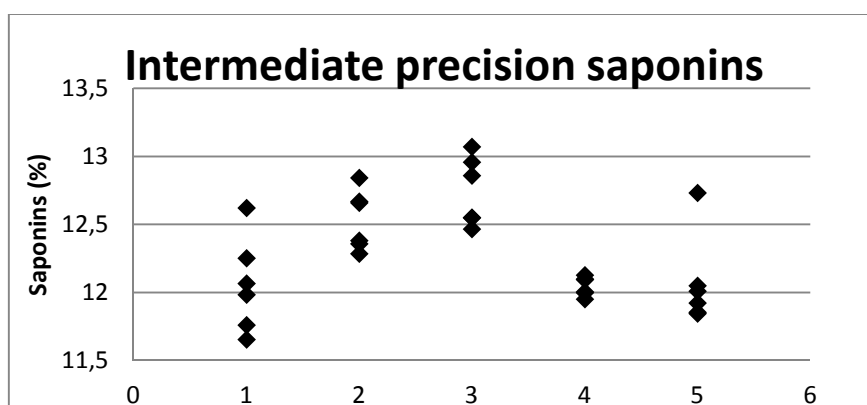


Figure 6.42 Results from intermediate precision for saponins: 1 = concentration level 50%; 2 = concentration level 100%, day 1; 3 = concentration level 100%, day 2; 4 = concentration level 100%, day 3; 5 = concentration level 150%.

Table 6.4 Precision results for flavonoids (1-5) and saponins (6-8); $F_{\text{theoretical}} = 2.67$ (different days, $n = 18$); $F_{\text{theoretical}} = 3.68$ (different concentration levels, $n = 30$).

Compound	Mean	s	RSD%	RSD _{within}	RSD _{between}	RSD _{max}	Cochran	F-value
1	concentration 50%	2.046	0.043	2.09				
	concentration 150%	2.039	0.046	2.28	1.16	1.72	2.40	1.84
	day1-100%	2.003	0.022	1.12				
	day2-100%	2.016	0.026	1.30	1.06	1.12	2.40	0.5001
	day3-100%	2.026	0.013	0.66				

Table 6.4 continued Precision results for flavonoids (1-5) and saponins (6-8); $F_{\text{theoretical}} = 2.67$ (different days, n = 18); $F_{\text{theoretical}} = 3.68$ (different concentration levels, n = 30).

Compound		Mean	s	RSD%	RSD _{within}	RSD _{between}	RSD _{max}	Cochran	F-value
2	concentration 50%	0.2653	0.0045	1.71					
	concentration 150%	0.2673	0.0060	2.23	1.43	2.02	3.26	0.5024	6.88
	day1-100%	0.2617	0.0018	0.67					
	day2-100%	0.2630	0.0028	1.05	0.85	1.49	3.27	0.5186	19.58
	day3-100%	0.2567	0.0020	0.77					
3	concentration 50%	0.3713	0.0051	1.38					
	concentration 150%	0.3705	0.0086	2.32	1.55	1.95	3.10	0.4592	4.48
	day1-100%	0.3630	0.0038	1.05					
	day2-100%	0.3626	0.0064	1.76	1.24	1.18	3.11	0.6706	0.46
	day3-100%	0.3607	0.0024	0.65					
4	concentration 50%	0.944	0.022	2.37					
	concentration 150%	0.935	0.025	2.63	1.81	2.66	2.69	0.4237	7.90
	day1-100%	0.922	0.011	1.22					
	day2-100%	0.909	0.014	1.50	1.12	2.97	2.70	0.5774	37.54
	day3-100%	0.9587	0.0032	0.33					
5	concentration 50%	0.683	0.020	2.88					
	concentration 150%	0.672	0.021	3.07	2.16	2.56	2.83	0.4102	3.45
	day1-100%	0.674	0.011	1.60					
	day2-100%	0.659	0.010	1.51	1.31	1.86	2.84	0.5168	7.51
	day3-100%	0.6565	0.0031	0.47					
Total flavonoid	concentration 50%	4.309	0.090	2.10					
	concentration 150%	4.28	0.10	2.43	1.64	1.81	2.14	0.4878	2.27
	day1-100%	4.224	0.048	1.14					
	day2-100%	4.203	0.052	1.23	1.01	1.14	2.15	0.4425	2.60
	day3-100%	4.259	0.022	0.51					
6	concentration 50%	2.87	0.13	4.68					
	concentration 150%	3.205	0.094	2.95	2.84	6.72	2.24	0.4387	28.53
	day1-100%	3.247	0.061	1.88					
	day2-100%	3.411	0.035	1.02	2.07	3.81	2.23	0.6488	15.40
	day3-100%	3.195	0.096	2.99					

Table 6.4 continued Precision results for flavonoids (1-5) and saponins (6-8); $F_{\text{theoretical}} = 2.67$ (different days, n = 18); $F_{\text{theoretical}} = 3.68$ (different concentration levels, n = 30).

Compound		Mean	s	RSD%	RSD _{within}	RSD _{between}	RSD _{max}	Cochran	F-value
7	concentration 50%	1.133	0.097	6.93	4.13	14.54	2.53	0.3663	69.34
	concentration 150%	1.412	0.055	3,93					
	day1-100%	1.335	0.060	4.50					
	day2-100%	1.673	0.056	3.32					
	day3-100%	1.477	0.030	2.04					
8	concentration 50%	8.14	0.17	2.08	2.28	4.70	1.96	0.3289	20.52
	concentration 150%	7.46	0.23	3.02					
	day1-100%	7.95	0.20	2.53					
	day2-100%	7.66	0.17	2.19					
	day3-100%	7.36	0.082	1.11					
Total saponin	concentration 50%	12.14	0.26	2.18	1.99	3.13	1.83	0.2330	9.86
	concentration 150%	12.07	0.34	0.58					
	day1-100%	12.53	0.22	1.77					
	day2-100%	12.74	0.25	1.98					
	day3-100%	12.05	0.070	2.78					

The accuracy of the method was determined by means of a recovery experiment. For the flavonoids, a mean recovery of 99.18% was found with an RSD% of 0.64% while for the saponins 109.20% was recovered with an RSD% of 5.51%. Although for both groups of compounds 100% was not included in the 95% confidence interval of the recovery results, for the flavonoids the method can be considered as accurate since a recovery% of 97% - 103% is generally accepted. For the saponins, however, the acceptable recovery limits were not reached; therefore, recovery% should be mentioned with every result obtained by this method. The lyophilized infusion was analyzed with the validated method and contained 4.51% flavonoids and 12.74% saponins, taking in account the amount of moisture present in the lyophilizate. An F-test was performed to check that the recovery experiment was performed with an equal precision as during the precision experiments. For flavonoids, this was the case, but for saponins, the calculated F-value was slightly higher than the critical F-value. An RSD% of 5.51% was found for the recovery results while according to the critical F-value a maximal RSD% value of 5.35% was allowed. Despite this statistical difference, the similarity between the precision could still be regarded as acceptable.

6.4 Coumarin, flavonoid and saponin profiles of different *Herniaria hirsuta* extracts and comparison with *Herniaria glabra* and *Herniariae herba*

6.4.1 Introduction

In addition to the Mediterranean region, *Herniaria hirsuta* grows in other parts of the world such as Central Europe and Asia as well as other *Herniaria species* such as *H. glabra*.¹ Regional climate differences such as temperature and humidity can cause variations in plant constituents. The effect of origin and species was evaluated by analysis of different *Herniaria hirsuta* and *Herniaria glabra* extracts. Therefore, chromatographic profiling using TLC and the abovementioned developed and validated HPLC method were applied to characterize the different species. In addition, flavonoids and saponins were quantified in all *Herniaria hirsuta* samples.

6.4.2 Material and methods

6.4.2.1 Plant material

Herniaria hirsuta was grown in Morocco, Belgium, and Bulgaria. Samples 1 and 2 were grown in Morocco in the wild (sample 1 as described in section 6.2.2.1) and cultivated (sample 2). From the seeds of this first sample, a plant was grown in Belgium by an unskilled hobbyist (sample 7). The seeds from both sample 1 and 7 were used to grow plants in Belgium under controlled conditions by a cultivator (Akuna) (sample 5 and 6), respectively. In addition, two samples from Bulgaria were obtained. In Bulgaria, herbs are sold in pharmacies and in special outlets where only herbs are sold. Sample 3 is a sample from a special herb outlet shop and sample 4 is a sample derived from an industrial manufacturer. In addition to the *Herniaria hirsuta* samples described above, plant material of *Herniaria glabra* was obtained from the National Botanical Garden of Belgium (sample 9) and from an industrial manufacturer in Bulgaria (sample 10 and sample 11). Sample 10 was a methanolic extract of *H. glabra* prepared by the industrial manufacturer. A sample *Herniariae herba* – *Herniaria vulgaris* (sample 8) was obtained from Fagron (Capelle aan den IJssel, The Netherlands) and the analytical certificate states that its origin is Bulgaria and it complies to the monograph of the Deutscher Arzneimittel Codex. All plant material was air-dried. Extracts were prepared as described under 6.2.2.1.

6.4.2.2 General experimental methods

TLC analysis

For coumarins, a solvent mixture of toluene and diethyl ether 1:1 (saturated with 10% glacial acetic acid) was used, for flavonoids, a mixture of ethyl acetate, formic acid, acetic acid and water 100:11:11:26, and for saponins, the composition of the solvent mixture was butanol, acetic acid and water 93:21:36. Detection was done at 254 and 365 nm and after spraying with different specific spraying reagents. Coumarins were visualized using a potassium hydroxide solution (5% in ethanol). Visualization of flavonoids was achieved after spraying with NEU reagent in combination with a PEG 4000 solution while saponins were revealed after using anisaldehyde reagent. Solutions of herniarin, umbelliferon, rutin, alfa-hederine and hederacoside C (1 mg/mL) were used as references.

HPLC-DAD

All samples were analyzed with the abovementioned developed and validated HPLC method. HPLC-DAD analysis was performed on an Agilent 1200 HPLC.

6.4.3 Results and discussion

6.4.3.1 Coumarins

Results are shown in Figure 6.43. Only sample 3, *Herniaria hirsuta* from the Bulgarian herbal outlet shop, and sample 9, *Herniaria glabra* obtained from the National Botanical Garden of Belgium, showed a zone of herniarin. A small zone of umbelliferon was present for sample 3.

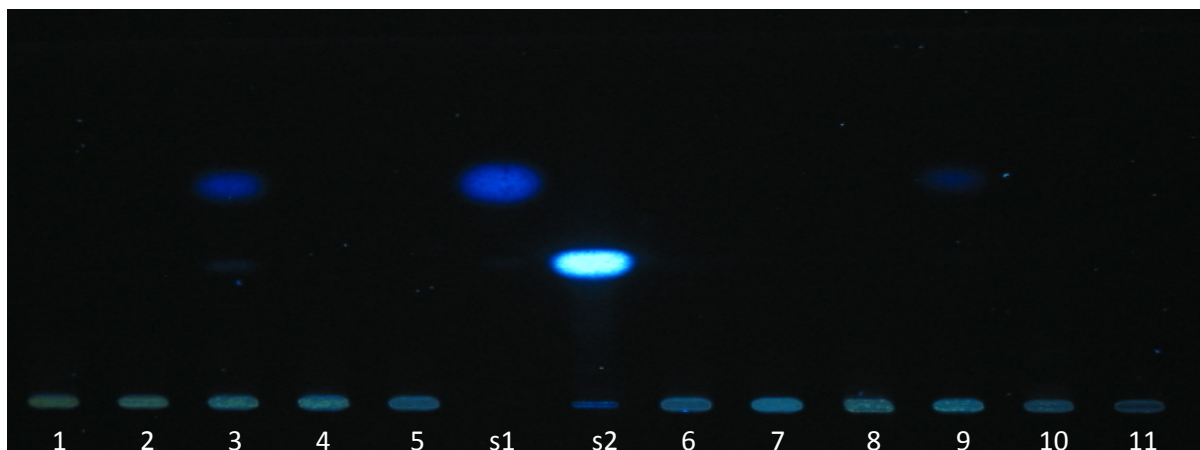


Figure 6.43 TLC chromatograms at 365 nm after spraying with a potassium hydroxide solution. Numbers indicate the sample number. 1: *H. hirsuta* from Morocco grown in the wild; 2: *H. hirsuta* from Morocco – cultivated; 3: *H. hirsuta* from Bulgarian herbal outlet shop; 4: *H. hirsuta* from Bulgarian industry; 5: *H. hirsuta* from seeds of 1 – grown in Belgium by cultivator; 6: *H. hirsuta* from seeds of 7 – grown in Belgium by cultivator; 7: *H. hirsuta* from seeds of 1 – grown in Belgium by hobbyist; 8: *Herniariae herba*; 9: *H. glabra* from Belgium; 10: *H. glabra* extract from Bulgarian industrial manufacturer; 11: *H. glabra* from Bulgarian industry; s1: standard solution 1 being herniarin and s2: standard solution 2 being umbelliferon.

6.4.3.2 Saponins

TLC chromatograms are shown in Figure 6.44. Saponins can turn purple to pink or green after spraying with anisaldehyde. All profiles of *Herniaria hirsuta* extracts, grown in Belgium or Morocco (samples 1, 2, 5, 6, and 7), were quite similar except for the additional greenish spot at Rf 0.12 that is visible for *H. hirsuta* grown in Belgium by an unskilled hobbyist (sample 7). *Herniaria hirsuta* samples from Bulgaria (samples 3 and 4) showed high similarity with the profiles obtained with *Herniariae herba* (sample 8). *H. glabra* obtained in Belgium (sample 9) showed a rather different profile having some similarities with sample 3, being a *Herniaria hirsuta* sample from Bulgaria. This was not the case for both *H. glabra* samples from Bulgaria (samples 10 and 11) which showed more similarities with *Herniariae herba* (sample 8) than with *H. glabra* from Belgium (sample 9) illustrating the influence of climate differences for *H. glabra*. Pink spots at Rf 0.70 were only visible for sample 3 and 9 and another pink spot at Rf 0.76 was present in sample 10. Differences in yellow spots, which originated from flavonoids, will be further discussed by means of the TLC chromatograms obtained after spraying with NEU reagent and a PEG 4000 solution. Differences in the HPLC profiles were also present (Figure 6.45) but these profiles were less informative than the TLC profiles.

The saponin content (Table 6.5) ranged from 7.74% to 14.82% and the content of plant material originating from Morocco was higher than that of plant material grown in Belgium or Bulgaria.

Regarding the variation in saponin content of plant material from the same origin, for example, Belgium, it could not be concluded that the origin of the plant material had a significant effect.

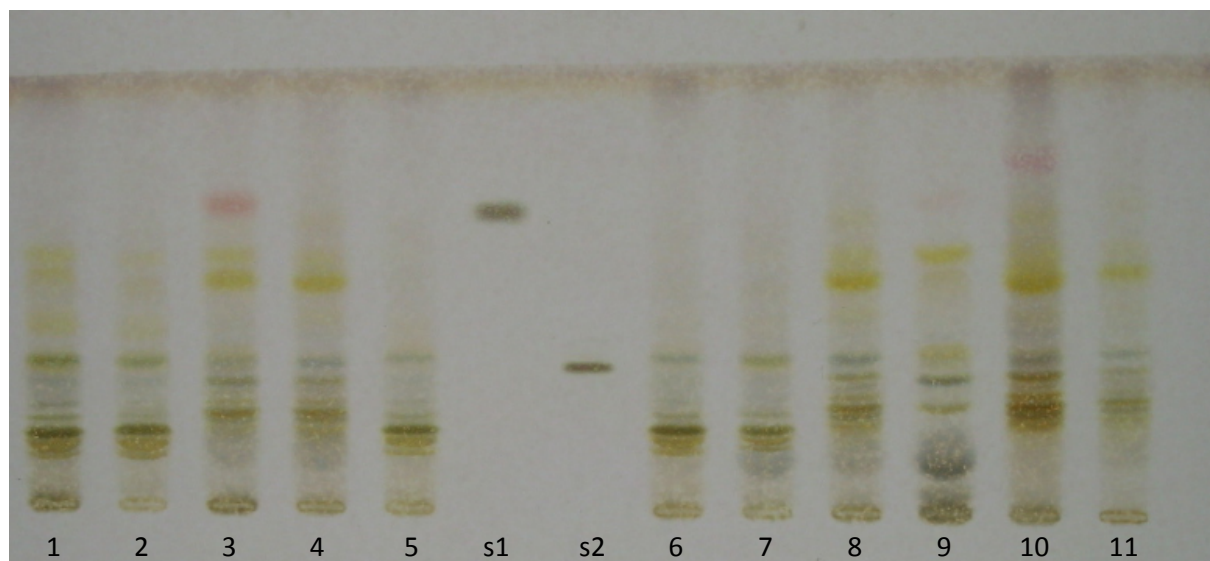


Figure 6.44 TLC chromatograms after spraying with anisaldehyde reagent. Numbers indicate sample numbers. 1: *H. hirsuta* from Morocco grown in the wild; 2: *H. hirsuta* from Morocco – cultivated; 3: *H. hirsuta* from Bulgarian herbal outlet shop; 4: *H. hirsuta* from Bulgarian industry; 5: *H. hirsuta* from seeds of 1 – grown in Belgium by cultivator; 6: *H. hirsuta* from seeds of 7 – grown in Belgium by cultivator; 7: *H. hirsuta* from seeds of 1 – grown in Belgium by hobbyist; 8: *Herniariae herba*; 9: *H. glabra* from Belgium; 10: *H. glabra* extract from Bulgarian industrial manufacturer; 11: *H. glabra* from Bulgarian industry; s1: standard solution being hederacoside C and s2: standard solution being α -hederine.

Table 6.5 Saponin content of different *H. hirsuta* extracts.

Sample (origin)	Saponin content (%)
1 (Morocco)	12.74
2 (Morocco)	14.82
3 (Bulgaria)	8.58
4 (Bulgaria)	8.47
5 (Belgium)	10.74
6 (Belgium)	10.38
7 (Belgium)	7.74

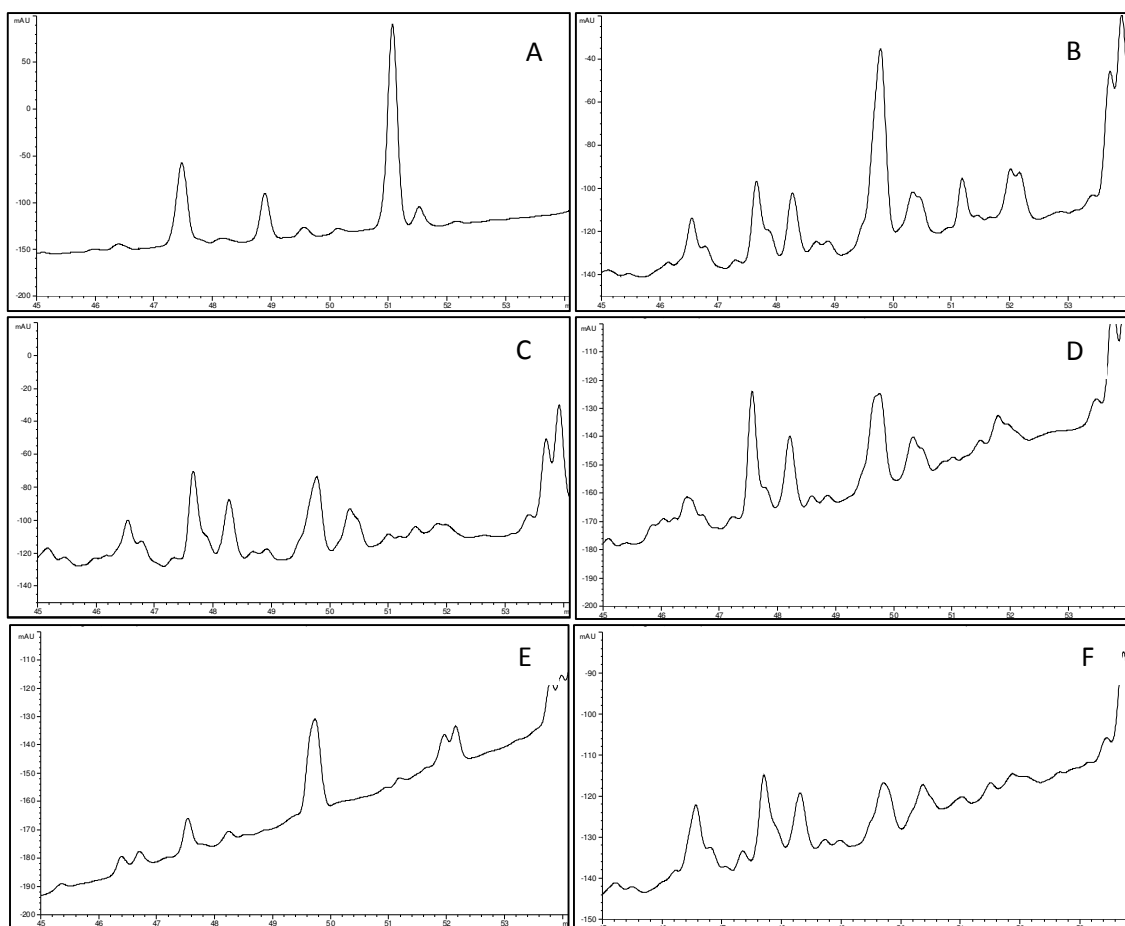


Figure 6.45 HPLC saponin profiles of different extracts. A: sample 1 (profiles of samples 2, 5, 6 and 7 were similar to that of sample 1 and are not shown); B: sample 3; C: sample 4; D: sample 8; E: sample 9; F: sample 10 (the profile of sample 11 was similar to that of sample 10 and is not shown).

6.4.3.3 Flavonoids

TLC and HPLC chromatograms are shown in Figures 6.46 and 6.47. After spraying with NEU reagent, flavonols were colored orange and flavones tended to be yellow/greenish. The blue spots originated from phenolic acids, such as chlorogenic acid. TLC and HPLC profiles of *Herniaria hirsuta* samples 1, 2, 5, 6 and 7 showed a high degree of similarity, but samples 5, 6 and 7 had a much lower content of flavonoids. There was a remarkable similarity between samples 4, 8, 10 and 11, *H. hirsuta* from the Bulgarian industry, *Herniariae herba* and two *Herniaria glabra* samples from Bulgaria, respectively, especially in the upper half of the thin layer chromatogram, being the green spots at R_f 0.65, 0.72 and 0.8 but also in the HPLC fingerprints. Sample 3 and 9, a *Herniaria hirsuta* sample from a Bulgarian herbal shop and *Herniaria glabra* from Belgium showed some similarities. Table 6.6 shows the total flavonoid content of all extracts ranging from 0.41% to 4.64%. As already mentioned, the flavonoid content of *H. hirsuta* grown in Belgium, 0.54%, 0.41% and 1.47% (samples 5, 6 and 7), respectively,

was much lower than that of *H. hirsuta* grown in Morocco, 4.50% and 2.72% (samples 1 and 2), respectively. Therefore, it could be concluded that the temperate maritime climate of Belgium resulted in a lower flavonoid yield in contrast with the Mediterranean climate of Oujda (Morocco).

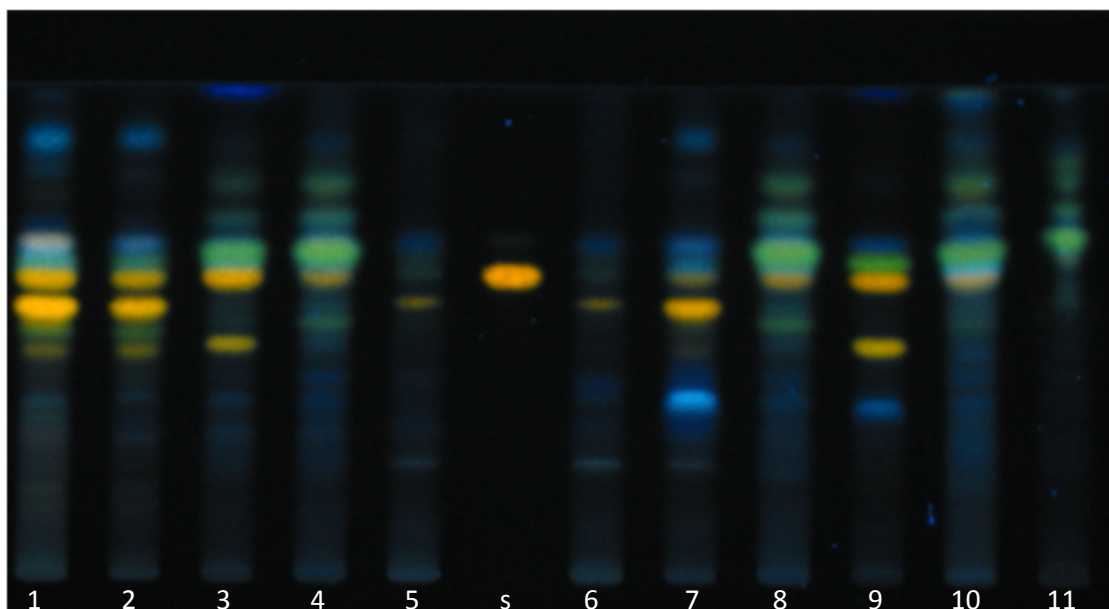


Figure 6.46 TLC chromatograms at 365 nm after spraying with NEU reagent and a PEG 4000 solution. Numbers indicate the sample number. 1: *H. hirsuta* from Morocco grown in the wild; 2: *H. hirsuta* from Morocco – cultivated; 3: *H. hirsuta* from Bulgarian herbal outlet shop; 4: *H. hirsuta* from Bulgarian industry; 5: *H. hirsuta* from seeds of 1 – grown in Belgium by cultivator; 6: *H. hirsuta* from seeds of 7 – grown in Belgium by cultivator; 7: *H. hirsuta* from seeds of 1 – grown in Belgium by hobbyist; 8: *Herniariae herba*; 9: *H. glabra* from Belgium; 10: *H. glabra* extract from Bulgarian industrial manufacturer; 11: *H. glabra* from Bulgarian industry; s: standard solution being rutin.

Table 6.6 Flavonoid content of different *H. hirsuta* extracts.

Sample	Flavonoid content (%)
1 (Morocco)	4.50
2 (Morocco)	2.72
3 (Bulgaria)	3.84
4 (Bulgaria)	3.60
5 (Belgium)	0.54
6 (Belgium)	0.41
7 (Belgium)	1.47

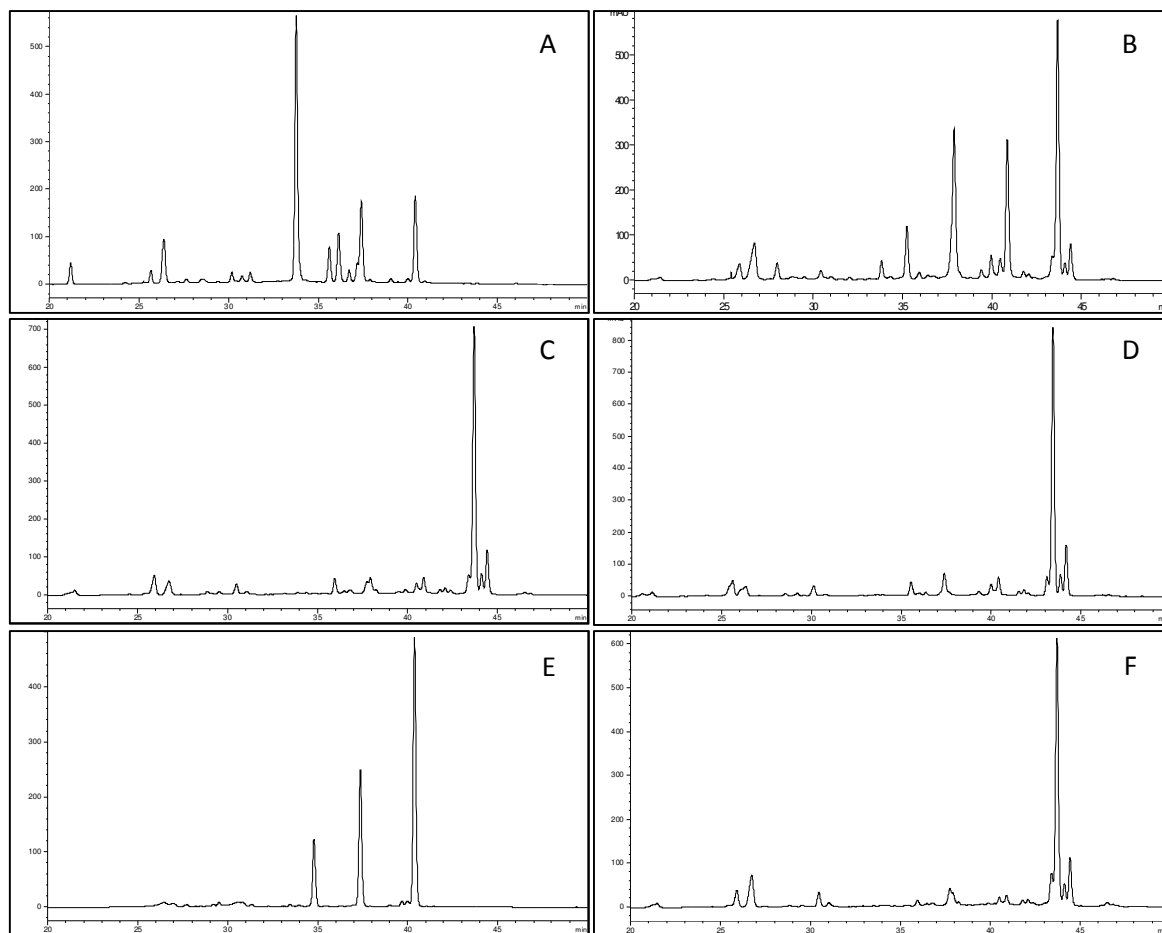


Figure 6.47 HPLC flavonoid profiles of different extracts. A: sample 1 (profiles of samples 2, 5, 6 and 7 were similar to that of sample 1 and are not shown); B: sample 3; C: sample 4; D: sample 8; E: sample 9; F: sample 10 (the profile of sample 11 was similar to that of sample 10 and is not shown).

6.5 Cholesterol lowering effect in the gallbladder of dogs by a standardized infusion of *Herniaria hirsuta* L.*

6.5.1 Introduction

Because of the promising activity of *H. hirsuta* on bile cholesterol in normal conditions the standardized extract of this plant was investigated for its efficacy against gallstones in dogs receiving a cholesterol-rich diet.⁸ Since no toxicity was reported in folk medicine and in the *in vivo* experiments, an extract of *Herniaria hirsuta* can be considered as non-toxic according to the legislation on herbal medicinal products (traditional use). However, since pharmacovigilance and long-standing use cannot be used as evidence for the absence of genotoxic risks, the genotoxicity must be evaluated according to the European guideline on the assessment of genotoxicity of herbal substances/preparations. The basic requirement is to assess genotoxicity in a bacterial reverse mutation test using a test battery of different bacterial strains (Ames test) (EMA/HMPC/107079/2007).⁴⁸

6.5.2 Materials and methods

6.5.2.1 Experimental protocol for the *in vivo* evaluation

All experiments were approved by the Ethical Committee of the University of Rabat, Morocco. 21 dogs (14.5 ± 4.9 kg) were collected for the experiment; temperature in the animalarium ranged between 16 – 35 °C on a natural light-dark cycle. Dogs used in the experiment were divided into one group of control dogs (CG, seven dogs), one group of dogs treated with UDCA (UG, seven dogs) and one group of dogs treated with a standardized extract of *H. hirsuta* (HG, seven dogs). Each dog was caged individually and was subjected to an acclimatization period of 15 days in the new environment before starting the experiment. During this period all dogs received an anti-parasitic treatment. Subsequently, all dogs were daily fed 200 g horse meat containing 50% sheep fat during 120 days, after which all dogs were daily fed 200 g horse meat without sheep fat till the end of the experiment (day 180). At day 30 of the experiment, treatment of the different groups started. While CG dogs received no additional treatment, UG dogs received twice a day a dose of 7.35 mg/kg body weight

*Published: van Dooren, I.; Faouzi, M.E.A.; Foubert, K.; Theunis, M.; Pieters, L.; Cherrah, Y.; Apers, S. Cholesterol lowering effect in gall bladder of dogs by a standardized infusion of *Herniaria hirsuta* L. *J. Ethnopharmacol.* **2015**, *169*, 69-75. Contribution: preparation of infusions.

UDCA (based on the human posology using the extrapolation of animal dose to human dose) and HG dogs received twice a day a dose of 48.5 mg/kg body weight of the herbal extract (patent filed, Pieters et al., 2013) until the end of the experiment (day 180).^{47,61} UDCA or the herbal extract were mixed with a small quantity of meat making sure the entire treatment dose was administered to each dog. A bile and blood sample of each dog was collected every 30 days, after which the concentration of cholesterol was determined. For the collection of the bile the following surgical method was used: All dogs received marbofloxacin 2% (1 mg/kg body weight), acepromazine (0.05 mg/kg body weight, intramuscular (IM)), atropine (0.04 mg/kg body weight, IM) and tolfenamic acid (4 mg/kg body weight, IM) before surgery. Induction of anesthesia was done depending on the weight of the dogs with sodium thiopental (15 mg/kg body weight, intravenous (IV)) or xylazine (0.5 mg/kg body weight, IV) combined with ketamine (15 mg/kg body weight, IV). For the maintenance of sedation isoflurane (1 L/min) (xylazine, ketamine) was used. During surgery, all dogs received artificial breathing through a tracheal tube. Each surgery bile was collected by puncturing the gallbladder. Bile and blood samples were immediately stored at -20 °C after which quantification of the cholesterol in both bile and blood was performed by an enzymatic method. After each surgical procedure, each dog received marbofloxacin 2% (1 mg/kg body weight) during 4 days. The body weight of all dogs was monitored during the entire experiment. Data are expressed as mean \pm SEM. Data were analyzed using one-way analysis of variance (ANOVA), followed by the Bonferroni test or Kruskal-Wallis analysis and Dunnett T3. $P \leq 0.05$ was considered significant.

6.5.2.2 Genotoxicity: Ames test

An Ames test was performed according to the organization for economic co-operation and development (OECD)-guideline. The standardized extract was tested on 5 *Salmonella typhimurium* strains (TA 1535, TA 100, TA 98, TA 1537, TA 102), whether or not in the presence of metabolizing S9-fraction. Six concentrations of the extract were tested (5 mg/plate, 1.5 mg/plate, 0.5 mg/plate, 0.15 mg/plate, 0.05 mg/plate, and 0.015 mg/plate) and depending on the bacterial strain and the absence and presence of the S9-fraction, different positive controls were included in the test. The respective positive controls for TA 1535 were sodium azide (50 μ g/mL) and 2-aminoanthracene (25 μ g/mL), for TA 100 sodium azide (50 μ g/mL) and 2-aminoanthracene (10 μ g/mL), for TA 98 4-nitroquinoline-1-oxide (2 μ g/mL) and 2-aminoanthracene (25 μ g/mL), for TA 1537 9-aminoacridine (500 μ g/mL) in

both cases, and for TA 102 4-nitroquinoline-1-oxide (10 µg/mL) and 2-aminoanthracene (25 µg/mL). Each concentration was tested in triplicate, while negative controls were performed in quadruplicate. Results are expressed as mean number of revertants ± SEM.

6.5.3 Results and discussion

6.5.3.1 In vivo evaluation

The level of cholesterol in the bile was determined for all dogs starting at day 30 of the experiment and with time intervals of 30 days (Figure 6.48). It was observed that the control group (CG) and the group that received UDCA (UG) showed an increase in bile cholesterol over time, until day 120 (90 days of treatment) when the cholesterol-rich diet was stopped. However, the bile cholesterol values of the group which received the standardized extract of *H. hirsuta* (HG) remained at the starting levels in spite of the continuous administration of a cholesterol-rich diet. Although a minor difference ($p \leq 0.05$) was observed between CG and HG after 30 days of treatment with the extract, this dissimilarity between CG and HG was more profound after 90 days of treatment ($p \leq 0.001$). Even 30 days after discontinuation of the cholesterol-rich diet a significant difference ($p \leq 0.001$) remained between the untreated group and the group which received the standardized extract of *Herniaria hirsuta*. At 150 days of treatment, a large standard deviation could be observed in CG, due to the bile cholesterol values of one dog. However, since this value was not marked as an extreme outlier by statistical analysis it was not excluded. Also, elimination of this value did not cause any profound difference in the statistical results after 150 days of treatment, as all three groups remained statistically equal. At any time-point, no statistical difference could be observed between CG and UG.

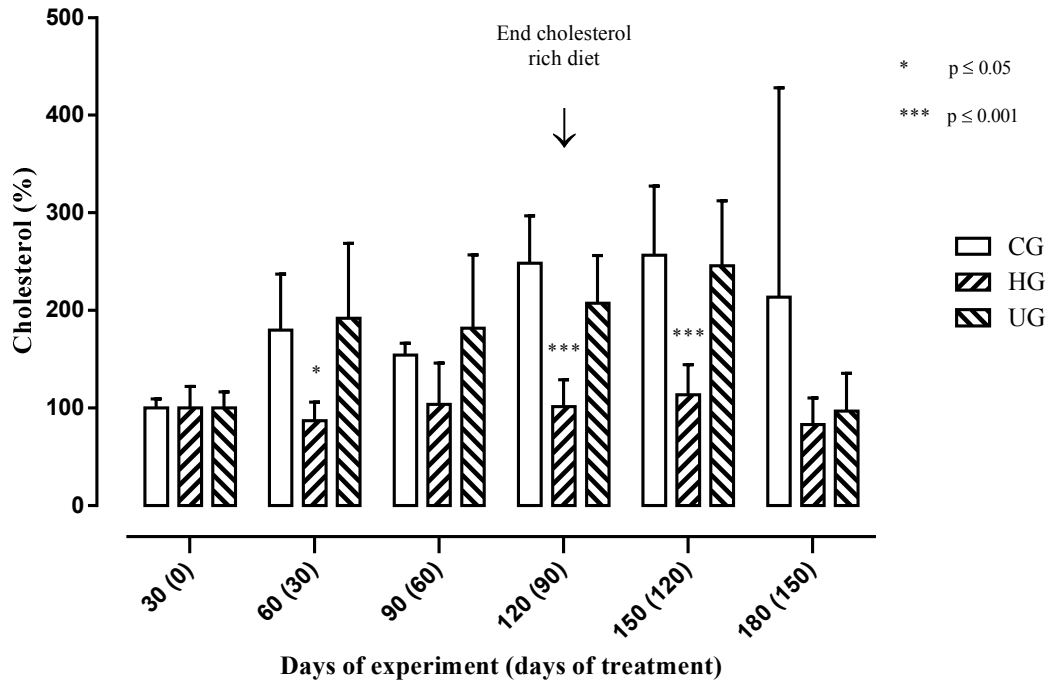


Figure 6.48 Cholesterol level in the bile for the three groups. CG: control group; HG: *H. hirsuta* group; UG: UDCA group.

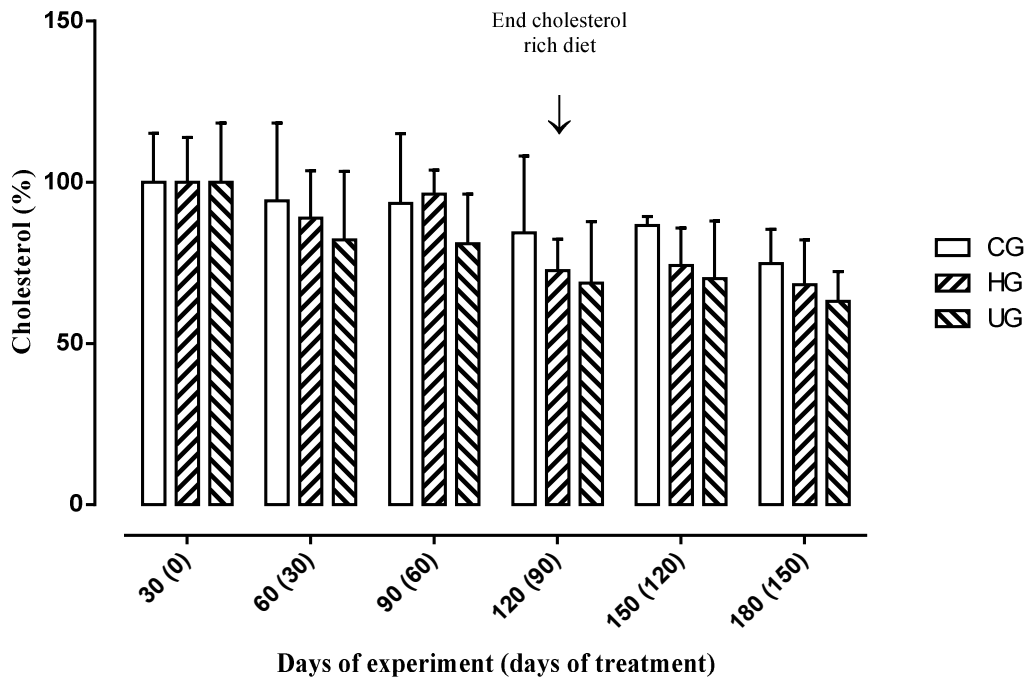


Figure 6.49 Cholesterol level in blood for the three groups. CG: control group; HG: *H. hirsuta* group; UG: UDCA group.

Although the values for cholesterol in blood seem to have a tendency to decrease over time (Figure 6.49), no statistically significant difference could be observed for CG and UG between the different time-points. For HG a difference could be observed which started after 90 days of treatment with the

standardized extract and remained until the end of the experiment. Despite this difference over time, all three groups (CG, UG, and HG) remained statistically equal for cholesterol values in blood at the different time-points. Concerning the body weight of the dogs, all groups were statistically equal and dogs gained or lost no body weight over time.

Because of the promising activity of *H. hirsuta* on bile cholesterol in normal conditions, the standardized extract of this plant was investigated for its efficacy against gallstones in dogs receiving a cholesterol-rich diet. In spite of the continuous administration of a cholesterol-rich diet, the standardized extract of *Herniaria hirsuta* was able to retain the level of cholesterol in the bile nearly constant at the starting level and to induce a difference with the untreated group. In the present study administration of a standardized extract of *H. hirsuta* had no significant effect on blood cholesterol levels.

UDCA is often used in the treatment of gallstones because of the production of unsaturated gallbladder bile resulting from a decreased hepatic secretion of biliary cholesterol and reduced intestinal absorption of cholesterol.⁶² However, in the current study this drug was unable to reduce the level of cholesterol in the bile or in the blood of the treated dogs. This can possibly be explained by compensatory mechanisms, for example, increased cholesterol synthesis or decreased excretion of fecal bile acids.⁶³⁻⁶⁴ It is clear that the standardized extract of *H. hirsuta* either has different mechanisms of action than UDCA and/or eliminates the compensatory mechanisms which may arise in dogs treated with UDCA.

6.5.3.2 Genotoxicity: Ames test

The results obtained for the Ames test are displayed in Table 6.7. For none of the tested strains, a dose-response relationship was observed. In addition, for none of the strains, there was a doubling of the amount of revertants in comparison with the negative control. Therefore, it can be concluded the extract is not genotoxic. These results were in line with its established traditional use in Morocco and European countries, and the absence of reported toxicity in folk medicine and in the *in vivo* experiments. The extract of *Herniaria hirsuta* can be considered as non-toxic according to the legislation on herbal medicinal products (traditional use).

Table 6.7 The amount of revertants seen for the different bacterial strains in the Ames test. (n=3, negative control n=4, *=high amount of revertants not counted, but considered ok)

	TA 98		TA 100		TA 1535		TA 1537		TA 102	
S9	X		X		X		X		X	
Negative control	38.8 ± 8.5	34.7 ± 2.9	187 ± 16	191 ± 34	8.8 ± 4.0	11.3 ± 4.3	8.5 ± 1.3	6.5 ± 1.3	218.5 ± 7.8	270 ± 34
Positive control	221 ± 20	1841 ± 349	904 ± 111	499 ± 49	715 ± 64	50.1 ± 5.5	136 ± 53	517 ± 24	*	*
Extract 0.015 mg/plate	47 ± 16	29.0 ± 7.9	249 ± 39	203 ± 47	8.7 ± 4.7	11.0 ± 4.4	8.7 ± 5.5	6.3 ± 1.5	369 ± 58	259 ± 10
Extract 0.05 mg/plate	53 ± 18	31.7 ± 2.1	263 ± 11	137.0 ± 4.2	7.0 ± 5.0	10.3 ± 2.1	4.3 ± 1.5	6.0 ± 3.5	356 ± 10	298 ± 21
Extract 0.15 mg/plate	30.3 ± 3.1	31.3 ± 2.1	257 ± 24	156 ± 51	13.3 ± 3.0	13.7 ± 2.5	12.0 ± 1.4	5.3 ± 1.2	296 ± 29	255 ± 12
Extract 0.5 mg/plate	44 ± 19	37.7 ± 9.3	220 ± 11	197 ± 56	12.0 ± 2.7	9.0 ± 2.7	8.7 ± 1.5	7.0 ± 2.7	309 ± 18	375 ± 28
Extract 1.5 mg/plate	31.0 ± 5.3	35.0 ± 1.7	275 ± 46	212 ± 43	9.3 ± 2.5	13.0 ± 4.4	9.0 ± 1.7	11.7 ± 1.5	420.0 ± 9.1	441 ± 52
Extract 5 mg/plate	28.7 ± 1.5	64.0 ± 6.6	290 ± 41	261 ± 69	15.7 ± 4.0	12.0 ± 7.0	11.3 ± 2.9	11.3 ± 2.1	429 ± 42	514 ± 41

6.5.4 Conclusions

Prolonged use of a standardized *H. hirsuta* extract results in a cholesterol-lowering effect in the bile but not in blood of dogs when maintaining a cholesterol-rich diet. Since this pharmacological effect prevents the formation of gallstones and can contribute to solving existing gallstones, a standardized preparation of *H. hirsuta*, showing no genotoxicity, may have a positive effect in the treatment of gallstones in human patients.

References

1. Brinckmann, J.; Lindemaier, M. *Herbal drugs and phytopharmaceuticals. A handbook for practice on a scientific basis*; Wichtl, M., Ed.; 3rd edition; CRC Press: Boca Raton, 2004; pp 289-291.
2. Austrian Pharmacopoeia. Österreichisches Arzneibuch. Verlag Österreich: Wien, 2010; p 335-336.
3. Gubler, E. *Herniaria hirsuta* Behaartes Bruchkraut. <http://www.alpenbotaniker.ch/Bruchkraut-Behaartes.html> (accessed May, 2016).
4. Mifsud, S. Hairy rupture wort. http://www.maltawildplants.com/CRYO/Herniaria_hirsuta.php (accessed May, 2016).
5. Kramer, N. *Herniaria hirsuta*. http://calphotos.berkeley.edu/cgi/img_query?enlarge=0000+0000+1210+2792 (accessed May, 2016).
6. Atmani, F.; Slimani, Y.; Mimouni, M.; Aziz, M.; Hacht, B.; Ziyat, A. Effect of aqueous extract from *Herniaria hirsuta* L. on experimentally nephrolithiasic rats. *J. Ethnopharmacol.* **2004**, *95* (1), 87-93.
7. Atmani, F.; Farell, G.; Lieske, J. Extract from *Herniaria hirsuta* coats calcium oxalate monohydrate crystals and blocks their adhesion to renal epithelial cells. *J. Urol.* **2004**, *172* (4), 1510-1514.
8. Settaf, A.; Labhal, A.; Cherrah, Y.; Slaoui, A.; Hassar, M. *Herniaria hirsuta* dissout les calculs biliaires cholestéroliques. *Espérance Médicale* **1999**, *6* (47), 79-82.
9. Eddouks, M.; Maghrani, M.; Lemhadri, A.; Ouahidi, M. L.; Jouad, H. Ethnopharmacological survey of medicinal plants used for the treatment of diabetes mellitus, hypertension and cardiac diseases in the southeast region of Morocco (Tafilalet). *J. Ethnopharmacol.* **2002**, *82* (2-3), 97-103.
10. Mbark, A. N.; Charouf, Z.; Wray, V.; Nimtz, M.; Schopke, T. Monodesmosidic saponins from *Herniaria hirsuta*. *Pharmazie* **2000**, *55* (9), 690-692.
11. Mbark, A. N.; Guillaume, D.; Kol, O.; Charrouf, Z. Triterpenoid saponins from *Herniaria fontanesii*. *Phytochemistry* **1996**, *43* (5), 1075-1077.
12. Rhiouani, H.; El-Hilaly, J.; Israili, Z. H.; Lyoussi, B. Acute and sub-chronic toxicity of an aqueous extract of the leaves of *Herniaria glabra* in rodents. *J. Ethnopharmacol.* **2008**, *118* (3), 378-386.
13. Al-Qura'n, S. Ethnopharmacological survey of wild medicinal plants in Showbak, Jordan. *J. Ethnopharmacol.* **2009**, *123* (1), 45-50.
14. Carrio, E.; Valles, J. Ethnobotany of medicinal plants used in Eastern Mallorca (Balearic Islands, Mediterranean Sea). *J. Ethnopharmacol.* **2012**, *141* (3), 1021-1040.
15. Ali-Shtayeh, M. S.; Yaniv, Z.; Mahajna, J. Ethnobotanical survey in the Palestinian area: a classification of the healing potential of medicinal plants. *J. Ethnopharmacol.* **2000**, *73* (1-2), 221-232.
16. Freiler, M.; Reznicek, G.; Jorenitsch, J.; Kubelka, W.; Schmidt, W.; SchubertZsilavec, M.; Haslinger, E.; Reiner, J. New triterpene saponins from *Herniaria glabra*. *Helv. Chim. Acta* **1996**, *79* (2), 385-390.
17. Mbark, A. N.; Charrouf, Z.; Wieruszkeski, J. M.; Leroy, Y.; Kol, O. *Herniaria* saponin-a, a novel saponin from *Herniaria fontanesii*. *Nat. Prod. Lett.* **1995**, *6* (3), 233-240.

18. Charrouf, Z.; Mbark, A. N.; Guillaume, D.; Leroy, Y.; Kol, O. New triterpenoid saponin from *Herniaria fontanesii*. *Abstracts of Papers*, 210th National Meeting of the American Chemical Society, Chicago, IL, Aug 20-24, 1995; American Chemical Society: Washington DC, **1995**.
19. Schroder, H.; Schubertszilavec, M.; Reznicek, G.; Cart, J.; Jurenitsch, J.; Haslinger, E. A triterpene saponin from *Herniaria glabra*. *Phytochemistry* **1993**, *34* (6), 1609-1613.
20. Reznicek, G.; Cart, J.; Korhammer, S.; Kubelka, W.; Jurenitsch, J.; Haslinger, E. The 1st 2 spectroscopically confirmed saponins from *Herniaria glabra* L. *Pharmazie* **1993**, *48* (6), 450-452.
21. Freiler, M.; Reznicek, G.; Schubert-Zsilavec, M.; Kubelka, W. Structures of triterpene saponins from *Herniaria glabra*. *Sci. Pharm.* **1996**, *64*, 7.
22. Wagner, H.; Bladt, S.; Zgainski, E. Flavonoid-Drogen. *Drogen analyse. Dünnschicht-chromatographische Analyse von Arzneidrogen*; Springer-Verlag: Berlin Heidelberg New York, 1983; pp 163-193.
23. Mbark, A. N.; Guillaume, D.; Cherrah, Y.; Wieruszeki, J. M.; Ricart, G.; Charrouf, Z. An acylated isorhamnetin glycoside from *Herniaria fontanesii*. *Phytochemistry* **1996**, *41* (3), 989-990.
24. *Dictionary of natural products on DVD* [DVD]; CRC Press, 2015.
25. Wagner, H.; Bladt, S.; Zgainski, E. Cumarin-Drogen. *Drogen analyse. Dünnschicht-chromatographische Analyse von Arzneidrogen*; Springer-Verlag: Berlin Heidelberg, New York 1983; pp 145-161.
26. Knoll, T. Stone disease. *Eur. Urol., Suppl.* **2007**, *6* (12), 717-722.
27. Moe, O. W. Kidney stones: pathophysiology and medical management. *Lancet* **2006**, *367* (9507), 333-344.
28. Schafmayer, C.; Hartleb, J.; Tepel, J.; Albers, S.; Freitag, S.; Volzke, H.; Buch, S.; Seeger, M.; Timm, B.; Kremer, B.; Folsch, U. R.; Fandrich, F.; Krawczak, M.; Schreiber, S.; Hampe, J. Predictors of gallstone composition in 1025 symptomatic gallstones from Northern Germany. *BMC Gastroenterol* **2006**, *6*, 36.
29. Stinton, L. M.; Myers, R. P.; Shaffer, E. A. Epidemiology of gallstones. *Gastroenterol. Clin. North Am.* **2010**, *39* (2), 157-169.
30. Tiselius, H. G. Epidemiology and medical management of stone disease. *BJU Int.* **2003**, *91* (8), 758-767.
31. Kum, F.; Mahmalji, W.; Hale, J.; Thomas, K.; Bultitude, M.; Glass, J. Do stones still kill? An analysis of death from stone disease 1999-2013 in England and Wales. *BJU Int.* **2016**, *118* (1), 140-4.
32. Butterweck, V.; Khan, S. R., Herbal medicines in the management of urolithiasis: alternative or complementary? *Planta Med.* **2009**, *75* (10), 1095-1103.
33. Sakhaee, K.; Maalouf, N. M.; Sinnott, B. Kidney stones 2012: pathogenesis, diagnosis, and management. *J. Clin. Endocrinol. Metab.* **2012**, *97* (6), 1847-1860.
34. Spernat, D.; Kourambas, J. Urolithiasis - medical therapies. *BJU Int.* **2011**, *108*, 9-13.
35. Bio-Stilgit Pharmaceuticals. Renalit Combi Colic. <http://www.biostilgit.it/product/renalit-combi-colic/> (accessed 24 June).
36. Bundesamt für Sicherheit im Gesundheitswesen. https://aspregister.basg.gv.at/aspregister/faces/aspregister.jspx?_afLoop=24021319537153280&_afWindowMode=0&_adf.ctrl-state=4hsfxyole_4 (accessed 24 June).

37. Atmani, F.; Slimani, Y.; Mbark, A. N.; Bnouham, M.; Ramdani, A. *In vitro* and *in vivo* antilithiasic effect of saponin rich fraction isolated from *Herniaria hirsuta*. *J Bras Nefrol* **2006**, *28* (4), 199-203.
38. Lambou-Gianoukos, S.; Heller, S. J. Lithogenesis and bile metabolism. *Surg.Clin. North Am.* **2008**, *88* (6), 1175-1194.
39. Das, I.; Verma, S. Human stones: Dissolution of calcium phosphate and cholesterol by edible plant extracts and bile acids. *J. Sci. Ind. Res.* **2008**, *67* (4), 291-294.
40. Di Ciaula, A.; Wang, D. Q.; Bonfrate, L.; Portincasa, P. Current views on genetics and epigenetics of cholesterol gallstone disease. *Cholesterol* **2013**, *2013*, Article ID 298421.
41. Castro-Torres, I. G.; de Jesus Cardenas-Vazquez, R.; Velazquez-Gonzalez, C.; Ventura-Martinez, R.; De la, O. A. M.; Naranjo-Rodriguez, E. B.; Martinez-Vazquez, M. Future therapeutic targets for the treatment and prevention of cholesterol gallstones. *Eur. J. Pharmacol.* **2015**, *765*, 366-374.
42. Wang, D. Q.; Cohen, D. E.; Carey, M. C. Biliary lipids and cholesterol gallstone disease. *J. Lipid Res.* **2009**, *50 Suppl*, S406-411.
43. Wang, H. H.; Portincasa, P.; de Bari, O.; Liu, K. J.; Garruti, G.; Neuschwander-Tetri, B. A.; Wang, D. Q. H. Prevention of cholesterol gallstones by inhibiting hepatic biosynthesis and intestinal absorption of cholesterol. *Eur. J. Clin. Invest.* **2013**, *43* (4), 413-426.
44. Gaillard, M.; Tranchart, H.; Lainas, P.; Dagher, I. New minimally invasive approaches for cholecystectomy: Review of literature. *World J Gastrointest Surg* **2015**, *7* (10), 243-248.
45. Konikoff, F. M. Gallstones - approach to medical management. *MedGenMed* **2003**, *5* (4), 8.
46. Portincasa, P.; Ciaula, A. D.; Bonfrate, L.; Wang, D. Q. Therapy of gallstone disease: What it was, what it is, what it will be. *World J Gastrointest Pharmacol Therap* **2012**, *3* (2), 7-20.
47. Settaf, A.; El Kabbaj, S.; Labhal, A.; Cherrah, Y.; Slaoui, A.; Hassar, M. *Herniaria hirsuta* reduces biliary cholesterol in dogs. Induced changes in bile composition. *Biologie et Santé* **2000**, *1*, 6.
48. European Medicines Agency. Guideline on the assessment of genotoxic constituents in herbal substances/preparations. *EMA/HMPC/107079/2007*. London, **2007**.
49. De Paepe, P.; Servaes, K.; Noten, B.; Diels, L.; De Loose, M.; Van Droogenbroeck, B.; Voorspoels, S. An improved mass spectrometric method for identification and quantification of phenolic compounds in apple fruits. *Food Chem.* **2013**, *136* (2), 368-375.
50. Medeiros, P.; Simoneit, B. Analysis of sugars in environmental samples by gas chromatography-mass spectrometry. *J. Chromatogr. A* **2007**, *1141* (2), 271-278.
51. Pollier, J.; Morreel, K.; Geelen, D.; Goossens, A. Metabolite profiling of triterpene saponins in *Medicago truncatula* hairy roots by liquid chromatography Fourier transform ion cyclotron resonance mass spectrometry. *J. Nat. Prod.* **2011**, *74* (6), 1462-76.
52. Tan, N.; Zhou, J.; Zhaob, S. Advances in structural elucidation of glucuronide oleanane-type triterpene carboxylic acid 3,28-O-bidesmosides (1962-1997). *Phytochemistry* **1999**, *52* (2), 153-192.
53. Agrawal, K. NMR spectroscopy in the structural elucidation of oligosaccharides and glycosides. *Phytochemistry* **1992**, *31* (10), 3307-3330.

54. Mshvildadze, V.; Elias, R.; Faure, R.; Debrauwer, L.; Dekanosidze, G.; Kemertelidze, E.; Balansard, G. Triterpenoid saponins from berries of *Hedera colchica*. *Chem. Pharm. Bull.* **2001**, *49* 6, 752-754.
55. Borges, R.; Tinoco, L.; Filho, J.; Barbi, N.; da Silva, A. Two new oleanane saponins from *Chicocca alba* (L.) Hitch. *J. Braz. Chem. Soc.* **2009**, *20* (9), 1738-1741.
56. Pinheiro, P.; Justino, G. Structural analysis of flavonoids and related compounds - a review of spectroscopic applications. In: *Phytochemicals - A global perspective of their role in nutrition and health* [Online]; Rao, V. Ed.; InTech: 2012; Chapter 2, 33-56.
<http://www.intechopen.com/books/phytochemicals-a-global-perspective-of-their-role-in-nutrition-and-health/structural-analysis-of-flavonoids-and-related-compounds-a-review-of-spectroscopic-applications> (accessed March 22, 2016).
57. Felser, C.; Schimmer, O., Flavonoid glycosides from *Alchemilla speciosa*. *Planta Med.* **1999**, *65* (7), 668-670.
58. Böttger, S.; Melzig, M. F. Triterpenoid saponins of the Caryophyllaceae and Illecebraceae family. *Phytochem. Lett.* **2011**, *4* (2), 59-68.
59. International Conference on Harmonisation of Technical Requirements for Registration of Pharmaceuticals for Human Use. Text on validation of analytical procedures: ICH Harmonised Tripartite guideline. **1996**.
60. International Conference on Harmonisation of Technical Requirements for Registration of Pharmaceuticals for Human Use. Validation of analytical procedures: methodology: ICH Harmonised Tripartite Guideline. **1996**.
61. Pieters, L.; Apers, S.; Theunis, M.; Vaeck, M.; El Mazouari, K.; Cherray, Y. Medicinal Plant Extract. EP2014/071987, April 23, 2015.
62. Di Ciaula, A.; Wang, D. Q.; Wang, H. H.; Bonfrate, L.; Portincasa, P. Targets for current pharmacologic therapy in cholesterol gallstone disease. *Gastroenterol. Clin. North Am.* **2010**, *39* (2), 245-64, viii-ix.
63. Pertsemlidis, D.; Kirchman, E. H.; Ahrens, E. H., Jr. Regulation of cholesterol metabolism in the dog. I. Effects of complete bile diversion and of cholesterol feeding on absorption, synthesis, accumulation, and excretion rates measured during life. *J. Clin. Invest.* **1973**, *52* (9), 2353-2367.
64. Pertsemlidis, D.; Kirchman, E. H.; Ahrens, E. H., Jr. Regulation of cholesterol metabolism in the dog. II. Effects of complete bile diversion and of cholesterol feeding on pool sizes of tissue cholesterol measured at autopsy. *J. Clin. Invest.* **1973**, *52* (9), 2368-2378.

Chapter 7

***VACCINIUM MACROCARPON* – CRANBERRY**

7.1 General introduction

7.1.1 Urinary tract infections

Urinary tract infections (UTIs) are widespread and affect a large part of the population. They are among the most common medical conditions that require outpatient treatment and persistent and recurrent infections often lead to hospitalization. Therefore, it is a major medical and economical burden. UTIs refer to the presence of a certain amount of bacteria in the urine and consist of cystitis, which is an infection of the bladder, and pyelonephritis, an infection of the kidneys. Typical symptoms of cystitis are dysuria, urgency and frequency of urination, suprapubic tenderness or pain, and hematuria, while pyelonephritis also includes flank and back pain and fever. Depending on the part that is involved they are divided in lower and upper urinary tract infections. When only the bladder is involved they are called lower urinary tract infections, while upper urinary tract infections involve the kidneys. The latter type can be severe in certain groups such as elderly people, infants, and immunodeficient persons. UTIs are more common in women but can also occur in men. Almost 30-40% of women will have a UTI during their lifetime and about 25% of them will suffer from recurrent UTIs, which are defined as two episodes of uncomplicated UTIs in the last six months or more than three in the last twelve months. Specific subpopulations are at higher risk to develop a UTI including infants, elderly people, pregnant women, patients with urologic abnormalities, spinal cord injuries and catheters, immunodeficient persons, and people with diabetes and multiple sclerosis. Most UTIs are caused by *Escherichia coli* bacteria. The infection starts through migration of these bacteria from the rectal area to the ureter and adhesion of *E. coli* to the uroepithelium through their fimbriae, such as the well-known type 1 and P-type fimbriae. This latter type plays an important role in the pathogenesis of ascending UTIs and pyelonephritis. Bearing in mind the increasing resistance of bacteria against antibiotics used in the prophylaxis or treatment of urinary tract infections, such as trimethoprim/sulfamethoxazole, the search for non-antibiotic treatment options has become more and more important.¹⁻¹¹

7.1.2 *Vaccinium macrocarpon*

Vaccinium macrocarpon Aiton or cranberry (Figure 7.1) is a small trailing evergreen scrub which can become 20 cm tall and grows aside bogs and swamps on acidic soils, peat, and clay. The stem is

slender, glabrous to hairy with roots starting at the nodes of the horizontal growing stems to form a dense mat. The leaves are green, elliptic, 7-10 cm long and have a slightly revolute margin. They are sessile and the arrangement is alternate. The flowers are attached to a 2 to 3 cm long pedicel with 2 greenish white bracteoles and consist of a 4-lobed calyx and cup-shaped corolla, which is white to pink and highly reflexed. The flowers have an inferior ovary, one style, a capitate stigma, and eight stamens. The fruit of cranberry is a globose red to black berry with a diameter of 9 to 20 mm. The mesocarp and endocarp are off-white to dull-red. The seeds are located in the four loculi of the fruit.¹² Phytochemical research proved the presence of flavan-3-ols, such as catechin and epicatechin, proanthocyanidins (PACs), flavonols such as quercetin-, myricetin- and kaempferol glycosides, cyanidin and peonidin anthocyanidins, which are shown in Figure 7.2, terpenes, organic acids, sugars, and complex carbohydrates.^{2,9,13-18}

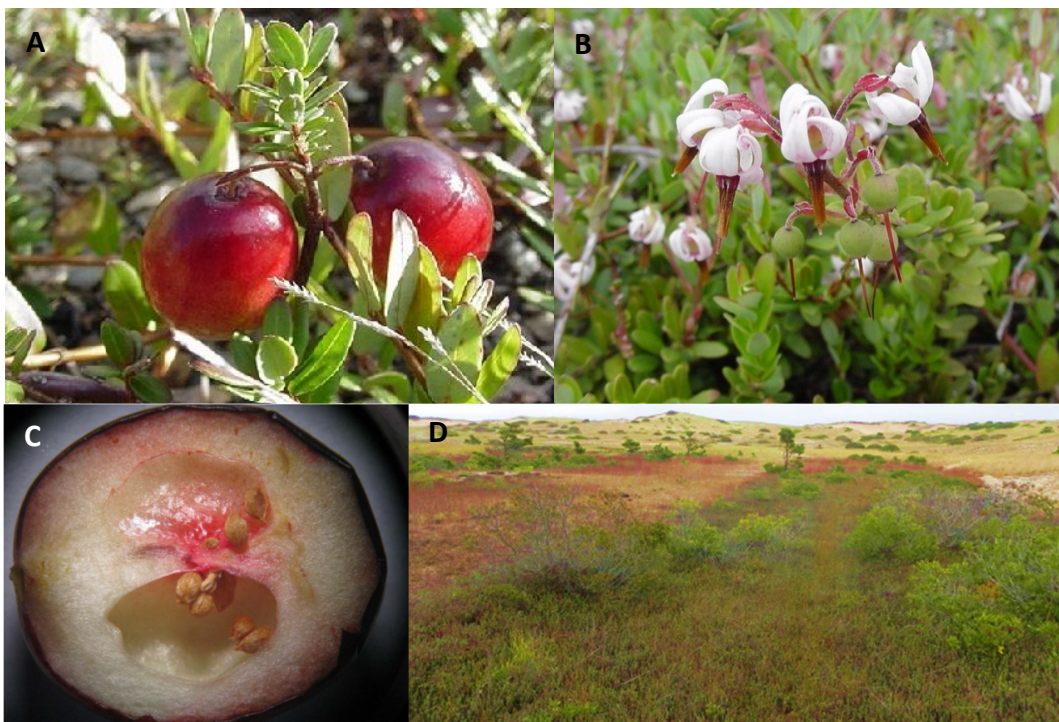
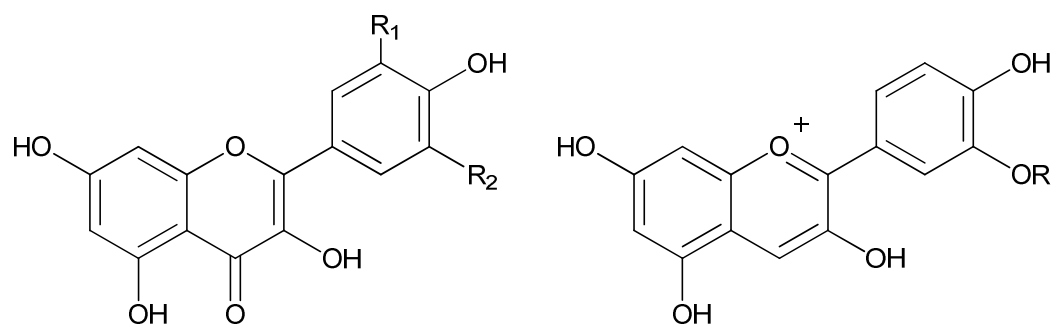
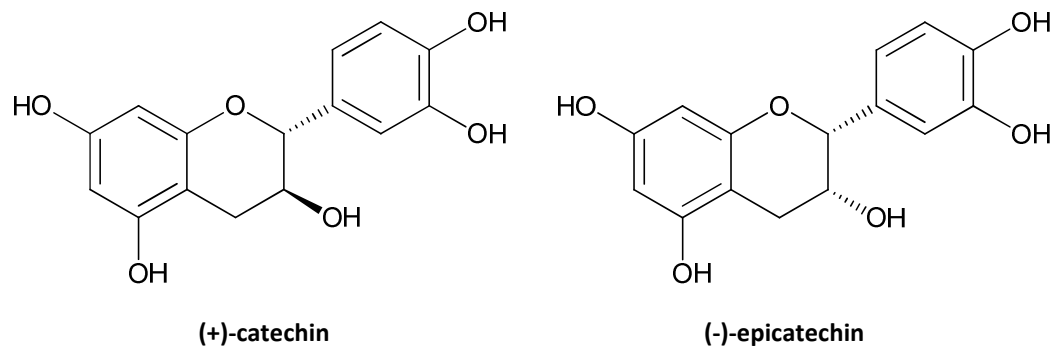


Figure 7.1: A) fruits; B) flowers; C) coupe of fruit with seeds; D) habitat of *V. macrocarpon*.¹²



	R ₁	R ₂		R
quercetin	H	OH	cyanidin	H
myricetin	OH	OH	peonidin	CH ₃
kaempferol	H	H		

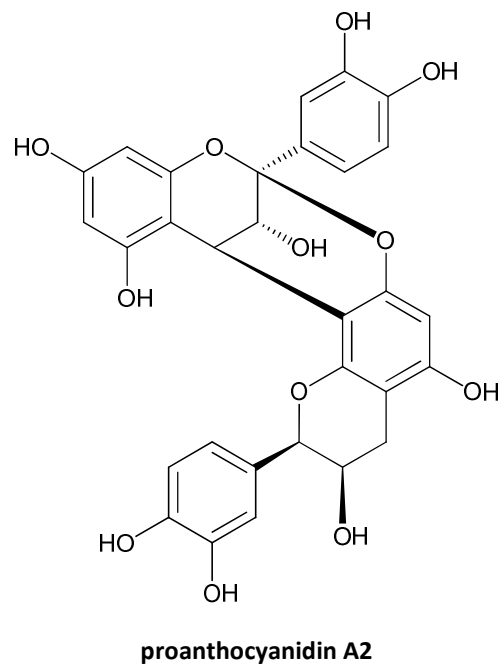


Figure 7.2 Structures of compounds present in *V. macrocarpon*.

The plant is native to northeastern North America and was already used as food and medicine by native Americans.^{2,12} The oldest record about the medicinal use of cranberry dates from the 17th century and describes the use against scurvy and fever. Later on, people used cranberry as a diuretic, anti-pyretic, laxative, for its anti-inflammatory properties, and for its positive effect on the urinary tract.¹² Nowadays it is widely used for the prevention of urinary tract infections. A large number of clinical studies has been performed to evaluate the use of cranberry for the prevention of UTIs. Unfortunately, these studies used different cranberry preparations, which were poorly standardized, making it hard to compare and sometimes leading to mixed results. Although most studies support the use of cranberry for the prevention of recurrent UTIs in young and middle-aged women, some studies could not confirm the effect.^{1,2,4-8,12} For other patient groups, clinical evidence remains insufficient. In order to obtain more comparative clinical studies, new analytical methods for the quantification and standardization of different cranberry preparations are still needed.

The positive effect of cranberry in the prevention of urinary tract infections is probably the result of multiple actions. Many *in vitro* and *ex vivo* studies were carried out in order to elucidate the mechanism of action. Many years ago it was believed that cranberry prevented infection by lowering the urinary pH, but this hypothesis was abandoned since it was shown that the consumption of a normal amount of cranberry could never sufficiently change the urinary pH.^{2,12,19} One mechanism, probably the most well-known, is the prevention of the adherence of *E. coli* by their P-type fimbriae to uroepithelial cells, a first step in the development of urinary tract infections.²⁰ This effect was ascribed to the A-type PACs, which are unusual PACs present in a limited number of foods such as cranberry.^{15,19,21} Howell et al.^{22,23} proved the anti-adherence activity of A-type PACs and of urine after consumption of cranberry, while this beneficial effect was not observed for urine after consumption of non A-type PACs containing juices, such as grape juice and apple juice. Although this effect is proven *in vitro*, these compounds have to reach the urine. Therefore, PACs need to be absorbed in the intestine first and it is well known that they are poorly absorbed *in vivo*, especially when the degree of polymerization is relatively high.²⁴ In literature, B-type dimers and trimers were found to be transported across Caco-2 cells and were also found in the urine of rats after feeding with grape seed extracts or after adding them to the feed.²⁵⁻²⁸ In addition, PAC B1 was found in human serum after intake of a PAC-rich grape seed extract.²⁹ Appeldoorn et al.³⁰ have proven the absorption of PAC dimers A1 and A2 in rats but trimers and tetramers were not absorbed, although Ou et al.³¹ found

very low absorption of A-type dimers to tetramers using Caco-2 cells. Recently, the presence of procyanidin A2 was proven in urine of older adults after consumption of a cranberry juice cocktail.³² Unabsorbed PACs reach the colon and are catabolized by colon bacteria into phenolic metabolites such as hydroxyphenylacetic acids, hydroxypropionic acids, hydroxybenzoic acids and hydroxyvaleric acids, which can be absorbed and reach the urine.³³⁻³⁶ It was proven by de Llano et al.³⁷ that these cranberry-derived metabolites were also capable of inhibiting the attachment of *E. coli* to the uroepithelium.

It is not fully understood how cranberry inhibits the attachment of *E. coli* but this can be caused by cranberry components, acting as receptor analogs for fimbriae and in this way competing with the uroepithelial cells, by alteration of the morphology of the bacteria, or by reduction of the expression of the fimbriae.¹⁹ Hidalgo et al.³⁸ found that the flagellin gene expression was inhibited by cranberry PACs and this resulted in reduced flagellum-mediated motility. This reduced swimming motility, together with reduced hydrophobicity, which is thought to be important for binding to uroepithelial cells, was also seen by Wojnicz et al.³⁹ after treatment of *E. coli* with a commercial cranberry extract. This way of action could prevent uropathogenic *E. coli* bacteria to reach the upper urinary tract.

In addition to inhibition of adherence, the prevention of the formation of biofilms, which are typically associated with catheter-associated UTIs, was shown when *E. coli* was treated with a commercial cranberry extract.³⁹ Another interesting possible mode of action which is suggested is the reduction of pathogenic *E. coli* in the gut by binding of PACs to bacteria rendering them anti-adherent or by modifying the bacterial selection pressure towards nonadherent strains.²⁴ A comparison of the metabolization of polyphenols of a cranberry and a grape seed extract using a dynamic gastrointestinal simulator showed a higher extent of metabolization of the former. The lower extent of metabolization of the grape seed extract was related to a higher degree of degradation of the colon microbiota. This means that the survival of colon bacteria, including beneficial bacteria, is higher for cranberry, which can also play a role in the bacterial selection pressure towards nonadherent strains.³³

7.1.3 Proanthocyanidins

PACs are a major group of phenolic compounds and consist of monomeric flavan-3-ol units, which can be attached to each other by interflavan bonds, mostly between C-4 and C-8 and sometimes

between C-4 and C-6. These proanthocyanidins are called B-type PACs. When an additional ether linkage between C-2 and C-7 is present these PACs are referred to as A-type PACs, which are less common than B-type PACs and only present in a small number of plants and foods, such as cranberry, peanuts, plums, cacao, and avocados (Figure 7.3).⁴⁰⁻⁴²

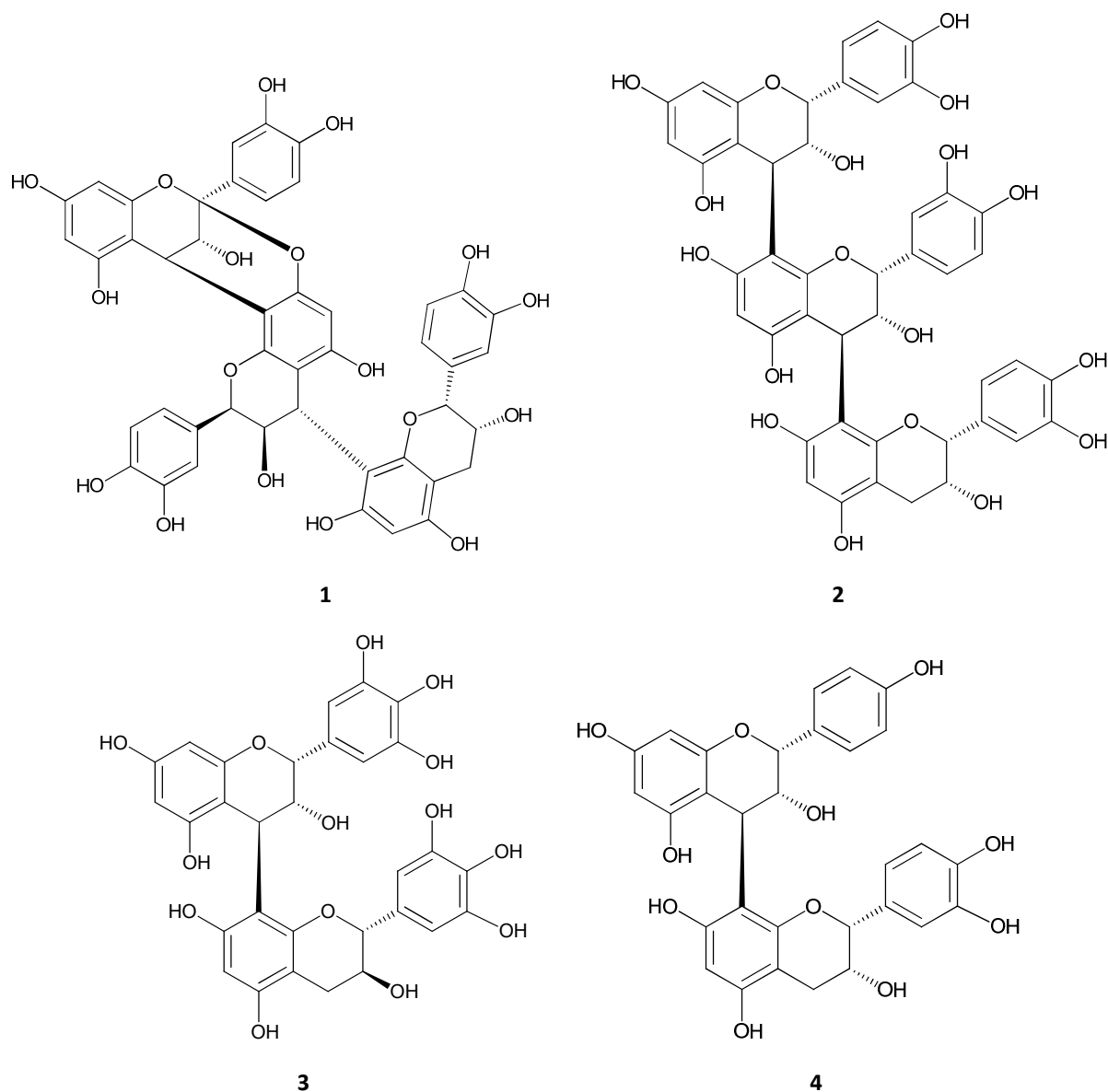


Figure 7.3 1: trimeric A-type procyanidin, cinnamtannin B1; 2: trimeric B-type procyanidin C1; 3: dimeric B-type prodelphinidin B1; 4: dimeric B-type propelargonidin.

Within proanthocyanidins, different classes exist depending on their monomeric units. Some common classes are procyanidins, consisting of catechin or epicatechin units, prodelphinidins, which also contain galocatechin or epigallocatechin units, and propelargonidins, also consisting of

afzelechin and epiafzelechin. Depending on the number of subunits and thus their degree of polymerization, they are categorized in oligomers and polymers, both groups occurring in nature.⁴³ Many health benefits are attributed to PACs. Epidemiological studies associated PACs with a lower risk of cardiovascular diseases and cancer.⁴⁴⁻⁴⁶ An antiatherogenic effect was observed through a hypolipidemic effect and a reduction of vascular inflammation. In addition, cocoa procyanidins increased the formation of prostacyclin and decreased the level of leukotrienes, leading to an antithrombotic effect. A positive effect on hypertension and obesity was also observed.^{45,46} Cranberry PACs showed a beneficial effect on periodontitis, an inflammatory disease of tooth gums.⁴⁷ These positive effects are related to different mechanisms of action including their antioxidant properties, specific interactions with different proteins and enzymes, leading to an increased expression of antioxidant enzymes and modulation of pro-inflammatory factors, and epigenetic mechanisms.^{45,46}

7.1.4 Herbal medicinal products and food supplements containing *V. macrocarpon*

An evaluation of cranberry-containing HMPs or food supplements on the market in Belgium was performed. Therefore, the information of the Belgian Center of Pharmacotherapeutical Information, which gives an overview of all registered drugs and Pharmacopendium Plus, containing all food supplements currently on the market, were consulted.^{48,49} This search indicated that there were 41 food supplements but no herbal medicinal products containing cranberry. Nineteen supplements were mono-preparations. From the 22 combination preparations, seven were combined with vitamin C, three with probiotics and in the other supplements, a variety of other plant species was found such as *Acerola*, *Vitis vinifera*, *Vaccinium vitis-idaea*, *Viola tricolor*, *Asparagus officinalis*, and *Salix alba*. Only five supplements explicitly mentioned the use of whole berry extracts and four mentioned the use of juice of *Vaccinium macrocarpon*. For only 28 products, the equivalent amount of PACs was indicated although only two leaflets mentioned the analytical technique used. In addition, for some products, the amount of PACs remained unclear due to a confusing description. Only half of the supplements with a PAC indication will ensure an intake of 36 mg PACs a day. This is the dose, measured by means of the dimethylaminocinnamaldehyde (DMAC) method, for which the French Health Products Safety Agency (AFSSA) has approved the following health claim “helps to reduce the adherence of certain *E. coli* bacteria to the urinary tract walls”.⁵⁰

7.1.5 Methods of analysis

Various methods are described for the analysis of proanthocyanidins going from simple to more sophisticated methods.

Quantification of PACs can be done by gravimetry after isolation of the constituents. To determine the total amount of PACs, different spectrophotometrical methods are available, namely the acid-butanol assay, vanillin assay, and the DMAC assay. The first assay is based on the formation of anthocyanidins, for example, cyanidin, out of PACs in acidic environment. The amount of anthocyanidins formed is measured spectrophotometrically at 545 nm. Although this method is simple and cheap, there are some disadvantages. PACs with a higher degree of polymerization will form more anthocyanidins than those with a lower degree of polymerization and the yield and kinetics of the reaction depend on the nature of the proanthocyanidins. Interference of colored samples, which already contain anthocyanidins, will overestimate the amount of PACs present. In addition, the choice of the standard used will influence the result since for cyanidin the amount of PACs will be underestimated because only a certain percentage of PACs will form cyanidin (procyanidins). The vanillin and DMAC assay both rely on the linking of vanillin or dimethylaminocinnamaldehyde to the flavan-3-ols resulting in a colored reaction product that can be measured spectrophotometrically at 500 and 640 nm, respectively. Different molar extinction coefficients, interference of anthocyanidins from the sample, and time and temperature dependency are the main disadvantages of the vanillin assay. Since reaction products formed with DMAC and PACs are measured at 640 nm, there is no risk of interference of anthocyanidins. An extra benefit of this assay over the vanillin assay is the measurement at room temperature. The formed dye tends to be unstable and since the reaction only occurs at the terminal unit, the presence of PACs with a high degree of polymerization will lead to underestimation.⁵¹⁻⁵³ All aforementioned spectrophotometrical assays do not distinguish different PACs and only estimate the total amount of both A-type and B-type PACs present in the sample.

For the separation of proanthocyanidins, chromatographic methods are used. Normal phase, using silica columns, and also hydrophilic interaction chromatography, using diol and amide stationary phases, are well known to separate PACs based on their degree of polymerization (DP) mostly up to 10, although PACs with a very high DP tend to elute incompletely when silica is used as stationary phase. This technique was used to separate B-type procyanidins in different samples, such as apple,

cacao, birch inner bark and grape seed extracts, and to quantify the proanthocyanidin content of various foods including chocolate, cranberry juice, wine, and apples.^{40,54-63} Besides HPLC, NP-HPTLC was described for the quantification of epicatechin and procyanidin B2 in chocolate and of procyanidin A2 in cranberry.⁶⁴⁻⁶⁵

Since reversed phase chromatography is able to separate oligomers with a good resolution, it is possible to quantify individual PACs.^{59,66-72} Procyanidins B2 and B5 were quantified in *Crataegus* leaves and flowers, proanthocyanidin B3 in *Jatropha macarantha* stems and procyanidins B1 and B2 in grapes, wine, and in different parts of *Vaccinium angustifolium*. During the development of our analytical method for the quantification of A-type dimers and trimers, two articles were published which described the quantification of A and B-type procyanidin dimers and trimers in cranberry, proving that also A and B-type procyanidin oligomers can be clearly separated by reversed phase chromatography.⁷¹⁻⁷² Although oligomers are well separated using reversed phase chromatography, compounds with a higher degree of polymerization tend to elute as one unresolved peak since the number of possible structures increases exponentially with their DP.

Recently, 2-dimensional hydrophilic interaction x reversed phase liquid chromatography was described for the separation of cacao procyanidins. In this way, separation of tetrameric to hexameric isomers was achieved.⁷³⁻⁷⁴

Since commercially available standards of PACs are very limited, isolated but well-characterized standards are used in many studies. Some authors calculated results using catechin or epicatechin as standard, which will lead to under/overestimation due to different response factors of monomers, oligomers, and polymers.

Detection can be done by UV at 280 nm, fluorescence detection, or mass spectrometric detection. These first two detection systems were used for quantification, where fluorescence detection showed higher sensitivity.^{41,52,54,63,67,75} Mass spectrometric detection is extensively used for identification and characterization purposes but is also used for quantification of proanthocyanidins. For this purpose, different types of mass spectrometers and ionization techniques are described including ESI-ion trap-MS, ESI-ion trap MS-MS, ESI-time of flight (TOF)-MS, matrix-assisted laser desorption ionization (MALDI)-TOF-MS, ESI-Triple Quadrupole MS.^{14,42,56,57,59,68,76-80} This latter technique was used for the characterization of proanthocyanidins in *Vaccinium macrocarpon*. A

drawback of mass spectrometric detection is the formation of doubly- and triply-charged ions, starting from tetramers, which can make structure elucidation harder.

Besides mass spectrometry, degradation of PACs in the presence of benzyl mercaptan or phloroglucinol is used to obtain structural information. This reaction cleaves PACs and results into benzylthioethers/benzylthiols and phloroglucinol adducts, obtained from the extension units and free flavan-3-ols from terminal units.^{63,81} Care has to be taken to obtain complete cleavage by using correct reaction conditions. Successive quantification and characterization using reversed phase HPLC analysis allow the calculation of the mean degree of polymerization and the nature and proportion of the subunits present.⁴⁰

Although a lot of research has been carried out on the characterization of cranberry procyanidins, much less has been done in order to quantify A-type procyanidins separately. Recently, a NP-HPTLC-densitometric method, a HPLC-UV method and three LC-MS methods for quantification of PAC A2 were published.^{65,71,72,82,83} All these methods include some imperfections and errors.

Boudesocque et al.⁶⁵ developed and validated an HPTLC method for quantification of PAC A2 in a cranberry extract and, similar to the HPLC-UV method published by Iswaldi et al.⁸² for the quantification of PAC A2 in cranberry syrup, this method will most probably not be applicable for quantification of both dimers and trimers because of its lower sensitivity and specificity. UPLC-MS² was used to quantify PAC A2 in urine samples. This method included a long and complicated sample preparation. Although an internal standard was used, losses could not be fully excluded since quercetin, a monomer, was used, while a dimer was analyzed, and these compounds may not behave similarly. This method was validated by analyzing spiked urine from three different persons in triplicate for all precision and accuracy measurements. No interday experiments were done and the RSD% ranged from 3.85% to 11.13% for one concentration level of urine of one person and had an accuracy of 91.7%. The other two UPLC-MS² methods described the quantification of both dimeric and trimeric procyanidins, in berries of different *Vaccinium spp.* including *Vaccinium macrocarpon* and in commercial cranberry products.⁷¹⁻⁷² Although very useful, these latter two methods were never validated and were found to encounter some problems. For example, one method used procyanidin C1, a B-type trimer to calculate the content of trimeric A-type PACs and methanol/water 20:80 with 0.2% HCl as extraction solvent, which can lead to degradation of procyanidins. The

possibility of matrix effects was not taken into consideration. The other method used solid phase extraction as sample clean-up which can give rise to losses since no internal standard was used. These authors tried to account for matrix effects by using a raspberry extract, which was free of procyanidin A2. Since one cannot expect the matrix of raspberry to be the same as that of cranberry, this is not an ideal way of dealing with matrix effects and can be an additional source of variation or error.

Therefore, a new, fast and sensitive analytical UPLC-MS/MS method for the quantification of the main PACs of interest present in a cranberry dry extract, using standard addition, was developed and validated in this work.

7.2 Development and validation of a UPLC-MS/MS method for the quantification of A-type dimeric and trimeric procyanidins in a cranberry extract

7.2.1 Materials and methods

7.2.1.1 Plant material

Several *Vaccinium macrocarpon* extracts were selected for the development of an analytical method to overcome problems such as peak interference and matrix effects. In total, twelve different extracts were obtained from different manufacturers.

Extract 1 was an extract used in capsules. It was produced by spray drying of the concentrated juice of the cranberry fruits. Extract 2 was obtained from an industrial producer of natural ingredients. Extract 3 was an extract used in capsules. It was a concentrate of the juice from cranberry fruits. Extract 4 was an extract used for the production of capsules. This extract was produced by extraction of the cranberry fruits with ethanol and water. Extract 5 was an extract used in a solid dosage form, namely, tablets and was a concentrated juice extract on a carrier of maltodextrin. Extract 6 was a whole berry-derived extract produced by an industrial natural ingredient manufacturer. Extract 7 was an extract of the fruits of *Vaccinium macrocarpon* and *Vaccinium oxycoccus* produced by a manufacturer specialized in the development of active plant extracts, by extraction of the fruits with water and a carrier of maltodextrin. Extract 8 was obtained from a natural ingredient manufacturer and was a dehydrated 100% cranberry extract. Extract 9 was an extract from the same manufacturer as extract 8. Extract 10 was a whole fruit extract from a manufacturer of value-added ingredients derived from fruits. In addition, cranberry fibers, extract 11, were produced by a food ingredient manufacturer. Later on, extract 12 was obtained from a manufacturer of fruit, vegetables, and medicinal extracts.

7.2.1.2 General experimental procedures

All experiments were carried out using an Acquity Ultra Performance LC with a triple quadrupole mass detector (TQD).

7.2.1.3 Method development

Extraction

The extraction part of the method was developed using extract 3. Different extraction solvent mixtures were evaluated for their extraction power of procyanidin dimers and trimers. The use of water, methanol and acetone, with and without acid has been described for the extraction of procyanidins from various sources, including cranberry. These solvents are mostly only used in binary solvent mixtures, sometimes combined with acid.^{40,42,52,55,67,75,77,79,84,85} In this work, both binary and ternary solvent mixtures of water, methanol and acetone were tested in order to obtain a broader view on the extraction of procyanidins from cranberry. In Table 7.1, the composition of the different test mixtures is shown.

Table 7.1 Overview of different extraction mixtures.

Mixture	Water (%)	Acetone (%)	Methanol (%)
1	10	50	40
2	25	35	40
3	10	35	55
4	40	35	25
5	25	65	10
6	40	50	10
7	25	50	25
8	10	10	80
9	20	20	60
10	0	80	20
11	0	50	50
12	0	20	80
13	20	0	80
14	20	80	0

Chromatographic conditions

Different columns, mobile phases and gradients were tested. Two different columns, available in our research group, were compared: an HSS T3 column (2.1 x 100 mm; 1.8 μ m) and a BEH C18 column (2.1 x 100 mm; 1.8 μ m) from Waters. As mobile phases, water and acetonitrile with 0.1 and 1% formic acid were used. During the course of our investigations, two articles, in which different finished cranberry products and *Vaccinium* species were investigated for their dimeric and trimeric

procyanidin content using UPLC-MS, were published.⁷¹⁻⁷² Therefore, we decided to compare our optimized gradient with the gradient systems used in these publications with minor changes. The first gradient started at 0 min with 5% B; 1 min, 5% B; 8 min, 20% B; 10 min, 40% B; 12 min, 100% B; 14 min, 100% B; 15 min, 5% B; 17 min, 5% B. The second gradient was based on Sanchez-Patan et al.⁷¹ and was as follows 0 min, 2% B; 8.56 min, 16.3% B; 8.86 min, 18.4% B; 11.36 min, 18.4% B; 11.46 min, 99.9% B; 12.86 min, 99.9% B; 12.96 min, 2% B; 14.36 min, 2% B. The third gradient was based on Jungfer et al.⁷² and started at 0 min with 5% B; 1 min, 5% B; 20 min, 18.4% B; 21 min, 100% B; 22 min, 100% B; 23 min, 5% B; 25 min, 5% B. A quick screening was done for all extracts with gradient 1. In order to have a thorough evaluation of the separation, extracts with different profiles were evaluated with all aforementioned parameters.

Mass spectrometric conditions

Tuning was done with a standard of procyanidin A2 in negative ion mode. Source parameters were as follows: capillary voltage 2.5 kV, extractor voltage 3 V, RF lens 0.1 V. The source temperature was set at 150 °C and the desolvation temperature at 450 °C. Desolvation gas flow was 900 L/hr and the cone gas flow was 50 L/hr. The analyzer parameters were 15.0 for LM Resolution1 and HM Resolution1 and the ion energy was set at 1.0 in MS/MS mode. The entrance and exit voltages were 1 and 0.5 V, respectively. LM Resolution2 and HM Resolution2 were set at 14.0 and the ion energy at 1.0. The gain was 1.0. The collision flow was set at 0.1 mL/min.

The extract was analyzed in full scan and single ion monitoring mode to locate the dimers and trimers. For each dimer or trimer, a product ion scan was done at different collision energies to obtain an idea of the fragmentation pattern of the compounds. From these product ion scan spectra, the most abundant product ion and another specific product ion were selected, as quantifier and qualifier, respectively, for the development of the MRM (multiple reaction monitoring) method. For every compound, the optimal cone voltage and collision energy were obtained by evaluating different cone voltages and collision energies.

Matrix effects

In order to evaluate possible matrix effects, a regression line with standard PAC A2 (0.082 – 11.42 µg/mL) and a standard addition regression line of solution containing 1.0 mg/mL sample, in this case extract 3, 4 or 5 and different concentrations of a standard solution of PAC A2 (0.082 – 11.42 µg/mL) were constructed. The slope of both lines was evaluated. In addition, the area of PAC A2 from the sample was subtracted from the area of the standard addition line and plotted. When no matrix effects are present, this latter regression line should be identical to the regression line of PAC A2.

In addition, another experiment was conducted to search for possible matrix effects. Different dilutions of the extracts, i.e. extract 1 (1.6 - 25 mg/mL), 2 (0.2 – 2.0 mg/mL) and 3 (0.075 – 1.8 mg/mL) were made. The areas of PAC A2 and of the different trimeric procyanidins were plotted as a function of their concentration. When matrix effects were present, a deviation of the linear regression line was visible, i.e. when ions were suppressed the area decreased and when ion formation was enhanced the area of the analyte increased.

Final method

A standard solution of procyanidin A2 was prepared by dissolving 5.0 mg in 10.0 mL methanol. From this solution, 4.0 mL was diluted to 100.0 mL with 45% methanol. 125.0 mg of the cranberry extract was weighed and 25.0 mL of the extraction solvent (methanol/acetone/water, 1:2:1) was added. This mixture was sonicated for 30 minutes and filtrated through a Nylon membrane filter (0.45 µm). To 2.5 mL of the test solution, 0, 2.0, 5.0 and 9.0 mL, respectively, of the PAC A2 standard solution was added in a volumetrical flask and diluted to 25.0 mL with 45% methanol.

Separation was performed using an Acquity BEH RP18 column (100 mm x 2.1 mm, 1.8 µm). The solvents were H₂O and acetonitrile, both with 0.1% formic acid. The following two gradients were used: gradient 1: 0-1 min, 5 %B; 1-8 min, 5-20% B; 8-10 min, 20-40% B; 10-12 min, 40-100% B; 12-14 min, 100% B; 14-15 min, 100-5% B; 15-17 min, 5% B; gradient 2: 0-1 min, 5 %B; 1-20 min, 5-18.4% B; 20-21 min, 18.4-100% B; 21-23 min, 100% B; 23-24 min, 100-5% B; 24-26 min, 5% B. For both methods, 5 µL sample was injected, while the column was kept at 40 °C and the sample manager was kept at 4 °C. The detection was done with MRM in the negative ion mode, using the transitions and collision energies/cone voltages as shown in Table 7.2 (see Results).

7.2.1.4 Method validation

The developed method was fully validated according to the ICH guidelines (chapter 4). For the validation of the method, extract 3 was used.

Calibration model

The calibration model of procyanidin A2 was investigated. For this purpose, five concentrations of a stock solution of 0.02 mg/mL of procyanidin A2 were added to a 1/10 dilution of the 100% sample (125 mg) (high concentrations). This was repeated with a 1/10 dilution of the 50% sample (62.5 mg) (low concentrations). The final concentrations of procyanidin A2 ranged from 0.25 µg/mL to 10.3 µg/mL. All solutions were injected twice. The area of procyanidin A2 was plotted as a function of the concentration of procyanidin A2 added to the sample. In this way, the percentage of procyanidin A2 and other dimers were calculated by standard addition. For calculation of the amount of trimers, one should first subtract the area of procyanidin A2 from the sample itself and set up a calibration line with these values. The logarithm of the area of procyanidin A2 after subtraction of the area of procyanidin A2 from the sample itself was plotted as a function of the logarithm of the concentration of PAC A2 added. In this way, trimers are calculated and expressed as PAC A2. Regression analysis was performed using Excel.

Precision

Precision experiments were performed on four independent samples (about 125.0 mg extract) which were analyzed on four different days using standard addition. Standard PAC A2 was added to three of the four dilutions. In addition, different concentration levels were tested, i.e. 62.5 mg (50%) and 187.5 mg (150%) of the sample.

The mean, the standard deviation and the RSD% were calculated for each day and each concentration level. The overall mean, standard deviation and RSD% were calculated for the three days and also for the three concentration levels. The repeatability and intermediate precision were evaluated by an ANOVA single factor. For the repeatability, the “within” mean squares were used to calculate the standard deviation and RSD%. For the intermediate precision, the standard deviation was calculated using the following formula:

$$s = \sqrt{\frac{MS_{between} - MS_{within}}{n_j} + MS_{within}}$$

Before performing the ANOVA single factor, a Cochran test and/or Levene's test was done.

Accuracy

Because of the nature of standard addition, no evaluation of the accuracy by standard addition can be performed. In addition, no blank sample existed and no standards of all trimeric procyanidins of the extract were commercially available.

Specificity

The specificity could not be tested since no blank sample existed and no standards of all trimeric procyanidins of the extract were commercially available. By using the MRM technique, the highest level of specificity possible for the apparatus is used, taking into account that a specific transition for these compounds was selected.

7.2.2 Results and discussion

7.2.2.1 Method development

Extraction

Binary solvent experiments showed that more than 50% of organic modifier was needed to extract procyanidins. Based on these findings, all ternary solvent mixtures were composed of maximum 40% of water. Eight out of nine ternary mixtures gave better extraction results than binary solvent mixtures, except for binary mixture 13 which was as good as ternary mixtures (Figure 7.5). Within the ternary mixtures, there were almost no differences, except for mixture 9, which only gave partial extraction of procyanidins.

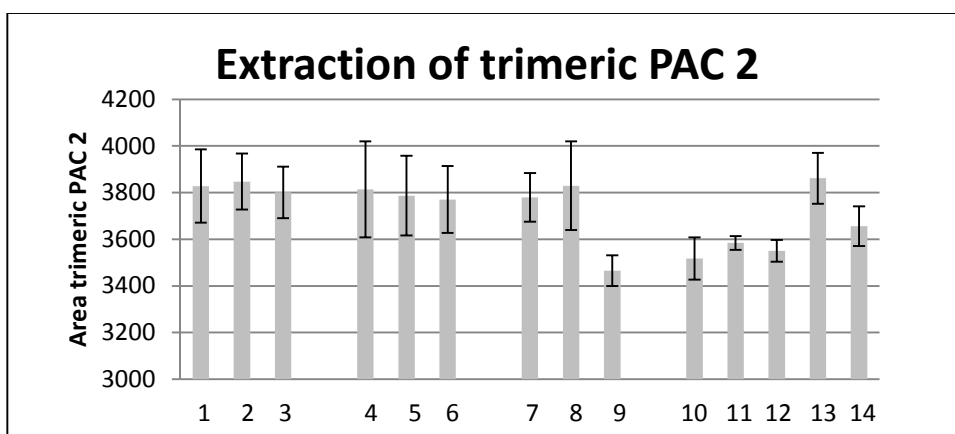
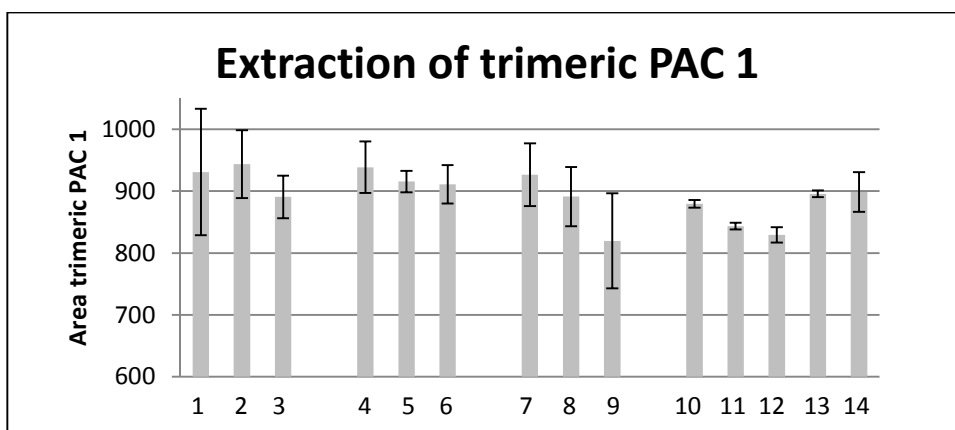
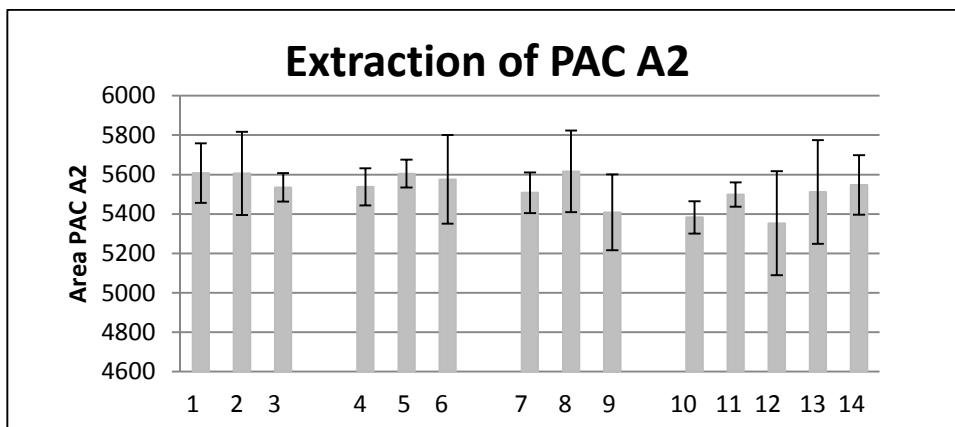


Figure 7.4 Overview of extraction results obtained with water/acetone/methanol mixtures: 1: 10/50/40; 2: 25/35/40; 3: 10/35/55; 4: 40/35/25; 5: 25/65/10; 6: 40/50/10; 7: 25/50/25; 8: 10/10/80; 9: 20/20/60; 10: 0/80/20; 11: 0/50/50; 12: 0/20/80; 13: 20/0/80; 14: 20/80/0.

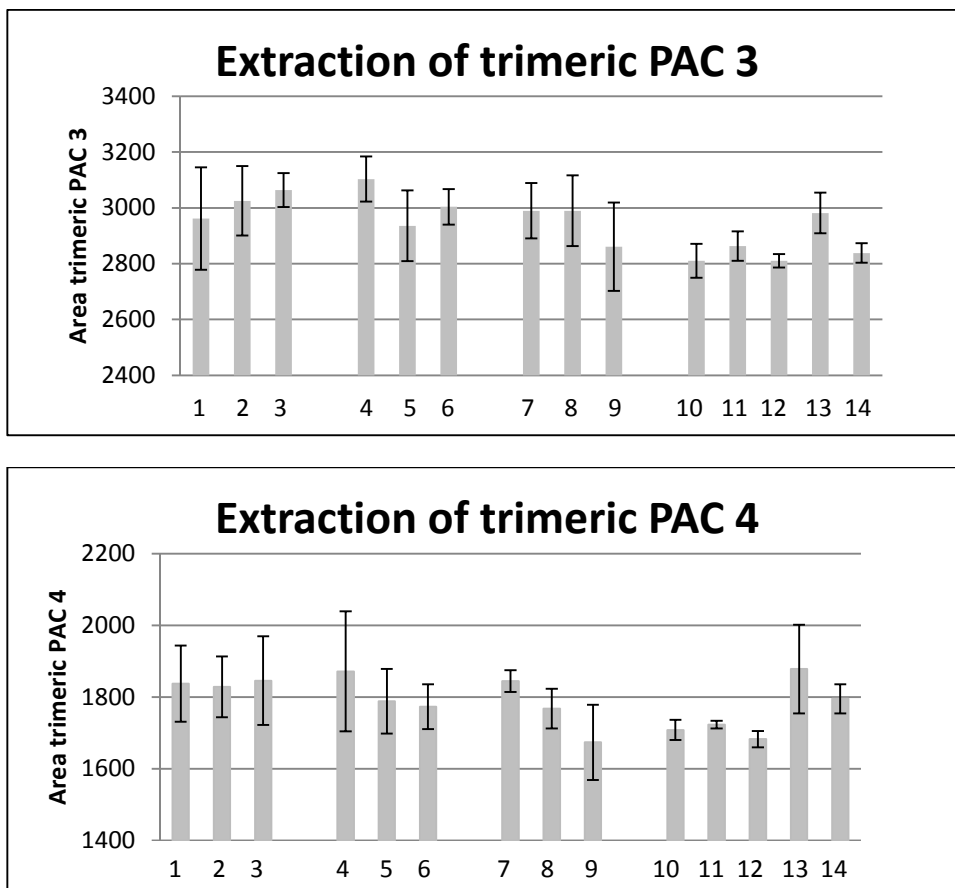


Figure 7.5 continued Overview of extraction results obtained with water/acetone/methanol mixtures: 1: 10/50/40; 2: 25/35/40; 3: 10/35/55; 4: 40/35/25; 5: 25/65/10; 6: 40/50/10; 7: 25/50/25; 8: 10/10/80; 9: 20/20/60; 10: 0/80/20; 11: 0/50/50; 12: 0/20/80; 13: 20/0/80; 14: 20/80/0.

In order to be able to extract procyanidins from different cranberry extracts, a ternary mixture was chosen over a binary mixture because of its robustness. Based on overall extraction yield and variation, mixture 7 was chosen as extraction solvent, which combined a high yield with low variation.

Chromatographic conditions

Preliminary screening of all extracts indicated that only one extract (extract 4) showed a different, more complex chromatographic profile. All other extracts resulted in similar chromatograms showing one dimer and four trimer peaks or even fewer peaks were present. Extract 3 was selected for further method development. All experiments using the HSS T3 column resulted in chromatograms with poor peak shape and a lot of noise, while the BEH C18 column gave a more optimal chromatographic profile (Figure 7.6). Based on these results, the BEH C18 column was selected.

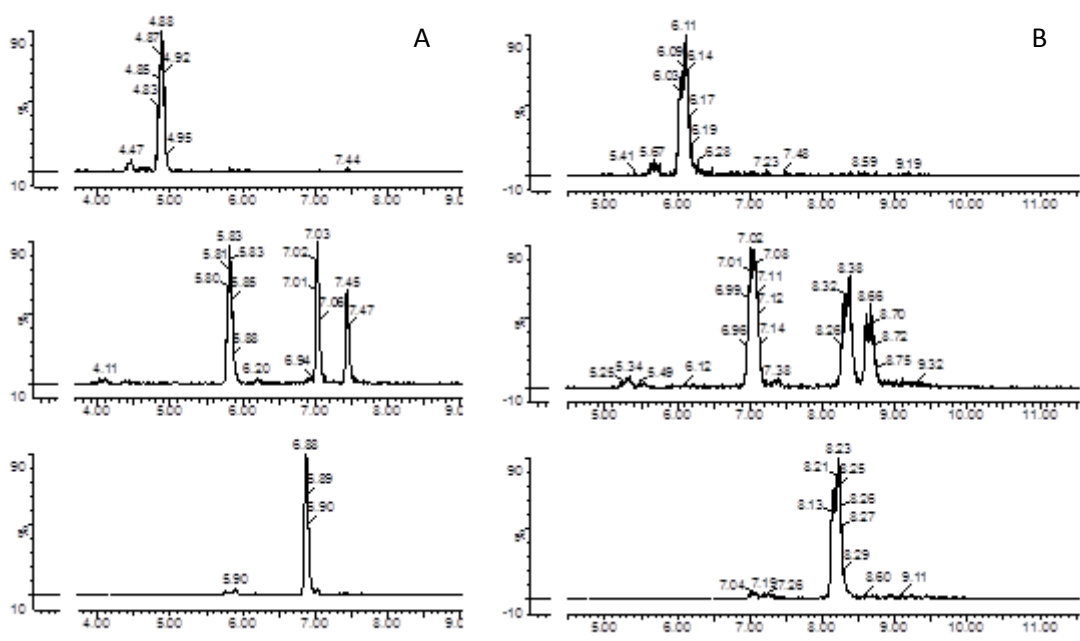


Figure 7.6 Chromatograms of extract 3: A) obtained with the BEH C18 column; B) obtained with the HSS T3 column. In the two upper chromatograms trimers are shown and in the lower chromatogram, a dimer is shown.

Separation of extract 3 was achieved with all three gradients but the separation of the more complex sample 4 was improved using the third gradient (Figure 7.7). As shown in Figure 7.7, the resolution of some peaks was higher than with gradient 1 and 2. Although the separation of cranberry samples with a different profile than the extracts in our screening panel will be better using gradient 3, it was the most time-consuming of all gradients. Gradient 1 was less time-consuming and was able to separate all procyanidins in 90% of the samples. For those above mentioned reasons, both gradient 1 and 3 were validated.

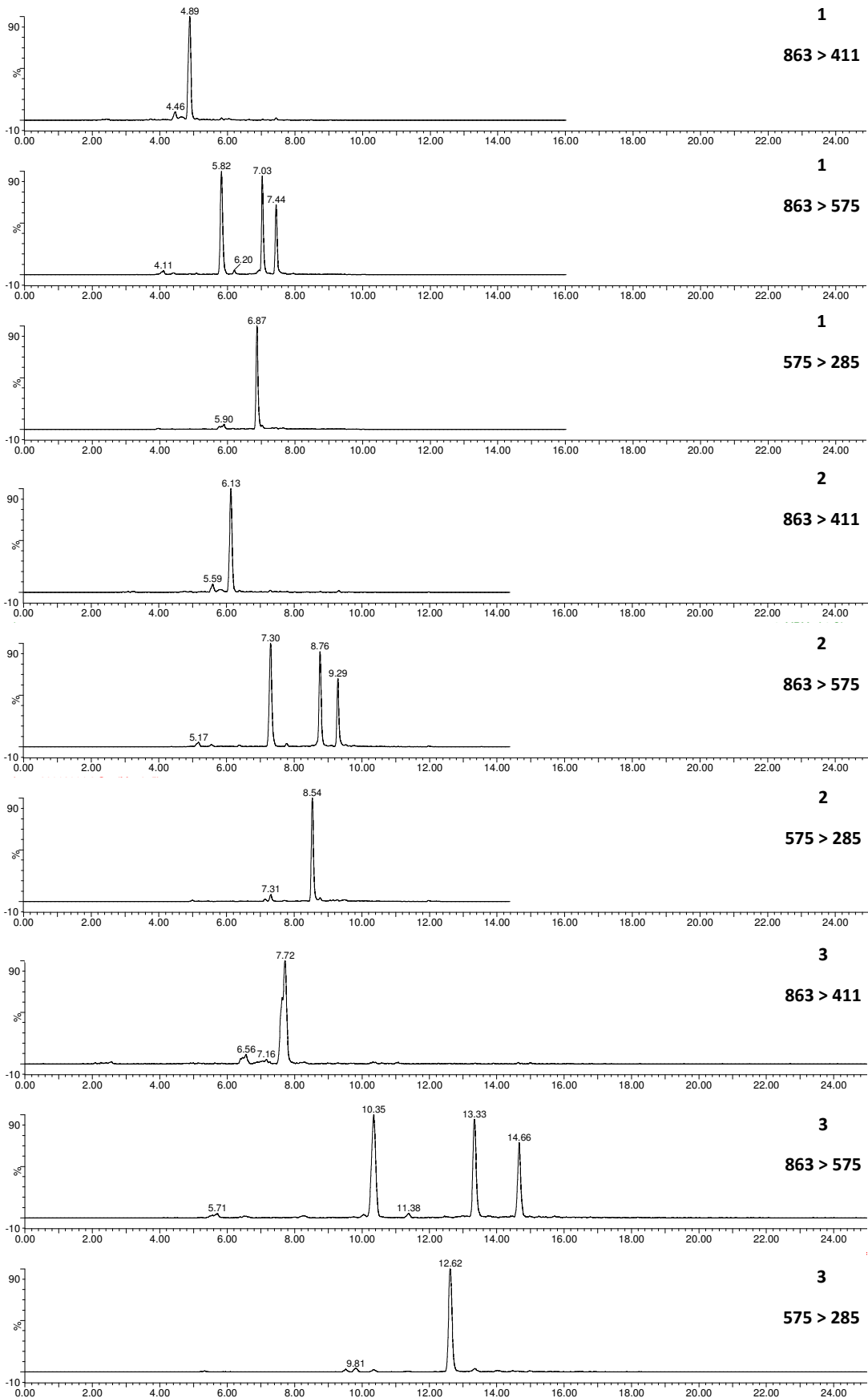


Figure 7.7 Chromatograms of cranberry extract 3 with 1) gradient 1; 2) gradient 2; 3) gradient 3 for trimeric procyanidins (863 > 411 and 863 > 575) and dimeric procyanidins (575 > 285).

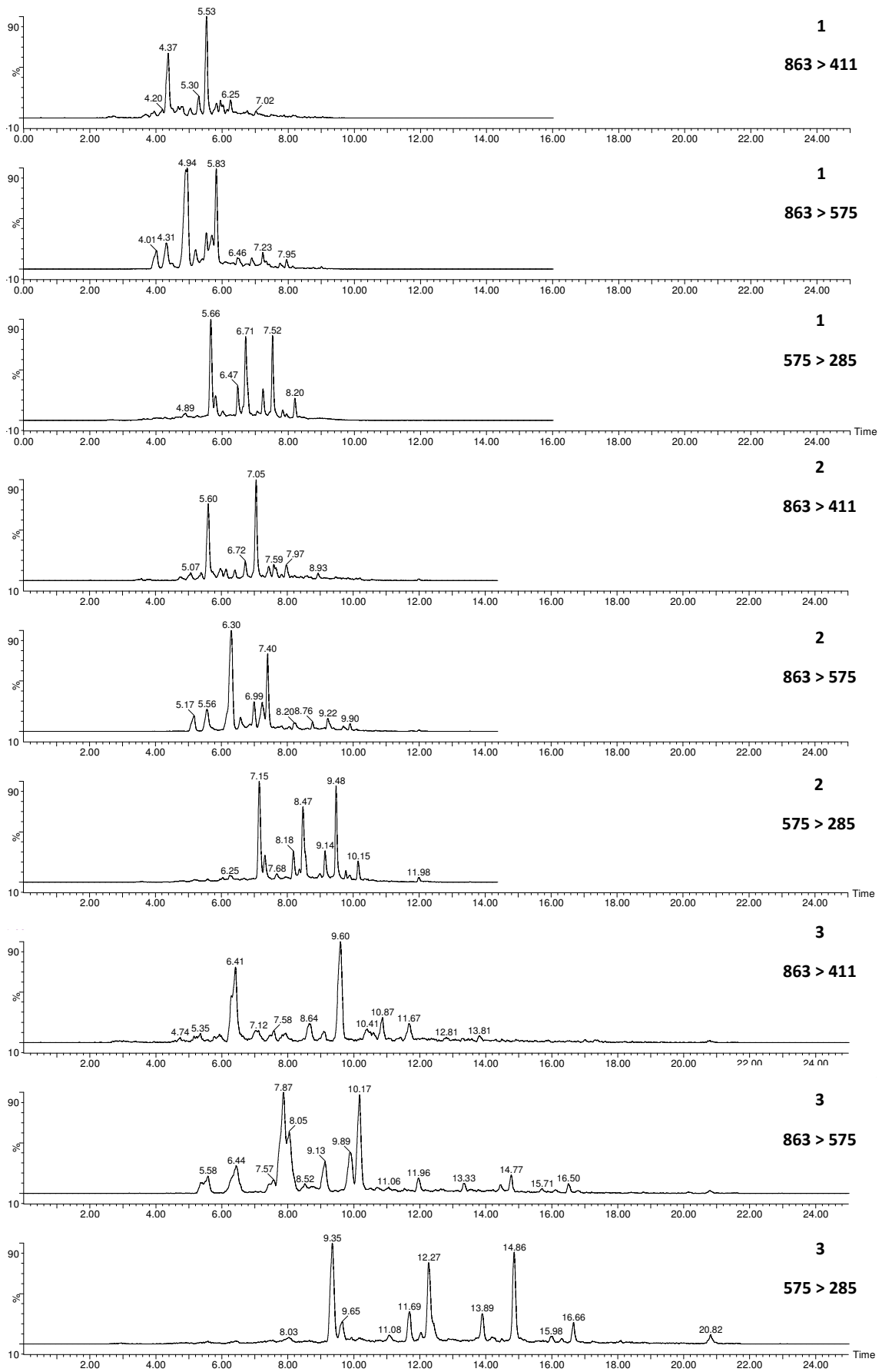


Figure 7.8 Chromatograms of cranberry extract 4 with 1) gradient 1; 2) gradient 2; 3) gradient 3 for trimeric procyanidins (863 > 411 and 863 > 575) and dimeric procyanidins (575 > 285).

The last parameter that was evaluated was the concentration of acid in the mobile phase. Based on literature, concentrations of 0.1% and 1% were compared. For extract 3, there was no influence on the peak shape or resolution, only a small shift in retention time was observed (average of 0.5 min extra). For extract 4, depending on the concentration of acid used, the separation was partially improved and partially reduced as indicated in Figure 7.9. Keeping in mind that procyanidins are not stable in an acidic environment, it should be avoided as much as possible, and a concentration of 0.1% formic acid was preferred.

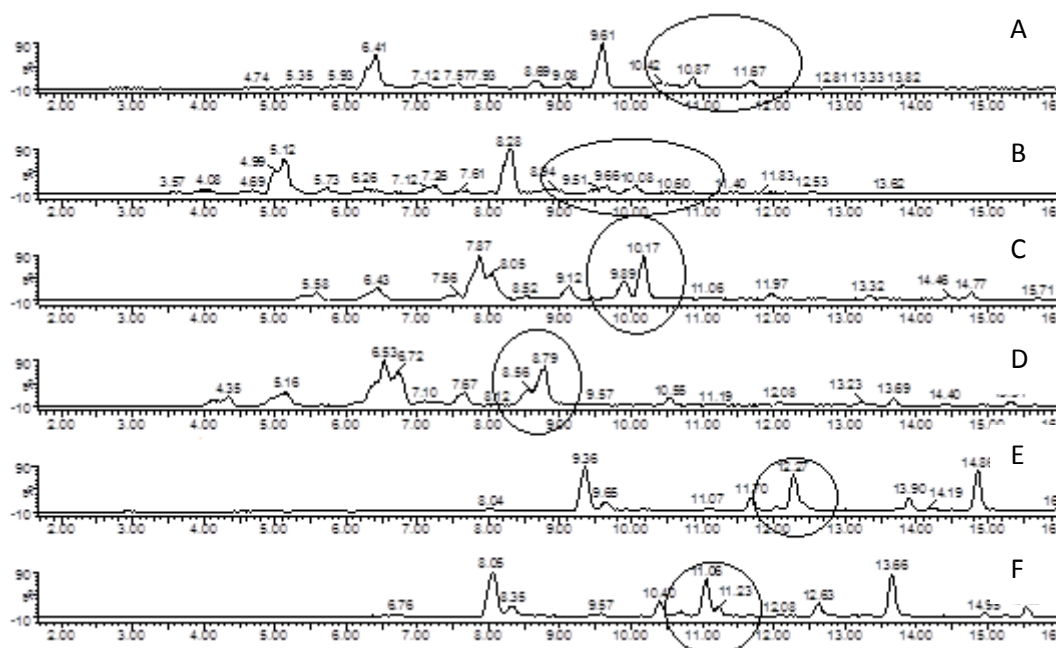


Figure 7.9 Chromatograms using mobile phase with 0.1 (A, C, E) and 1% (B, D, F) formic acid. A and B: MRM 863 \rightarrow 411; C and D: MRM 863 \rightarrow 575; E and F: MRM 575 \rightarrow 285.

In course of the experiments a reference solution of procyanidin A2 seemed to be unstable when the autosampler was kept at room temperature overnight; therefore, the autosampler temperature was set at 4 °C and at this temperature the standard solution remained stable for at least 24 h.

Mass spectrometric conditions

The optimal collision energy and cone voltage for the transitions used for quantitative as well as for qualitative purposes for each compound, giving maximal intensity, are shown in Table 7.2.

Table 7.2 Overview of the optimal collision energy and cone voltage for every transition.

Transition	Optimal collision energy (eV)	Optimal cone voltage (V)
574.9 → 285.2	27	45
574.9 → 449.2	21	50
863.0 → 575.2	24	45
863.0 → 711.2	18	40
863.0 → 411.2	32	50
863.0 → 573.2	22	55

Matrix effects

The regression line of PAC A2, the standard addition line (sample + PAC A2) and the regression line constructed with the difference between sample and standard addition line are plotted in Figures 7.9 and 7.10. For extract 3, the slope of the regression line of PAC A2 is steeper than that of the standard addition line, suggesting matrix effects, more specifically ion suppression. This effect was not seen for extract 4 (not shown) and 5, meaning that there were no matrix effects.

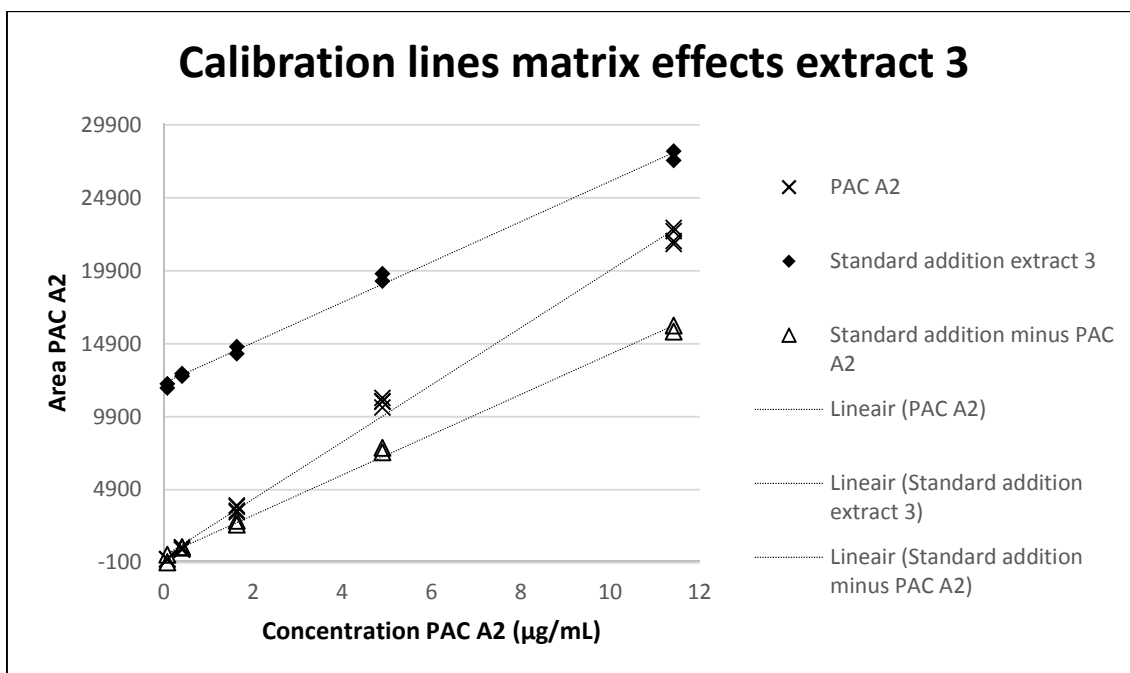


Figure 7.10 Calibration lines for extract 3.

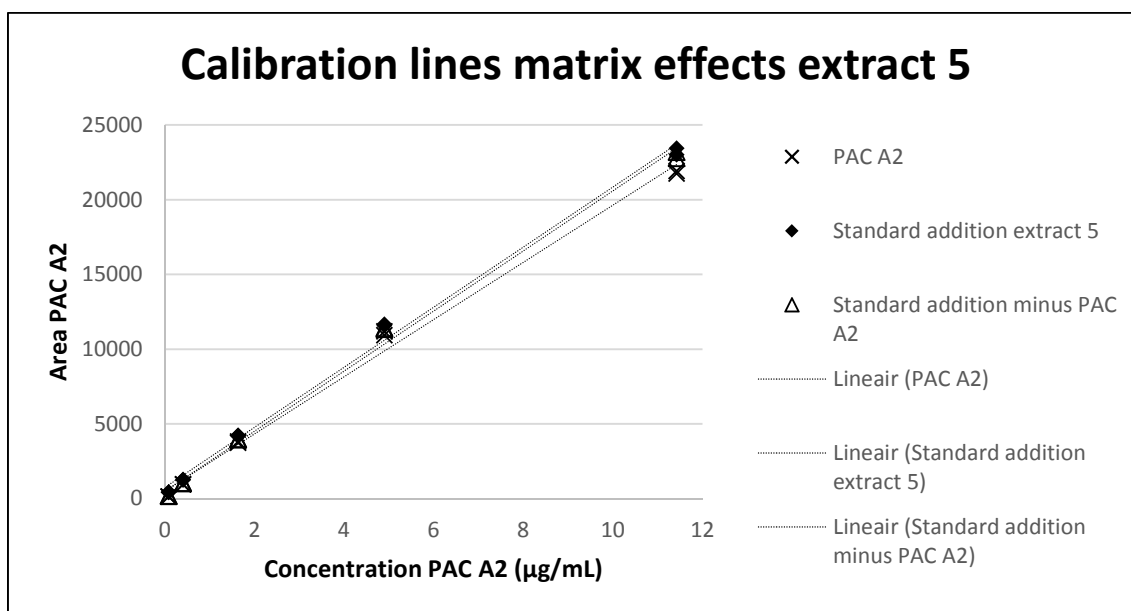


Figure 7.11 Calibration lines for extract 5.

The results of the dilution experiments for dimers of extracts 2 and 3 and for trimers of extract 3 are presented in Figures 7.11, 7.12 and 7.13. This experiment is based on the fact that the matrix effects disappear when the product that causes ion suppression or enhancement has a low concentration but the analyte is still measurable. A drawback of this experiment is that matrix effects are only observed if the targeted constituent reaches a low enough concentration in one of the dilutions, i.e. when this is not the case the matrix effects will be present in all dilutions and this will still result in a linear regression line.

For PAC A2 of all extracts (1-3), the same effect was observed, i.e. the curve became flatter with increasing concentration indicating ion suppression at higher concentrations. This was not seen for trimeric procyanidins, but as already mentioned above, these findings could not rule out possible matrix effects for trimeric procyanidins.

Theoretically, this means that when the dilution of the sample is sufficient, the results will not be influenced by ion suppression. In routine analysis, this implies that before analyzing a sample, multiple dilutions should be made and the dilution where no matrix effect is present should be chosen (for analysis without standard addition). Besides the unpractical aspect, there are other reasons that favor a standard addition method, namely the fact that the sample cannot be endlessly diluted, since next to dimeric procyanidins also the trimeric variants should be measurable. For example, for extract 3, areas of trimers are smaller than for PAC A2, creating a challenge. Bearing in

mind that this test was only performed on three samples, more specifically crude extracts, but no finished products, it was not sure that matrix effects could always be solved by diluting. Hence, it was decided to develop a standard addition method in order to be able to analyze all possible types of cranberry products.

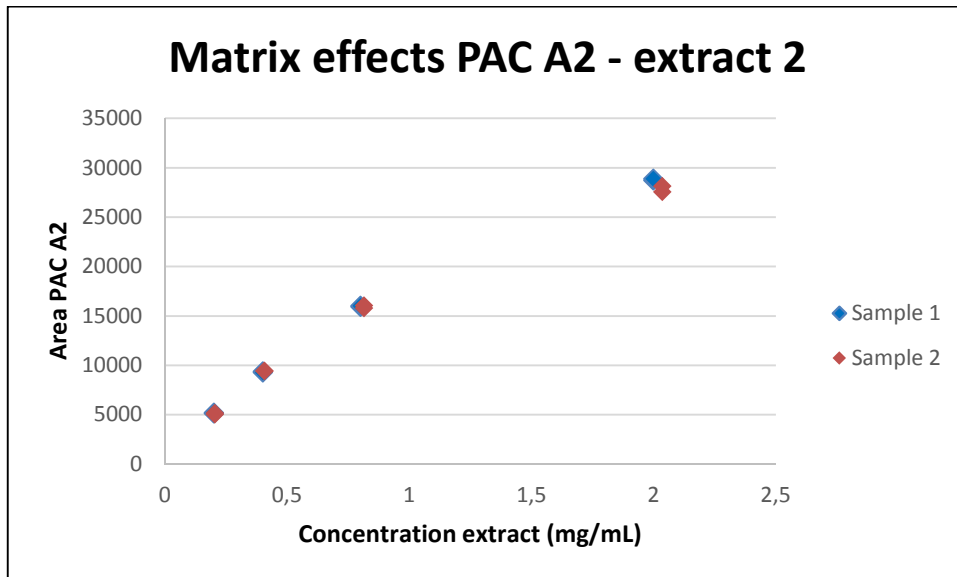


Figure 7.12 Results of the dilution experiment for PAC A2 in extract 2 (in duplicate).

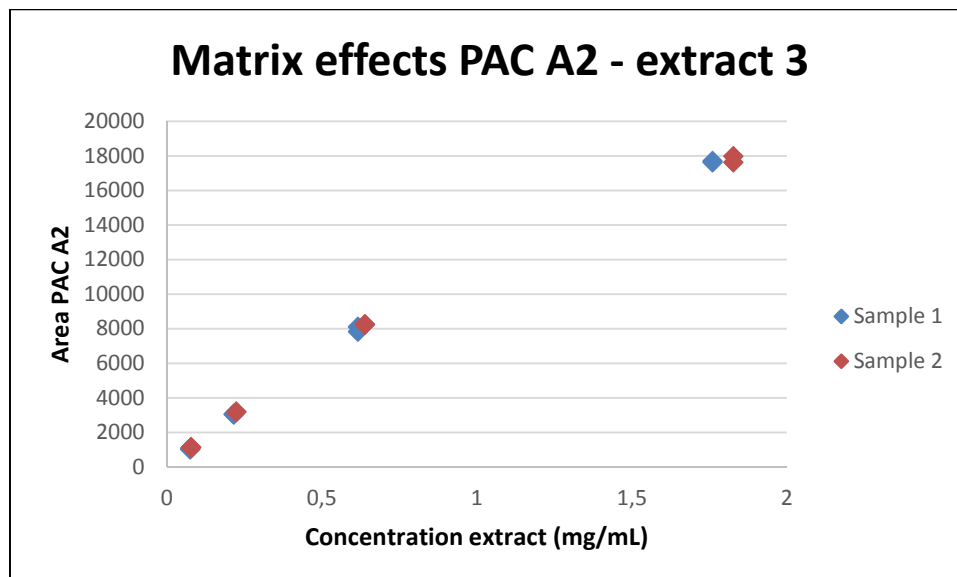


Figure 7.13 Results of the dilution experiment for PAC A2 in extract 3 (in duplicate).

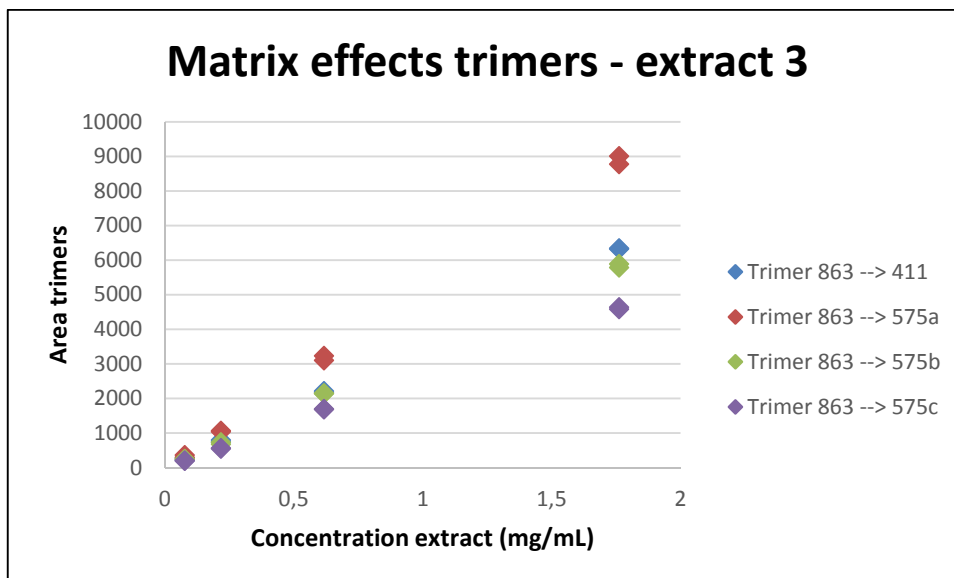


Figure 7.14 Results of the dilution experiment for trimeric procyanidins in extract 3 (in duplo).

7.2.2.2 Final method

Based on the findings during the method development, the following two final methods, i.e. method A and method B, were validated. For both methods, samples were prepared as described in 7.2.1.3. Separation was performed using an Acquity BEH RP18 column (100 mm x 2.1 mm, 1.8 μ m). The solvents were H₂O and acetonitrile, both with 0.1% formic acid. For method A, gradient 1 was used: 0-1 min, 5 %B; 1-8 min, 5-20% B; 8-10 min, 20-40% B; 10-12 min, 40-100% B; 12-14 min, 100% B; 14-15 min, 100-5% B; 15-17 min, 5% B. For method B, gradient 3 was used: 0-1 min, 5 %B; 1-20 min, 5-18.4% B; 20-21 min, 18.4-100% B; 21-23 min, 100% B; 23-24 min, 100-5% B; 24-26 min, 5% B. For both methods, 5 μ L sample was injected, while the column was kept at 40 °C and the sample manager was kept at 4 °C. The detection was done as described in 7.2.1.3.

7.2.2.3 Method validation

Calibration model

A visual inspection of all calibration lines and their corresponding residuals plots showed that these were linear. Figures 7.15 and 7.16 show the standard addition calibration lines for PAC A2 added to 100% sample and 50% sample, obtained with gradient 3. All correlation coefficients were higher than 0.99 and the slopes of the regression lines were significant. All residuals were randomly scattered and showed no heteroscedasticity (Figures 7.17 and 7.18). Since it is not possible to compare the

maximal residual value with the area of the expected value (100% sample) when using standard addition, the maximal residual value was compared with the middle and the lowest point of the standard addition curve in order to obtain a good idea of the deviation. For PAC A2 (dimers) none of the residuals were higher than 7.05 % of the area of the middle or 14.87% of the area of the lowest concentration of PAC A2 of the regression line obtained with gradient 1 and none of the residuals were higher than 6.82% of the area of the middle or 13.96% of the area of the lowest concentration of PAC A2 of the regression line obtained with gradient 3. These values are still acceptable for LC-MS methods.

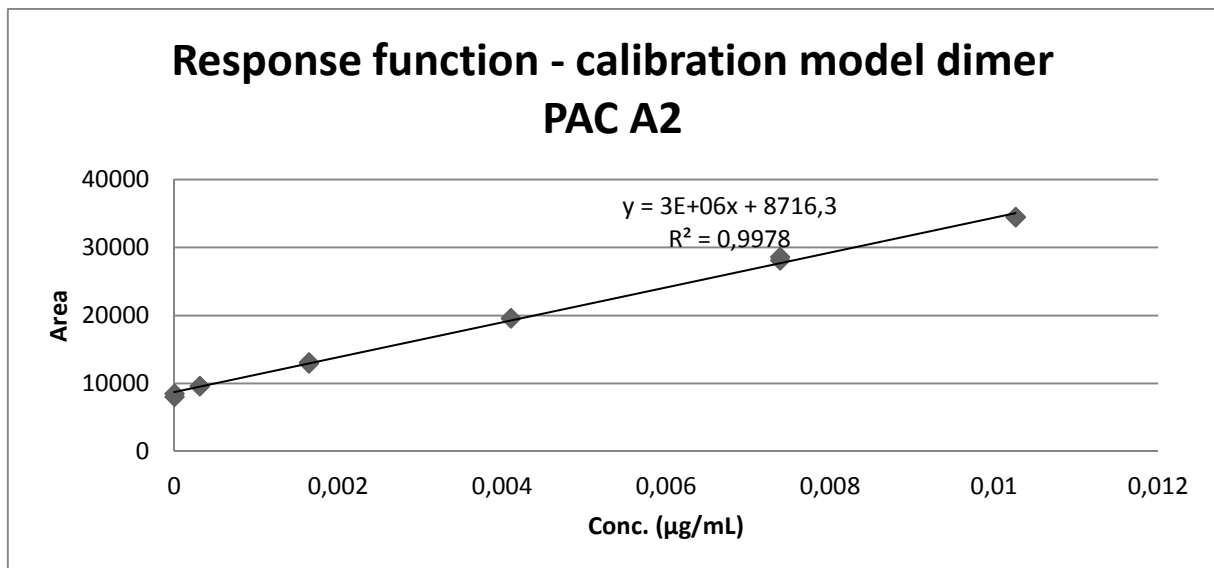


Figure 7.15 Calibration line of PAC A2 in 100% sample.

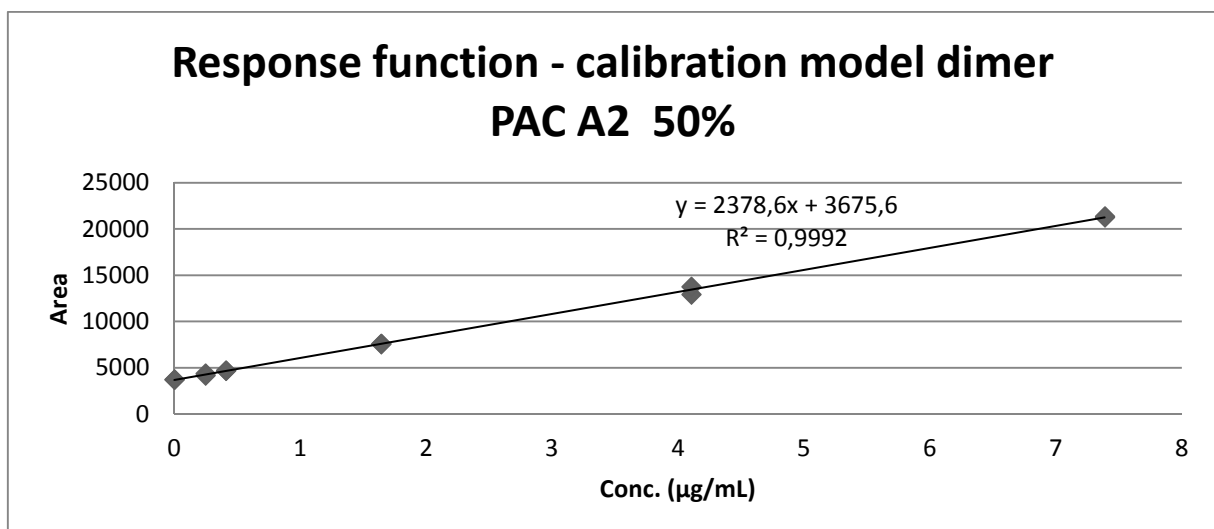


Figure 7.16 Calibration line for PAC A2 in 50% sample.

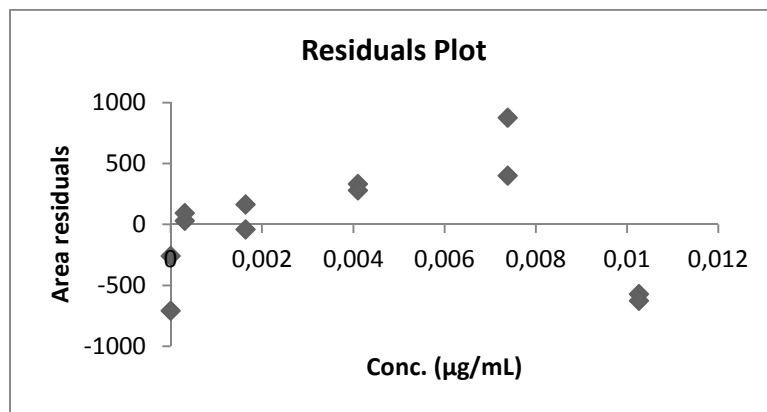


Figure 7.17 Residual plot for PAC A2 – 100% sample.

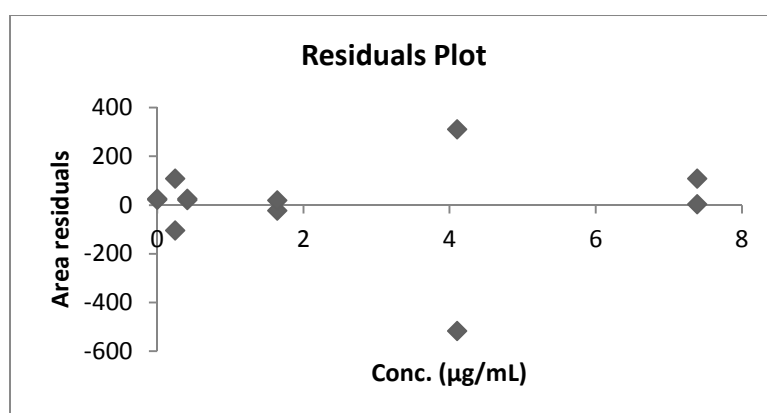


Figure 7.18 Residual plot for PAC A2 – 50% sample.

For the calculation of trimeric procyanidins, calibration lines were constructed by plotting the concentrations and corresponding areas after subtracting the area of PAC A2 in the sample without PAC A2 addition from the area of PAC A2 at the different addition levels. These calibration lines were visually linear and the correlation coefficients were larger than 0.99. Residual values were 13.30% and 6.88% calculated with reference to the middle concentration level of the regression line and 97.03% and 82.86% calculated with reference to the lowest concentration level obtained with gradient 1 for standard addition with 50% and 100% of the sample, respectively. For gradient 3, the residual values were 13.20% and 6.70% calculated with reference to the middle concentration level of the regression line and 112.32% and 56.83% calculated with reference to the lowest concentration level for standard addition with 50% and 100% of the sample, respectively. These high values obtained when the residuals were calculated with reference to the lowest concentration level could be explained by the large range of concentrations and thus the large range of areas covered by the

regression lines. For trimers, a linear model could be adopted and was used to calculate the trimer content during precision experiments. Unfortunately, this gave unacceptable RSD% values as high as 34.04% for one trimer and 24.52% for the total trimer content on the same day. Therefore, different transformations were evaluated such as $1/x$, $1/x^2$, and a logarithmic transformation. Although all transformations resulted in visual linear regression lines, a $1/x^2$ transformation resulted in lower correlation coefficients, sometimes lower than 0.99. The lowest residuals were obtained by a logarithmic transformation (Figures 7.19 and 7.20) with the maximum residual being 3.46% of the lowest concentration of the regression line, as shown in Figures 7.21 and 7.22. Therefore, this transformation was chosen for further calculations, which turned out to give acceptable precision results as will be discussed later.

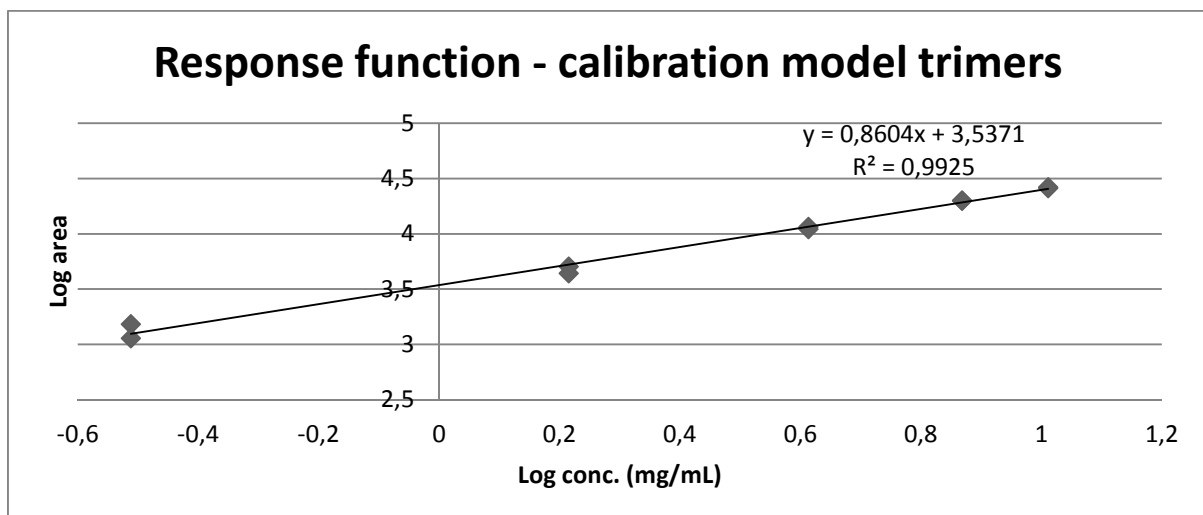


Figure 7.19 Calibration line for trimers in 100% sample.

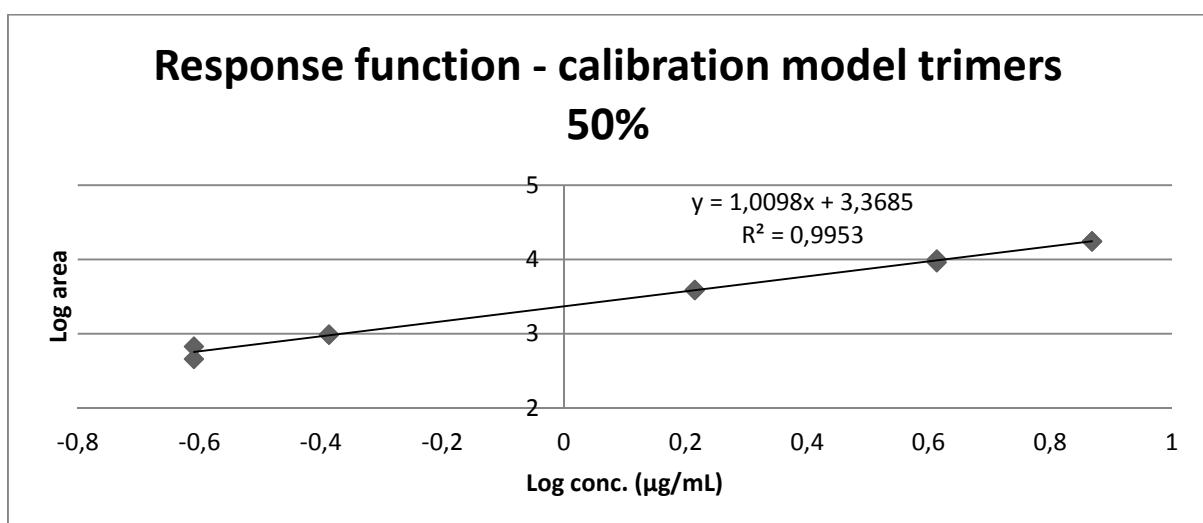


Figure 7.20 Calibration line for trimers in 50% sample.

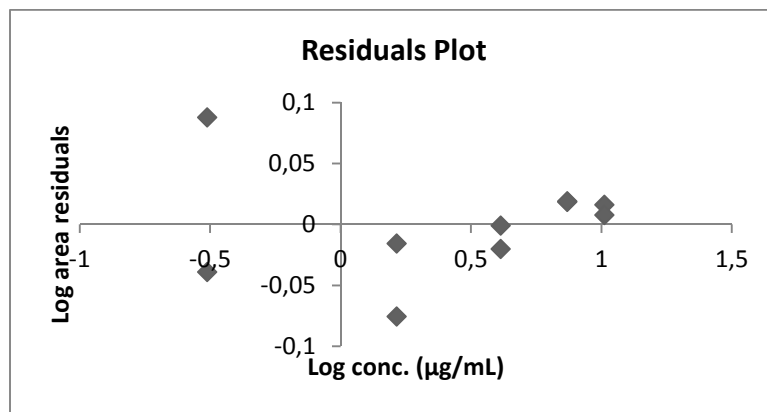


Figure 7.21 Residual plot for PAC A2 – 50% sample.

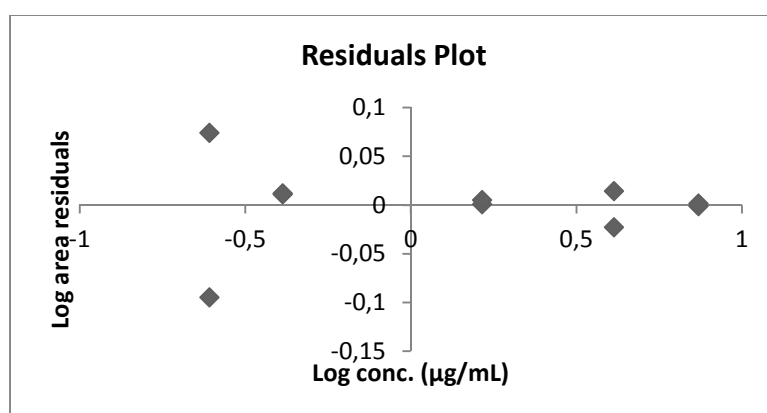


Figure 7.22 Residual plot for PAC A2 – 50% sample.

Precision

Procyanidin A2 – dimeric procyanidins

The results for both gradients 1 and 3 are shown in Table 7.3. In case of different days, the calculated Cochran values were smaller than the critical C-value, implying that the variances were not significantly different and an ANOVA single factor could be carried out. This latter test showed for both gradients 1 and 3 a calculated F-value that was higher than the critical F-value, meaning that the results between the days were significantly different.

Table 7.3 Results of precision and intermediate precision experiments for PAC A2 (%) using gradient 1 and 3.

	Gradient 1				Gradient 3			
	<x>	s	RSD%		<x>	s	RSD%	
Day 1 – 100%	0.763	0.011	1.40	RSD _{within} = 1.84	0.580	0.011	1.75	RSD _{within} = 2.77
Day 2 – 100%	0.7216	0.0089	1.23	RSD _{between} = 3.53	0.638	0.022	3.49	RSD _{between} = 4.86
Day 3 – 100%	0.7612	0.0096	1.26	RSD _{Horwitz} = 4.18	0.627	0.022	3.52	RSD _{Horwitz} = 4.30
Day 4 – 100%	0.721	0.021	2.97	RSD _{max} = 2.79	0.6287	0.0094	1.50	RSD _{max} = 2.87
Overall days	0.742	0.024	3.26	F _{critical} = 3.49 F _{calculated} = 11.73	0.618	0.028	4.52	F _{critical} = 3.49 F _{calculated} = 9.28
Concentration level 50%	0.715	0.019	2.68	RSD _{within} = 2.49 RSD _{between} = 3.72	0.604	0.013	2.13	RSD _{within} = 2.98 RSD _{between} = 4.28
Concentration level 150%	0.718	0.030	4.14	RSD _{Horwitz} = 4.19 RSD _{max} = 2.79	0.617	0.026	4.21	RSD _{Horwitz} = 4.30 RSD _{max} = 2.87
Overall levels	0.733	0.026	3.58	F _{critical} = 2.77 F _{calculated} = 5.93	0.616	0.025	4.13	F _{critical} = 2.77 F _{calculated} = 5.26

The RSD_{between} for gradients 1 and 3 were 3.53% and 4.86%, respectively, and were higher than the calculated maximum RSD%, based on RSD_{Horwitz}.

In case of the different concentration levels, the calculated C-value was smaller than the critical C-value. The ANOVA single factor test showed for both gradients 1 and 3 a significant difference for results on the concentration levels since the calculated F-value was higher than the critical F-value. RSD_{between} values were 3.72% and 4.28%, respectively, and also higher than the calculated maximum RSD%.

Since RSD_{between} values for different days and on different concentrations levels were still smaller than 5%, which is generally accepted in complex analyses, the method can still be considered as precise.

The graphical representation of the results (Figure 7.23) revealed that no trend could be observed between the results obtained at different concentration levels, proving the completeness of extraction. The overall mean content of PAC A2 was 0.73% and 0.62% for gradient 1 and 3, respectively. This difference can be explained by the peak shape of standard PAC A2, which had an additional small peak attached to the main peak when using gradient 1 and therefore a split peak integration was done, which can lead to a slightly smaller area.

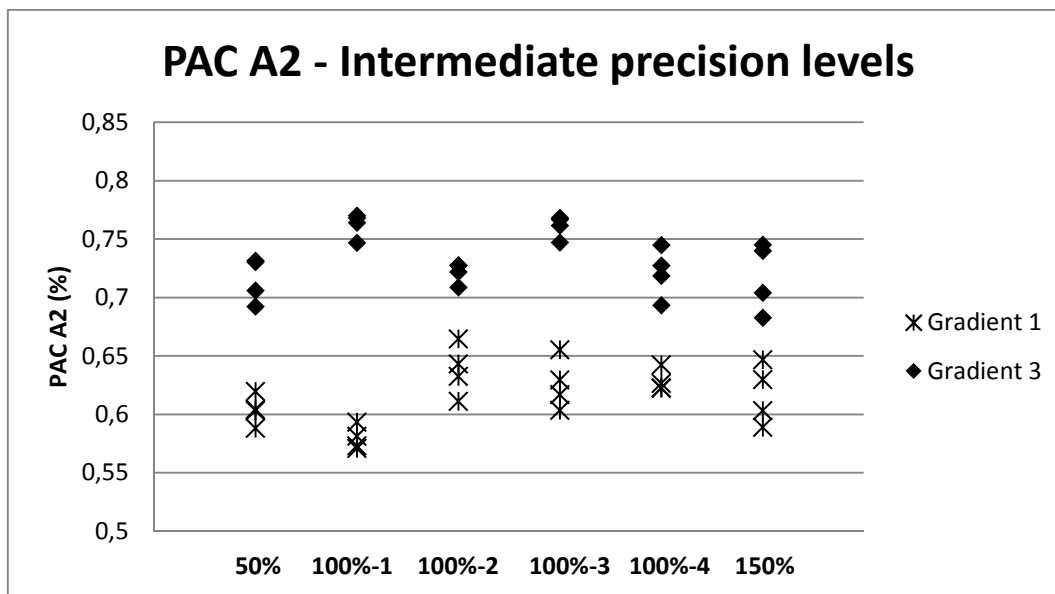


Figure 7.23 Precision and intermediate precision results for PAC A2.

Trimeric procyanidins

The results for both gradients 1 and 3 are shown in Tables 7.4 and 7.5. Calculations were done for all trimeric procyanidins separately and for the total content of trimeric PACs. For gradient 3, the calculated Cochran values were smaller than the critical C-value, implying that the variances obtained on different days were not significantly different and an ANOVA single factor could be carried out. Calculated Cochran values obtained with gradient 1 were much higher than the critical value. This would imply that no ANOVA single factor test could be carried out since the different variances were not considered equal. Since it was important to have an estimation of the “between variation” and bearing in mind that a Cochran’s test assumes normally distributed values which was hard to achieve for only four results per day, another test was done to assess the equality of the variances. A Levene’s test was performed using SPSS. All variances obtained with gradient 1 were considered equal according to this latter test and an ANOVA single factor test was performed.

Table 7.4 Results of precision and intermediate precision experiments for trimeric procyanidins (%) using gradient 1.

Gradient 1						
		Trimer 1 (%)	Trimer 2 (%)	Trimer 3 (%)	Trimer 4 (%)	Total trimers (%)
Day 1 – 100%	<x>	0.173	0.266	0.180	0.136	0.75
	s	0.025	0.036	0.027	0.020	0.11
	RSD%	14.67	13.50	14.75	14.64	14.24
Day 2 – 100%	<x>	0.1684	0.258	0.179	0.1348	0.7401
	s	0.0080	0.013	0.010	0.0073	0.0038
	RSD%	4.77	4.92	5.70	5.38	5.12
Day 3 – 100%	<x>	0.1735	0.2659	0.1821	0.1371	0.759
	s	0.0049	0.0076	0.0043	0.0036	0.020
	RSD%	2.84	2.86	2.36	2.60	2.66
Day 4 – 100%	<x>	0.1482	0.2245	0.1533	0.1252	0.6512
	s	0.0037	0.0034	0.0035	0.0043	0.0093
	RSD%	2.48	1.50	2.25	3.46	1.43
Overall days	<x>	0.166	0.254	0.174	0.133	0.726
	s	0.016	0.025	0.018	0.011	0.069
	RSD%	9.77	9.76	10.23	8.23	9.48
Intermediate precision: inter day	F _{critical}	3.49				
	F _{calculated}	3.05	4.08	3.50	1.00	3.04
	RSD _{within}	8.23	7.68	8.35	8.23	7.99
	RSD _{between}	10.12	10.22	10.64	8.23	9.82
	RSD _{Horwitz}	5.24	4.92	5.21	5.42	4.20
	RSD _{max}	3.50	3.28	3.47	3.61	2.80
Concentration level 50%	<x>	0.172	0.268	0.175	0.132	0.747
	s	0.012	0.014	0.014	0.011	0.050
	RSD%	7.20	5.29	7.93	7.94	6.79
Concentration level 150%	<x>	0.203	0.308	0.215	0.162	0.888
	s	0.018	0.024	0.019	0.016	0.077
	RSD%	8.94	7.80	8.65	10.03	8.66
Overall levels	<x>	0.173	0.265	0.181	0.138	0.757
	s	0.021	0.030	0.023	0.016	0.089
	RSD%	12.00	11.38	12.61	11.49	11.72
Intermediate precision: inter level	F _{critical}	2.77				
	F _{calculated}	6.09	7.34	6.79	4.50	6.28
	RSD _{within}	8.27	7.38	8.39	8.66	8.00
	RSD _{between}	12.46	11.87	13.12	11.86	12.18
	RSD _{Horwitz}	5.21	4.89	5.18	5.39	4.17
	RSD _{max}	3.47	3.26	3.45	3.59	2.78

Table 7.5 Results of precision and intermediate precision experiments for trimeric procyanidins using gradient 3.

Gradient 3						
		Trimer 1 (%)	Trimer 2 (%)	Trimer 3 (%)	Trimer 4(%)	Total trimers (%)
Day 1 – 100%	<x>	0.1585	0.2216	0.1546	0.1169	0.6517
	s	0.0073	0.0078	0.0069	0.0052	0.0027
	RSD%	4.60	3.53	4.47	4.41	4.12
Day 2 – 100%	<x>	0.1578	0.2285	0.1630	0.1202	0.6696
	s	0.0082	0.0104	0.0087	0.0066	0.0335
	RSD%	5.20	4.55	5.33	5.47	5.01
Day 3 – 100%	<x>	0.1579	0.2286	0.1630	0.1202	0.6697
	s	0.0072	0.0087	0.0084	0.0065	0.0304
	RSD%	4.55	3.82	5.12	5.42	4.54
Day 4 – 100%	<x>	0.1676	0.2359	0.1707	0.1263	0.700
	s	0.0030	0.0027	0.0046	0.0042	0.014
	RSD%	1.80	1.13	2.72	3.36	2.02
Overall days	<x>	0.1605	0.2286	0.1628	0.1209	0.673
	s	0.0074	0.0088	0.0088	0.0062	0.030
	RSD%	4.59	3.85	5.41	5.12	4.51
Intermediate precision: inter day	F _{critical}	3.49				
	F _{calculated}	1.99	2.14	3.22	1.88	2.21
	RSD _{within}	4.19	3.48	4.50	4.72	4.05
	RSD _{between}	4.68	3.94	5.61	5.21	4.62
	RSD _{Horwitz}	5.27	4.99	5.26	5.50	4.25
	RSD _{max}	3.51	3.33	3.50	3.66	2.83
Concentration level 50%	<x>	0.155	0.220	0.1610	0.1259	0.663
	s	0.010	0.013	0.0089	0.0059	0.040
	RSD%	6.44	6.03	5.52	4.66	5.96
Concentration level 150%	<x>	0.173	0.247	0.178	0.134	0.732
	s	0.018	0.022	0.017	0.016	0.074
	RSD%	10.53	9.08	9.74	11.62	10.04
Overall levels	<x>	0.162	0.230	0.165	0.1240	0.681
	s	0.011	0.014	0.012	0.0093	0.045
	RSD%	6.79	6.21	7.09	7.52	6.66
Intermediate precision: inter level	F _{critical}	2.77				
	F _{calculated}	1.84	2.47	2.75	2.28	2.11
	RSD _{within}	6.24	5.41	6.03	6.65	5.97
	RSD _{between}	6.87	6.32	7.23	7.65	6.75
	RSD _{Horwitz}	5.26	4.99	5.25	5.48	4.24
	RSD _{max}	3.51	3.33	3.50	3.65	2.83

For gradient 3, the factor “day” had no significant effect on the results since all calculated F-values were lower than the critical F-value. Although all RSD_{between} values were higher than the maximal RSD, the highest RSD_{between} was 5.61% which is acceptable for an LC-MS method.

Results obtained with gradient 1 showed calculated F-values that were higher than the critical F-value for trimer 2 and trimer 3. For all other trimers and for the total content, no effect of the factor day was observed. All RSD_{between} values were twice as high as for gradient 3 with the highest one being 10.64%.

In case of different concentration levels, the calculated C-values were smaller than the critical C-value for gradient 1, except for trimer 2. For gradient 3, all calculated C-values, except for trimer 3, were slightly higher than the critical C-values. Because of the aforementioned reasons, a Levene’s test was executed and this test did not confirm unequal variances. The subsequently performed ANOVA single factor test did not show a significant effect of concentration levels on the results for gradient 3. This was confirmed by the graphically overlapping results (Figure 7.24). The opposite was found for gradient 1, for which all calculated F-values were higher than the critical F-value. For both gradients, as for the different days, the RSD_{between} was higher than the calculated maximum RSD% and the highest RSD_{between} values were 7.65% (gradient 3) and 13.12% (gradient 1).

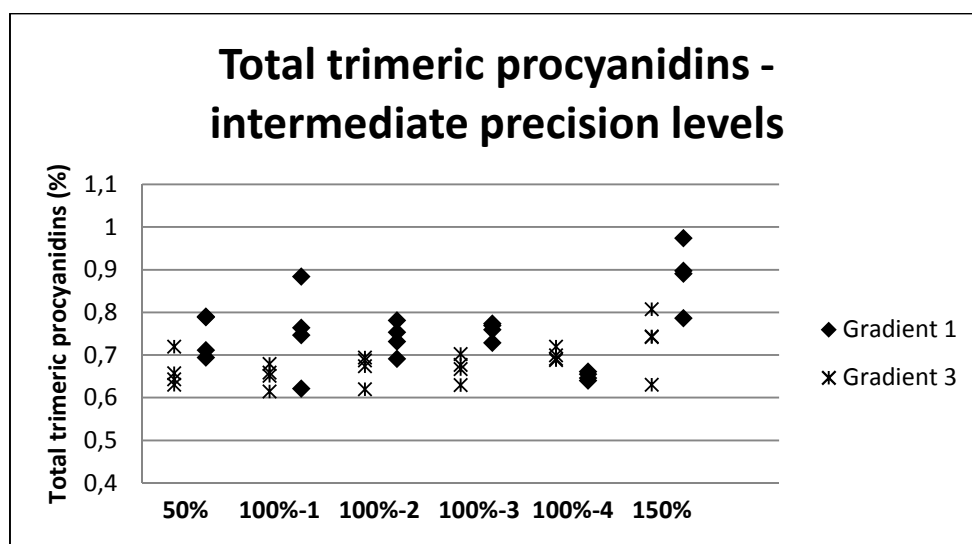


Figure 7.24 Precision and intermediate precision results for trimeric PACs.

Although an RSD% up to 15% is acceptable for LC-MS, this difference in variation between the two methods/gradients could not be ignored. Therefore, method 3 was selected as the best method.

7.2.3 Conclusions

A standard addition LC-MS² method for the simultaneous quantification of A-type dimers and trimers in cranberry extracts was developed and validated. A linear calibration model could be adopted for dimers and, after logarithmic transformation, for trimers. The maximal interday and interconcentration precision was found to be 4.86% and 4.28% for PAC A2 5.61% and 7.65% for trimeric PACs, which are all acceptable values for an analytical method using LC-MS².

7.3 Comparison of twelve cranberry-containing extracts using different commonly used analytical techniques

7.3.1 Materials and methods

7.3.1.1 Plant material

The extracts described under 7.2.1.1 were analyzed.

7.3.1.2 General experimental procedures

The instruments used for the experiments were an Acquity Ultra Performance LC with a triple quadrupole mass detector, a Lambda 35 double beam UV-VIS spectrophotometer (Perkin Elmer), an Infinite 200 96-well plate reader and a HPLC-DAD system from Beckmann.

The device used for ultrasonication was an ultrasonic cleaner Branson MHT 3510.

7.3.1.3 Analysis

Twelve different crude cranberry extracts were analyzed in triplicate (except profiling) by different analytical techniques. In this way, the total procyanidin content, the content of A-type procyanidin dimers and trimers, and a profile of procyanidins were determined and compared with each other.

LC-MS analysis

The concentration of A-type dimers and trimers was determined with the validated LC-MS method described above (7.2.2.2).

Butanol-HCl assay

The spectrophotometric method described in the Eur. Ph. for Hawthorn berries (*Crateagi fructus*), also known as the butanol-HCl assay, was used to quantify the procyanidin content expressed as cyanidin chloride.⁸⁶ Briefly, the sample was weighed in a round bottom flask and 30 mL of 70% ethanol (v/v) was added. This mixture was refluxed for 30 min and filtered. The filtrate was collected and 20 mL of 70% ethanol was added to the residue. This latter solution was refluxed for 15 min. This solution was also filtered and both filtrates were combined. 10 mL distilled water and 15 mL of an

HCl solution (25%) were added and the mixture was refluxed for 80 min. The solution was filtered and diluted to 250.0 mL. Depending on the sample, a given volume was concentrated under reduced pressure to about 3 mL. This 3 mL was extracted three times with 15 mL butanol and organic phases were combined and diluted to 100.0 mL. From this solution, the absorbance was measured at 555 nm using a double beam UV-VIS spectrophotometer.

DMAC assay

Procyanidins were quantified with the DMAC colorimetric method as described by Prior et al.⁵³ Briefly, extracts were weighed and extraction solvent (40% of the volume of the measuring flask) (acetone/water/acetic acid 75:24.5:0.5) was added. The samples were vortexed for 30 s and sonicated for 30 min. After this, all samples were stirred for 1 h and centrifuged at 785 g (2000 rpm) for 10 min. Dilutions of the supernatant were made using 73% ethanol as dilution solvent. A stock solution of standard PAC A2 (100 µg/mL) was prepared in ethanol 91% and dilutions, ranging from 10 to 50 µg/mL, were made with the same solvent. 70 µL of a 0.1% DMAC solution, prepared freshly each day in acidified ethanol, was mixed with either 210 µL dilution solvent, standard solution or dilutions of the samples in a 96-well plate. The plate was read (640 nm) every minute during 25 min at 25 °C using an Infinite 200 well plate reader. In addition, the method was adapted and samples were processed sample by sample. To this aim, 300 µL of a 0.1% DMAC solution was mixed with either 900 µL of the dilution solution, standard solution or sample dilution in a test tube and shortly vortexed. The absorption (640 nm) of the mixture was then analyzed every minute, during 50 min, using a UV-VIS double beam spectrophotometer. Results were calculated using a calibration line constructed with standard dilutions of PAC A2.

Normal phase chromatographic profile

A profile of the procyanidins present in the extracts was created by normal phase HPLC-UV (Beckmann). This method was partially based on the analysis described by Romani et al.⁸⁷ To 100.0 - 1000.0 mg sample (depending on the sample), 2 parts of absolute ethanol were added and the solution was sonicated for 30 min. Thereafter, 8 parts of dichloromethane were added and the solution was homogenized and filtered (0.45 µm). Samples were analyzed on a Purospher Star Si-column (250 x 4 mm, 5µm). Mobile phase A was methanol/formic acid/water (97:2:1) and mobile

phase B dichloromethane/methanol/formic acid (83:15:2). The following gradient was used: 0 min – 100% B; 20 minutes – 89% B; 30 min – 100% B; 40 min – 100% B. 15 µL of each sample was injected. The flow rate was set at 0.75 mL/min and detection was performed at 280 nm. Catechin, epicatechin, gallic acid and procyanidins B1 and B2 were used as standards.

Thin layer chromatography

The NP-HPTLC method as described by Boudesocque et al.⁶⁵ was used to quantify the PAC A2 content in all cranberry extracts. Different PAC A2 standard solutions (0.07, 0.1, 0.3, and 0.5 mg/mL) and extracts dissolved in methanol (70 mg/mL) were applied to NP-HPTLC plates by an Automatic TLC sampler and developed with CH₂Cl₂/ethyl acetate/formic acid (6:10:1) in an automatic developing chamber. After drying, the plates were dipped in an HCl solution containing 1% of vanillin and heated for 2 min at 110 °C. Densitometric detection was done by scanning at 500 nm using a TLC Scanner 3.

7.3.2 Results and discussion

7.3.2.1 Analysis

LC-MS method

During analysis, it became clear that the extraction mixture which was optimal for extract 3, the extract used for development and validation of the method, was not applicable to all other extracts. When the extraction mixture was added to extracts 1, 4, 5 and 7, aggregates were formed which can hinder full extraction of PACs. During dilution of extracts 6, 10, and 11, which were two whole berry extracts and cranberry fibers, respectively, the solution became opaque. Therefore, the extraction solvent was optimized for all problematic extracts. This resulted in water as extraction solvent for extracts 1, 5 and 7 since all three extracts were fully soluble in water, while extraction with methanol was the best alternative for extract 4, the only extract that was manufactured using water and ethanol. A mixture of water and methanol 50:50 was optimal for extracts 10 and 11, and a mixture of water and acetone 50:50 was chosen for extract 6.

All extracts were analyzed with both gradients 1 and 3. Although gradient 3 showed much lower variation during the validation, the applicability of gradient 1 on a broader range of extracts was further evaluated. Results obtained with both methods are shown in Tables 7.6, 7.7, and 7.8. It was clear that gradient 1 resulted again in much higher variations, independently from the extract

analyzed, with RSD% values higher than the acceptable 15%. Therefore, only the results obtained with method 3 will be discussed. Results for dimers were as follows (Table 7.6): one extract, namely, extract 2, showed a concentration higher than 1%, 1.12%, respectively; extracts 3, 4, 8 and 12 had a concentration between 0.1 and 1% and all other extracts had a concentration below 0.1 % with extract 7 showing a concentration even lower than 0.01%. For trimers (Table 7.8), extract 4 showed the highest concentration with 1.44% and extracts 5, 7 and 11 had the lowest content (<0.01%). All other extracts were situated between 0.01 and 1%: extracts 1, 6, 9 and 10 ranged between 0.01 and 0.1% and extracts 2, 3, 8 and 12 between 0.1 and 1%.

Table 7.6 Results for PAC A2 (%) measured with gradient 1 and 3 with and without standard addition.

	Gradient 1 standard addition	Gradient 1 without standard addition	Gradient 3 standard addition	Gradient 3 without standard addition
Extract 1				
<x>	0.0652	0.0050	0.0570	0.0515
s	0.0077	0.0027	0.0037	0.0010
Extract 2				
<x>	1.261	1.082	1.121	1.0578
s	0.077	0.013	0.033	0.0090
Extract 3				
<x>	0.666	0.602	0.614	0.581
s	0.018	0.019	0.015	0.020
Extract 4				
<x>	Not applicable	Not applicable	0.0287	0.0242
s	Not applicable	Not applicable	0.0025	0.0015
Extract 5				
<x>	0.0176	0.01407	0.0147	0.01408
s	0.0011	0.00019	0.0010	0.00034
Extract 6				
<x>	0.0434	0.0356	0.0409	0.0375
s	0.0040	0.0021	0.0037	0.0006
Extract 7				
<x>	0.001692	0.001214	0.001587	0.00126
s	0.000064	0.000062	0.000090	0.00013
Extract 8				
<x>	0.671	0.584	0.575	0.56
s	0.020	0.012	0.012	0.12
Extract 9				
<x>	0.1098	0.0908	0.0982	0.0960
s	0.0026	0.0047	0.0025	0.0019
Extract 10				
<x>	0.0597	0.0504	0.05185	0.0523
s	0.0014	0.0039	0.00042	0.0016
Extract 11				
<x>	0.0170	0.01664	0.01559	0.01605
s	0.0010	0.00013	0.00045	0.00069
Extract 12				
<x>	0.991	0.6752	0.846	0.690
s	0.032	0.0088	0.030	0.012

Table 7.7 Overview of trimeric procyanidin content (%) obtained with method A (gradient 1).

	Trimer 1 (%)	Trimer 2 (%)	Trimer 3 (%)	Trimer 4 (%)	Total (%)
Extract 1					
<x>	0.0148	0.0212	0.0122	0.0109	0.059
s	0.0028	0.0032	0.0027	0.0025	0.011
Extract 2					
<x>	0.223	0.341	0.214	0.186	0.96
s	0.028	0.028	0.030	0.026	0.11
Extract 3					
<x>	0.165	0.263	0.177	0.136	0.74
s	0.035	0.040	0.028	0.022	0.12
Extract 4	Not applicable				
<x>					
s					
Extract 5					
<x>	0.00425	0.00138	0.00132	0.001251	0.00820
s	0.00038	0.00012	0.00012	0.000099	0.00072
Extract 6					
<x>	0.00960	0.00815	0.00649	0.00526	0.02950
s	0.00042	0.00047	0.00064	0.00087	0.00203
Extract 7		Not applicable			
<x>	0.001799				0.001799
s	0.000058				0.000058
Extract 8					
<x>	0.1948	0.1870	0.1196	0.1038	0.605
s	0.0045	0.0052	0.0037	0.0023	0.016
Extract 9					
<x>	0.0225	0.00699	0.00641	0.00596	0.0418
s	0.0022	0.00076	0.00072	0.00067	0.0043
Extract 10					
<x>	0.0111	0.00593	0.00420	0.00483	0.0261
s	0.0012	0.00094	0.00083	0.00076	0.0035
Extract 11					
<x>	0.00199	0.00130	0.00125	0.00130	0.0058
s	0.00049	0.00034	0.00032	0.00034	0.0015
Extract 12					
<x>	0.179	0.4046	0.313	0.2224	1.119
s	0.020	0.0031	0.031	0.0024	0.011

Table 7.8 Overview of trimeric procyanidin content (%) obtained with method B (gradient 3).

	Trimer 1 (%)	Trimer 2 (%)	Trimer 3 (%)	Trimer 4 (%)	Total (%)
Extract 1					
<x>	0.0113	0.0191	0.0111	0.0089	0.0503
s	0.0010	0.0010	0.0012	0.0012	0.0026
Extract 2					
<x>	0.195	0.299	0.182	0.163	0.839
s	0.012	0.018	0.012	0.013	0.054
Extract 3					
<x>	0.1492	0.2306	0.1642	0.1114	0.655
s	0.0040	0.0069	0.0036	0.0039	0.016
Extract 4					
<x>	0.3473*	1.090*			1.437
s	0.0058	0.074			0.079
Extract 5					
<x>	0.00323	0.001049	0.000993	0.000914	0.00618
s	0.00011	0.000070	0.000093	0.000087	0.00035
Extract 6					
<x>	0.0074	0.00626	0.00492	0.00401	0.0226
s	0.0010	0.00083	0.00062	0.00065	0.0031
Extract 7		Not applicable			
<x>	0.001842				0.001842
s	0.000053				0.000053
Extract 8					
<x>	0.1651	0.1437	0.0922	0.0835	0.484
s	0.0049	0.0058	0.0044	0.0045	0.020
Extract 9					
<x>	0.01935	0.00582	0.00546	0.00527	0.0359
s	0.00048	0.00024	0.00014	0.00029	0.0011
Extract 10					
<x>	0.09957	0.00538	0.00383	0.00454	0.0237
s	0.00092	0.00095	0.00085	0.00091	0.0036
Extract 11					
<x>	0.00205	0.001270	0.001170	0.001270	0.00577
s	0.00017	0.000062	0.000067	0.000095	0.00039
Extract 12					
<x>	0.1344	0.2934	0.2149	0.1489	0.792
s	0.0029	0.0038	0.0042	0.0023	0.011

* More trimeric procyanidins with transition of 863 → 411 were present in extract 4 and trimeric procyanidins with transition 863 → 575 were different from those of the other extracts.

The ratio between dimeric and trimeric PACs ranged from 52% to 273%. In addition, it should be mentioned, as already done before, that extract 4 showed a totally different profile of dimers and trimers. This could be caused by the extraction solvent, ethanol/water, used by the manufacturer to produce the extract. This extraction solvent was different from that of all the other extracts. During

the analysis of different commercial cranberry products, most preparations showed only four trimeric PACs, while some preparations also showed a more complex profile.⁷¹ So the PAC profile can differ between preparations, depending on the origin, cultivar variety, and processing.

The dimer content of all extracts was also analyzed without standard addition and compared with results obtained with standard addition. For all results, the mean and standard deviation are given (Table 7.6). For almost all extracts there is a trend that a higher percentage PAC A2 is found when using the standard addition method, suggesting potential matrix effects (Figures 7.25 and 7.26). This trend is more pronounced for method A, especially for extracts 5, 7, 8, 9, and 12. For PAC A2 contents obtained with method B, this trend is observed for extracts 1, 2, 4, 7, and 12.

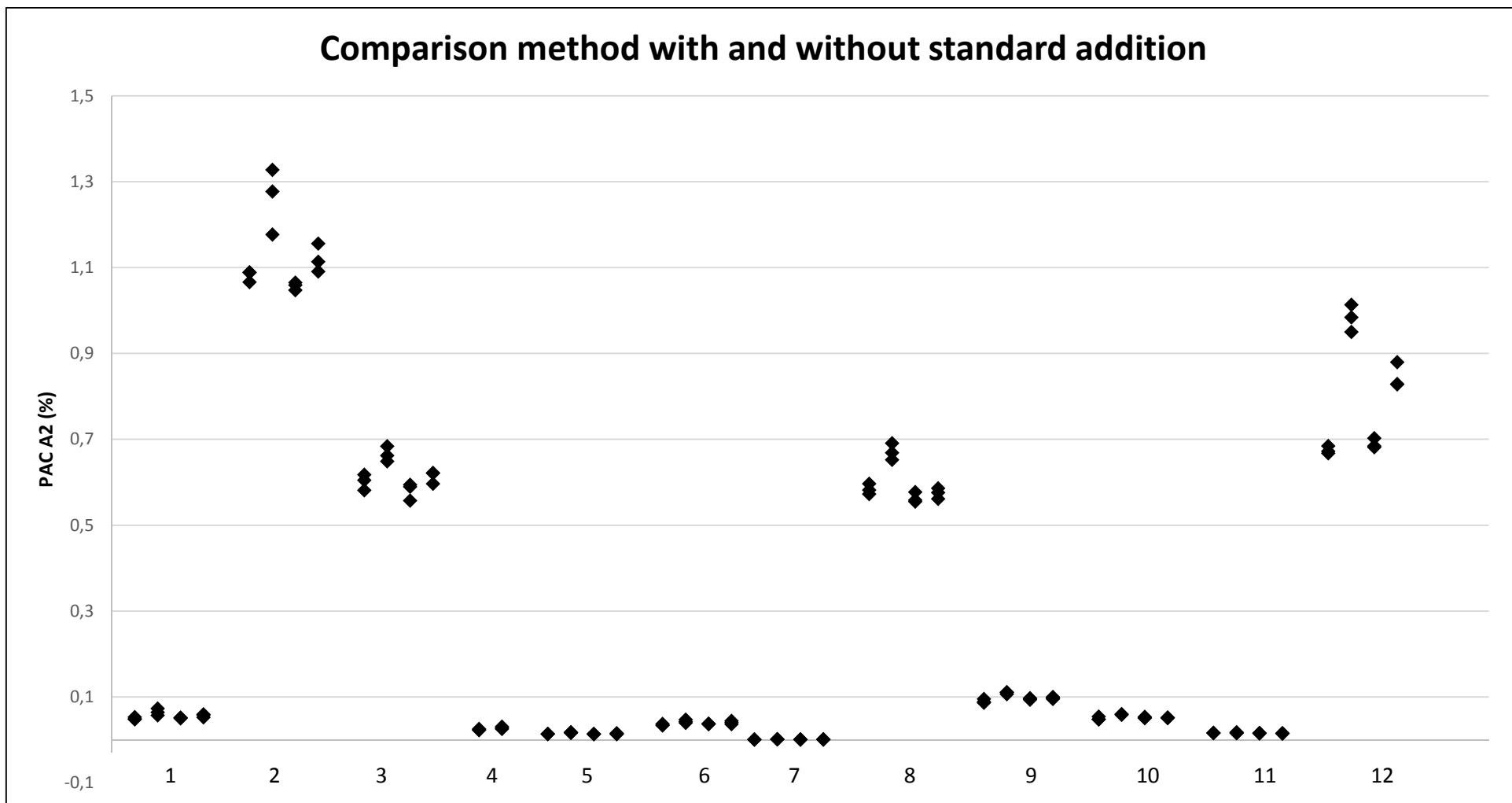


Figure 7.25 % PAC A2 measured with gradients 1 and 3 both without and with standard addition. For each extract the results are shown in the following order: gradient 1, gradient 1 with standard addition, gradient 3, gradient 3 with standard addition. The number of the extract is written below.

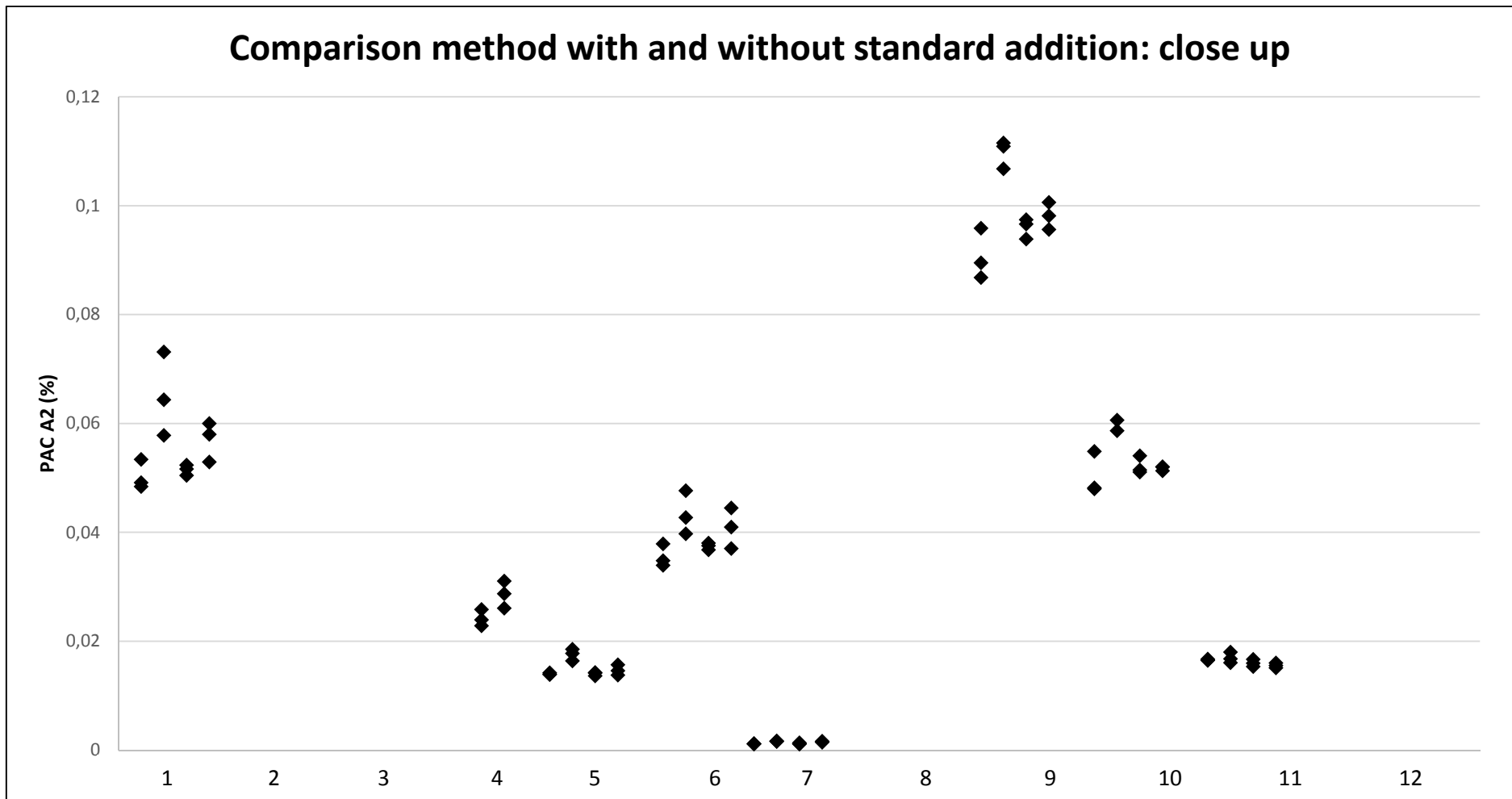


Figure 7.26 Close up of extracts with a lower PAC A2 content: extracts 1, 4, 5, 6, 7, 9, 10 and 11. Extracts 2, 3, 8 and 12 are not visible.

NP-HPLC-UV method

For all extracts (except extract 12), a NP-HPLC profile was obtained. Extract 12 was not analyzed with this method since it was only obtained after all measurements had already been performed. The profiles of extracts 3 and 10 are shown in Figures 7.27 and 7.28. The chromatogram of the extract is shown in black, monomeric standards are shown in blue and the oligomeric standards are shown in red. The division between monomers and oligomers/polymers is indicated by the green line. These chromatograms demonstrate that the ratio between polymers and monomers was much higher for extract 3 than it was for extract 10. The ratio was visually interpreted and was the highest for extracts 2, 3 and 8 followed by extract 9. An intermediate ratio was observed for extract 1, 4 and 7 and almost no oligomeric and polymeric PACs were present in extracts 6, 10, and 11. Extract 5 hardly showed any signal neither for monomers nor for polymers although a highly concentrated solution was injected.

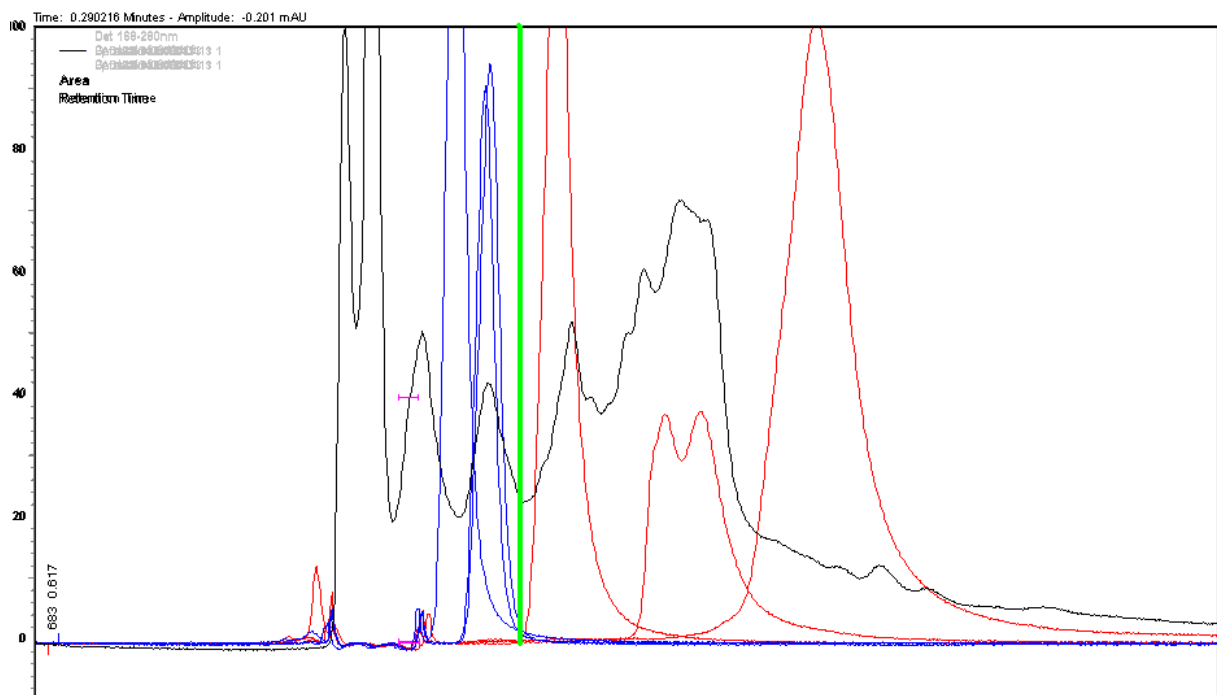


Figure 7.27 Chromatogram of cranberry extract 3 (black) and standard compounds epicatechin, catechin, gallic acid (in blue), PAC A2, PAC B1, and PAC B2 (in red). The green line shows the separation of monomers and oligomers/polymers.

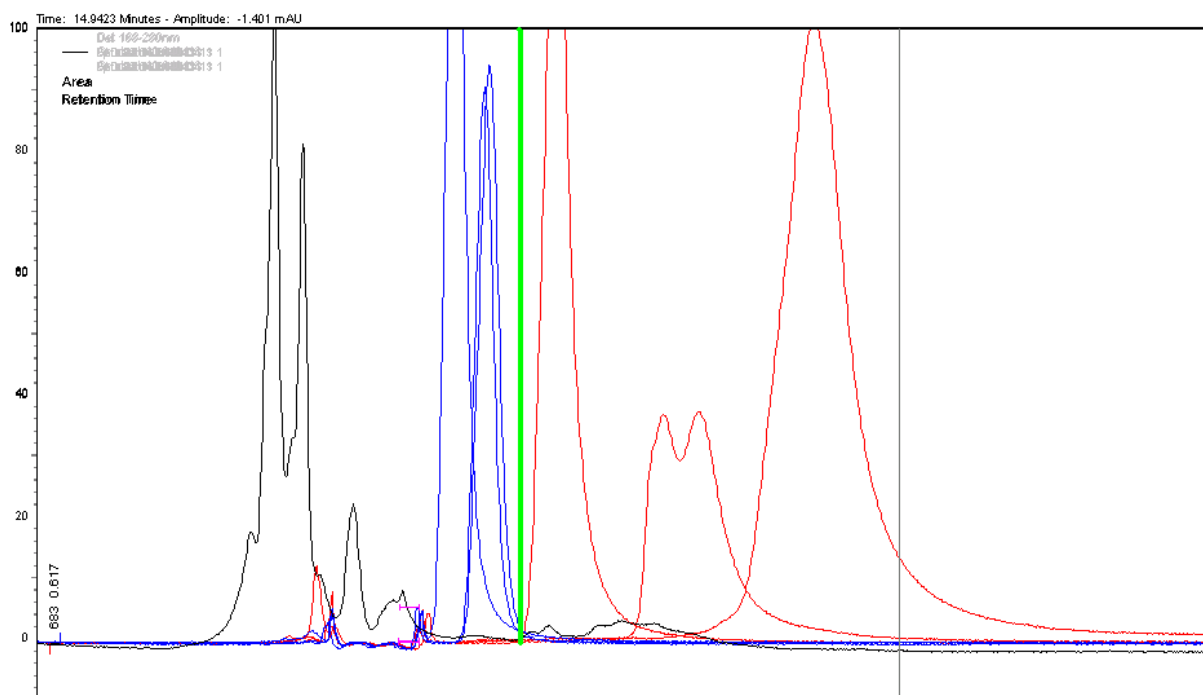


Figure 7.28 Chromatogram of cranberry extract 10 (black) and standard compounds epicatechin, catechin, gallic acid (in blue), PAC A2, PAC B1, and PAC B2 (in red). The green line shows the separation of monomers and oligomers/polymers.

Spectrophotometric assay/butanol-HCl assay

During sample preparation, it became clear that the extraction solvent, ethanol/water 70:30, caused some problems. When the solvent was added to extracts 1, 4, 5 and 7, an aggregate was formed. Therefore, the extracts were first fully dissolved in water and afterwards the ethanol was added. Since extracts 4 and 5 blocked the filter paper, centrifugation (10 min, 2397 g - 3500 rpm) was used instead. Results are shown in Table 7.9 and ranged from 0.1340% to 7.58%.

Table 7.9 Overview of results obtained with the spectrophotometrical method/butanol-HCl assay.

extract	% PACs expressed as cyanidin HCl		
	<x>	s	RSD%
1	0.344	0.020	5.67
2	4.955	0.034	0.68
3	4.63	0.19	4.01
4	4.87	0.13	2.68
5	0.1340	0.0053	3.97
6	0.2720	0.0075	2.76
7	1.115	0.026	2.34
8	6.93	0.23	3.27

Table 7.9 continued Overview of results obtained with the spectrophotometrical method/butanol-HCl assay.

extract	% PACs expressed as cyanidin HCl		
	<x>	s	RSD%
9	1.56	0.11	6.79
10	0.2083	0.0068	3.28
11	0.160	0.012	7.51
12	7.58	0.29	3.85

DMAC

As for the other methods described the extraction solvent was not optimal for all extracts and again the formation of aggregates was observed for extracts 1, 4, 5, and 7. Therefore, samples were first fully dissolved in water (with 0.5% acetic acid) before the acetone was added to ensure complete extraction of PACs.

The semi-automatic DMAC analysis, using 96-well plates, resulted in unacceptable calibration lines and results. This could be a result of the use of multichannel pipets and 96-microwell plates. Therefore, the protocol was adjusted as described above and samples were prepared in larger volumes and measured using a double beam UV/VIS spectrophotometer. This resulted in calibration lines with correlation coefficients larger than 0.99. PAC concentrations ranged from 0.155 to 32.77% (Table 7.10).

Table 7.10 Overview of results obtained with the DMAC method.

extract	% PACs expressed as PAC A2		
	<x>	s	RSD%
1	0.654	0.037	5.59
2	14.82	0.29	1.97
3	18.03	0.16	0.91
4	32.77	0.83	2.54
5	0.155	0.010	6.55
6	0.654	0.027	4.10
7	0.223	0.017	7.55
8	15.897	0.099	0.62
9	2.880	0.084	2.92
10	0.6397	0.0090	1.41
11	0.337	0.017	5.14
12	15.71	0.49	3.09

NP-HPTLC method

All samples were analyzed with the method described by Boudesocque et al.⁶⁵ but, unfortunately, this method was not sensitive enough to quantify the PAC 2 content of the cranberry crude extracts.

Comparison of different techniques

Table 7.11 Overview of all results from different analytical techniques.

Extract	LC-MS		Butanol-HCl assay	DMAC assay	NP-HPLC profile
	% PAC A2	% trimeric procyanidins expressed as PAC A2	% procyanidins expressed as cyanidin HCl	% procyanidins expressed as PAC A2	Ratio monomers/polymers
1	0.0570	0.0503	0.344	0.654	+/-
2	1.121	0.839	4.955	14.82	+
3	0.614	0.655	4.63	18.03	+
4	0.0287	1.090	4.87	32.77	+/-
5	0.0147	0.00618	0.1340	0.155	-
6	0.0409	0.0226	0.2720	0.654	-
7	0.00159	0.001842	1.115	0.223	+/-
8	0.575	0.484	6.93	15.897	+
9	0.0982	0.0359	1.56	2.880	+
10	0.05185	0.0237	0.2083	0.6397	-
11	0.01559	0.00577	0.160	0.337	-
12	0.846	0.792	7.58	15.71	n.a.

-: low ratio of monomers/polymers; +/-: intermediate ratio of monomers/polymers; +: high ratio of monomers/polymers.

The results obtained with all analytical techniques discussed are summarized in Table 7.11. Between the butanol-HCl assay and the total content of dimers and trimers obtained with LC-MS, there was a correlation of R^2 0.74 – R 0.86, meaning that when a higher concentration of A-type PACs was found by LC-MS the % PACs expressed as cyanidin HCl also roughly increased (Figure 7.29). Deviations between these two techniques could be explained by the fact that the butanol-HCl assay does not distinguish between A-type and B-type PACs and is biased by the interference of anthocyanidins. This

means that samples containing a high amount of cyanidins and/or B-type PACs but a low amount of A-type PACs will result in a high procyanidin content making this method on its own unsuitable for quality analysis of cranberry. In addition, because the LC-MS assay only gives the content of dimeric and trimeric A-type PACs and not of higher polymers, the % PACs measured with the butanol-HCl assay of samples with a similar dimer and trimer content measured by LC-MS can differ depending on their polymeric PAC content.

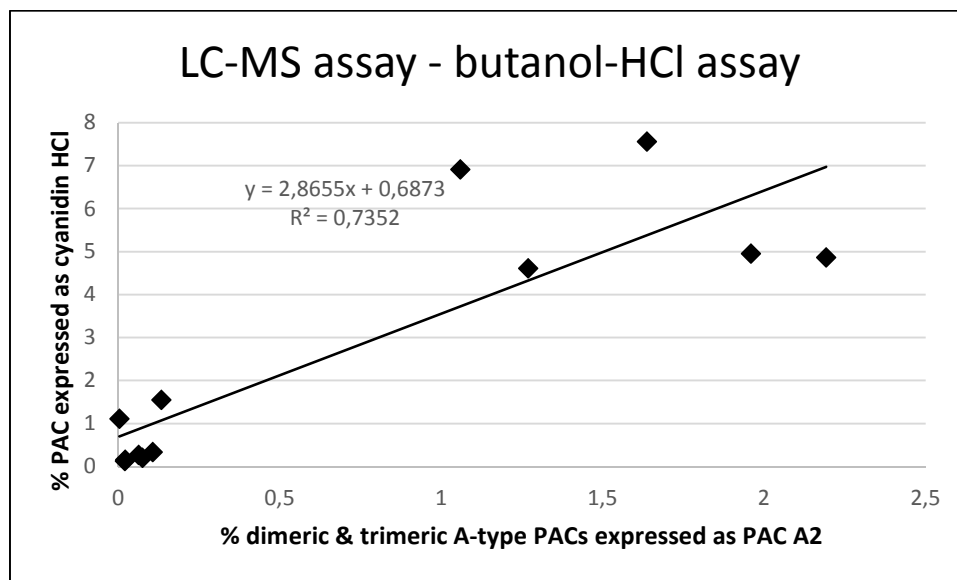


Figure 7.29 Graphical presentation of correlation between the LC-MS assay and the butanol-HCl assay.

A correlation coefficient of 0.88 was found between the LC-MS assay and DMAC assay (Figure 7.30). Deviations between both methods can be explained by the fact that the DMAC assay, as already mentioned for the butanol-HCl assay, cannot distinguish between A and B-type PACs and by the fact that the LC-MS assay only measures dimeric and trimeric A-type PACs. In addition, this technique also measures monomers which can overestimate the amount of PACs and, on the other hand, an underestimation is also possible for samples with a high content of polymers with a high degree of polymerization since DMAC only reacts with one PAC molecule. This implies that, when a sample not identified as cranberry is tested with this method, a high PAC content can be obtained for a sample containing mainly B-type monomers, and a lower PAC content for a sample that mainly consists of high weight A-type PACs. This problem could be overcome by combining the DMAC assay with the LC-MS assay.

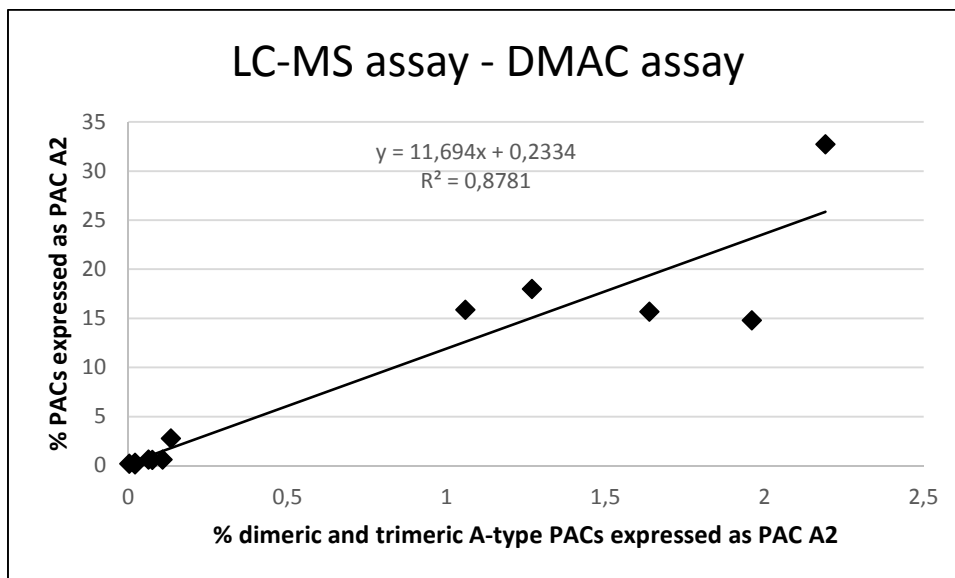


Figure 7.30 Graphical presentation of correlation between the LC-MS assay and the DMAC assay.

The correlation between the DMAC and butanol-HCl assay was 0.65 (Figure 7.31). It was clear that one sample, extract 4, deviated largely from the regression line. When this point was eliminated from the plot, the correlation coefficient increased to 0.89 (Figure 7.32). A possible explanation for extract 4 could be the higher content of monomers present, in comparison with extracts 2, 3, 8 and 12, which was found by analysis with NP-HPLC-UV. These monomers are also measured with the DMAC assay but not with the butanol-HCl assay. Another remarkable deviation is seen for extract 7 (combination with grape seed extract) which has a very low PAC content according to the DMAC method as for extracts 1, 5, 6, 10 and 11, whereas it showed a much higher PAC content than the other extracts according to the butanol-HCl assay. Since the solution of this extract was extremely colored due to the presence of anthocyanidins, this could have led to an overestimation of the PAC content using the butanol-HCl assay.

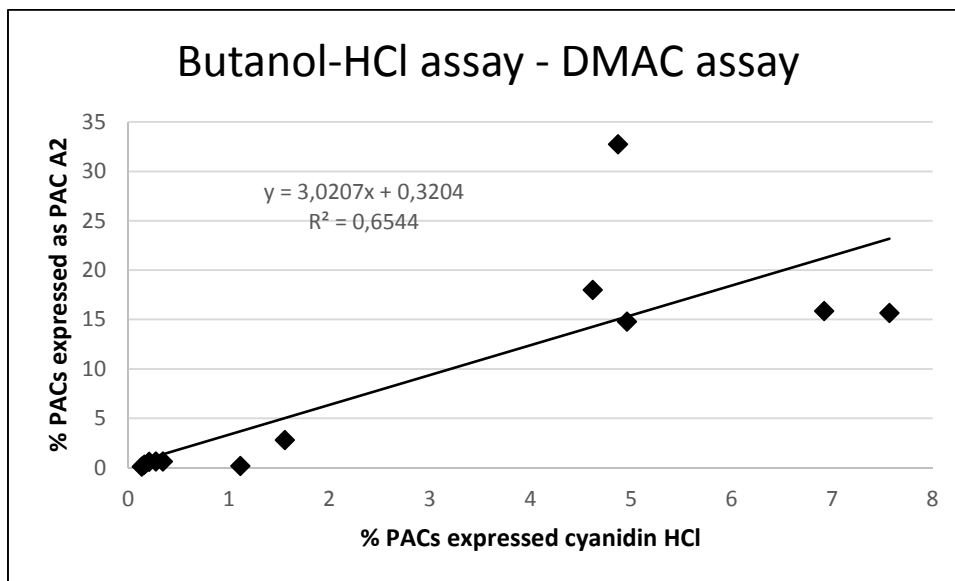


Figure 7.31 Graphical presentation of correlation between the butanol-HCl assay and the DMAC assay including extract 4.

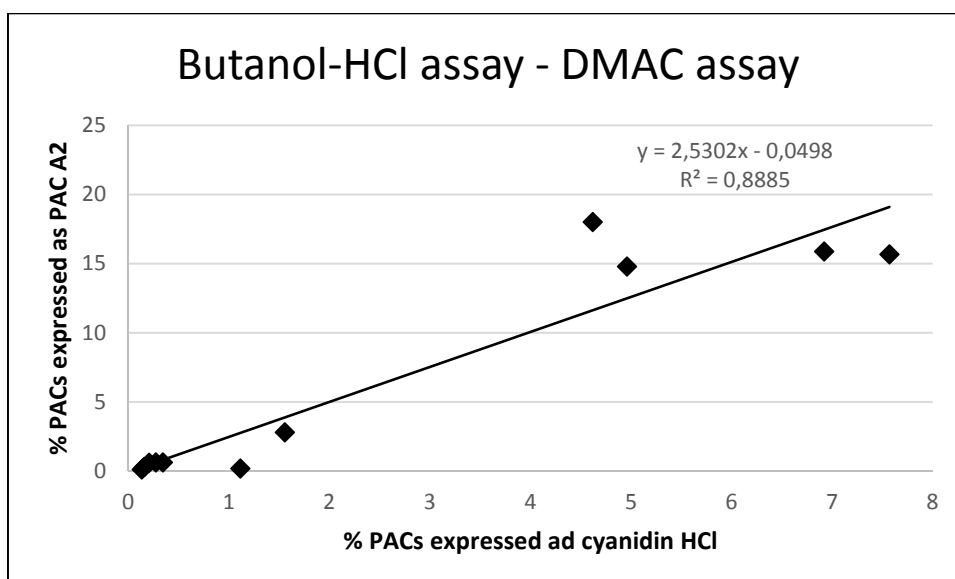


Figure 7.32 Graphical presentation of correlation between the butanol-HCl assay and the DMAC assay without extract 4.

7.3.3 Conclusion

Analysis of twelve different extracts using the abovementioned LC-MS standard addition method highlighted the enormous variation in dimeric and trimeric PAC content. Comparison of these results with LC-MS² analysis without standard addition showed the presence of matrix effects for some of the extracts and proved the necessity of standard addition.

A comparison of the results obtained with the well-known and widely used DMAC method, the butanol assay, and our newly developed LC-MS² method showed that, generally, extracts 2, 3, 4, 8

and 12 contained the highest total PAC content and A-type dimer and trimer concentration. Further in-depth comparison clearly indicated the need for a reliable method able to quantify A-type PACs, which are considered to be the pharmacologically active constituents of cranberry, since neither the DMAC or the butanol-HCl assay are capable of distinguishing between A and B-type PACs and therefore cannot detect adulterations with, for example, extracts with a high B-type PAC content. Hence, the combination of the DMAC method or butanol-HCl assay with our more specific LC-MS² assay could overcome these existing shortcomings.

References

1. Jepson, R. G.; Williams, G.; Craig, J. C. Cranberries for preventing urinary tract infections. *Cochrane Database of Systematic Reviews* **2012**.
2. Micali, S.; Isgro, G.; Bianchi, G.; Miceli, N.; Calapai, G.; Navarra, M. Cranberry and recurrent cystitis: more than marketing? *Crit. Rev. Food Sci. Nutr.* **2014**, *54* (8), 1063-1075.
3. Aydin, A.; Ahmed, K.; Zaman, I.; Khan, M. S.; Dasgupta, P. Recurrent urinary tract infections in women. *Int Urogynecol J* **2015**, *26* (6), 795-804.
4. Occhipinti, A.; Germano, A.; Maffei, M. E. Prevention of urinary tract infection with Oximacro (R), a cranberry extract with a high content of A-type proanthocyanidins: A pre-clinical double-blind controlled study. *Urol J* **2016**, *13* (2), 2640-2649.
5. Burleigh, A. E.; Benck, S. M.; McAchran, S. E.; Reed, J. D.; Krueger, C. G.; Hopkins, W. J. Consumption of sweetened, dried cranberries may reduce urinary tract infection incidence in susceptible women - a modified observational study. *Nutr. J.* **2013**, *12*.
6. Wang, C. H.; Fang, C. C.; Chen, N. C.; Liu, S. S. H.; Yu, P. H.; Wu, T. Y.; Chen, W. T.; Lee, C. C.; Chen, S. C. Cranberry-containing products for prevention of urinary tract infections in susceptible populations A systematic review and meta-analysis of randomized controlled trials. *Arch. Intern. Med.* **2012**, *172* (13), 988-996.
7. Vasileiou, I.; Katsargyris, A.; Theocharis, S.; Giaginis, C. Current clinical status on the preventive effects of cranberry consumption against urinary tract infections. *Nutr. Res.* **2013**, *33* (8), 595-607.
8. Barbosa-Cesnik, C.; Brown, M. B.; Buxton, M.; Zhang, L. X.; DeBusscher, J.; Foxman, B. Cranberry juice fails to prevent recurrent urinary tract infection: results from a randomized placebo-controlled trial. *Clin. Infect. Dis.* **2011**, *52* (1), 23-30.
9. Krueger, C. G.; Reed, J. D.; Feliciano, R. P.; Howell, A. B. Quantifying and characterizing proanthocyanidins in cranberries in relation to urinary tract health. *Anal. Bioanal. Chem.* **2013**, *405* (13), 4385-4395.
10. Schito, G. C.; Naber, K. G.; Botto, H.; Palou, J.; Mazzei, T.; Gualco, L.; Marchese, A. The ARESC study: an international survey on the antimicrobial resistance of pathogens involved in uncomplicated urinary tract infections. *Int. J. Antimicrob. Agents* **2009**, *34* (5), 407-413.
11. Bien, J.; Sokolova, O.; Bozko, P. Role of uropathogenic *Escherichia coli* virulence factors in development of urinary tract infection and kidney damage. *Int. J. Nephrol.* **2012**, *2012*, Article ID 681473.
12. Cranberry Fruit *Vaccinium macrocarpon* Aiton Revision. *American Herbal Pharmacopoeia and Therapeutic Compendium*; R. DipAyu, T. B., Ed.; Scotts Valley: CA, 2016.
13. Singh, A. P.; Wilson, T.; Kalk, A. J.; Cheong, J.; Vorsa, N. Isolation of specific cranberry flavonoids for biological activity assessment. *Food Chem* **2009**, *116* (4), 963-968.
14. Neto, C. C.; Krueger, C. G.; Lamoureaux, T. L.; Kondo, M.; Vaisberg, A. J.; Hurta, R. A. R.; Curtis, S.; Matchett, M. D.; Yeung, H.; Sweeney, M. I.; Reed, J. D. MALDI-TOF MS characterization of proanthocyanidins from cranberry fruit (*Vaccinium macrocarpon*) that inhibit tumor cell growth and matrix metalloproteinase expression *in vitro*. *J. Sci. Food Agric.* **2006**, *86* (1), 18-25.

15. Foo, L. Y.; Lu, Y. R.; Howell, A. B.; Vorsa, N. A-type proanthocyanidin trimers from cranberry that inhibit adherence of uropathogenic P-fimbriated *Escherichia coli*. *J. Nat. Prod.* **2000**, *63* (9), 1225-1228.
16. Cote, J.; Caillet, S.; Doyon, G.; Sylvain, J. F.; Lacroix, M. Bioactive compounds in cranberries and their biological properties. *Crit. Rev. Food Sci. Nutr.* **2010**, *50* (7), 666-679.
17. Vvedenskaya, I. O.; Rosen, R. T.; Guido, J. E.; Russell, D. J.; Mills, K. A.; Vorsa, N. Characterization of flavonols in cranberry (*Vaccinium macrocarpon*) powder. *J. Agric. Food Chem.* **2004**, *52* (2), 188-195.
18. Kylli, P.; Nohynek, L.; Puupponen-Pimia, R.; Westerlund-Wikstrom, B.; Leppanen, T.; Welling, J.; Moilanen, E.; Heinonen, M. Lingonberry (*Vaccinium vitis-idaea*) and European cranberry (*Vaccinium microcarpon*) proanthocyanidins: isolation, identification, and bioactivities. *J. Agric. Food Chem.* **2011**, *59* (7), 3373-3384.
19. Howell, A. B. Bioactive compounds in cranberries and their role in prevention of urinary tract infections. *Mol. Nutr. Food Res.* **2007**, *51* (6), 732-737.
20. Gupta, K.; Chou, M. Y.; Howell, A.; Wobbe, C.; Grady, R.; Stapleton, A. E. Cranberry products inhibit adherence of P-fimbriated *Escherichia coli* to primary cultured bladder and vaginal epithelial cells. *J. Urol.* **2007**, *177* (6), 2357-2360.
21. Foo, L. Y.; Lu, Y. R.; Howell, A. B.; Vorsa, N. The structure of cranberry proanthocyanidins which inhibit adherence of uropathogenic P-fimbriated *Escherichia coli* *in vitro*. *Phytochemistry* **2000**, *54* (2), 173-181.
22. Howell, A.; Souza, D.; Roller, M.; Fromentin, E. Comparison of the anti-adhesion activity of three different cranberry extracts on uropathogenic P-fimbriated *Escherichia coli*: a randomized, double-blind, placebo-controlled, *ex vivo*, acute study. *Nat. Prod. Comm.* **2015**, *10* (7), 1215-1218.
23. Howell, A. B.; Botto, H.; Combescure, C.; Blanc-Potard, A. B.; Gausa, L.; Matsumoto, T.; Tenke, P.; Sotto, A.; Lavigne, J. P. Dosage effect on uropathogenic *Escherichia coli* anti-adhesion activity in urine following consumption of cranberry powder standardized for proanthocyanidin content: a multicentric randomized double-blind study. *BMC Infect. Dis.* **2010**, *10*.
24. Feliciano, R. P.; Krueger, C. G.; Reed, J. D. Methods to determine effects of cranberry proanthocyanidins on extraintestinal infections: Relevance for urinary tract health. *Mol. Nutr. Food Res.* **2015**, *59* (7), 1292-1306.
25. Deprez, S.; Mila, I.; Huneau, J. F.; Tome, D.; Scalbert, A. Transport of proanthocyanidin dimer, trimer, and polymer across monolayers of human intestinal epithelial Caco-2 cells. *Antioxid. Redox Signaling* **2001**, *3* (6), 957-967.
26. Tsang, C.; Auger, C.; Mullen, W.; Bornet, A.; Rouanet, J. M.; Crozier, A.; Teissedre, P. L. The absorption, metabolism and excretion of flavan-3-ols and procyanidins following the ingestion of a grape seed extract by rats. *Br. J. Nutr.* **2005**, *94* (2), 170-181.
27. Gonthier, M. P.; Donovan, J. L.; Texier, O.; Felgines, C.; Remesy, C.; Scalbert, A. Metabolism of dietary procyanidins in rats. *Free Radical Biol. Med.* **2003**, *35* (8), 837-844.
28. Serra, A.; Macia, A.; Romero, M. P.; Valls, J.; Blade, C.; Arola, L.; Motilva, M. J. Bioavailability of procyanidin dimers and trimers and matrix food effects in *in vitro* and *in vivo* models. *Br. J. Nutr.* **2010**, *103* (7), 944-52.

29. Sano, A.; Yamakoshi, J.; Tokutake, S.; Tobe, K.; Kubota, Y.; Kikuchi, M. Procyanidin B1 is detected in human serum after intake of proanthocyanidin-rich grape seed extract. *Biosci., Biotechnol., Biochem.* **2003**, *67* (5), 1140-1143.
30. Appeldoorn, M. M.; Vincken, J. P.; Gruppen, H.; Hollman, P. C. H. Procyanidin dimers a1, a2, and b2 are absorbed without conjugation or methylation from the small intestine of rats. *J. Nutr.* **2009**, *139* (8), 1469-1473.
31. Ou, K. Q.; Percival, S. S.; Zou, T.; Khoo, C.; Gu, L. W. Transport of cranberry A-type procyanidin dimers, trimers, and tetramers across monolayers of human intestinal epithelial Caco-2 cells. *J. Agric. Food Chem.* **2012**, *60* (6), 1390-1396.
32. McKay, D. L.; Chen, C. Y. O.; Zampariello, C. A.; Blumberg, J. B. Flavonoids and phenolic acids from cranberry juice are bioavailable and bioactive in healthy older adults. *Food Chem.* **2015**, *168*, 233-240.
33. Sanchez-Patan, F.; Barroso, E.; van de Wiele, T.; Jimenez-Giron, A.; Martin-Alvarez, P. J.; Moreno-Arribas, M. V.; Martinez-Cuesta, M. C.; Pelaez, C.; Requena, T.; Bartolome, B. Comparative *in vitro* fermentations of cranberry and grape seed polyphenols with colonic microbiota. *Food Chem.* **2015**, *183*, 273-282.
34. Sanchez-Patan, F.; Cueva, C.; Monagas, M.; Walton, G. E.; Gibson, G. R.; Martin-Alvarez, P. J.; Moreno-Arribas, M. V.; Bartolome, B. Gut microbial catabolism of grape seed flavan-3-ols by human faecal microbiota. Targetted analysis of precursor compounds, intermediate metabolites and end-products. *Food Chem.* **2012**, *131* (1), 337-347.
35. Serra, A.; Macia, A.; Romero, M. P.; Angles, N.; Morello, J. R.; Motilva, M. J. Metabolic pathways of the colonic metabolism of procyanidins (monomers and dimers) and alkaloids. *Food Chem.* **2011**, *126* (3), 1127-1137.
36. Cueva, C.; Sanchez-Patan, F.; Monagas, M.; Walton, G. E.; Gibson, G. R.; Martin-Alvarez, P. J.; Bartolome, B.; Moreno-Arribas, M. V. *In vitro* fermentation of grape seed flavan-3-ol fractions by human faecal microbiota: changes in microbial groups and phenolic metabolites. *FEMS Microbiol. Ecol.* **2013**, *83* (3), 792-805.
37. de Llano, D. G.; Esteban-Fernandez, A.; Sanchez-Patan, F.; Martin-Alvarez, P. J.; Moreno-Arribas, M. V.; Bartolome, B. Anti-adhesive activity of cranberry phenolic compounds and their microbial-derived metabolites against uropathogenic *Escherichia coli* in bladder epithelial cell cultures. *Int. J. Mol. Sci.* **2015**, *16* (6), 12119-12130.
38. Hidalgo, G.; Chan, M.; Tufenkji, N. Inhibition of *Escherichia coli* CFT073 fliC expression and motility by cranberry materials. *Appl. Environ. Microbiol.* **2011**, *77* (19), 6852-6857.
39. Wojnicz, D.; Sycz, Z.; Walkowski, S.; Gabrielska, J.; Aleksandra, W.; Alicja, K.; Anna, S. L.; Hendrich, A. B. Study on the influence of cranberry extract Zuravit S.O.S((R)) on the properties of uropathogenic *Escherichia coli* strains, their ability to form biofilm and its antioxidant properties. *Phytomedicine* **2012**, *19* (6), 506-14.
40. Gu, L. W.; Kelm, M. A.; Hammerstone, J. F.; Beecher, G.; Holden, J.; Haytowitz, D.; Prior, R. L. Screening of foods containing proanthocyanidins and their structural characterization using LC-MS/MS and thiolytic degradation. *J. Agric. Food Chem.* **2003**, *51* (25), 7513-7521.

41. Maatta-Riihinen, K. R.; Kahkonen, M. P.; Torronen, A. R.; Heinonen, I. M. Catechins and procyanidins in berries of *Vaccinium* species and their antioxidant activity. *J. Agric. Food Chem.* **2005**, *53* (22), 8485-8491.
42. Prior, R. L.; Lazarus, S. A.; Cao, G. H.; Muccitelli, H.; Hammerstone, J. F. Identification of procyanidins and anthocyanins in blueberries and cranberries (*Vaccinium* spp.) using high-performance liquid chromatography/mass spectrometry. *J. Agric. Food Chem.* **2001**, *49* (3), 1270-1276.
43. Ferreira, D.; Slade, D.; Marais, J. Flavans and proanthocyanidins. In *Flavonoids Chemistry, biochemistry and applications*, Andersen, O.; Markham, K., Eds. CRC Press: Boca Raton, Florida, 2006; pp 553-616.
44. Turati, F.; Rossi, M.; Pelucchi, C.; Levi, F.; La Vecchia, C. Fruit and vegetables and cancer risk: a review of southern European studies. *Br. J. Nutr.* **2015**, *113 Suppl 2*, S102-10.
45. Quinones, M.; Miguel, M.; Aleixandre, A. Beneficial effects of polyphenols on cardiovascular disease. *Pharmacol. Res.* **2013**, *68* (1), 125-131.
46. Blade, C.; Aragones, G.; Arola-Arnal, A.; Muguerza, B.; Bravo, F. I.; Salvado, M. J.; Arola, L.; Suarez, M. Proanthocyanidins in health and disease. *Biofactors* **2016**, *42* (1), 5-12.
47. Feghali, K.; Feldman, M.; La, V. D.; Santos, J.; Grenier, D. Cranberry proanthocyanidins: natural weapons against periodontal diseases. *J. Agric. Food Chem.* **2012**, *60* (23), 5728-5735.
48. Belgian Center for Pharmaceutical Center. <http://www.bcfi.be/nl/start> (accessed May, 2016)
49. Pharmacopendium Plus. <http://www.farmacopendium.be/farma/> (accessed May, 2016)
50. French Agency for Food Environmental and Occupational Health Safety. Cranberry and urinary tract infections: state of scientific knowledge. <https://www.anses.fr/en/content/cranberry-and-urinary-tract-infections-state-scientific-knowledge> (accessed July, 2016).
51. Krenn, L.; Steitz, M.; Schlicht, C.; Kurth, H.; Gaedcke, F. Anthocyanin- and proanthocyanidin-rich extracts of berries in food supplements - analysis with problems. *Pharmazie* **2007**, *62* (11), 803-812.
52. Hummer, W.; Schreier, P. Analysis of proanthocyanidins. *Mol. Nutr. Food Res.* **2008**, *52* (12), 1381-1398.
53. Prior, R. L.; Fan, E.; Ji, H.; Howell, A.; Nio, C.; Payne, M. J.; Reed, J. Multi-laboratory validation of a standard method for quantifying proanthocyanidins in cranberry powders. *J. Sci. Food Agric.* **2010**, *90* (9), 1473-1478.
54. Robbins, R. J.; Leonczak, J.; Johnson, J. C.; Li, J.; Kwik-Urbe, C.; Prior, R. L.; Gu, L. Method performance and multi-laboratory assessment of a normal phase high pressure liquid chromatography-fluorescence detection method for the quantitation of flavanols and procyanidins in cocoa and chocolate containing samples. *J. Chromatogr. A* **2009**, *1216* (24), 4831-4840.
55. Hammerstone, J. F.; Lazarus, S. A.; Schmitz, H. H. Procyanidin content and variation in some commonly consumed foods. *J. Nutr.* **2000**, *130* (8S Suppl), 2086s-2092s.
56. Kuhnert, S.; Lehmann, L.; Winterhalter, P. Rapid characterisation of grape seed extracts by a novel HPLC method on a diol stationary phase. *J. Funct. Foods* **2015**, *15*, 225-232.
57. Shoji, T.; Masumoto, S.; Moriichi, N.; Kanda, T.; Ohtake, Y. Apple (*Malus pumila*) procyanidins fractionated according to the degree of polymerization using normal-phase chromatography and characterized by HPLC-ESI/MS and MALDI-TOF/MS. *J. Chromatogr. A* **2006**, *1102* (1-2), 206-213.

58. Kelm, M. A.; Johnson, J. C.; Robbins, R. J.; Hammerstone, J. F.; Schmitz, H. H. High-performance liquid chromatography separation and purification of cacao (*Theobroma cacao* L.) procyanidins according to degree of polymerization using a diol stationary phase. *J. Agric. Food Chem.* **2006**, *54* (5), 1571-1576.
59. Karonen, M.; Liimatainen, J.; Sinkkonen, J. Birch inner bark procyanidins can be resolved with enhanced sensitivity by hydrophilic interaction HPLC-MS. *J.Sep. Sci.* **2011**, *34* (22), 3158-3165.
60. Counet, C.; Ouwerx, C.; Rosoux, D.; Collin, S. Relationship between procyanidin and flavor contents of cocoa liquors from different origins. *J. Agric. Food Chem.* **2004**, *52* (20), 6243-6249.
61. Yanagida, A.; Murao, H.; Ohnishi-Kameyama, M.; Yamakawa, Y.; Shoji, A.; Tagashira, M.; Kanda, T.; Shindo, H.; Shibusawa, Y. Retention behavior of oligomeric proanthocyanidins in hydrophilic interaction chromatography. *J. Chromatogr. A* **2007**, *1143* (1-2), 153-161.
62. Lazarus, S. A.; Adamson, G. E.; Hammerstone, J. F.; Schmitz, H. H. High-performance liquid chromatography/mass spectrometry analysis of proanthocyanidins in foods and beverages. *J. Agric. Food Chem.* **1999**, *47* (9), 3693-3701.
63. Gu, L.; Kelm, M.; Hammerstone, J. F.; Beecher, G.; Cunningham, D.; Vannozzi, S.; Prior, R. L. Fractionation of polymeric procyanidins from Lowbush Blueberry and quantification of procyanidins in selected foods with an optimized normal-phase HPLC-MS fluorescent detection method. *J. Agric. Food Chem.* **2002**, *50* (17), 4852-4860.
64. Glavnik, V.; Simonovska, B.; Vovk, I.; Pavlovic, D.; Asperger, D.; Babic, S. Quantification of (-)-epicatechin and procyanidin B2 in chocolates. *J. Planar Chromatogr. - Mod. TLC* **2011**, *24* (6), 482-486.
65. Boudesocque, L.; Dorat, J.; Pothier, J.; Gueiffier, A.; Enguehard-Gueiffier, C. High performance thin layer chromatography-densitometry: A step further for quality control of cranberry extracts. *Food Chem.* **2013**, *139* (1-4), 866-871.
66. Harris, C. S.; Burt, A. J.; Saleem, A.; Le, P. M.; Martineau, L. C.; Haddad, P. S.; Bennett, S. A.; Arnason, J. T. A single HPLC-PAD-APCI/MS method for the quantitative comparison of phenolic compounds found in leaf, stem, root and fruit extracts of *Vaccinium angustifolium*. *Phytochem. Anal.* **2007**, *18* (2), 161-169.
67. Gómez-Alonso, S.; García-Romero, E.; Hermosín-Gutiérrez, I. HPLC analysis of diverse grape and wine phenolics using direct injection and multidetection by DAD and fluorescence. *J. Food Compos. Anal.* **2007**, *20* (7), 618-626.
68. Benavides, A.; Montoro, P.; Bassarello, C.; Piacente, S.; Pizza, C. Catechin derivatives in *Jatropha macrantha* stems: characterisation and LC/ESI/MS/MS quali-quantitative analysis. *J. Pharm. Biomed. Anal.* **2006**, *40* (3), 639-647.
69. Rohr, G. E.; Meier, B.; Sticher, O. Quantitative reversed-phase high-performance liquid chromatography of procyanidins in *Crataegus* leaves and flowers. *J. Chromatogr. A* **1999**, *835* (1-2), 59-65.
70. Rzeppa, S.; Von Bargen, C.; Bittner, K.; Humpf, H. U. Analysis of Flavan-3-ols and procyanidins in food samples by reversed phase high-performance liquid chromatography coupled to electrospray ionization tandem mass spectrometry (RP-HPLC-ESI-MS/MS). *J. Agric. Food Chem.* **2011**, *59* (19), 10594-10603.

71. Sanchez-Patan, F.; Bartolome, B.; Martin-Alvarez, P. J.; Anderson, M.; Howell, A.; Monagas, M. Comprehensive assessment of the quality of commercial cranberry products. phenolic characterization and *in vitro* bioactivity. *J. Agric. Food Chem.* **2012**, *60* (13), 3396-3408.
72. Jungfer, E.; Zimmermann, B. F.; Ruttkat, A.; Galensa, R. Comparing procyanidins in selected *Vaccinium* species by UHPLC-MS(2) with regard to authenticity and health effects. *J. Agric. Food Chem.* **2012**, *60* (38), 9688-9696.
73. Kalili, K. M.; de Villiers, A. Systematic optimisation and evaluation of on-line, off-line and stop-flow comprehensive hydrophilic interaction chromatography x reversed phase liquid chromatographic analysis of procyanidins. Part II: application to cocoa procyanidins. *J. Chromatogr. A* **2013**, *1289*, 69-79.
74. Kalili, K. M.; de Villiers, A. Systematic optimisation and evaluation of on-line, off-line and stop-flow comprehensive hydrophilic interaction chromatography x reversed phase liquid chromatographic analysis of procyanidins, part I: theoretical considerations. *J. Chromatogr. A* **2013**, *1289*, 58-68.
75. Wallace, T. C.; Giusti, M. M. Extraction and normal-phase HPLC-fluorescence-electrospray MS characterization and quantification of procyanidins in cranberry extracts. *J. Food Sci.* **2010**, *75* (8), C690-6.
76. Jaiswal, R.; Jayasinghe, L.; Kuhnert, N. Identification and characterization of proanthocyanidins of 16 members of the *Rhododendron* genus (Ericaceae) by tandem LC-MS. *J. Mass Spectrom.* **2012**, *47* (4), 502-15.
77. Karonen, M.; Loponen, J.; Ossipov, V.; Pihlaja, K. Analysis of procyanidins in pine bark with reversed-phase and normal-phase high-performance liquid chromatography–electrospray ionization mass spectrometry. *Anal. Chim. Acta* **2004**, *522* (1), 105-112.
78. Gu, L.; House, S. E.; Wu, X.; Ou, B.; Prior, R. L. Procyanidin and catechin contents and antioxidant capacity of cocoa and chocolate products. *J. Agric. Food Chem.* **2006**, *54* (11), 4057-4061.
79. Sarnoski, P. J.; Johnson, J. V.; Reed, K. A.; Tanko, J. M.; O'Keefe, S. F. Separation and characterisation of proanthocyanidins in Virginia type peanut skins by LC-MSn. *Food Chem.* **2012**, *131* (3), 927-939.
80. Serra, A.; Macia, A.; Romero, M. P.; Pinol, C.; Motilva, M. J. Rapid methods to determine procyanidins, anthocyanins, theobromine and caffeine in rat tissues by liquid chromatography-tandem mass spectrometry. *J. Chromatogr. B: Anal. Technol. Biomed. Life Sci.* **2011**, *879* (19), 1519-1528.
81. Koerner, J. L.; Hsu, V. L.; Lee, J.; Kennedy, J. A. Determination of proanthocyanidin A2 content in phenolic polymer isolates by reversed-phase high-performance liquid chromatography. *J. Chromatogr. A* **2009**, *1216* (9), 1403-1409.
82. Iswaldi, I.; Gomez-Caravaca, A. M.; Arraez-Roman, D.; Uberos, J.; Lardon, M.; Segura-Carretero, A.; Fernandez-Gutierrez, A. Characterization by high-performance liquid chromatography with diode-array detection coupled to time-of-flight mass spectrometry of the phenolic fraction in a cranberry syrup used to prevent urinary tract diseases, together with a study of its antibacterial activity. *J. Pharm. Biomed. Anal.* **2012**, *58*, 34-41.

83. Walsh, J. M.; Ren, X. B.; Zampariello, C.; Polasky, D. A.; McKay, D. L.; Blumberg, J. B.; Chen, C. Y. O. Liquid chromatography with tandem mass spectrometry quantification of urinary proanthocyanin A2 dimer and its potential use as a biomarker of cranberry intake. *J. Sep. Sci.* **2016**, *39* (2), 342-349.
84. Naczk, M.; Shahidi, F. Extraction and analysis of phenolics in food. *J. Chromatogr. A* **2004**, *1054* (1-2), 95-111.
85. Travaglia, F.; Bordiga, M.; Locatelli, M.; Coisson, J. D.; Arlorio, M. Polymeric proanthocyanidins in skins and seeds of 37 *Vitis vinifera* L. cultivars: a methodological comparative study. *J. Food Sci.* **2011**, *76* (5), C742-749.
86. Council of Europe. Hawthorn berries. In: European Pharmacopoeia 8.7 [Online]; Council of Europe: Strasbourg, 2016. <http://online6.edqm.eu/ep706/> (accessed March 1, 2013).
87. Romani, A.; Ieri, F.; Turchetti, B.; Mulinacci, N.; Vincieri, F. F.; Buzzini, P. Analysis of condensed and hydrolysable tannins from commercial plant extracts. *J. Pharm. Biomed. Anal.* **2006**, *41* (2), 415-420.

Chapter 8

GENERAL CONCLUSIONS AND FUTURE PERSPECTIVES

Before a herbal product reaches the market, different phases have to be passed. First of all, a thorough scientific study needs to be performed, which includes characterization and method development in order to standardize or quantify the herbal product in addition to the evaluation of its efficacy. A suitable formulation needs to be developed, and the compatibility of the extracts with the excipients and primary packaging materials needs to be evaluated, to obtain a finished product, which will be produced in large amounts. Another important issue is the stability of the product. This should be tested during stability studies. The ICH guidelines describe the different parameters for stability testing. Depending on the intended shelf life of the product, the time period of the stability studies can be 6 or 12 months, each with their corresponding temperature and humidity conditions. The last hurdle that has to be taken is the filing of an application in order to obtain a marketing authorization using all the acquired data from the abovementioned phases.

Desmodium adscendens and Herniaria hirsuta

For both extracts, a thorough scientific study was performed. The extracts were characterized and a method was developed and validated for the standardization/quantification. In addition, the efficacy of the extracts was proven in an *in vivo* study. Further steps still need to be undertaken to develop a suitable formulation and to evaluate the stability of the herbal product. All these data need to be gathered and an application needs to be filed to obtain a marketing authorization.

In addition, although this information is not needed for the application, it would be interesting to thoroughly study their behavior during the passage through the gastro-intestinal tract. Taking into account that the GIDM only reflects passive diffusion, an expansion of this model with Caco-2 cells can overcome this problem. Furthermore, the colonic phase experiment could be performed with fecal slurry prepared from feces obtained from a more heterogenic population such as vegetarians, patients with gallstones for *H. hirsuta* and persons with a higher risk for liver damage, such as alcoholics and patients treated with specific drugs, for *D. adscendens*. Further metabolism studies with a human S9 fraction or liver microsomes, together with phase II co-factors, are necessary to complete these *in vitro* experiments.

For *H. hirsuta*, a follow-up study in which the standardized extract is tested against implanted gallstones in dogs would be interesting. From an ethical point of view, many efforts are made to lower the number of animal studies and replace them by alternative approaches. Therefore, it would

be interesting to first test the effect of a standardized extract of *H. hirsuta* on gallstone dissolution in an *in vitro* model. Since the extract was found not to be genotoxic and is already traditionally used for centuries, it would be interesting to evaluate the standardized extract in a clinical study with patients with moderate gallstones, as such and in addition to UDCA.

Vaccinium macrocarpon

Although many herbal products containing *V. macrocarpon* are already available on the market, most of them are poorly characterized and reliable analytical methods for the quantification of A-type procyanidins are still needed. To overcome this problem a new, fast and specific LC-MS² method using standard addition was developed and validated for the quantification of dimeric and trimeric A-type procyanidins in cranberry extracts. The next step would be to select a range of preparations available in pharmacies and sold in other shops. Therefore, I would suggest to select on the one hand a pool of scientifically based preparations for which information on the production and the final product is available, and on the other hand a pool of the most sold and used preparations on the market, independently of their scientific background. In this way, a representative pool of samples for analysis will be obtained. In the meantime, it would be valuable to keep searching for synthetic ways to produce better standard materials or fast and efficient ways to isolate them from *Vaccinium macrocarpon* itself in order to overcome the lack of polymeric procyanidin standards.

Chapter 9
SUMMARY

Medicinal plants have already been used for centuries in different parts of the world. Nowadays, herbal medicines are still an important part of health care for large parts of the population in developing countries, but also in industrialized developed countries the public interest and use of herbal products has tremendously increased during the past decades. Therefore, there is a high need for scientifically based and quality controlled herbal products.

In this work, three plant species with a well-established medicinal reputation were selected:

Desmodium adscendens (Sw.) DC., *Henriaria hirsuta* L., and *Vaccinium macrocarpon* Aiton.

D-pinitol had been characterized in our research group as the major component of a ***Desmodium adscendens*** (Sw.) DC. (*D. adscendens*) decoction. An analytical gas-chromatographic flame-ionization detection (GC-FID) method for this constituent was developed and validated according to the ICH guidelines, with the aim of preparing a quantified extract of *D. adscendens* with a known level of D-pinitol and performing quality control of herbal medicinal products and food supplements containing *D. adscendens*. The calibration model was linear and the precision was acceptable. The intermediate precision showed an RSD% of 1.27. The accuracy ranged from 103.38% to 105.84%. This method was used to prepare a quantified extract and to screen five food supplements. In addition, various production methods, including the use of different plant parts and extraction volumes were evaluated on laboratory scale by means of GC. The five food supplements that were investigated in this work showed a substantial difference in D-pinitol amount, which has major implications for the posology of different supplements. For industrial purposes, the most efficient production method would be the preparation of a decoction of leaves and twigs, also found to be used traditionally, using 15 L of water for each kg of dried plant material followed by lyophilization.

A patent has been filed on the use of *Desmodium*, especially *D. adscendens*, for treatment of viral or chemically-induced hepatitis. However, up to today no studies have been performed with a quantified extract of *D. adscendens*. In this work the protective and curative effect of this decoction, in which D-pinitol was quantified, and of pure D-pinitol, against liver damage induced by various chemicals in rats, was investigated.

These *in vivo* experiments showed a significant liver-protective effect of a *D. adscendens* decoction, which was already observed at a dose containing 5 mg/kg D-pinitol. The decoction was more active

(based on AST levels) or comparably active (ALT levels) as pure D-pinitol at a concentration of 20 mg/kg. The effect of a *Desmodium adscendens* decoction did not significantly increase when a higher concentration (corresponding to 20 mg/kg D-pinitol) was used and probably the maximal effect had already been achieved at a dose equivalent to 5 mg/kg D-pinitol. Therefore, the hepatoprotective effect of *D. adscendens* can be partially ascribed to D-pinitol, but there is a possible synergistic effect of other constituents of the decoction, which can explain the higher or comparable effect at a lower dose. For this reason, further phytochemical research was envisaged to characterize other constituents present in the decoction.

Phytochemical analysis of a decoction of *D. adscendens* was performed by flash chromatography, semi-preparative and solid phase extraction – liquid chromatography (SPE-LC). Their structure elucidation was performed by thorough investigation using NMR and MS. Hereby, the presence of a significant amount of flavonoids, more specifically flavone-*O*-glycosides and flavone-*C*-glycosides was revealed. Vitexin-2''-*O*-xyloside and 2-*O*-(*E*-coumaroyl)-malic acid were isolated and identified for the first time in *D. adscendens*. In addition, isoschaftoside, schaftoside and vicenin-2 were found to be present by comparison with an extract of *Passiflora incarnata*, used as a surrogate standard.

The *in vivo* study suggested that in addition to D-pinitol some other constituents contribute to the hepatoprotective effect and further phytochemical research proved the presence of flavonoids in the decoction, which could be responsible for the synergistic effect seen in the study. In addition, some authors described the antioxidative activity of *D. adscendens*. Therefore, and based on the traditional use of *D. adscendens* for the management of anti-inflammatory disorders and hepatitis and the hepatoprotective and antidiabetic activity of D-pinitol, it was decided to evaluate the ability of a decoction of *D. adscendens* to inhibit the formation of advanced glycation end products. Therefore, two *in vitro* tests, i.e. the BSA-glucose and the fructosamine assay, were performed. No significant anti-glycation activity was measured neither for D-pinitol nor for the decoction. During the execution of the BSA-glucose assay, some problems concerning fluorescence quenching arose and it could be concluded that, although this *in vitro* test is widely used, it is not suitable for all types of constituents.

Since data concerning the metabolization of the constituents of *D. adscendens* and of the decoction are scarce, vitexin, D-pinitol and a flavonoid-rich fraction of the decoction of *D. adscendens* were evaluated in a gastro-intestinal dialysis model with colonic phase. Investigations using the GIDM

resulted in valuable information concerning absorption and stability. Vitexin, glycosides of vitexin and isovitexin, and D-pinitol were found to be absorbed during the small intestinal phase of the model. Since this model only mimics absorption by passive diffusion, no information about absorption by active transport or enzymatic phenomena taking place in the brush borders of the small intestine is obtained. In addition, passive diffusion of polar compounds through the dialysis membrane may not reflect passive diffusion in the gastro-intestinal tract, which requires more lipophilic properties. Hence, no full absorption profile is obtained in this way. During the colonic phase, vitexin and C-glycosides thereof were found to be stable throughout their passage in the simulated gastro-intestinal tract. Only the O-glycosidic bonds of O,C-glycosides of vitexin or isovitexin were hydrolyzed in the colon compartment. This was confirmed by the absence of phenolic acids, or C-deglycosylated aglycones, products of the colonic metabolization of flavonoids.

The second plant species investigated was ***Herniaria hirsuta*** L. (*H. hirsuta*) An infusion of *H. hirsuta* is traditionally used in Morocco for the treatment of biliary dyskinesia and (uro)lithiasis or as a diuretic. The efficacy against cholelithiasis was proven in an *in vivo* study in dogs. However, the efficacy and use of a standardized extract against cholelithiasis have never been investigated. For the development of a standardized extract, the major constituents were characterized. Two previously undescribed triterpene saponins, 28-O-[[β -D-xylopyranosyl-(1 \rightarrow 4)- α -L-rhamnopyranosyl-(1 \rightarrow 2)]- β -D-glucopyranosyl-(1-6)]- β -D-glucopyranosyl}-medicagenic acid and 3-O-[α -L-rhamnopyranosyl-(1 \rightarrow 3)- β -D-glucuronopyranosyl]-28-O-[[β -D-glucopyranosyl-(1 \rightarrow 3)- β -D-xylopyranosyl-(1 \rightarrow 4)]- β -D-apiofuranosyl-(1 \rightarrow 3)]- α -L-rhamnopyranosyl-(1 \rightarrow 2)- β -D-fucopyranosyl}-medicagenic acid and three flavonoids, quercetin-3-O-(2''-O- α -L-rhamnopyranosyl)- β -D-glucuronopyranoside, rutin and narcissin (isorhamnetin-3-O-rutinoside), were isolated using flash chromatography and successive semi-preparative HPLC and were well characterized by MS and 1D and 2D NMR spectroscopic techniques. An analytical HPLC-UV method for the quantification of these constituents was developed and validated according to the ICH guidelines. The calibration model was linear and the precision was acceptable. The intermediate precision showed an RSD% smaller than 3% for flavonoids whereas the RSD%_{between} for saponins ranged from 3.1% to 14.5%. A mean accuracy of 99.2% and 109.2% was found for flavonoids and saponins, respectively. In addition to the preparation of a standardized

extract, this method can be used for quality control of herbal medicinal products and food supplements containing *H. hirsuta*.

Herniaria spp. samples from different regions were screened using this method. Significant differences in profiling were present due to origin and species. Although the flavonoid content of *H. hirsuta* was significantly influenced by the climate, the saponin content seemed to be stable. These findings emphasize the importance of standardization of the extracts.

Finally, the *in vivo* effect of the standardized extract of the plant on the level of cholesterol in the bile of dogs receiving a cholesterol-rich diet was investigated. Prolonged use of the standardized *H. hirsuta* extract resulted in a cholesterol-lowering effect in the bile but not in blood of dogs when maintaining a cholesterol-rich diet. In addition to the efficacy of the standardized extract, the genotoxicity was evaluated by means of an Ames test. The results of this test proved that the extract was not genotoxic.

The last plant species which was selected was *Vaccinium macrocarpon* Aiton. Cranberry is widely used for the prevention of urinary tract infections and is a rich source of proanthocyanidins, including the rather rare A-type procyanidins which are considered to be the pharmacologically active constituents. Despite the abovementioned use, mixed results were obtained in clinical studies. This could be caused by the use of different cranberry preparations, which were poorly standardized, making it hard to compare clinical studies with each other. To overcome this problem, new analytical methods for the quantification and standardization of different cranberry preparations are still needed. In literature, only a few potentially qualitative methods for quantification of dimeric and trimeric A-type proanthocyanidins are described and none of them was thoroughly developed and validated. In this study, a standard addition LC-MS² method for the simultaneous quantification of A-type dimers and trimers in cranberry extracts was developed and validated. A linear calibration model could be adopted for dimers and, after logarithmic transformation, for trimers. The maximal interday and interconcentration precision was found to be 4.86% and 4.28% for PAC A2 and 5.61% and 7.65% for trimeric PACs, which are all acceptable values for an analytical method using LC-MS². Analysis of twelve different extracts using the abovementioned LC-MS standard addition method highlighted the enormous variation in dimeric and trimeric PAC content. Comparison of these results with LC-MS² analysis without standard addition showed the presence of matrix effects for some of

the extracts and proved the necessity of standard addition. In addition, all abovementioned extracts were analyzed with the well-known and widely used DMAC method and the butanol-HCl assay and the results were compared with our newly developed LC-MS² method. The inability to distinguish between A and B-type PAC's by the two former assays and thereby the need for a reliable and specific method to quantify A-type PACs was underlined by the obtained results. Hence, the combination of the dimethylamminocinnamaldehyde (DMAC) method or butanol-HCl assay with our more specific LC-MS² assay could overcome these shortcomings.

SAMENVATTING

Geneeskrachtige planten worden al eeuwenlang gebruikt in verschillende delen van de wereld. Momenteel is dit nog steeds de enige vorm van gezondheidszorg voor een groot deel van de bevolking in ontwikkelingslanden, maar ook in de geïndustrialiseerde landen is de interesse in en het gebruik van geneeskrachtige planten gedurende de laatste decennia enorm gegroeid. Hierdoor is er een grote nood aan wetenschappelijk onderbouwde en kwaliteitsvolle medicinale kruidenpreparaten.

Voor dit werk werden drie planten met een gevestigde medicinale reputatie geselecteerd: *Desmodium adscendens* (Sw.) DC., *Herniaria hirsuta* L. en *Vaccinium macrocarpon* Aiton.

D-pinitol werd in onze onderzoeksgroep gekarakteriseerd als voornaamste inhoudsstof van ***Desmodium adscendens***. Met het oog op de ontwikkeling van een gekwantificeerd extract met een gekende concentratie aan D-pinitol en de kwaliteitscontrole van medicinale plantenpreparaten en voedingssupplementen die *Desmodium adscendens* decoct bevatten, werd een analytische GC-FID methode ontwikkeld en gevalideerd volgens de ICH richtlijnen. De calibratiecurve was lineair en de precisie van de methode was aanvaardbaar. De intermediaire precisie resulteerde in een RSD% van 1.27%. De recovery varieerde van 103.38% tot 105.84%. Deze methode werd gebruikt voor de bereiding van een gekwantificeerd extract en de screening van vijf voedingssupplementen. Daarnaast werden verschillende productiemethoden geëvalueerd waarbij verschillende plantendelen, extractievolumes en droogprocedures werden vergeleken op laboratoriumschaal d.m.v. de hierboven beschreven GC methode. De vijf onderzochte voedingssupplementen vertoonden een substantieel verschillende concentratie aan D-pinitol, wat grote gevolgen heeft naar posologie van deze supplementen toe. Wat betreft de industriële doelstelling werd aangetoond dat de traditionele bereidingsmethode, waarbij een kilogram gedroogd plantenmateriaal opgekookt wordt met 15 liter water gevolgd door lyofilisatie, de meest efficiënte productiemethode is.

Een patent werd reeds genomen op het gebruik van *Desmodium*, meer specifiek *D. adscendens* voor de behandeling van virale en chemisch geïnduceerde hepatitis, maar tot op vandaag werden nog geen studies uitgevoerd met een gekwantificeerd *D. adscendens* extract. Tijdens dit onderzoek werd de preventieve en curatieve activiteit van een decoct, waarin D-pinitol gekwantificeerd werd, en van het zuivere D-pinitol tegen chemisch geïnduceerde leverschade bij ratten onderzocht. Deze *in vivo* experimenten toonden aan dat een decoct van *D. adscendens* een significant leverbeschermend

effect heeft, dat reeds aanwezig was bij een dosis equivalent aan 5 mg/kg D-pinitol. Het decoct vertoonde een hogere (gebaseerd op de AST levels) of gelijkaardige activiteit (gebaseerd op de ALT levels) dan het zuivere D-pinitol, toegediend aan een concentratie van 20 mg/kg. Het effect van het decoct steeg niet significant wanneer een hogere dosis gegeven werd (overeenkomend met 20 mg/kg D-pinitol). Hoogstwaarschijnlijk werd het maximale effect reeds bereikt bij een dosis overeenkomend met 5 mg/kg D-pinitol. Het leverbeschermend effect kan dus gedeeltelijk toegeschreven worden aan D-pinitol, maar vermoedelijk is er een synergetisch effect met andere inhoudsstoffen van het decoct, wat de hogere of gelijkaardige activiteit van het decoct kan verklaren ten opzichte van een lagere dosis D-pinitol.

Fytochemisch onderzoek van het decoct van *D. adscendens* werd uitgevoerd d.m.v. isolatie van de inhoudsstoffen met behulp van flash chromatografie, semi-preparatieve vloeistofchromatografie en vaste fase extractie gekoppeld aan vloeistofchromatografie. Grondige analyse van NMR en MS spectra leidde tot de structuuropheldering van een aantal inhoudsstoffen. Op deze wijze werd de significante aanwezigheid van flavonoïden, meer specifiek flavon-*O*-glycosiden en flavon-*C*-glycosiden, aangetoond. Vitexin-2''-*O*-xyloside en 2-*O*-(*E*-coumaroyl)-malic acid werden voor het eerst geïsoleerd en geïdentificeerd in *D. adscendens*. Daarnaast werd de aanwezigheid van isoschaftoside en schaftoside aangetoond door vergelijking met een extract van *Passiflora incarnata*, gebruikt als surrogaat standaard.

Aangezien D-pinitol een antihyperglycemische werking heeft *in vivo* en het decoct flavonoïden bevatte, welke gekend zijn voor hun anti-oxidatieve werking, rees de vraag of D-pinitol en een decoct dat D-pinitol bevat de vorming van gevorderde glycatie eindproducten zou kunnen inhiberen. Om dit te onderzoeken werden twee *in vitro* testen uitgevoerd, zijnde de BSA glucose en de fructosamine test. Voor zowel D-pinitol als het decoct van *D. adscendens* kon geen significant inhiberend effect aangetoond worden. Tijdens de uitvoering van de BSA glucose test traden er problemen op, waaronder fluorescentie quenching, en hieruit kon besloten worden dat, alhoewel deze test een wijd verspreid gebruik kent, hij niet geschikt is voor alle soorten inhoudsstoffen.

Aangezien er weinig informatie beschikbaar is over het gedrag in het maag-darmkanaal en de metabolisatie van de inhoudsstoffen van *D. adscendens* en het decoct, werden verschillende standaarden, waaronder vitexine en D-pinitol, en een fractie van het decoct rijk aan flavonoïden onderzocht m.b.v. een gastro-intestinaal dialyse model (GIDM) met colon fase. De experimenten die

uitgevoerd werden in het GIDM leverden waardevolle informatie op betreffende de absorptie en stabiliteit doorheen het maagdarmkanaal. Vitexine, vitexine- en isovitexine glycosiden en D-pinitol werden geabsorbeerd tijdens hun verblijf in het GIDM. Hierbij dient wel opgemerkt te worden dat dit model slechts de absorptie via passieve diffusie nabootst en geen informatie oplevert betreffende absorptie d.m.v. actief transport of enzymatische fenomenen die plaatsvinden in de brush borders van de dunne darm. Daarnaast weerspiegelt de passieve diffusie van polaire componenten doorheen de dialysemembranen van het model de passieve diffusie in het gastro-intestinaal systeem niet, aangezien hiervoor eerder lipofiele eigenschappen nodig zijn. Omwille van deze redenen kon geen volledig absorptieprofiel bepaald worden. Vitexine en vitexine C-glycosiden waren stabiel tijdens de colonfase en enkel de O-glycosidische bindingen van O,C-glycosiden van vitexine en van isovitexine werden gehydrolyseerd door de colonbacteriën. Deze bevindingen werden bevestigd door de afwezigheid van fenolische zuren, welke metabolisatie producten zijn van flavonoïden, gevormd door de bacteriën in de darm.

De tweede plant die onderzocht werd was *Herniaria hirsuta*. Een infuus van deze plant wordt in Marokko traditioneel gebruikt voor de behandeling van dyskinesie van de gal, (nier)stenen en wordt ook gebruikt als diureticum. De werkzaamheid van deze plant tegen galstenen werd aangetoond in een *in vivo* studie met honden. Niettegenstaande werd het effect van een gestandaardiseerd extract tegen galstenen nooit onderzocht. Om een gestandaardiseerd extract te bereiden werden eerst de hoofdcomponenten van het infuus gekarakteriseerd. Twee nooit eerder beschreven triterpeen saponinen, 28-O-[[β -D-xylopyranosyl-(1 \rightarrow 4)- α -L-rhamnopyranosyl-(1 \rightarrow 2)]- β -D-glucopyranosyl-(1-6)]- β -D-glucopyranosyl-medicagenic acid en 3-O-[α -L-rhamnopyranosyl-(1 \rightarrow 3)- β -D-glucuronopyranosyl]-28-O-[[β -D-glucopyranosyl-(1 \rightarrow 3)- β -D-xylopyranosyl-(1 \rightarrow 4)]- β -D-apiofuranosyl-(1 \rightarrow 3)]- α -L-rhamnopyranosyl-(1 \rightarrow 2)- β -D-fucopyranosyl}-medicagenic acid en drie gekende flavonoïden, quercetine-3-O-(2''-O- α -L-rhamnopyranosyl)- β -D-glucuronopyranoside, rutine en narcissine (isorhamnetin-3-O-rutinoside) werden geïsoleerd met behulp van flash chromatografie en semi-preparatieve HPLC en werden gekarakteriseerd d.m.v. MS en 1D en 2D spectroscopische NMR technieken. Voor de kwantificatie van deze hoofdcomponenten werd een analytische HPLC-UV methode ontwikkeld en gevalideerd volgens de ICH richtlijnen. Het calibratiemodel was lineair en de precisie van de methode was aanvaardbaar. De intermediaire precisie resulteerde in een RSD%

kleiner dan 3% voor de flavonoïden en een RSD% gaande van 3.1% tot 14.5% voor de saponinen. De gemiddelde recovery bedroeg 99.2% en 109.2%, respectievelijk voor flavonoïden en saponinen. Naast de bereiding van een gestandaardiseerd extract kan deze methode gebruikt worden voor de kwaliteitscontrole van medicinale plantenpreparaten en voedingssupplementen die een infuus van *H. hirsuta* bevatten. *Herniaria spp.* stalen van verschillende regio's werden gescreend met deze methode. Significante verschillen in de bekomen profielen werden aangetoond afhankelijk van de groeiplaats en de soort. Alhoewel de concentratie aan flavonoïden een significante invloed kende van het klimaat, leek de concentratie aan saponinen eerder stabiel te zijn. Deze resultaten tonen het belang van standaardisatie van extracten nog maar eens aan. Uiteindelijk werd het *in vivo* effect van het gestandaardiseerd extract op de cholesterolconcentratie in de gal onderzocht in honden die op een cholesterolrijk dieet stonden. Een langer gebruik van het gestandaardiseerd extract van *H. hirsuta* resulteerde in een cholesterolverlagend effect in de gal wanneer het cholesterolrijk dieet werd verdergezet, maar dit effect was niet zichtbaar voor het cholesterolgehalte in het bloed. Naast de werkzaamheid van het extract werd ook de genotoxiciteit onderzocht m.b.v. een AMES test. Deze test toonde aan dat het extract niet genotoxisch is.

De laatste plant die geselecteerd werd was ***Vaccinium macrocarpon*** Aiton. De grote veenbes wordt wereldwijd gebruikt voor de preventie van urinaire infecties en is rijk aan proanthocyanidines (PACs), ook de eerder zeldzame, weinig voorkomende A-type procyanidines, welke worden beschouwd als de farmacologisch actieve componenten van cranberry. In tegenstelling tot het hierboven vermelde gebruik, werden uiteenlopende resultaten gevonden tijdens verschillende klinische studies. Dit kan het resultaat zijn van het gebruik van verschillende soorten en slecht gekarakteriseerde veenbespreparaten, waardoor de resultaten van verschillende studies onderling moeilijk vergelijkbaar waren. Om dit probleem te overwinnen, is er nood aan nieuwe analytische methoden voor de kwantificatie en standaardisatie van veenbespreparaten.

In de literatuur zijn slechts enkele potentieel kwalitatieve methoden voor de kwantificatie van dimere en trimere A-type procyanidines beschreven, en hiervan werd geen enkele grondig ontwikkeld en gevalideerd. In deze studie werd een LC-MS² methode met standaardadditie ontwikkeld voor de gelijktijdige kwantificatie van A-type dimeren en trimeren aanwezig in veenbessen. Voor de kwantificatie van de dimeren kon een lineair model gebruikt worden evenals

voor de trimeren na logaritmische transformatie. De maximale intermediaire precisie bedroeg 4.86% voor de verschillende dagen en 4.28% voor de verschillende concentraties voor PAC A2 en 5.61% voor de verschillende dagen en 7.65% voor de verschillende concentraties voor de trimere PACs, wat aanvaardbare waarden zijn voor LC-MS² methoden.

Analyse van twaalf verschillende veenbesextracten m.b.v. de bovenstaande LC-MS² methode brachten enorme verschillen in de concentratie aan dimere en trimere PACs aan het licht. Vergelijking van deze resultaten met resultaten bekomen met de LC-MS² methode zonder standaardadditie, toonde de aanwezigheid van matrixeffecten aan en de daaruit volgende noodzakelijkheid een van standaardadditie methode. Daarnaast werden alle hierboven vermelde extracten geanalyseerd met de welgekende en wijdverspreide DMAC methode en de butanol-HCl methode. Deze resultaten werden vergeleken met de nieuw ontwikkelde LC-MS² methode. Het feit dat A-type en B-type PACs niet van elkaar te onderscheiden zijn m.b.v. de DMAC assay en butanol-HCl methode en de nood aan een betrouwbare en specifieke methode voor de kwantificatie van A-type PACs werden nogmaals benadrukt door de bekomen resultaten. Hieruit volgt dat de combinatie van de DMAC methode of butanol-HCl methode met de meer specifieke LC-MS² methode de bestaande analytische tekortkomingen kan overwinnen.

ACKNOWLEDGMENTS - DANKWOORD

Ondanks dat het enorm cliché klinkt, is het toch waar: een doctoraatsthesis schrijf je niet alleen, maar komt tot stand dankzij de medewerking en ondersteuning van een heel aantal mensen die ik nu graag wil bedanken!

Allereerst wil ik Prof. dr. Sandra Apers en Prof. dr. Luc Pieters bedanken voor de kans die ze me hebben gegeven om een doctoraat te maken op het laboratorium NatuRA. **Sandra**, van u heb ik enorm veel kunnen opsteken over analyse en uw passie voor alles wat met het analytische vakgebied te maken had, werkte aanstekelijk. Uw deur stond altijd open en u stond me steeds bij met goede raad. Ook zou ik u willen bedanken voor de didactische vrijheid, het vertrouwen, de fijne babbels en goede samenwerking. Bedankt daarvoor! **Luc**, ook bij u kon ik steeds terecht wanneer ik vragen had. Bedankt voor uw begeleiding en goede raad tijdens dit doctoraat.

Daarnaast bedank ik alle collega's en ex-collega's van het het labo NatuRA voor de leerrijke en gezellige tijd. Enkele personen wil ik in het bijzonder danken voor de hulp tijdens mijn doctoraat.

Roger, jij leerde me de kneepjes van het practicum en ik heb enorm veel van je geleerd. Bij jou kon ik steeds terecht met vragen gaande over practicumverslagen en planningen tot een printer die plots niet meer werkte of wanneer ik weer eens een computerprobleem had. Bedankt voor de didactische vrijheid en het vertrouwen! Bedankt voor de fijne samenwerking.

Het bureau A 1.14 was mijn eerste stekje en daar heb ik een hele tijd met **Kenn**, **Hans** en **Rica** samen gezeten. Bedankt voor de leuke tijd en de fijne samenwerking! Nadien in bureau A 1.12 kreeg ik een aantal nieuwe bureaugenootjes. **Mart** en **Tania**, bedankt voor alles, jullie onvoorwaardelijke steun, al de antwoorden op de ontelbare vragen, de hulp, de gezellige babbels,... **Hanne**, bedankt voor de fijne samenwerking! Zonder jou zou cranberry niet dezelfde betekenis hebben. Bedankt voor je hulp bij de deze analyses. Na een tijdje kwam **Laura** erbij. Hoofdletters, kleine letters, velden bijwerken met een druk op de knop,... alle Word en Excel problemen verdwenen als sneeuw voor de zon met onze expert Laura als mede-eilandbewoner. Veel succes met je doctoraat en alle practica! Op het laatst vervoegde **Kenn** ons op dit eiland. Reeds vanaf het begin van mijn onderzoek stond Kenn klaar met woord en daad. Ze heeft me ingewijd in de wondere wereld van de veenbessen, maar ook het

Herniaria-project werd door haar opgevolgd. Bedankt voor alle wijze raad, de grappige en leuke gesprekken en de dolle autoritjes.

Daarnaast wil ik ook **Emmy** bedanken, mijn AGes-bondgenoot, voor de vele fijne momenten en babbels. Je optimisme en doorzettingsvermogen zijn inspirerend en ik wens je veel succes bij het afronden van je doctoraat! I also want to express my gratitude to **Stefaniya** for her help as an Erasmus student on the *Herniaria*-project. Your funny messages made me laugh and I will never forget the cookies on my desk before my internal defense! Good luck, Stefaniya and all the best!

Dankzij **Annelies (V.)** was ik nooit alleen wanneer er laat gewerkt werd. Bedankt voor de vele fijne babbels in de transit bureau en het bewaren en bewaken van mijn stalen die in de -80°C verbleven. Ik wens je veel succes niet alleen met je studie maar met je hele doctoraat! **Sebastiaan**, bedankt voor je hulp bij de analyse met de super LC-MS en voor de wissels van de gasflessen! **Anastasia**, bedankt voor je hulp bij het S9 experiment. **Annelies (B.)**, bedankt voor de hulp met het gastro-intestinaal model.

Vasiliki, thanks for all the nice talks and your infinite NMR support. Your passion and knowledge about NMR were legendary. I wish you all the best! **Adnan**, thanks for your help in the lab and with the gas bottles!

Hanne, Hans, Rica, Emmy, Laura, Maxime, Kenn, Lisbeth, Freya, Maarten, Nina, Sabine, Mart, Annelies (B.), Rudy, Francis en **Steven**, bedankt voor de fijne samenwerking tijdens de practica!

Mijn collega's van een verdiep lager, **Arnout, Sofie, Shari** en **Géraldine**, bedankt voor de fijne samenwerking tijdens het practicum Industriegame en de hulp bij het autoclaveren. Veel succes met jullie doctoraat! **Arnout**, bedankt voor de mooie foto's voor de kaft van mijn thesis.

Adrian, Alexander, Walid en **Steven**, bedankt voor jullie gastvrijheid en hulp bij de LC-MS analyses.

Prof. dr. Anne-Marie Lambeir en **Lesley** zou ik willen bedanken voor de gastvrijheid en de hulp bij de metingen met de Tecan.

Ook iedereen van de PBW werkgroep CDE bedankt voor de fijne samenwerking, in het bijzonder **Kris** en **Sophie**!

Prof. Magda Claeys en **Reinhilde** zou ik willen bedanken voor de gastvrijheid en hulp bij de analyses. Ook alle leden van mijn doctoraatsjury zou ik willen bedanken voor het nalezen van dit werk.

Daarnaast zou ik nog enkele fantastische mensen in mijn leven willen bedanken. Mijn ouders, **mama** en **papa**, zou ik willen bedanken voor alles wat ze voor me hebben gedaan. Zij hebben mij van kleins af aan aangemoedigd in alles wat ik deed en ook tijdens mij studies en doctoraat stonden ze steeds voor mij klaar: van een verplichte pauze-wandeling, al dan niet met de hond, tijdens de blokperiodes tot vers gemaakte soep die nog steeds aan huis geleverd wordt, jullie waren er altijd.

Thomas, mijn broer(tje), wil ik hierbij bedanken voor zijn interesse die hij toonde in mijn doctoraat, in het bijzonder de veenbes die ik bestudeerde. Jouw ambitieus en ondernemend karakter werkt inspirerend!

Christa en Patrick, bedankt voor jullie interesse in mijn werk en jullie gastvrijheid.

Gitta en Dennis, bedankt voor alle hulp met Word en de Engelse taal!

Lien en **Lotte**, bedankt voor alle interesse die jullie toonden voor mijn doctoraat. Elk jaar kijk ik uit naar onze kerstuitstap om er eens helemaal tussenuit te zijn! Bedankt voor jullie jarenlange vriendschap!

Anja en **Aster**, bedankt voor jullie interesse in mijn doctoraat en de fijne etentjes met of zonder gezelschapsspelen. Bedankt voor jullie jarenlange vriendschap!

Nils, schat, u wil ik bedanken voor alle wetenschappelijke en huishoudelijke hulp. Zonder jouw begrip, geduld, steun en aanmoedigen zou dit werk zoveel moeilijker gegaan zijn. Je wist steeds de juiste woorden te vinden als het even wat minder ging of ik gefrustreerd thuis kwam. Het is fijn om samen met jou mijn wetenschappelijke problemen te bespreken. Bedankt om me te vergezellen naar de universiteit als ik er weer op een avond of tijdens het weekend een analyse ging opstarten of afronden, als er weer eens iets mis liep met teamviewer of wanneer ik nog enkele documenten nodig had. Bedankt om me bij te staan wanneer de computer of Word het weer eens liet afweten. Bedankt voor alles, ik zie je graag!

SCIENTIFIC CURRICULUM VITAE

- October 2009 – January 2010 Master thesis (Industrial Pharmacy): Development and validation of a method for the quantification of D-pinitol in a decoction of *D. adscendens* – Determination of the hepatoprotective effect
Prof. dr. S. Apers
University of Antwerp, Belgium
- March 2009 – June 2009 Laboratory of Microbiology, Parasitology and Hygiene
Master thesis: Pharmacodynamics of new antifungal compounds for the treatment of topical mycosis
Prof. dr. P. Cos
University of Antwerp, Belgium

PUBLICATIONS

van Dooren, I; Foubert, K; Bijttebier, S; Theunis, M; Velichkova, S; Claeys, M; Pieters, L; Exarchou, V; Apers, S. Saponins and flavonoids from an infusion of *Herniaria hirsuta*. *Planta Med.* **2016**, Published online DOI 10.1055/s-0042-118710.

van Dooren, I; Hermans, N; Dhooghe, L; Naessens, T; Vermeyelen, R; Claeys, M; Vlietinck, A; Pieters, L; Apers, S. Development and validation of a gas chromatographic method for the quantification of D-pinitol in decoctions of *Desmodium adscendens*. *Phytochem Lett*, **2014**, 7, 19-25.

van Dooren, I; Faouzi, M.E.A; Foubert, K; Theunis, M; Pieters, L; Cherrah, Y; Apers, S. Cholesterol lowering effect in the gall bladder of dogs by a standardized infusion of *Herniaria hirsuta* L. *J. Ethnopharmacol.* **2014**, 169 (1), 69-75.

Magielse, J; Arcoraci, T; Breynaert, A; van Dooren, I; Kanyanga, C; Fransen, E; Van Hoof, V; Vlietinck, A; Apers, S; Pieters, L; Hermans, N. Antihepatotoxic activity of a quantified *Desmodium adscendens* decoction and D-pinitol against chemically-induced liver damage in rats. *J. Ethnopharmacol.* **2013**, 146 (1), 250-256.

ORAL PRESENTATIONS

Development and validation of a method for standardization of infusions of *Herniaria hirsuta*, 18th Forum of Pharmaceutical Sciences, 2014 – Blankenberge, Belgium

Phytochemical analysis of *Desmodium adscendens* - 17th of Pharmaceutical Sciences, 2013 – Spa, Belgium

Development and validation of a gas chromatographic method for the quantification of D-pinitol in a decoction of *Desmodium adscendens* - 16th Forum of Pharmaceutical Sciences, 2012 – Blankenberge, Belgium

POSTER PRESENTATIONS

Development and validation of a method for standardization of infusions of *Herniaria hirsuta* – International Congress and Annual Meeting for Medicinal Plant and Natural Product Research, 2015 – Budapest, Hungary

Development and validation of a method for standardization of infusions of *Herniaria hirsuta* - Drug Analysis: 10th International Symposium on Drug Analysis, 25th International Symposium on Pharmaceutical and Biomedical Analysis 2014 – Liège, Belgium